ABSTRACT

Over the last few years considerable doubt has been cast on the accuracy of the values of the transport properties of the inert gases available in the literature (1,2,3). Barker and Pompe in a careful analysis (2) have shown that the high temperature transport data of argon are inconsistent with potential energy functions obtained by reference to molecular beam experiments, second virial coefficient measurements and direct theoretical calculation. Similar considerations have led Hanley and Childs (3) to suggest that the published tables of inert gas viscosities may be incorrect by as much as 10 percent above 600°K.

This thesis reports a new determination of the low pressure viscosity coefficients up to high temperatures for all the rare gases and nitrogen. The determination was made using a specially designed capillary viscometer capable of making measurements up to 1600°K.

Accurate viscometry requires numerous corrections to be applied to the basic Poiseuille formula. The apparatus was designed to allow these corrections to be made simply and accurately. Thus the effects due to gas imperfection and the kinetic energy of the gas accelerating along the capillary (Hagenbach correction) were usually reduced to less than 0.1%. To maintain the capillary at a uniform temperature it was necessary to wind it in a close helix. However at high flow rates extra resistance due to centrifugal forces on the molecules, the so-called curved pipe flow effect, occurs. A separate study of curved pipe flow was made and the results and conclusions are given in the final chapter.

The viscosity coefficients were determined from an analysis of the times of flow, in practice the time for a mercury surface to pass between electrical contacts, at various mean pressures in the capillary. Thus the slip factor, which arises from the finite velocity of the gas at the wall surface, can be eliminated by

a suitable analysis, since it is dependent on the mean free path in the gas, which itself is inversely proportional to the pressure. It is shown that the slip coefficient, widely thought to be constant, in fact can vary with the thermal history, composition and temperature of the capillary.

Two comparative methods of calculating the viscosities were employed; the so-called RELATIVE method where the ratio of one gas to a standard gas at the same temperature is determined, and the so-called STANDARD method where the viscosity of a gas at a given temperature is taken as a standard and the viscosity at another temperature calculated relative to it. This method requires accurate measurement of the temperature of the capillary. The results were fitted to polynomials of the form,

$$\text{Log}_{10}(\text{Ratio}) = A \log_{10} T + B/T + C/T^2 + D$$

and are presented in the Summary tables (4-1) to (4-3). These ratios are believed accurate to within 0.5% and the standard deviations of the observed ratios from the smooth curves given by the polynomials are less than 0.2%.

The viscosities were calculated from these ratios using standard values taken from the literature and are given in Summary tables (4-4) and (4-5). The absolute accuracy of the results depends on the choice of a suitable standard viscosity. It is believed that the standards of viscosity are accurate to within our experimental error but the results in Summary tables (4-4) and (4-5) can easily be recalculated should the accepted values be proved to be in error. The viscosities of the inert gases given in our Tables are believed to be accurate to within 1%. The literature has been surveyed and the data of other workers for both viscosity and thermal conductivity coefficients are presented in an appendix. The results of this work are critically compared with the earlier data. For the inert gases the thermal conductivity coefficient is directly proportional to the viscosity coefficient and interconversion is straightforward. The widely quoted viscosity data of Trautz

et al. (4) and Vasilesco (5) are shown to be in error by over 5% at the highest temperatures.

The new data in this thesis have been examined carefully to see if they give better agreement with intermolecular potential functions derived from other sources. It is shown that the new data satisfy the law of corresponding states within experimental error and that much of the discrepancy between viscosity data and other sources of information is reconciled.

(1) E.A. Mason and W.E. Rice, J.Chem.Phys. 22 843 (1954)

(2) J.A. Barker and A. Pompe, private communication to be published: see E.B. Smith Ann,Rep.Chem.Soc. (London) 83 13 (1966)

(3) H.J.M. Hanley and G.E. Childs, Science 159 1114 (1968)

(4) M. Trautz and R. Zink, Ann.Physik 7 427 (1930)

(5) V. Vasilesco, Ann.Physique (Paris) 20 137, 292 (1945)

8-XI-68

THE VISCOSITY OF SIMPLE GASES

A Thesis submitted for the degree of

Doctor of Philosophy

by

R. A. DAWE

St. Catherine's College
OXFORD

Physical Chemistry Laboratory
OXFORD

September 1968

ACKNOWLEDGEMENTS

I should like to thank warmly all who have helped me during this period of research, in particular:-

Professor R.E. Richards, head of the Physical Chemistry Department, for allowing me the facilities of the Department,

Dr. E.B. Smith, my supervisor, for his constant and valuable guidance, and friendly encouragement.

The Gas Council for a Research Scholarship and for their interest.

My colleagues, especially Mr. A.G. Clarke, for much useful discussion and many fruitful arguments,

The Staff of the Physical Chemistry Laboratory, especially Mr. A. Duncan for making and repairing the platinum and platinum-rhodium helices so skilfully and Mr. K. Calkin, the laboratory glassblower, for making the inlet and back vessels and much helpful advice.

My wife, Deborah, for her encouragement especially in moments of gloom and for help in preparing some of the Tables.

R.A. Dawe

CONTENTS

INTRODUCTION

CHAPTER 1 - INTERMOLECULAR FORCES

The Origin of Forces 3

Analytical Models for the Pair Potential Function 6

The Relation between the Bulk Properties and Intermolecular Forces 10

CHAPTER 2 - VISCOSITY

Definitions 18

The Gaseous Viscosity Coefficient - Elementary Kinetic Theory 19

Rigorous Kinetic Theory 21

Measurement of Viscosity 32

The Standard Value 33

Agreement between Various Methods 34

The Theory of the Flow of Gases through Capillaries 35

Formulation of the Flow of Gases through Capillary Tubes 44

Correction to Poiseuille Flow - Kinetic Energy 47

- Gas Imperfections 49

- Curved Pipe Flow 50

CHAPTER 3 - EXPERIMENTAL

Introduction 53

The Apparatus 54

Apparatus Description - The Thermostat Tank 55

- The Front Vessel V_f 55

- The Backing Vessel V_b 56

- The Capillary 57

- The Furnace 60

- Temperature Measurement 63

- The Vacuum Line 64

- The Gas Line 65

- Materials Used 65

Experimental Procedure 67

CHAPTER 4 - RESULTS

Introduction 69

Equations Used 70

- The Relative Method 72
- The Standard Method 73

Corrections Applied 73

- Kinetic Energy 74
- Gas Imperfection 76
- Curved Pipe Flow 79

Method of Correcting Results 80

The Expansion Coefficient 81

Analysis of Times of Flow 83

Specimen Calculation by the Relative Method 83

The Relative Ratios 86

Specimen Calculation by the Standard Method 93

The Standard Ratios 95

Summary Table (4-1) The Coefficients for the Smoothed Curves 102

Summary Table (4-2) Ratios Relative to N_2 103

Summary Table (4-3) Standard Ratios 104

Summary Table (4-4) The Viscosities calculated by the Standard Method 105

Summary Table (4-5) The Viscosities calculated by the Relative Method 106

Figures Showing the Smoothed Curves and Deviations of Various Data from Them

A Comparison with other Data 107

Errors and Accuracy 114

CHAPTER 5 - DISCUSSION

Introduction 119

Viscosity and the Potential Function 120

The Slip Coefficient 126

Curved Pipe Flow 133

APPENDIX 1 - Glossary of Symbols

APPENDIX 2 - Useful Data for the Gases

APPENDIX 3 - Pressure Measurements

APPENDIX 4 - Volume Measurements

APPENDIX 5 - Times of Flow

APPENDIX 6 - The Statistics of the Straight Line

APPENDIX 7 - Review of Previous Data

APPENDIX 8 - Curved Pipe Flow Evaluation

APPENDIX 9 - Reduced Collision Integrals for the Potential $\phi(r^*) = 10{,}000 \exp(-8r^*)$

REFERENCES

INTRODUCTION

Molecules attract and repel each other. Without the attractive forces, gases would not condense to liquids, and without the repulsive forces liquids and solids would not have such small compressibility coefficients and the volume of solids at absolute zero would be nil. A knowledge of these intermolecular forces is basic to the understanding of the properties of matter.

The simplest interactions which can be studied are two body problems. These only occur in the gaseous phase, and then only when the gas is so dilute that the probability of three molecules being close enough to interact is negligible. Information is available from second virial coefficients, molecular beam scattering measurements and low pressure transport properties. Other bulk properties such as crystal lattice energies, high pressure transport properties or third virial coefficients involve third or higher order interactions.

Statistical mechanics can provide a link between the measureable bulk properties and the potential energy function, ϕ (r), often conveniently expressed as a mathematical function summing the attractions and repulsions between pairs of molecules. In principle, the potential function can be calculated as a function of separation by quantum mechanical considerations. All the electrons in each molecule have to be included which usually leads to a complicated many body problem at present insoluble in its exact form, except in the simplest cases (e.g. 4, 5).

Gross simplifications have to be introduced. A functional form for the potential, ϕ (r), is assumed, with the adjustable parameters often chosen in part on theoretical grounds, and certain of the bulk properties calculated through the statistical mechanical expressions developed for that property. The adequacy of the potential is assessed by comparison with the experimental data. As yet it is not possible to obtain the intermolecular potential from the bulk properties without

first invoking some model, since the statistical mechanical integrals for the macroscopic properties cannot be inverted except for a very simple case (6).

Reasonable agreement has been reached with second virial coefficients and molecular beam scattering measurements for the same potential function, but attempts to reconcile the low pressure transport properties, which since the advent of high speed computers can be calculated easily and accurately with the more realistic potential functions, have not been successful. The reason for this failure has been ascribed by some writers to incorrect determinations of the transport data (7-10) and recently it has been stated that the transport data are in urgent need of critical re-examination (11).

A potential function needs to be tested with data over a wide temperature range. The low pressure transport property easiest to obtain experimentally over a wide range of temperature is the viscosity coefficient determined by a capillary flow technique; other methods require complicated temperature dependent corrections such as the torsional wire corrections needed with oscillating disc viscometers (12) and accommodation coefficients in thermal conductivity measurements (13-16).

This thesis reports a new determination of the low pressure viscosity coefficient by a capillary flow technique for all the rare gases and nitrogen over the wide temperature range 300-1530°K. A summary of the techniques of viscometry and the theory on which the capillary flow method is based are given in Chapter 2, while the apparatus and experimental results are recorded in Chapters 3 and 4. In the remaining chapter these results are discussed in the light of the intermolecular force theory briefly reviewed in Chapter 1 and the effects of the major corrections, slip and curved-pipe flow, to capillary flow data are then further considered.

CHAPTER 1

INTERMOLECULAR FORCES

The force of interaction between two molecules (the word 'molecule' here includes the rare gas atoms) is a function of their intermolecular separation and their mutual orientation. Usually it is more convenient to consider the intermolecular potential energy than the force: for spherical non-polar molecules the potential energy of interaction, $\phi(r)$, is related to the force $F(r)$ by

$$F(r) = -\frac{d\phi(r)}{dr} \quad \text{i.e.} \quad \phi(r) = \int_r^\infty F(r)\,dr .$$

Molecules which have an angular dependent potential, such as dipolar or non-spherical molecules (e.g. long chain hydrocarbons) have in addition a torque tending to rotate the molecule.

The Origin of Forces

The forces which can act on a particle may be classified according to their origin:-

1. Strong nuclear — e.g. forces binding protons and neutrons, and are of a very short range $\sim 10^{-5}$ A.
2. Weak nuclear — e.g. forces associated with μ -mesons, again of very short range.
3. Gravitational — these act on all systems and are proportional to the masses and r^{-2}.
4. Electromagnetic forces.

The forces between atoms and molecules are almost entirely electromagnetic in origin and may be further subdivided into the following groups (5).

1. Chemical bonding ~ 60 kcal/mole } Valence forces.
2. Ionic interactions ~ 30 kcal/mole }
3. Metallic bonding ~ varies in strength, as shown by the range of melting points of metals.
4. Hydrogen bonding ~ 5 kcal/mole
5. Intermolecular forces ~ 1 kcal/mole

Room temperature (kT) is equivalent to 0.6 kcal/mole or 0.025 e.v./mole.

Since the intermolecular forces of electromagnetic origin are the main contributors to the bulk properties discussed in this thesis, only these will be considered further.

Intermolecular Forces (1-3, 17-22)

These forces are generally very weak, 10^{-3} - 10^{-1} e.v., and may be regarded as extending over distances of about 5 σ, where σ is the hard sphere radius of the molecule (page 6). They may be classified into two groups: short range repulsive forces and long range attractive forces.

Short range repulsive forces:- these forces result from the violation of the Pauli Exclusion Principle due to the overlap of the electron charge clouds. Quantum mechanical calculations indicate that they fall off exponentially with separation of the molecules. (1, 23, 24) Except in the most elementary cases, such calculations are not accurate, due to the complex exchange, overlap and correlation effects which involve most of the electrons in both molecules. An expression, A exp (-Br) where A and B are constants, is often used for calculations where the kinetic energy of the molecules is not more than about 5 kT. For simple potential functions in order to keep the mathematical computations manageable, the repulsive force is approximated by a term in r^{-n}.

Long range forces:- these forces are attractive and can arise in essentially three ways (1) :-

1. Electrostatic or Orientation forces - these result from the interaction of the various permanent multipole moments in the molecules. Two dipoles interact with an energy proportional to r^{-3}, which over all orientations would average to zero were it not for the Boltzmann exponential weighting factor taking into account that statistically the molecules prefer the lower energy configurations. The leading term for dipole-dipole attraction at long range is $-\frac{2\mu_a^2\mu_b^2}{3kTr^6}$ where μ is the dipole moment). Similar considerations apply to other multipole interactions (25).

2. Induction forces - these arise when a permanent multipole can induce a multipole in a polarisable molecule and the two moments interacting. For a dipole-induced dipole, the energy is $-\frac{\mu_a^2\alpha_b^2(3\cos^2\theta_a+1)}{2r^6}$ (where α is the polarisability) which when averaged over all orientations results in the attractive energy of $-\frac{\mu_a^2\alpha_b^2}{r^6}$.

3. Dispersion (London) forces - when the electrons in molecule 'a' are in some configuration which results in an instantaneous dipole moment, then this instantaneous dipole moment will induce a dipole in molecule 'b' and the two instantaneous dipoles will interact to produce an energy of attraction.

London (26, 27) using second order perturbation theory expressed this dispersion effect as

$$\phi(r) = C_6 r^{-6} + C_8 r^{-8} + C_{10} r^{-10} + \ldots$$

where for the simplest model, when the atom is considered to be an harmonic and isotropic oscillator with a single characteristic frequency, ν_0, the 'induced-dipole induced-dipole' coefficient is given by

$$C_6 = -\frac{3}{4}\alpha^2(h\nu_0)$$

where α is the polarisability and $h\nu_0$ approximates to the ionisation potential.

C_6 may also be calculated by variational methods (28) or by oscillator strength sums (22, 29-31), there being good agreement between the various methods. These theoretical results may be compared with the values derived from potential functions (page 8).

Higher terms such as C_8, the induced dipole-induced quadrupole and C_{10}, the induced dipole-induced octopole interactions, have been calculated for the inert gases (32).

Analytical Models for the Pair Potential Function (1)

A suitable pair potential function $\phi(r)$ must have the general shape shown in figure 1. The potential energy is by convention chosen to be zero when the molecules are infinitely far apart. For small values of r, the potential is very large due to the repulsive forces; as r increases $\phi(r)$ becomes negative due to the attractive forces and asymptotically approaches zero

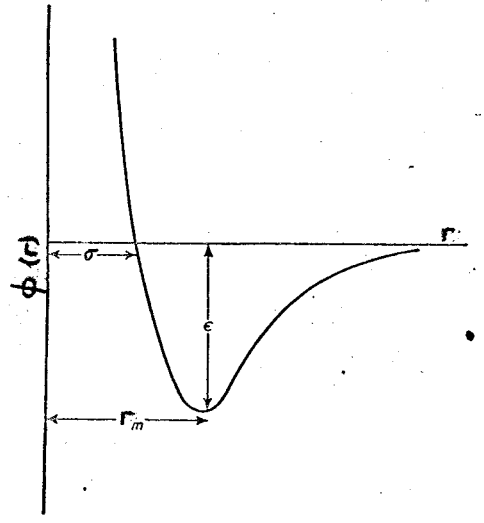


FIGURE 1.1 *Intermolecular potential energy as a function of separation.*

σ, the collision diameter, is the value of r when $\phi(r) = 0$ and r_m is the position of maximum attractive energy, $-\varepsilon$.

For systems where more than two body interactions occur, the intermolecular energy of a number of molecules is frequently assumed to be the sum of the pair

energies,

$$\text{i.e.} \quad \phi(r) = \frac{1}{2} \sum_{i} \sum_{\substack{j \\ i \neq j}} \phi(r_{ij})$$

Axilrod and Teller (33) showed this assumption to be false, thus for a three body interaction an extra contribution, (the so called triple dipole term) is at large distances

$$\phi = \beta (1 + 3 \cos \theta_{12} \cos \theta_{13} \cos \theta_{23})(r_{12} r_{13} r_{23})^{-3}$$

where r_{ij}, θ_{ij} are the sides and interior angles formed by the three particles. For three identical oscillators (34) $\beta = \frac{3}{4} \alpha C_6$ where α is the polarisability. Neglect of this term causes the calculated interaction for an equilateral triangle array to be too large, and for a linear array too small (35). At close distances exchange effects become important and the correction term becomes more complicated (35). Non additivity can make a significant error to the calculated values for many physical properties. For example, the third virial coefficient for argon is increased by about 50% over the pairwise value (36), and for the lattice energies of the solid inert gases, the correction is some 5-10% of the total value (37). Whether there are any significant non-pairwise corrections other than triple dipole corrections is still a matter of debate (38, 39, 40).

On account of these difficulties emphasis for the determination of the parameters of the inert gases has recently been placed on the properties involving only pair interactions. Since the calculation of the pair potential from first principles by quantum mechanics is not at present practicable (4, 22) many simplified analytical functions have been used to describe it. The functional forms are selected to have the general shape of figure 1, and contain two or more parameters obtained by a comparison of theoretical and experimental physical properties. The

form, though, must be sufficiently simple to enable it to be used in calculations. For a study of the relationship between physical properties and statistical mechanical theory rather than the intermolecular forces, simplified potentials are often used. These are not realistic and do not have the general shape of figure 1. Examples are (41):-

hard sphere model - $\phi(r) = \infty$, $r < \sigma$; $\phi(r) = 0$, $r > \sigma$

square well model - $\phi(r) = \infty$, $r < \sigma$; $\phi(r) = -\varepsilon$, $\sigma < r < k\sigma$;

$\phi(r) = 0$, $r > k\sigma$, where $k \approx 3$.

point centres of repulsion model - $\phi(r) = dr^{-\delta}$. δ is the index of repulsion often 9-15. If $\delta = 4$, the molecules are known as Maxwell molecules.

Sutherland model - $\phi(r) = \infty$, $r < \sigma$; $\phi(r) = -cr^{-\gamma}$, $r > \sigma$

This is fairly realistic.

Examples of the more realistic potentials in common use are:-

Lennard-Jones n-m potential (42)

$$\phi(r) = \frac{n\varepsilon}{n-m}\left[\frac{m}{n}\left(\frac{r_m}{r}\right)^{n} - \left(\frac{r_m}{r}\right)^{m}\right]$$

where n represents the repulsive part of the potential and m the attractive part. Since the asymptotic behaviour of $\phi(r)$ is of the form, $-C_6 r^{-6}$ (page 5), m is usually taken as 6. If n is taken as 12, the potential becomes

$$\phi(r) = \varepsilon\left[\left(\frac{r_m}{r}\right)^{12} - 2\left(\frac{r_m}{r}\right)^{6}\right] \quad ; \quad r_m = 2^{1/6}\sigma$$

This form is known as the Lennard-Jones 12-6 potential, and due to its mathematical simplicity has been much used with fair success (1). However $C_6 (= -4\varepsilon\sigma^6)$ is found to be a factor of two too high when compared with the best theoretical values (17).

Other forms of the n-m potential often used are 16-6, 18-6 (43) and 28-7 (44), where the C_6 values agree more closely with the theoretical values.

The Kihara Potential (45)

$$\phi(r) = \infty, \; r < \gamma\sigma \; ; \quad \phi(r) = \frac{n\epsilon}{n-m}\left(\frac{n}{m}\right)^{\frac{n}{n+m}}\left[\left(\frac{\sigma-\gamma\sigma}{r-\gamma\sigma}\right)^{n} - \left(\frac{\sigma-\gamma\sigma}{r-\gamma\sigma}\right)^{m}\right], \; r \geqslant \gamma\sigma$$

Kihara replaced the point centre model with a molecule having an inpenetrable core of radius $\gamma\sigma$. $\phi(r)$ is now a function of the minimum distance between the cores. Usually $n = 12$, $m = 6$ and γ is a third variable parameter. If $\gamma = 0$, the Kihara potential reduces to the Lennard-Jones potential.

The Modified Buckingham Exp-6 Potential (46)

$$\phi(r) = \infty, \; r \leqslant r_{max} \; ; \quad \phi(r) = \frac{\epsilon}{(1-6/\alpha)}\left[\frac{6}{\alpha}\exp\left(\alpha(1-r/r_m)\right) - (r_m/r)^6\right], \quad r \geqslant r_{max}$$

α is a parameter which is a measure of the steepness of the repulsive energy. As α increases, the repulsive part of $\phi(r)$ becomes steeper. The function has a spurious maximum at r_m and then goes to minus infinity as r further approaches zero, so it is modified by a cut-off at r_m. The potential approximates the repulsive part of the potential to the more theoretical realistic exponential form.

As more accurate data become available, these fairly simple potentials have appeared inadequate in correlating the different properties, so more complex forms have been devised.

Guggenheim and McGlashan (47) devised a potential by fitting the different regions of the potential to data most sensitive to that region. They fitted the low

energy repulsive region using high temperature viscosity data, the region of the minimum in the potential energy using lattice energies and the attractive long range area to quantum mechanical calculations. The function has however been recently strongly criticized (20).

Multiterm potentials where the function has a number of higher order terms in r^{-m} (48) or adjustable parameters (49, 50) have also been used. These functions are often a modification of one of the common potentials described above, but they still do not seem capable of fitting the data for all available properties (17).

The Relation between the Bulk Properties and Intermolecular Forces.

Accurate information about the forces between molecules can only be obtained if the statistical mechanical theory connecting the physical property with the intermolecular potential is well established. Otherwise the comparison between experimental and theoretical values serves to test the statistical mechanical theory rather than the potential function. The calculation procedure is somewhat indirect, since all that is available are certain weighted averages of functions of the potential, as in virial coefficients, or some function of the deflections suffered by colliding molecules averaged over all possible trajections, as in transport coefficients. Information can be derived from any phase but unambiguous interpretation is often very difficult.

Solids.

The regularity of the crystal lattice causes the potential energy of interaction, E, of one molecule with all its neighbours to be determined by the type of lattice and the distance between molecules. If pairwise additivity is assumed, the energy can be written,

$$E = \sum_{k} n_k \quad \phi\,(r)_{rk}$$

where rk is the distance from a lattice point to the k^{th} shell of lattice points

surrounding it; n_k the number of lattice points in the k^{th} shell and $\phi(r)_{rk}$ the pair potential energy at rk.

The total internal energy, Eo, of a crystal at absolute zero is the sum of the static potential energy $\frac{1}{2}$NE of the lattice and the zero point energy Ko, associated with the zero point vibrations of the molecules in the lattice.

$$Eo = \tfrac{1}{2}NE + Ko$$

Corrections for non-pairwise additivity have to be made (37), but because there are uncertainties in the value and number of these corrections, the usefulness of crystal lattice data in determining detail about the intermolecular potential is limited (38-40, 52,53).

Liquids (19,54,55,56)

Liquids and dense gases are even more difficult to use than solids for the determination of intermolecular forces, for not only are there the problems of non-pairwise additivity but the basic statistical-mechanical theory of liquids is still in a rudimentary state. Limited success has been made with the various proposed models such as the cell model (i.e. a disordered solid) (57) and the dense gas model (58). Statistical methods based on Monte Carlo techniques (59,60) or molecular dynamics (61) are now being developed and giving much information about the behaviour of liquids. X-ray scattering data has been used to determine the experimental pair distribution function for liquids (62) but the many body problems still exist (56).

Dilute Gases

The physical properties of dilute gases, where three body interactions are negligible, can be calculated with fair success through classical statistical mechanics using only the pair potential (1).

Thermodynamic or Equilibrium Properties

Experimental P-V isotherms may be fitted over a wide temperature and pressure range by the virial equation of state, which is a power series relation

$$\frac{\tilde{PV}}{RT} = 1 + \frac{B(T)}{\tilde{V}} + \frac{C(T)}{\tilde{V}^2} + \ldots.$$

where $\tilde{V}$ is the molar volume and the temperature dependent functions B(T), C(T) are known as the second, third ... virial coefficients. B(T) relates the deviations from ideality due to two body interactions, C(T) to the three body interactions. For a dilute gas only the second virial coefficient need be considered. From statistical mechanics it can be shown that (63)

$$B(T) = 2\pi N \int_0^\infty \left[1 - \exp\left(-\phi(r)/kT\right)\right] r^2 \, dr$$

where N is Avogadro's number. Unfortunately only the ratio width/depth of the potential well is defined due to r being a double valued function of $\phi(r)$ where $r > \sigma$, so an uniquely defined potential is not deducible from the second virial coefficient (64). Investigations (65, 66) of the mathematical problem of inverting this integral to find $\phi(r)$ have shown that only the positive, single valued (repulsive) part of $\phi(r)$ (i.e. $r < \sigma$) is determined uniquely. Jonah and Rowlinson (6) for helium at high temperatures have attempted this by means of an inverse Laplace transform. Their results agree well with Phillipson's quantal calculations (67), although corrections for the small potential well and for quantum effects have to be made. In the low temperature limit B(T) is determined by the shape and depth of $\phi(r)$ near its minimum (68), but this limit is difficult to approach experimentally and its relation to $\phi(r)$ is complicated by quantum effects.

Experimentally B(T) may be determined by accurate P-V measurements e.g. (69, 70), or independently from the zero pressure Joule Thomson coefficient, (71) where

$$\mu = \left(\frac{\partial T}{\partial P}\right)_H = \frac{\left(T\left(\frac{\partial V}{\partial T}\right)_P - V\right)}{C_P} = \frac{1}{C_P}\left(T\left(\frac{dB}{dT}\right) - B\right)$$

where C_P is the zero pressure limit of the molar heat capacity at constant pressure.

$$\text{whence} \quad \mu = -\frac{2\pi N}{C_P kT} \int_0^\infty \exp\left(-\phi(r)/kT\right) \cdot \left(\phi(r) - \frac{1}{3} r\left(\frac{d\phi(r)}{dr}\right)\right) r^2 \, dr$$

Third or higher virial coefficients are very difficult to measure experimentally and the uncertainty of non-pairwise additivity makesthem difficult to interpret.

Transport Properties

Information concerning the pair potential may be obtained from the temperature variation of low density transport coefficients (viscosity, thermal conductivity and diffusion factors) by means of the Chapman-Enskog theory (3). According to this theory, the various transport coefficients for dilute gases depend on the collision integrals $\Omega^{(l,s)}$, defined by

$$\Omega^{(l,s)}(T) = \left(\frac{2\pi kT}{\mu}\right)^{1/2} \int_0^\infty \int_0^\infty e^{-\gamma^2} \gamma^{2s+3} \left(1 - \cos^l \chi\right) b \, db \, d\gamma$$

where $\gamma^2 = \frac{1}{2} g^2/kT$, g the relative initial velocity, μ the reduced mass of the pair of colliding molecules, χ the relative scattering angle and b the impact parameter. The scattering angle χ is a function of b and g, and its values are related to the form and parameters of the pair potential (see chapter 2 for further discussion). In the lowest order approximation, the coefficient of viscosity and the coefficient of thermal conductivity are directly related to $\Omega^{(2,2)}$, while the self diffusion coefficient is given in terms of $\Omega^{(1,1)}$.

The calculation of these collision integrals (in effect temperature dependent

cross-sections) involve extensive numerical integrations which the Oxford University K.D.F.9 computer can evaluate for a given potential in about 3 minutes, using the programme of Dr. M. Rigby based on the method of Barker, Fock and Smith (72). The transport properties can then be calculated assuming suitable parameters in the potential and compared with the experimental values (see chapter 2).

Thermal diffusion factors (73-77) have been suggested to be very sensitive to the form of the intermolecular potential function (78). However the data are rather sparse and have large experimental uncertainties (79), so as yet have not shed a clearer light onto the subject.

Molecular Beams (21, 80-85)

In principle one of the most direct ways of studying interactions experimentally is to investigate the scattering of a beam of particles by a collection of other particles.

A molecular beam is a directed ray of neutral atoms or molecules in a high vacuum, with a particle density such that collisions do not occur between atoms within the beam, and the vacuum high enough (10^{-6} torr) to make improbable collisions between beam particles and chamber particles. An elastic collision is one in which no internal energy state nor material composition change occurs; only this type of collision will be considered here. Information can be obtained from the scattering of the molecular beams hitting a surface or interacting with another beam of molecules.

Two regions of molecular beam energy have been used.

a) High Energy (5-5000 e.v.) beams which provide information about the repulsive potential (17, 80, 83, 86). These beams are often produced by accelerating the atoms as ions and then neutralising them by resonant-charge exchange with neutral atoms (83). The scattering intensity $I(\chi_o, E)$ beyond some angle χ_o, which

depends on the apparatus geometry is measured, and the so called total cross section $S(\chi_o, E)$ given by

$$S(\chi_o, E) = 2\pi \int_{\theta_o}^{\pi} I(\chi_o, E) \sin\chi \, d\chi$$

is determined as a function of beam energy E. At high energies, only the repulsive potential need be considered. For small ranges of r, $\phi(r) = a r^{-n}$ is often used, but the more correct exponential form $\phi(r) = A \exp(-Br)$ can represent the conditions over a wider range. A suitable plot of $I(\chi, E)$ against log E gives the value of the coefficients (86).

For helium, over the range 0.5 - 2.3 Å, the potential

$$\phi(r) = 196 \exp(-4.21\, r) \text{ ev. } (r \text{ in Å})$$

gives good agreement with high energy beam results and theoretical calculations (87, 88).

b) Low Energy (10^{-3} - 1 e.v. i.e. thermal energies) beams provide information about the attractive forces between molecules (21, 80, 81, 89). The beams are often produced by carefully designed thermal sources (21). The thermal energy of the beam is comparable to the depth of the potential well and because of this and the angle of deflection, χ, being controlled by both attractive and repulsive forces (page 23), interference phenomena are observed at various values of χ (89). With a suitable analysis of these phenomena much detail of the potential around the minimum may be elucidated.

By measuring the total cross-section, determined by passing the beam through a scattering chamber at known density and measuring the intensity of the transmitted beam, details concerning the attractive potential C_6 may be obtained. The values of C_6 agree with theoretically derived values (17). From differential cross section measurements, which are related to the intensity $I(\chi)$ scattered at the measuring

angle X , and using the functions developed through quantum mechanics with an assumed potential function, further detail about the interactions between molecules has been deduced (21).

Other Methods

Information concerning the intermolecular potential between molecules may be gained from a variety of other techniques. For example, pressure broadening of spectral lines, where the absorption of radiation by a molecule is affected by the presence of other molecules nearby (90-92), nuclear magnetic resonance (93), and sound dispersion in gases (94). Since these methods are concerned mainly with polyatomic molecules which have internal degrees of freedom, they will not be considered further here.

The Principle of Corresponding States (95-97)

The Principle of Corresponding States (P.C.S.) is of great value in studies of intermolecular energy functions. It was first proposed by van der Waals (98) and formalised by Pitzer (95).

Suppose a bulk property, A, of a number of molecules of similar type could be related to two experimental quantities, X and Y, then $A = f(X,Y)$. The P.C.S. says that if the quantities X and Y are reduced to dimensionless numbers by dividing by some characteristic parameters of the molecules (e.g. the critical properties), then the reduced property $A^* = A/z = f(X/\alpha),(Y/\beta) = f(X^*,Y^*)$, (where * denotes a reduced quantity: z, α and β are the characteristic parameters, in such a form as to have the same dimensions as A, X and Y)and is a function of the dimensionless variables X^* and Y^*. It is thus independent of the individuality of the molecules; for when two species have the same values of X^* and Y^*, they will have the same value of A^* and are said to be in corresponding states. Hence data from many sources and substances may be correlated on one graph. This has been carried out for many properties of a large number of gases (96, 97), confirming the

principle for many simple substances.

The value of the P.C.S. is due to it widening the range of a property under investigation. Every species has a different set of reducing parameters, thus results for a number of substances obtained under the same experimental conditions will give a range of reduced values. Another valuable feature is that data not available for some molecules can be estimated from a suitable corresponding states plot, provided the reducing parameters are known.

If the potential function is dependent on only two parameters i.e. $\phi(r) = Ef(r)$ - for example the Lennard-Jones potential, (E is an energy term and f(r) some function of the potential with intermolecular distance) then taking the reducing parameters to be ϵ, an energy, and σ a length (e.g. see figure 1) then

$$\phi^* = \phi/\epsilon = kf(r/\sigma) = kf(r^*) .$$

ϕ^* is dependent only in the reduced distance r^*; it is independent of the particular species. The effectiveness of a potential can be seen by comparing the reduced property calculated by the reduced potential with the suitably reduced experimental data. Thus in a single operation data from many molecules can be compared with the values predicted by the potential.

If however the potential is dependent on more than two parameters e.g. polar or non-spherical molecules, then more than two reduction parameters are required.

The value of the viscosity coefficients reported in this thesis in helping to elucidate the potential function for the inert gases will be appraised in Chapter 5.

CHAPTER 2

VISCOSITY

Definitions (2, 16)

Viscosity is concerned with the transport of momentum through a fluid due to a gradient in velocity. Consider a fluid flowing past a plane surface such that the velocity of flow increases uniformly from it, and imagine the fluid subdivided into many thin layers. Each layer of fluid parallel to the direction of flow exerts a tangential force on the adjacent layers, tending to decrease the velocity of the faster moving and to increase that of the slower moving layer. A result of this internal friction is that force must be applied in order to maintain the velocity gradient. The retarding influence due to this exchange of momentum is called viscosity.

For a Newtonian fluid (e.g. water; non-Newtonian e.g. tar) this retarding force, F, (really a shearing stress) in the moving fluid is proportional to the area of interface, A, and its velocity gradient (dv/dz),

$$\text{i.e.} \quad F = \eta \; A \; (dv/dz) \tag{2.1}$$

where the proportionality constant η is termed the coefficient of viscosity. η is formally defined as the tangential force per unit area needed to maintain a unit velocity gradient. Its dimensions are $ML^{-1}T^{-1}$, so in the c.g.s. system the unit is g cm^{-1} sec^{-1} called the poise (in s.i. units, 10^{-1} kg m^{-1} s^{-1}). At 20°C, η for water is 10.1×10^{-3} poise and for argon 222.8×10^{-6} poise. Often in fluid mechanics, the kinematic viscosity, ν, is used. This is defined by $\nu = \eta/\rho$, where ρ is the fluid density. ν is dimensionally L^2T^{-1}, which in the c.g.s. system is cm^2 sec^{-1}, called the stoke (in s.i. units 10^{-4} m^2 s^{-1}).

The type of flow governed by viscous forces is called laminar or streamline flow. It is quite different from turbulent or diffusive flow discussed later.

Viscous effects occur in both liquids and gases, although the mechanism of internal friction is different (19). In liquids, the molecules are close together, their movement restricted and permanently subjected to the intermolecular forces of their neighbours. These forces govern the transport of momentum by collision, and, since their effects decrease with temperature rise, the viscosity would be expected to decrease. In gases, molecules can travel long distances without coming near a neighbour, and since the intermolecular forces only have an effect at close distances, it is the transport of momentum by positional change of molecules which causes the viscous stresses. Since the molecular velocity increases as the temperature rises, the viscosity would be expected to rise. Both these predictions of temperature effects are experimentally observed.

Only gases will be considered further here.

The Gaseous Viscosity Coefficient

Elementary Kinetic Theory (2,16,99-102)

By imagining the molecules to be rigid non-attracting spheres with diameter σ and all travelling with the same speed $\bar{c}$, a simple derivation of momentum transfer may be made. Consider again a gas, subdivided into thin layers, flowing past a plane surface with a velocity gradient uniformly increasing from it, then owing to this gradient momentum is transfered from the faster moving to the slower moving layers, so giving the viscous drag. The momentum transfered to a layer by a molecule is the momentum it received at its last collision: this is on average a mean free path (λ) away. By equating the net momentum transfered by the molecules to a layer with the frictional resistance of that layer, it can be shown that,

$$\eta = \frac{1}{3} \rho \bar{c} \lambda \quad . \ (\rho \text{ is the density}) \tag{2.2}$$

From the Maxwell distribution of velocities,

the mean speed $$\bar{c} = \left(\frac{8RT}{\pi M}\right)^{\frac{1}{2}} = \left(\frac{8kT}{\pi m}\right)^{\frac{1}{2}} \tag{2.3}$$

where $R = Nk$ is the gas constant, and $M = Nm$ is the molecular weight. λ, the mean free path, is the average distance a molecule travels between collisions, and is given by (2).

$$\lambda = \frac{1}{\sqrt{2}\ \pi\ \sigma^2 n} \qquad \text{n is the number density of molecules} \qquad (2.4)$$

Hence $$= \frac{2}{3\ \pi} \sqrt{\frac{mkT}{\pi}}\ \frac{1}{\pi\sigma^2} \qquad (2.5)$$

Thus the coefficient of viscosity should be independent of pressure, depend inversely on the square of the molecular size and have a temperature coefficient of $T^{\frac{1}{2}}$.

At pressures of about an atmosphere, the viscosity coefficient is experimentally found to be independent of pressure (16,102). At low pressures, when the molecules collide more frequently with the walls of the containing vessel rather than with each other, and at high pressures where $\lambda \approx \sigma$, deviations occur. The temperature dependence of η is found to be nearer $T^{0.7}$ than $T^{0.5}$. This is due to the attractions and repulsions of real molecules which the hard sphere model do not consider.

For equation (2.2) it was assumed that all the molecules possess the same velocity and that on collision the 'past history' of the molecules was 'forgotten'. The treatment may be modified to take into account the distribution of velocities and the influence of prior collisions. Jeans (103) has shown that the persistance of velocities, where the molecules show a tendency to continue to move in their original direction after a collision, result in modifications to λ. However these amendments are not very satisfactory and the most rigorous results are obtained by other treatments due to Chapman and Enskog (3) where their conclusion for hard sphere molecules is

$$\eta = 0.499\ \rho\ \bar{c}\ \lambda \qquad (\lambda \text{ as in 2.4}) \qquad (2.6)$$

Similar considerations may be made for other transport properties including the coefficient of thermal conductivity, κ , and isotopic and thermal diffusion factors. These are related respectively to the transport of energy and mass within the gas arising from gradients of temperature and concentration.

Rigorous Kinetic Theory (1,2,3)

A gas is considered as an aggregation of unconnected molecules in rapid thermal motion, where the mean thermal energy is sufficiently great to prevent condensation. The fluid properties of a gas result from the propagation of disturbances by the mechanism of intermolecular and molecule-surface collision. Although the molecular nature of a gas ultimately determines its macroscopic properties, a consideration of the time variation of the molecular density in an element of phase space enables the Boltzmann transport equation to be established and the general fluid mechanical equations derived. Thus the coefficient of viscosity of a gas could be calculated if the distribution of velocities in the shearing gas were known. The distribution function $f_i(r, v_i, t)$ which describes the number of molecules of the species which at time t lie in a unit volume element about the point r and which have velocities within the unit range about v_i., would reduce to the Maxwellian distribution if there were no gradients

$$\text{i.e.} \quad f_i^o = n_i \left(\frac{m_i}{2 \pi kT} \right)^{3/2} \exp(-m_i v_i^2 / 2kT) .$$

When the system is only slightly perturbed from this equilibrium position,

$$f_i = f_i^o (1 + \Delta)$$

which satisfies the Boltzmann integro differential equation and may be solved under a number of limiting conditions. Namely (1) the density of the gas must be low enough to ensure that only binary collisions need be considered; (2) the

dimensions of the container must be very much larger than the mean free path so that collisions with the walls are unimportant; (3) elastic collisions must occur; this will only be true for monatomic gases, since inelastic collisions can occur between molecules with internal degrees of freedom and although mass and momentum will still be conserved, kinetic energy will not. This means that the viscosity and diffusion coefficients should not be appreciably affected but the thermal conductivity coefficient will, hence more complex treatments (104) have been proposed for polyatomic molecules; (4) the intermolecular force between the molecules must be spherically symmetrical and vanish at large separations;(5) the de Broglie wavelength (h/mv) must be small compared with the molecular dimensions, otherwise quantum effects will be observed and the use of classical mechanisms become invalid. This will occur at low temperatures when the molecular velocity becomes small. At 200°K however the effects are less than 1% even for helium;(6) the temperature must not be so high that excited energy states become important; (7) the gradients of the physical quantities (e.g. for viscosity - the velocity gradient) must be small; the extreme gradients set up in shock waves would be expected to give large deviations.

The equations were first solved by Chapman (105) and Enskog (106), where the transport coefficients were expressed in terms of a set of integrals, $\Omega^{(l,s)*}(T^*)$ which involve explicitly the dynamics of molecular encounter and hence the intermolecular force law. The collisions change the directions and velocities of the colliding particles and when there is a gradient of temperature velocity or mass will effect the distribution of velocities.

Although the final expressions must relate to collisions between two particles in three dimensions with respect to the laboratory frame of reference, it is more convenient initially to consider the motion of a single particle under a central force field. This treatment can be related to the centre of mass frame with two colliding molecules which can in turn be transformed to relate it to the

rest frame (1).

Accordingly a collision may be characterised in terms of a particle of reduced mass μ $(m_1 m_2/(m_1 + m_2))$ moving with an initial relative velocity of approach g . If $\phi(r)$ is a symmetric potential energy function, and b the impact parameter defined as the distance of closest approach in the absence of the potential, then a typical trajectory and characteristic parameters appear as in figure 2.1. As a particle approaches, the centre of force, it will either be attracted or repelled so that its orbit will deviate from the incident straight line trajectory. After passing the centre of force, the forces acting on the particle diminish and the path again approaches a straight line. In general, the final motion is not the same as the incident direction and the particle is said to be scattered.

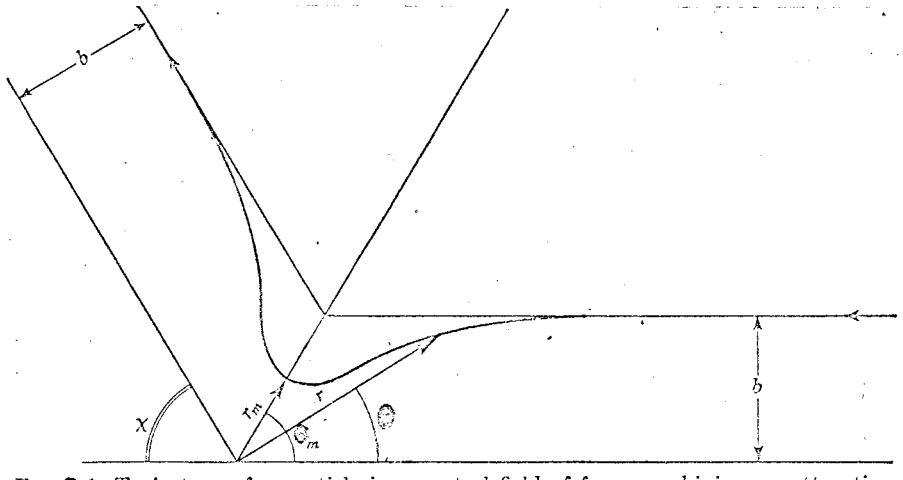


FIG. 2-1. Trajectory of a particle in a central field of force combining an attraction with a shorter-range repulsion: b is the impact parameter, χ is the angle of deflection, and (r_m, θ_m) are the polar coordinates of the point of closest approach.

θ and r are the plane polar co-ordinates specifying the position of the particle with the centre of force as the origin. r_m is the distance of closest approach and θ_c the value of θ at this distance. The trajectory is symmetrical about r_m, so the angle of deflection χ, (the angle between the

asymptotes measured from the initial to the final direction of motion) is

$$\chi = \pi - 2\theta_c .$$

From the conservation of energy and angular momentum (1,2)

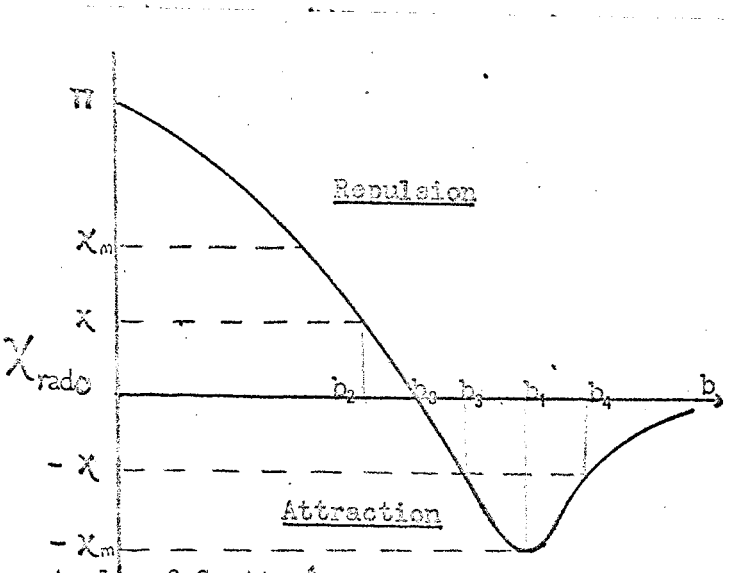
$$\theta_c = \int_{r_m}^{\infty} d\theta = \int_{r_m}^{\infty} (1 - \phi(r)/\tfrac{1}{2}\mu g^2 - b^2/r^2)^{-\frac{1}{2}} r^{-2} dr \qquad (2.7)$$

hence $$\chi = \pi - 2b\int_{r_m}^{\infty} (1 - b^2/r^2 - \phi(r)/\tfrac{1}{2}\mu g^2)^{-\frac{1}{2}} r^{-2} dr \qquad (2.8)$$

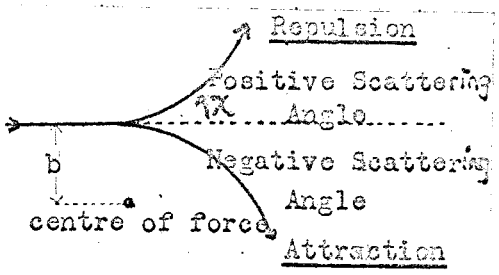
and r_m may be obtained from

$$b^2/r_m^2 = 1 - \phi(r)/\tfrac{1}{2}\mu g^2 \qquad (2.9)$$

If ϕ (r) is known, then for a given initial relative velocity, χ may be calculated. Each value of the impact parameter b results in a definite value of χ . For a realistic potential with an attractive and repulsive part (e.g. the Lennard Jones potential) figure 2.2 shows the typical behaviour of the deflection function.



Angle of Scattering as a function of b at constant energy.



Path of Scattered Molecule.

Figure (2.2) Scattering for a Realistic Potential.

Collisions with a large positive scattering angle can be attributed to the repulsive portion of the potential at small impact parameters. The scattering angle decreases with increasing impact parameter until no deflection is observed when the impact parameter is b_o; this is where the average repulsive and attractive forces just cancel. For larger impact parameters the long range attractive forces lead to a change in the direction of deflection to negative angles. After going to a maximum at b_1 the deflection function converges to zero as b tends to infinity. For small values of g (the exact value depending on the potential) the maximum negative angle χ_m corresponding to the inpact parameter b_1 goes to infinity (the so called orbiting value). As g increases the value of χ_m tends to zero when there is no longer any contribution to scattering due to attractive forces.

For angles $\chi < \chi_m$, there are three different impact parameters b_2, b_3, b_4 for the same value of χ and g, whereas for $\chi > \chi_m$ there is only one. If the potential assumed has only a repulsive term, as when the relative velocity g is very large, there will be no negative (attractive) scattering, and so for each value of at each value of g there will be only one value of b.

The angle of deflection of a molecule is related to the intermolecular potential, the initial velocity and the impact parameter by equation (2.8). There can be several impact parameters leading to the same angle of deflection for the same initial relative velocity, so it is necessary to sum the contributions from all impact parameters leading to the same scattering angle. The measure of the distribution in angle of the scattered molecules is given in terms of the differential scattering cross-section $d\sigma$, when for scattering into an element of solid angle $d\omega$, $d\sigma$ is defined by

$$d\sigma \; d\omega = \frac{\text{Number of molecules scattered per sec. into } d\omega}{\text{Intensity of incident molecules}} \qquad (2.10)$$

For molecules interacting with centrosymmetric forces there is complete symmetry about the incident direction, so

$$d\omega = 2\pi \sin\chi \, .d\chi \quad . \text{ and } \quad d\sigma = I(\chi)\, d\omega = 2\pi I(\chi) \sin\chi \, .d\chi$$

where $I(\chi)$ is the angular distribution function. For a given initial velocity, the number of molecules deflected into the solid angle $d\omega$ lying between χ and $(\chi + d\chi)$ per unit time is equal to the number of incident molecules with an impact parameter lying between the corresponding b and b + db (see diagram of (109)). Since there can be a number of b's giving the same value of χ (i.e. when $\chi < \chi_m$) it follows that the total number of particles scattered into $d\omega$ is $\sum_{i=1}^{N} 2\pi n\, b.db$, where N is the number of b's contributing to the scattering at the angle χ, and n is the intensity of incident particles: hence from the definition of $d\sigma$ (equation 2.10)

$$d\sigma = \sum_{i=1}^{N} 2\pi \, b db$$

and so

$$I(\chi, g) = \sum_{i=1}^{N} \frac{b}{\sin\chi} \left| \frac{db}{d\chi} \right| \qquad (2.11)$$

$db/d\chi$ can be positive or negative for realistic potentials.

The total cross section S is obtained by integrating the differential cross section over all angles of deflection i.e. over the complete solid angle of 4π

$$S = 2\pi \int_0^{\pi} I(\chi, g) \sin\chi \, d\chi \qquad (2.12)$$

S is the effective area which a target molecule presents to the incident beam. For a force field which extends to infinity, as for example the intermolecular potential, there is no upper limit to the impact parameter because deflections occur, although very small, no matter how large the value of b. The value of S is then infinite. This difficulty is overcome when the scattering processes are considered by a quantum mechanical treatment (21, 22,81,82,108,109) and the quantum mechanically derived

value of $I(\chi, g)$ of equation (2.11) is substituted for the classical value when the integral in (2.12) becomes convergent. In the treatment of transport phenomena, the cross section as defined above is replaced by Q, defined by

$$Q(g) = 2\pi \int_0^{\pi} (1-\cos^l \chi)\, I(\chi, g) \sin\chi \, d\chi \qquad (2.13)$$

where l is a positive integer, its value depending on the property under investigation and the degree of approximation to which the calculations are carried. In the first approximation (22), most of the contribution to $Q(g)$ comes from angles near some most effective angle ($\chi = \pi$ for $l = 1$ (diffusion) and $\chi = \pi/2$ for $l = 2$ (thermal conductivity and viscosity)). The angular weighting function $(1 - \cos^l \chi)$ suppresses the small angle contributions to $I(\chi, g)$, which in any case have negligible effects on transport phenomena, and since it rapidly tends to zero for small values of χ, the integral in (2.13) converges. From (2.11), (2.13) becomes

$$Q(g) = 2\pi \int_0^{\infty} (1 - \cos^l \chi)\, b\, db \qquad (2.14)$$

The transport properties are finally expressed in terms of temperature dependent collision integrals, $\Omega^{(l,s)}(T)$, which are obtained by integration over the whole range of relative velocities with a probability density defined in terms of the Maxwell-Boltzmann velocity distribution. The complete expressions for the transport properties consist of an infinite series, whose terms are functions of these collision integrals defined by

$$\Omega^{(l,s)}(T) = \sqrt{\frac{2\pi kT}{\mu}} \int_0^{\infty}\int_0^{\infty} e^{-\gamma^2} \gamma^{(2s+3)} (1-\cos^l \chi)\, b\, db\, d\chi \qquad (2.15)$$

$$\text{or } \Omega^{(l,s)}(T) = \sqrt{\frac{kT}{2\pi\mu}} \int_0^{\infty} e^{-\gamma^2} \gamma^{(2s+3)}\, Q^{l}(g)\, d\gamma \qquad (2.16)$$

where $\gamma^2 = \mu g^2/2kT$ and $\mu = m_1 m_2/m_1 + m_2$

and $s = 1,2,3,4$ and $l = s, s+1, s+2,$

For rigid spheres where $\phi(r) = \infty$, $r < \sigma$, $\phi(r) = 0$, $r > \sigma$, equations (2,14) and (2.16) simplify to

$$Q_{r.s.} = \left[1 - \tfrac{1}{2}\left(\frac{1+(-1)^l}{1+l}\right)\right] \pi \sigma^2 \qquad (2.17)$$

and

$$\Omega^{(l,s)}{}_{r.s.} = \sqrt{\frac{kT}{2\pi\mu}} \; \frac{(s+1)!}{2} \; Q'_{r.s.} \qquad (2.18)$$

For real molecules, the various kinetic variables may be reduced to dimensionless quantities by a suitable combination of parameters appearing in the potential function $\phi(r) = \varepsilon f(r)$ (page 16)

$r^* = r/\sigma$, reduced intermolecular distance,

$T^* = kT/\varepsilon$, reduced temperature,

$b^* = b/\sigma$, reduced impact parameter,

$\phi^* = \phi/\varepsilon$, reduced intermolecular potential energy

$g^{*2} = \mu g^2/2$, reduced relative kinetic energy.

$Q^{(l)}(g)$ and $\Omega^{(l,s)}(T)$ may be reduced by division by their corresponding rigid sphere values thus:-

$$Q^{l*}(g^*) = \frac{Q^{(l)}(g)}{Q^{l}{}_{r.s}} = Q^{(l)}(g) \Big/ \left[1 - \tfrac{1}{2}\left(\frac{1-(-1)^l}{1+l}\right)\right] \pi \sigma^2 \qquad (2.19)$$

$$\Omega^{(l,s)*}(T^*) = \frac{\Omega^{(l,s)}(T)}{\Omega^{(l,s)}{}_{r.s.}} = \Omega^{(l,s)}(T) \Big/ \sqrt{kT/2\pi\mu} \; \frac{(s+1)!}{2} \left[1 - \tfrac{1}{2}\left(\frac{1-(-1)^l}{1+l}\right)\right] \pi \sigma^2 \qquad (2.20)$$

$Q^{l*}(g^*)$ and $\Omega^{(l,s)*}(T^*)$ have the physical significance that they indicate the deviation of any particular model from the idealised rigid sphere model.

(2.8), (2.14), (2.16) may now be rewritten in terms of reduced units

$$\chi(g^*, b^*) = \pi - 2b^* \int_{r_m^*}^{\infty} \left(1 - \frac{b^{*2}}{r^{*2}} - \frac{\phi(r^*)}{g^{*2}}\right)^{-1/2} r^{*-2} \, dr^* \qquad (2.21)$$

$$Q^{1^*}(g^*) = 2\left[1 - \frac{1}{2}\left(\frac{1+(-1)^1}{1+1}\right)\right]\int_0^\infty (1-\cos^1\chi)\, b^*\, db^* \qquad (2.22)$$

$$\Omega^{(1,s)^*}(T^*) = \frac{2}{(s+1)!\ T^{*s+2}}\int_0^\infty e^{-g^{*2}/T^*} \cdot g^{*(2s+3)} \cdot Q^{1^*}(g^*)\, dg^* \qquad (2.23)$$

The first approximation to the coefficients of viscosity, thermal conductivity and diffusion are (1)

$$\eta = \frac{5}{16\pi\sigma^2}\frac{\sqrt{\pi\, mkT}}{\Omega^{(2,2)^*}(T^*)} = \frac{2.6693\sqrt{MT}}{\sigma^2\,\Omega^{(2,2)^*}(T^*)} \times 10^{-5}\ \text{g cm}^{-1}\text{sec}^{-1} \qquad (2.24)$$

$$\kappa = \frac{25}{32\pi\sigma^2}\frac{\sqrt{\pi\, mkT}}{\Omega^{(2,2)^*}(T^*)} \quad \frac{C_v}{M} = \frac{1.9891\sqrt{T/M}}{\sigma^2\,\Omega^{(2,2)^*}(T^*)} \times 10^{-4}\ \text{cal cm}^{-1}\text{sec}^{-1}\,{}^{o}\text{K}^{-1}$$

$$C_v = \frac{3R}{2}\ \text{cal/mole} \qquad (2.25)$$

$$D = \frac{3}{16\pi}\frac{\sqrt{2\pi\, k^3T^3/M}}{P\,\sigma_{12}^2\,\Omega^{(1,1)^*}T^*} = \frac{2.628\sqrt{T^3(M_1+M_2)/2M_1M_2}}{P\,\sigma_{12}^2\,\Omega^{(1,1)^*}(T_{12}^*)} \times 10^{-3}\ \text{cm}^2\ \text{sec}^{-1}$$

P = pressure in atms. (2.26)

C_v is the molar specific heat at constant volume. η and κ depend on

$\Omega^{(2,2)*}$ whereas D depends on $\Omega^{(1,1)*}$.

The errors involved in the first approximation increase with temperature, but even at very high temperatures are less than 1%. More accurate expressions may be obtained by considering further terms in the series. Correction factors have been developed, and the simplest are due to Kihara (110) where the factors to multiply the first approximation are given by,

$$f_\eta = 1 + \frac{3}{49}\left(\frac{4\Omega^{(2,2)*}}{\Omega^{(2,3)*}} - \frac{7}{2}\right)^2 \qquad (2.27)$$

$$f_\kappa = 1 + \frac{2}{21}\left(\frac{4\Omega^{(2,2)*}}{\Omega^{(2,3)*}} - \frac{7}{2}\right)^2 \qquad (2.28)$$

$$f_D = 1 + \left(\frac{6\Omega^{(1,2)*}}{\Omega^{(1,1)*}} - 5\right)\left(\frac{16\Omega^{(2,2)*}}{\Omega^{(1,1)*}} + 40\right)^2 \qquad (2.29)$$

For the rigid sphere model, $\Omega^{(2,2)*}(T^*) = 1$, so from (2.24)

$$\eta = \frac{0.5}{16\pi\sigma^2}\sqrt{\frac{mkT}{\pi}} = 2.6693 \times 10^{-5}\frac{\sqrt{MT}}{\sigma^2}\ g.cm^{-1}sec^{-1} \qquad (2.30)$$

which using $\lambda = (2\pi n\sigma^2)^{-1}$ and $\bar{c} = (8RT/\pi M)^{\frac{1}{2}}$ from (2.5) and (2.3) give

$$\eta = \frac{5}{32}\pi\rho\bar{c}\lambda = 0.490\,\rho\bar{c}\lambda \qquad (2.31)$$

If the higher approximations are taken into account (3), $\eta = 0.499\,\rho\bar{c}\lambda$ (2.6), Comparing (2.24) with (2.25),

$$\kappa = \frac{5}{2}\frac{C_v}{M}\eta = \frac{15}{4}\frac{R}{M}\eta \qquad (2.32)$$

Thus the thermal conductivity may be calculated from viscosity measurements. For monatomic gases (2.32) is true, but for other molecules it becomes inaccurate because inelastic collisions occur when the internal modes take up some of the

translational energy. A correction can be made where the internal energy is also considered (1) and (2.32) becomes

$$K = \frac{15}{4}\frac{R}{M}\eta\left(\frac{4}{15}\frac{C_v}{R} + \frac{3}{5}\right) \qquad (2.33)$$

For some polyatomics this is not exact and more complex corrections have been devised (111-113).

The Measurement of Viscosity

The coefficient of viscosity may be determined by observing the effects of the frictional forces caused by viscosity. There are four basic techniques, each having many variations:-

1. To observe the damping of a body oscillating in a fluid.
2. To use the viscous drag to transmit a force to a measuring device.
3. To observe the retardation from free fall of a body in a fluid.
4. To displace a fluid through a tube, series of tubes or pores.

Examples of method one are the oscillating disc (114-117) and oscillating cylinder (118). The oscillating disc is essentially a thin circular plate suspended from a torsional fibre between two stationary plates and set into oscillatory motion. When the space between the plates is filled with a gas, the oscillations are damped and the decrement of the motion can be related to the viscosity. This method has been used for low temperature work (114,115) and for high pressure studies (119). Kestin has developed the method to a high precision for the absolute determination of the viscosity coefficient at room temperature (117). Recently he has described an instrument which will cover the temperature range 300-750°K (120), but the difficulties of the torsion fibre have not yet been fully overcome.

The rotating cylinder typifies method two. The gas is situated between two concentric cylinders. One cylinder is rotated with a constant angular velocity and the torque transmitted to the other by the gas is balanced by a torsion wire suspension. For laminar flow conditions, this torque is proportional to the viscosity. Bearden (121) using this method has obtained very accurate results for air at room temperature.

Millikan's oil drop experiment exemplifies technique three (122, 123). In the determination of the electronic charge e by this method, the value for the viscosity of air needs to be very accurate. If however e is known from some other

method, such as X-ray studies, η may be determined. This method is of limited value though due to the complex hydrodynamic equations involved.

Capillary flow viscometry uses method four. The rate at which a gas flows through a capillary tube under a pressure difference between the ends is measured. The flow rate is dependent on the viscosity but also on the fourth power of the radius of the tube. This limits the accuracy of any absolute determination, but by comparing the flow rate with that of a standard gas, the ratio of viscosities may be easily found. There have been many apparatuses described e.g. (124-126). It is a valuable technique for high temperature determinations since only the capillary need be at the high temperature. For this reason the apparatus described here uses the capillary flow technique.

The Standard Value

Most workers have used a comparative method; taking a value for some gas as standard and comparing the viscous effect of the gas to be measured with that of the known gas. Until recently, air at 23°C was taken as the absolute standard. From a consideration of many results, Hopper and Laby (127) showed that if $e = 4.8044 \pm 0.0007 \times 10^{-10}$ e.s.u. as determined from X-ray results, η_{23} air needed to be $1830.9 \pm 0.5 \times 10^{-7}$ g cm^{-1}sec^{-1}. for agreement with their oil-drop results. Earlier workers e.g. Trautz (125), used Millikan's value of 1823×10^{-7} g cm^{-1}sec^{-1} (122), while Birge (128-130) after a critical examination of all data available states that the more recent determinations of η_{23} air indicate the value should be $1832.45 \pm 0.69 \times 10^{-7}$ g cm^{-1}sec^{-1}. He also says that the present best value of e is that of DuMond and Cohen (131) which is $4.80286 (\pm 0.00009) \times 10^{-10}$ e.s.u.

These differing values have caused much confusion in the literature. Birge explains (130) that some of this confusion has arisen because Millikan obtained his value of η from the rotating cylinder instrument of Harrington (132), who did not allow for the torsion constant for a quartz fibre depending on the weight

suspended by it (121). Harrington used a quartz fibre to provide the torque but probably included a systematic error as the suspended mass used in his experiment differed from that with which he determined the torsion constant. The results of earlier workers quoted in this thesis have been suitably corrected to η_{23} air $= 1833 \times 10^{-7}$ g cm^{-1} sec^{-1}.

Kestin (133) has suggested that nitrogen ought to be taken as the standard; since it can be obtained pure and has the advantage of not being a mixture. For these reasons nitrogen has been used as the standard in this work.

Agreement between various methods

After correcting the values to the same standard, the agreement between the various workers using different techniques at room temperature is good. Thus argon is given variously at 20°C.

Authors	Method	$\eta \times 10^6$ poise
Kestin and Leidenfrost, 1959	oscillating disc	222.8
Johnson and Grilly, 1942	oscillating disc	222.7
De Rocco and Halford, 1957	high pressure capillary	222.0
Trautz and Zink, 1930	low pressure capillary	222.3
Wobser and Müller, 1941	rolling ball	223.9
Clarke and Smith, 1968	low pressure capillary	223.0

At other temperatures, data are not numerous and the agreement between the various sets is often poor. A comparison with the results obtained in this work is given in Chapter 4.

The Theory of the Flow of Gases through Capillaries

The flow of a gas through a capillary may be divided into a number of regimes according to the molecular dynamics:- turbulent, viscous (or continuum, Poiseuillian), slip, transition and free molecule flow. The different cases will be considered briefly and then in subsequent sections in more detail. Finally equations of flow valid over all regions will be discussed and the relevance to this work assessed.

Turbulent Flow

As the fluid velocity in a tube increases the pressure drop across the tube changes from being proportional to the quantity of fluid flow to being proportional to the square of fluid flow. The flow, which was smooth for the first condition becomes full of irregular eddying motions. This is seen very clearly in the case of a liquid flowing through a glass tube when a little coloured liquid is added by means of a small dropping tube (134). It forms a straight clean cut filament at the low fluid velocities, but at the higher velocities this filament breaks up and the coloured liquid is distributed throughout the fluid. The former fluid flow is said to be streamline flow and the latter turbulent. Reynolds (173) predicted the onset of this turbulent flow by the dimensionless number R_e ($= \frac{2r\rho v}{\eta}$, v the fluid velocity, ρ the density). When a certain numerical value of the Reynolds number was reached, turbulent flow occured. The critical value depended on the surface conditions of the tube but usually lay between 2340–4000.

It is found that for fluid flow through a large diameter pipe viscous forces act to effect the flow only in a small region immediately about the surface. The flow outside this boundary layer is inviscid so the viscous flow equations become invalid, and instead the flow rate is calculated through semi-empirical turbulent flow equations (135). Within the layer, viscous stresses take over and the velocity must decrease uniformly from that of the inviscid flow at the outer edge to zero at the surface. For a capillary, under the normal experimental conditions used in

this work R_e never exceeds 1000 so the flow throughout the tube is viscous, except perhaps just at the entrance and exit where irregularities can cause eddying, but this is minimised by careful design and construction of the capillary ends.

Viscous and Free-molecule flow definitions

As the flow rate decreases to below turbulent flow conditions the viscous stresses are propagated throughout the capillary, but as the density of the gas within the capillary becomes lower molecule-wall collisions become predominant, and the flow rate changes to that of free-molecule flow.

Continuum, laminar or Poiseuillian flow region

The continuum region has a very small Knudsen number K(= λ /d, where d is the diameter of the pipe) of about 10^{-5}. If the flow is laminar (i.e. non turbulent), a straight circular pipe will have shear stresses and velocities symmetrically distributed about the centre line, and the velocity at the wall surface is or can be assumed to be zero. The flow rate is given by Poiseuille's formula (page 37).

Slip region

Slip flow effects are expected when λ is 1-10% the diameter of the tube i.e. $K \approx 10^{-2} - 10^{-1}$. Here the velocity at the wall surface cannot be ignored and has to be included when calculating the flow rate.

Transition region

Where the mean free path is of the order of the diameter of the tube i.e. $K \approx 1$, and molecule-wall collisions and molecule-molecule collisions are both of importance in determining the flow rate.

Free Molecule flow

Here the mean free path is substantially larger than the diameter of the

tube i.e. $K > 5$, and the molecule-wall collisions govern the flow rate.

Viscous Flow Derivation of Poiseuille's Formula

Consider the laminar flow of an incompressible fluid through a capillary tube of radius r and length l. The steady state motion of the fluid will be governed by the viscosity. The flow velocity v of the fluid will be a function of the radial distance a (measured from the axis of the tube-x axis), decreasing from a maximum on the axis. The velocity gradient will be dv/da.

For a short cylinder of fluid of radius a and length dx in the steady flow, the pressure between its ends produces a force $\pi a^2 dP$ in the direction of the pressure drop, and is equal and opposite to the viscous shearing stress generated over its curved surface i.e. $2\pi a \eta dx \frac{dv}{da}$ thus equating forces in the x direction

$$-2\pi a \eta dx \frac{dv}{da} + \pi a^2 dP = 0$$

$$dv = \frac{1}{2\eta} \frac{dP}{dx} a\, da \qquad (2.35)$$

Integrating

$$v = \frac{1}{4\eta} \frac{dP}{dx} a^2 + c \qquad (2.36)$$

Assuming that there is zero velocity at the wall, then $v = 0$ when $a = r$

$$v = -\frac{1}{4\eta} \frac{dP}{dx} (r^2 - a^2) \qquad (2.37)$$

which gives a parabolic velocity profile. (dP/dx is negative in the x direction)

The volume flow dV/dt, flowing through the cylinder in unit time is given by,

$$\frac{dV}{dt} = \int_0^r v\, 2\pi a\, da$$

whence

$$\frac{dV}{dt} = -\frac{\pi r^4}{8\eta} \frac{dP}{dx} \qquad (2.38)$$

Conservation of molecules makes dV/dt independent of the position along the tube for an incompressible fluid, thus integrating for the whole tube, with a pressure P_f at the beginning of the capillary ($l = 0$) and P_b at the end

$$\frac{dV}{dt} = \frac{\pi r^4}{8 \eta l} (P_f - P_b)$$

A gas, though, is a compressible fluid, and the volume flow varies along the tube. Assuming the gas to be ideal, $PV = nRT$.

For the small cylinder of length dl,

$$\frac{dV}{dt} = \frac{RT}{P} \frac{dn}{dt} \tag{2.39}$$

where P is the mean pressure of the small volume dV, and dn the number of moles of gas contained in it.
Using (2.39) and (2.38),

$$\frac{dn}{dt} = - \frac{\pi r^4}{8 \eta RT} P \frac{dP}{dx} \tag{2.40}$$

Although the volume flow varies along the tube, the mole flow rate is independent of the position; hence integrating over the length of the tube,

$$\frac{dn}{dt} = \frac{\pi r^4}{16 \eta RTl} (P_f^2 - P_b^2) = \frac{\pi r^4}{8 \eta RTl} \Delta P . P \tag{2.41}$$

where $P = (P_f + P_b)/2$ and $\Delta P = (P_f - P_b)$.

This equation was first proposed by Meyer (136).

Slip Flow

In the continuum region the gas is assumed to be at rest at the wall. However if it is at some velocity v_o, then equation (2.37) becomes

$$v = -\frac{1}{4\eta}\frac{dP}{dx}(r^2 - a^2) + v_o \qquad (2.42)$$

and equation (2.38)

$$\frac{dV}{dt} = -\pi\left(\frac{r^4}{8\eta}\frac{dP}{dx} - v_o r^2\right)$$

and equation (2.40)

$$\frac{dn}{dt} = -\frac{\pi r^4 P}{8\eta RT}\frac{dP}{dx} + \frac{\pi P v_o r^2}{RT} \qquad (2.43)$$

There will be a viscous drag of 2π r.l. $v_o \varepsilon$ along the tube, where ε is a constant, termed the coefficient of external friction and is the tangential momentum given to the surface divided by the surface velocity. This viscous drag is equal to the driving force

so $\quad 2\pi$ r.l. $\varepsilon\, v_o = \pi r^2 (P_f - P_b)$

$$v_o = \frac{r}{2l\varepsilon}(P_f - P_b) \qquad (2.44)$$

which for a short length dx of the tube with a pressure drop of -dp (in the x direction) becomes

$$v_o = \frac{-r}{2\varepsilon}\frac{dP}{dx} \qquad (2.45)$$

Substituting (2.45) in (2.43),

$$\frac{dn}{dt} = -\frac{\pi r^4}{8\,\eta\,RT}\,p\,\frac{dP}{dx}\left(1 + \frac{4\eta}{r\varepsilon}\right) \qquad (2.46)$$

Thus the flow is increased by the factor $(1 + 4\eta/r\varepsilon)$. The fraction η/ε is called the coefficient of slip and has the dimensions of length. Its effect is the same as if the wall was moved back a distance η/ε and the velocity gradient continued uniformly to zero at the wall. It is negligible when r is large compared with η/ε, but when r is small the flow is largely controlled by this term, being proportional to r^3 instead of r^4 as in continuum flow.

An estimate of this factor may be obtained from mean free path considerations. All molecules are assumed to have the mean speed $\bar{c}$, and are referred to a frame of reference moving at $\bar{c}$. The surface layer of the molecules of the gas is constituted half of the molecules carrying the momentum of the gas molecules at the wall, and half carrying the momentum from their last collision in the gas. A complication is added by not all the tangential momentum being necessarily given to the wall surface. A model due to Maxwell (137) assumes a fraction (1-f) of the molecules to be specularly reflected, thus retaining the incident tangential momentum, and a fraction f of the molecules leaving at random angles, independent of the previous motion and having zero momentum in the tangential direction. The fraction (1-f) implies that there is a certain preponderancy of the molecules to retain their tangential momentum after collision with the walls.

Let the average tangential velocity of the surface layer of molecules be v_o. Since the number of collisions with the wall per unit time is $\frac{1}{4} n \bar{c}$, the surface layer is made up of $\frac{1}{4} n \bar{c}$ impinging molecules with tangential velocity u, $\frac{1}{4} n \bar{c}$ (1-f) specularly reflected molecules with tangential velocity u and $\frac{1}{4} n \bar{c} f$ diffusely scattered molecules with zero tangential velocity. The total number of molecules in the layer is the sum of those entering and leaving. It is $\frac{1}{2} n \bar{c}$, so the average momentum in the surface layer is

$$\tfrac{1}{2}\, mn\bar{c}\, v_o = \tfrac{1}{4} mn\bar{c}\, u + \tfrac{1}{4} mn\bar{c}\,(1-f)\, u + \tfrac{1}{4} mn\bar{c}\, f\, 0$$

hence $$v_o = (2-f)\,u/2 \qquad (2.47)$$

The momentum a molecule carries to the wall is determined by the site of its last collision before reaching the surface layer. The average distance of this site from the layer is $2/3\,\lambda$ (138) but Fryer (139) considers the persistence of velocities of molecules on collision would lengthen this distance to λ . The tangential velocity of a molecule would thus be

$$u = v_o - \lambda \left(\frac{dv}{da}\right)_{a=o}$$

where $\left(\frac{dv}{da}\right)_{a=o}$ is the velocity gradient in the midst of the gas away from the wall and decreases as a increases.

Hence $$v_o = -\left(\frac{2-f}{f}\right)\lambda \left(\frac{dv}{da}\right)_{a=o}$$

and from (2.35)

$$v_o = -\left(\frac{2-f}{f}\right)\lambda \frac{r}{2\eta} \frac{dP}{dx} \qquad (2.48)$$

so (2.43) becomes

$$\frac{dn}{dt} = -\frac{\bar{\pi}\, r^4}{8\eta RT}\, P \frac{dP}{dx}\left(1 + \left(\frac{2-f}{f}\right)\frac{4\lambda}{r}\right) \qquad (2.49)$$

Alternatively, since the tangential momentum given up to the surface per second is $\tfrac{1}{4}\, nm\bar{c}.f.u$, then from the definition of ε (page 39) and (2.47)

$$\varepsilon = \frac{n}{4} m\bar{c}\, f \frac{u}{v_o} = \frac{n m \bar{c} f}{2(2-f)}$$

Then substituting $\eta = \frac{1}{2} n m \bar{c} \lambda$ (2.6), $\epsilon = \frac{\eta f}{\pi(2-f)}$ and (2.46) becomes (2.49). Should the value of $\frac{2}{3}\lambda$ be used for the average distance, then the slip factor becomes that given by Present (138) $\left(1 + \left(\frac{2-f}{f}\right) \frac{8\lambda}{3r}\right)$.

If $k\lambda$ is used then the factor becomes $\left(1 + \left(\frac{2-f}{f}\right) \frac{4k\lambda}{r}\right)$, and (2.46) becomes

$$\frac{dn}{dt} = -\frac{\bar{\pi} r^4}{8\eta RT} P \frac{dP}{dx} \left(1 + C \frac{\lambda}{r}\right) \text{ where } C = \left(\frac{2-f}{f}\right) 4k \qquad (2.50)$$

k is a constant which may vary with temperature and the molecular species. The value of k will be discussed in Chapter 5, but it cannot be rigorously established until the state of the gas next to the surface has been more accurately described.

Molecular Flow

If the mean free path of the gas is larger than the diameter of the tube i.e. $K > 5$, a molecule of gas will collide many times with the wall of the tube before encountering another molecule. The flow of the gas will be determined almost entirely by the collisions with the wall and is practically unaffected by intermolecular collisions. The collision process is assumed to be diffusive i.e. to effect an erasure of the molecular history. The molecules are then re-emitted from the surface with a random (cosine) distribution in direction and a Maxwellian distribution in velocity. This assumption has been questioned (140, 174) on account of direct studies of molecular scattering from surfaces, although Knudsen (16, 141) found there was little specular reflection.

A specular reflection would require a surface that is smooth on the submicroscopic scale of molecular dimensions e.g. a cleavage plane of a perfect

single crystal. In practice, the wall surfaces are highly irregular on the submicroscopic level, so for free molecular flow the molecules are assumed to be diffusely scattered. If the impinging molecules adhere to the surface for an appreciable length of time, the reflections will not be specular even if the reflecting conditions were satisfied.

The steady flow rate is found to be (2,16,100)

$$\frac{dn}{dt} = -\frac{2\pi a^3}{3RT}\left(\frac{8RT}{\pi M}\right)^{\frac{1}{2}}\frac{dP}{dx} \qquad (2.51)$$

The transport is proportional to the density gradient, from the more to the less concentrated end, and the flow is of the nature of diffusion. Many workers (141-133) have confirmed (2.51) within an experimental error of about 1%. This verifies the assumption of diffuse reflection for molecular flow.

Free molecular flow differs from laminar flow in several respects. The former varies as the cube of the radius whereas the latter varies as the fourth power. Viscous flow depends on the average pressure and the pressure difference, whereas free molecular flow is proportional to the pressure difference.

Experiments have shown that the ratio of flow rate/pressure difference plotted against average pressure goes through a minimum at $r/\lambda \approx 0.3$. Equation (2.50) cannot be valid for the transition region ($\lambda \approx r$) since it does not predict this minimum, so cannot be further extended into the low pressure region. Also at these pressures (2.50) does not reduce to (2.51). A variable factor $16f/3\pi(2-f)k$ multiplying the slip term of (2.50) has been suggested (145), but it is not very satisfactory since to follow the minimum it would have to vary non-uniformly. A number of better formulations have been suggested to explain this minimum (139, 146,148).

Corrections to (2.50) to enable it to follow the experimental findings are discussed in the next section. Other methods for deriving the flow equations are then briefly considered.

Formulation of the flow of gases through capillary tubes (139,147-151)

A single equation describing the rate of flow of a gas through a capillary with a pressure difference of $(P_f - P_b)$ for the range viscous to free molecule flow would have to reduce to equation (2.50) when $K \sim 10^{-3}$, to equation (2.51) when $K > 5$ and predict the minimum found at $r/\lambda \approx 0.3$ i.e. $K \approx 1.3$, when the ratio of flow rate/$(P_f - P_b)$ is plotted against the average pressure $(P_f + P_b)/2$.

Weber (148) considered the total flow to be the sum of three components (a) a viscous component which increases more or less linearly with r/λ (b) a slip component which rises to a constant value at $r/\lambda \approx 2.0$ and (c) a diffusive component which decreases asymptotically to zero as r/λ increases.

Fryer (139) in a detailed discussion considers the relative importance of these components in order to make the momentum generated by the pressure gradient be completely transmitted to the wall of the tube. He modifies equation (2.50) using $k = 4/3$ and $f = 1$, to conform to this condition.

Equation (2.50) implies that as $P \rightarrow 0$, the slip and viscous flow terms must vanish, but Weber showed that slip flow exists at very low pressures when only isolated inter-molecular collisions occur. This is because a molecule striking another molecule is more likely to have come from upstream so giving the stricken molecule an additional flow momentum. By making allowances for the molecules at the wall having no slip velocity (as diffuse reflection is assumed, the molecules whose last collision was at the wall have no slip velocity), and for the diffusion of the molecules at the walls moving along the surface from the higher to the lower pressure end (pressure diffusion) and which add to the flow rate, Fryer amends (2.50) to

$$Q = -r^3 \left(\frac{2\pi RT}{M}\right)^{\frac{1}{2}} \left(\frac{\pi}{32} \frac{P}{P_1} + \frac{\pi}{3} \frac{P}{(P + P_1)} + \frac{4}{3} \frac{P_1}{(P + P_1)} \right) \frac{dP}{dx} \qquad (2.52)$$

where $P_1 = \lambda P/r$ and $G = \frac{dn}{dt} RT$. (2.53)

Barrer and Nicholson (152) quote the formula in another equivalent form

$$G = - r^2 \left(\frac{\pi r \bar{c}}{32}\right) \frac{dP}{dx} \left(\frac{r}{\lambda} + C \frac{2r/\lambda}{1 + 2r/\lambda} + \frac{64}{3} \left(\frac{1}{1 + 2r/\lambda} \right) \right) \quad (2.54)$$

The three terms in these equations represent Poiseuille flow, slip flow and molecular flow respectively. Thus at high pressures ($P \gg P_1$, $K \approx 10^{-5}$) the equation reduces to (2.50) and at low pressures ($P \ll P_1$) it becomes (251). The minimum value of the ratio G/dP against average pressure is however too high when compared with the experimental value.

At low pressures Fryer regards the Poiseuille term as being proportional to the probability of a molecule coming from an intermolecular collision suffering its next collision with another molecule rather than the wall. At low pressures some molecules are engaged on wall to wall paths and not available for molecular collision so cannot contribute to viscous flow. This fraction $f(p)$ of the molecules engaged on wall to wall paths must be subtracted from the flow rate. Scott and Dullien (147) suggest that $f(p) = \exp\left(-\sinh^{-1}(P/P_1)\right)$ and so Fryer's final equation for the flow rate is

$$G = -r^3 \left(\frac{2\pi RT}{M} \right)^{\frac{1}{2}} \left(\frac{\pi P}{32 P_1} \left[1 - \exp\left(-\sinh^{-1} \frac{P}{P_1} \right) \right] + \frac{\pi}{3} \frac{P}{P + P_1} + \frac{4}{3} \frac{P_1}{P + P_1} \right) \frac{dP}{dx} \quad (2.55)$$

which when dP/dx can be replaced by $\Delta P/l$, and P by $\bar{P}$, the average pressure, can be compared with Knudsen's experimental results (141) with excellent agreement.

For geometries other than long single cylinders, such as short capillaries, rectalinear cylinders, bundles of capillaries or porous membranes the above equations have to be modified (152).

Equations and derivations other than (2.55) describing the flow of gases have been described (149). Knudsen (141, 153) proposed a semi-empirical equation which describes his experimental results successfully.

$$C = -\left(a\bar{P} + \frac{b}{1 + c_2\bar{P}} + \frac{b\,c_1\bar{P}}{1 + c_2\bar{P}} \right) \Delta P \qquad (2.56)$$

where $\bar{P}$ is the mean gas pressure, a, b, c_1 and c_2 are constants and $\Delta P \ll \bar{P}$. The form of the constants can be obtained by comparing (2.56) with the limiting conditions of viscous and free molecule flow (100, 101).

Mason et al (150, 154, 155) have described a novel derivation where they consider the porous medium to be an array of dust particles held stationary in space. The dust particles are treated as giant molecules in terms of the classical kinetic theory of gases. Their solution (150) for a long single capillary for a pressure gradient at uniform temperature reduces to Knudsen's equation. If elastic gas-wall collisions (not necessarily specular collisions) are assumed, they find that k (250) is about 1.5.

Simons (156) amongst others (157, 158, 172) gives a theoretical treatment by solving the Boltzmann equation using some model and employing suitable boundary conditions for the gas flow. When integrated and compared with the experimental results, his model gives fair agreement.

Corrections to Poiseuille Flow

In the work described here, $K \approx 10^{-4} - 10^{-2}$ and the flow is effectively described by equation (2.50). The constant C in the slip term will be examined in Chapter 5.

The flow rate has to be further corrected for the kinetic energy of the moving fluid, imperfect streaming at the entrance of the tube, gaseous imperfection and curved pipe flow. These will now be considered in more detail.

Kinetic Energy

The gas molecules leave the capillary with a finite velocity, but the energy so carried away by the emergent jet has been assumed to have been used up in overcoming the viscous forces in the capillary. The viscous forces are thus smaller than Poiseuille's equation assumes, and the resulting viscosity calculated from equation (2.50) has to be corrected. This correction is commonly known as the Hagenbach correction (159,160).

Unlike an incompressible fluid, a gas accelerates down the capillary due to the pressure drop.* The kinetic energy imparted to an elemental anulus of radius a per second at $l = 0$, is $\frac{1}{2}\rho\,(v\,2\pi\,a\,da)v^2$, where ρ is the density and v the fluid velocity at $l=0$.

The total kinetic energy imparted per second at the entrance to the capillary is,

$$\int_0^r \tfrac{1}{2}\,\rho\,(v.\,2\pi\,a\,da)\,v^2$$

from (2.37), becomes $$-\pi\rho\frac{r^8}{8}\left(\frac{1}{4\eta}\frac{dP'}{dx}\right)^3 \qquad (2.56)$$

where dP' is the effective pressure difference which overcomes only the viscous resistance.

From (2.38), (2.56) becomes $$\frac{\rho}{\pi^2 r^4}\left(\frac{dV}{dt}\right)^3 \qquad (2.57)$$

* Only the initial kinetic energy need be considered, since the extra energy needed to accelerate the gas molecules down the tube is supplied by conduction through the walls of the capillary (p156 ref 160). Thus the flow may be considered as for an incompressible fluid.

See also M Brillouin - Book 2 - 3rd Lecon §=

The Viscosity of Gases and Liquids, 1907, for the original derivation for gases.

The total work in moving a volume of fluid dV against a pressure difference dP is $dP\,\frac{dV}{dt}$ per sec., and so the work done against the viscous forces is $dP'\,\frac{dV}{dt}$,

$$\text{thus } -dP'\frac{dV}{dt} = -dP\frac{dV}{dt} - \frac{\rho}{\pi^2 r^4}\left(\frac{dV}{dt}\right)^3 = \frac{dV}{dt}\left(-dP - \frac{\rho}{\pi^2 r^4}\left(\frac{dV}{dt}\right)^2\right) \qquad (2.58)$$

since dP is negative in the direction of flow,

rewriting (2.38) as

$$\eta' = -\frac{\pi r^4}{8(dV/dt)}\frac{dP'}{dx}$$, η' is the viscosity due to viscous forces.

Hence on rearranging (2.58)

$$-dP' = \frac{8\eta'}{\pi r^4}\frac{dV}{dt}dx = -dP - \frac{\rho}{\pi^2 r^4}\left(\frac{dV}{dt}\right)^2 \qquad (2.59)$$

$$\text{or} \quad \eta' dx = -\frac{\pi r^4}{8(dV/dt)}dP - \frac{\rho}{8\pi}\frac{dV}{dt} \qquad (2.60)$$

Since the fluid may be regarded as an incompressible fluid, $-dP = \Delta P = (P_f - P_0)$ and $dx = l$, thus

$$\eta' = \eta - \frac{\rho}{8\pi l}\frac{dV}{dt} = \eta\left(1 - \frac{\rho}{8\pi\eta l}\frac{dV}{dt}\right) = \eta\left(1 - \frac{M}{8\pi\eta l}\frac{dn}{dt}\right) \qquad (2.61)$$

where η' is the true viscosity, and η the apparent viscosity.

At the entrance of the capillary, there is a finite distance before the parabolic distribution of velocities across the tube (2.57) is set up and the flow streamlines parallel to the walls. This gives rise to a slight correction to the

NB 1. $\rho\left(\frac{dV}{dt}\right) = M\left(\frac{dn}{dt}\right)$ is a constant down the capillary for a compressible fluid.

2. If the integrated equations for an incompressible fluid are used (justification see note on p 47) $-dP/dx = \Delta P/l$, and the above derivation may be clearer (ref 160).

above factor, giving in the ideal case (160-163)

$$\eta' = \eta\left(1 - \frac{1.12\ M}{8\pi\eta l}\ \frac{dn}{dt}\right) \tag{2.62}$$

The actual value of the constant depends on the shape of the entrance (164). By careful design of the ends of the capillary, this non-viscous region can be minimised. In the case of all the capillaries used here, the length of the capillary is such that the kinetic energy corrections are so small that they can usually be ignored.

Gas Imperfection

In deriving the flow equations ideal gas conditions have been assumed. If the second virial coefficient is included in the derivation, thus

$$PV = n\ RT(1 + BP/RT) \tag{2.63}$$

on differentiating w.r.t. time

$$\frac{dV}{dt} = \frac{RT}{P}\left(1 + \frac{BP}{RT}\right)\frac{dn}{dt} \tag{2.64}$$

(2.40) becomes

$$\frac{dn}{dt} = -\frac{\pi r^4}{8\eta RT}\ \frac{P}{(1+BP/RT)}\ \frac{dP}{dx} \tag{2.65}$$

$$\simeq -\frac{\pi r^4}{8\eta RT}\ P(1 - BP/RT)\ \frac{dP}{dx} \tag{2.66}$$

Rewriting

$$\frac{dn}{dt} = -\frac{\pi r^4}{8\eta RT}\ P\ \frac{dP}{dx} + \frac{\pi r^4}{8\eta RT}\ \frac{BP^2}{RT}\ \frac{dP}{dx} \tag{2.67}$$

which on integrating and comparing with (2.40)

$$\eta' = \eta - \frac{2B}{3RT}\eta\left[\frac{(P_f^3 - P_b^3)}{(P_f^2 - P_b^2)}\right] \tag{2.68}$$

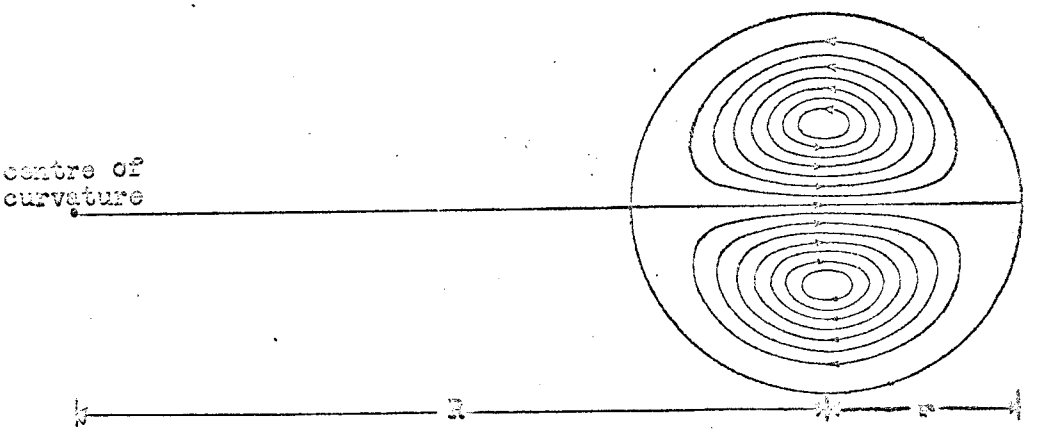
$$\eta' = \eta\left(1 - \frac{2B}{3RT}\left[\frac{(P_f^2 + P_fP_b + P_b^2)}{(P_f + P_b)}\right]\right) \tag{2.69}$$

where η' is the true viscosity and η the apparent viscosity when imperfection terms are not considered.

This correction is always less than 0.2% except for xenon. Further imperfection terms occur when the experimentally determined value of (dn/dt) is considered (see Chapter 4).

Curved Pipe Flow (165-168)

If the capillary is in the form of a helix, the curvature of the tube may cause an increased resistance to flow. When the fluid is moving along a curved pipe, there is a pressure gradient across the pipe to balance the centrifugal force. The pressure will be greatest at the outer part of the wall and least at the point nearest the centre of curvature. The fluid velocity near the centre of the tube is faster than that near the wall due to the viscous forces, so in consequence, a secondary flow is set up. The more rapidly flowing central parts are forced outwards and the slower parts along the walls are driven inwards towards the axis of the helix as shown in figure 2.3.



Figure(2.3) - showing the secondary flow due to curved-pipe flow.

The secondary flow is superposed on the main stream so that the resultant flow is helical in the top and bottom sections of the tube. This was experimentally shown by Taylor (169) in the case of a fluid, when he introduced into the running fluid a coloured thread through a small hole in the side of the helix. This type of secondary flow is set up whatever the section of channel; thus for a river at a bend, the region of maximum velocity is not as for a straight channel, at the centre of the stream, but is displaced toward the outer wall.

The derivation of the increased resistance to flow is complex, but has been achieved by Dean in the case when the flow velocity is small (164, 165). He showed that the correction term required for curved pipe flow compared with flow in a straight pipe, depends on a quantity D, the Dean Number. It is defined as $D = \frac{2r\rho v}{\eta}\sqrt{\frac{r}{R'}} = Re\sqrt{\frac{r}{R'}}$ where v is the fluid velocity, r the

radius of the capillary, R' the radius of the helix and Re the Reynolds number.

He obtained an expression for the ratio of flow of fluid in a coiled capillary to that in a straight capillary, Fc/Fs,

$$Fc/Fs = 1 - (J/576)^2\ 0.03058 + (J/576)^4\ 0.01195$$

where $J = 2D^2 = 2Re^2 (r/R)$.

Fc/Fs is less than 0.1% below D = 8. It is valid up to J = 576 (D = 17) i.e. about 2% curved pipe flow. For liquids, White (167) found that curved pipe flow was negligible below D = 11.6 and the expression

$$Fc/Fs = (1 - [1 - (11.6/D)^{0.45}]^{2.2})^{-1},\ D > 11.6;\ Fc/Fs = 1,\ D < 11.6.$$

fitted his results. Vasilesco (170) confirmed this figure with his experiments on gases, while Anfilogoff (102, 171) suggested a value of 9 for the critical value of D.

Dean's analysis was for very slow flow rates and incompressible fluids. The variation of the density of a gas from the inside to the outside of the tube makes the problem of the compressible fluid flowing in a coiled pipe formidable. The usual method of correction is a graphical method; assuming the increased resistance to be some universal function of D. This will be described in detail in Chapter 5.

CHAPTER 3

EXPERIMENTAL

The capillary viscometer is the best choice at the present time for the measurement of viscosity at high temperatures, although some work has been carried out at intermediate temperatures with other types of viscometers. It is relatively easy to operate since only the capillary need be at the high temperature, and the elementary theory of the instrument has been well tested. The main problem is a good evaluation of the necessary corrections. These corrections may be reduced by using a long straight capillary, but it is difficult to maintain a uniform temperature over the entire length of such capillaries. Coiling the capillary makes it easier to maintain a uniform temperature, while the additional corrections of curved pipe flow can be minimised by using slow flow rates and a large ratio of spiral-radius to channel-radius.

The instrument used in this work is a coiled capillary viscometer. It will be described in detail in this chapter, and the various corrections will be evaluated in Chapter 4.

The Apparatus

Experimental insight was obtained by using the apparatus built by Dr. M. Rigby (175,176). The slip correction for helium in the worst case amounted to over 20%, but this effect can be reduced by using higher pressures, and a new apparatus was built with this in mind. The range of temperature was widened to 1700°K by using a platinum-rhodium capillary and a furnace with platinum-rhodium windings.

With the new instrument the viscosity of a gas could be stated relative to its viscosity at another temperature or relative to another gas at the same temperature. Only the latter method was possible in the earlier viscometer. The apparatus was designed so that the numerical value and temperature variation of the slip coefficient and the effects of curved pipe flow could also be examined.

The second apparatus is shown in plate 1 and in diagramatic form in figures 3.1 and 3.2. The viscometer section (figure 3.2) consists essentially of two thermostatted vessels, V_f and V_b, connected by a coiled capillary, which itself is enclosed in a furnace. A gas train and vacuum line complete the apparatus.

The time taken for a gas to pass from V_f to V_b for a set of measured pressure differences is recorded for a series of gases. From these times the relative viscosities may be calculated. By repeating the runs over a range of temperatures, the ratio of the viscosities relative to that at some reference temperature may be determined.

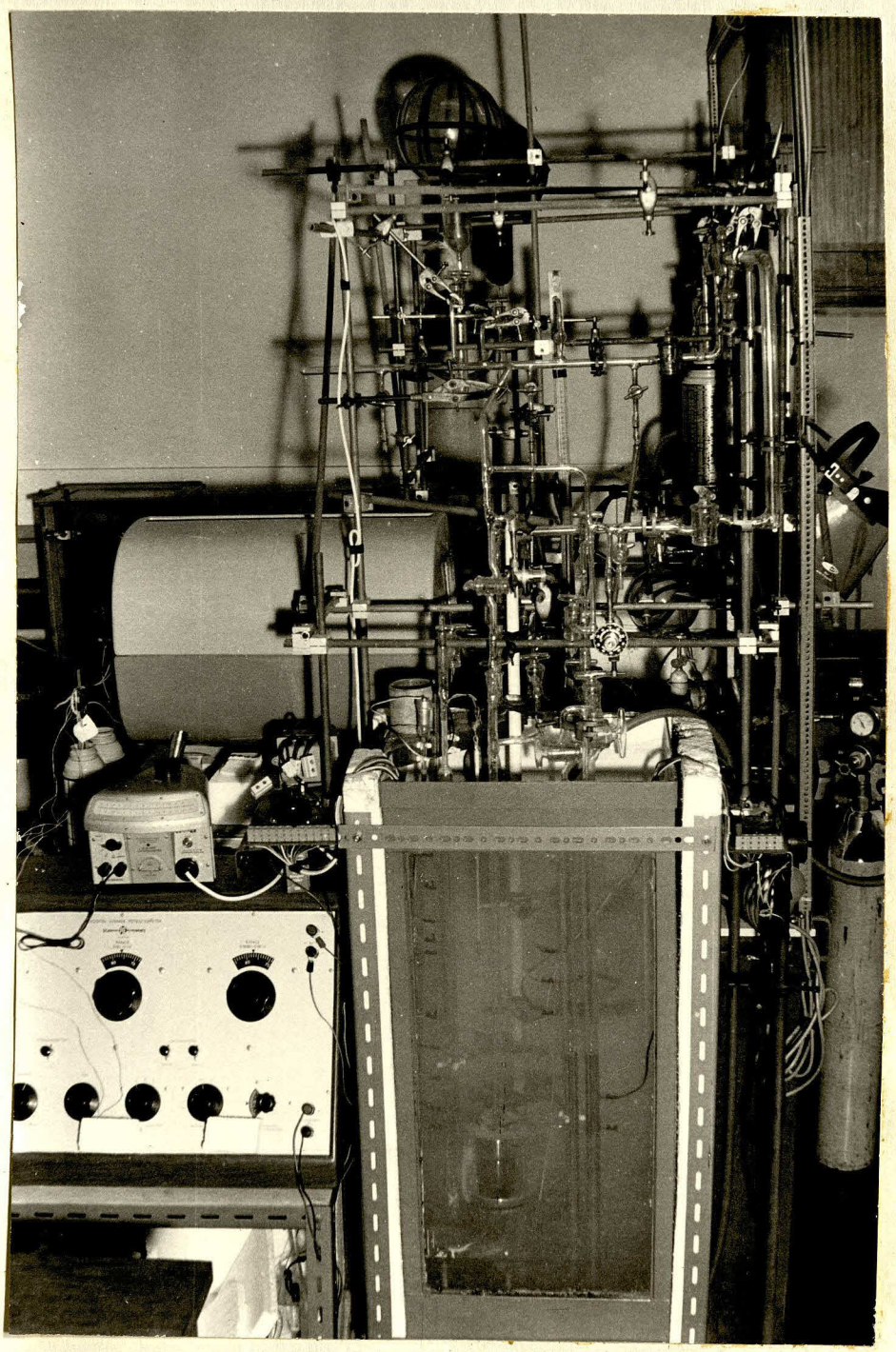
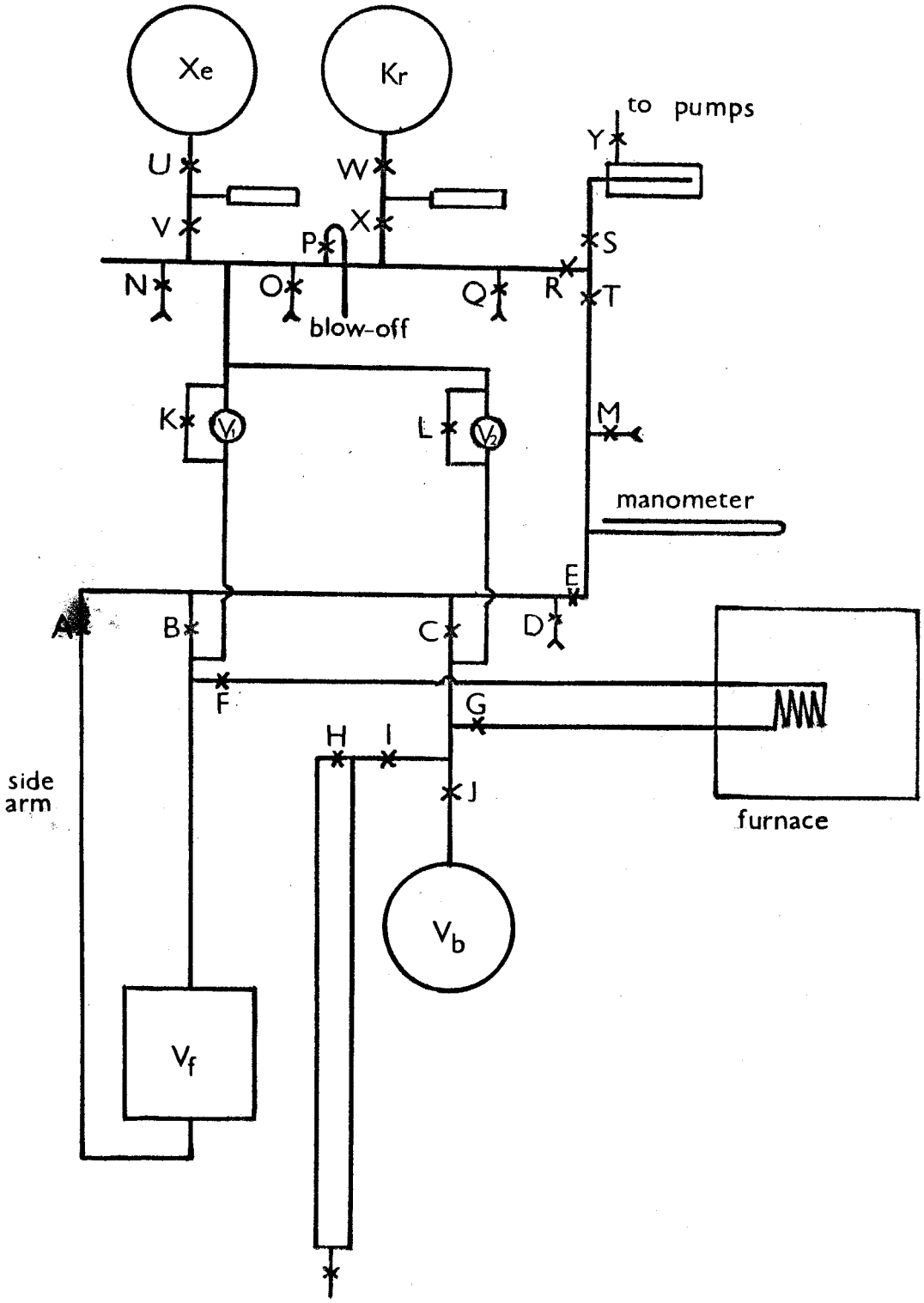
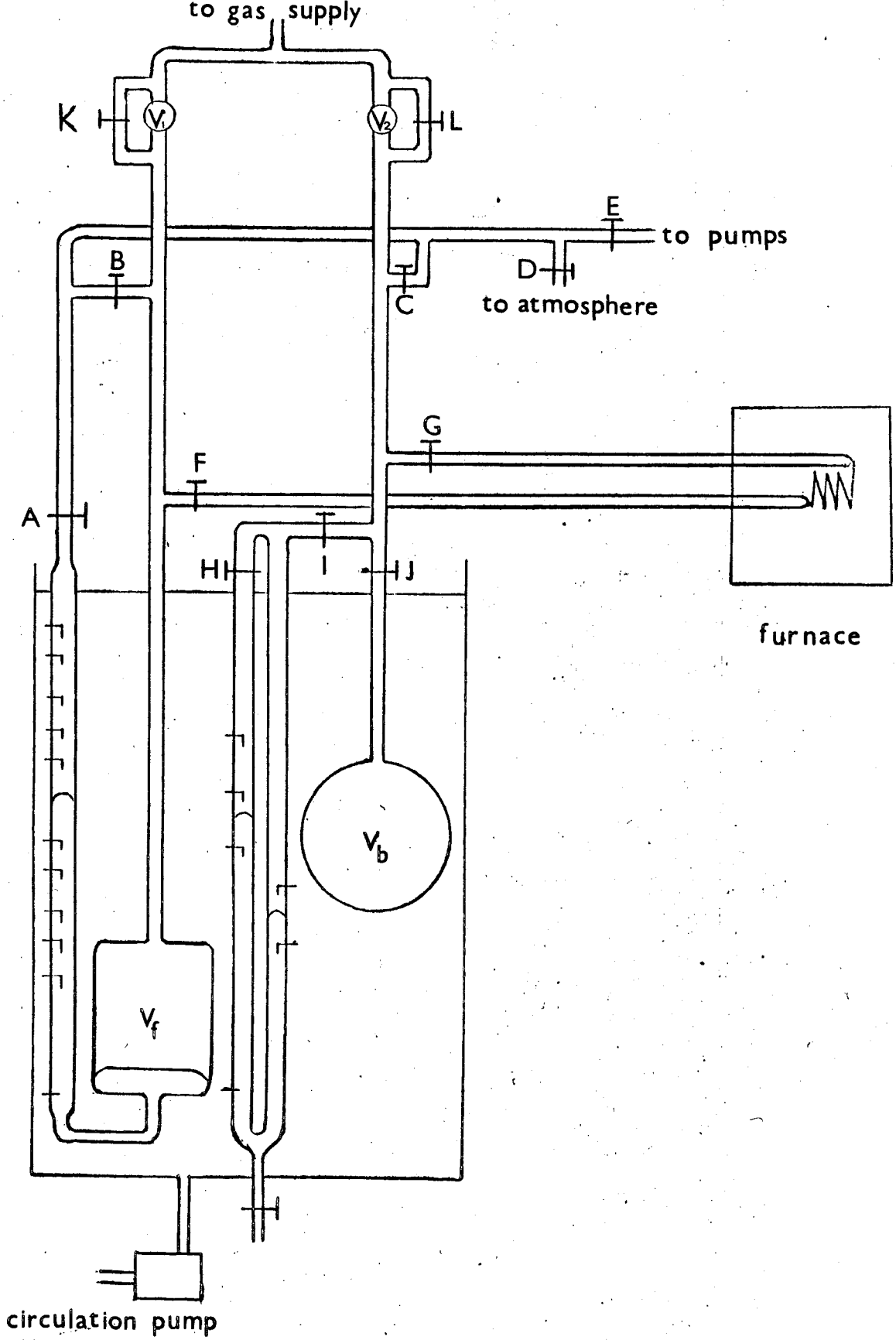


PLATE 1 : THE VISCOMETER.



SCHEMATIC DIAGRAM OF APPARATUS

(FIGURE 3.1)



SCHEMATIC DIAGRAM OF APPARATUS. (FIGURE 3.2)

Apparatus Description

The Thermostat Tank

The glass fronted thermostat tank housed both the front vessel V_f with its side-arm and the backing vessel V_b with its manometer. It was a large copper tank of approximately 90 litres in volume with dimensions 80 x 30 x 40 cms and was painted white to aid illumination of mercury menisci. It was lagged with polystyrene foam and filled with distilled water. There were two holes in the bottom; these were screwcapped so that an o-ring seal could give a water-tight connection with the tube which passed through it. The base of the manometer for V_b passed through one hole, so that the manometer could be drained of its mercury, and the other was connected to a circulation pump. Water could be pumped from the (colder) bottom of the tank to the (warmer) top at the rate of about 3 litres/minute. A 250 watt carbon filament bulb heated the water, and the temperature was regulated to better than 25.00 $\pm$0.02°C by a toluene regulator with a long regulating bulb made from a tube, 60 x 1.2 cms. No detectable variation of a 0.01°C thermometer was observed over a period of weeks for a thermometer kept at one spot in the bath, although small gradients close to the edges of up to 0.08° were found.

The Front Vessel V_f

The pyrex cylindrical vessel V_f of approximately 1 litre in volume (radius 5 cm, height 16 cms) was sited in the thermostat tank. It was linked from its base to a side-arm by 1.0 cm.i.d. tubing and from its top by 55 x 1.2 cm.i.d. tubing to the capillary lead via tap F, to the gas train by taps V_1 and K and to the vacuum line by tap B. Some 200 ccs of doubly distilled mercury were poured down the side tube into the vessel through a special inlet, closed by a B.10 stopper. The accurate volume of the vessel was determined by a series of pressure

measurements on a given mass of gas (appendix 4).

The side arm was a 70 cm length of 2 cm.i.d. tubing and was connected at its top end to the vacuum line through tap A. It acted as a manometer for the front vessel. Inserted into this tube were 11 pointers (tungsten rod sealed into the glass and platinum wire filed to a point welded on to the rod). These were positioned so that the tips corresponded to pressures of approximately 55, 52, 47, 42, 38, 36, 26, 21,16 , 11 and 8 cms of mercury. These pressures were measured accurately using a cathetometer telescope (appendix 3). Near the bottom another tungsten rod was sealed into the glass so that a small electric current could be passed through the mercury whilst there was still contact with a given pointer tip. Each pointer was connected by a brass terminal connector and plastic coated wire (a different colour for each) to a selection switch. A 2 volt A.C. supply and 3 volt torch bulb completed the circuit. The moment the mercury left a tip was clearly defined by the bulb going out. Using A.C. prevented corrosion of the connectors, and with only 2 volts there was a minimum of arcing between the mercury surface and pointers.

The Backing Vessel V_b

The backing vessel V_b was a 2l globe also sited in the thermostat tank. Its volume was deduced from pressure measurements (appendix 4). V_b was connected to stopcock J and from there through tap G to the capillary, by taps V_2 and L to the gas train, by tap C to the vacuum line and by tap I to a wide bore manometer, sited near the front of the thermostat tank. Pointers, similar to the front vessel, were inserted into the manometer walls so that pressures of approximately 10, 15, 20, 25 and 30 cms of mercury could be accurately set. These pressures were accurately measured using a cathetometer telescope (appendix 3). Another rod was sealed near the bottom of one of the tubes so that an electrical circuit, similar to the front vessel, could be made. The pressure in V_b could be

set easily, since when the mercury meniscus was just on a pointer tip the light flickered when the manometer was tapped. The pressure could be set more accurately (better than ±0.1 mm) using a telescope, with graticule eyepiece, accurately fixed at 45°. At this angle the image of the tip and the tip appear in a straight line. The pointer could be set to n ± 1 divisions of the graticule (1 graticule division ≡ 0.03 mm).

The Capillary

Three capillaries were used. These were made of:-

(a) Platinum industrial grade - 99.9% platinum.

(b) Platinum - 20% Rhodium.

(The straight tubes were bought from Johnson Matthey Metals Limited and the helices wound in the Physical Chemistry workshops.)

(c) Silica.

All three capillaries were of the same design. The capillary tube was joined smoothly to the wider bore tubing while still in the plane of the helix. The wider tubes were then bent to give the shape as shown in Plates 2, 3 and 4. The inlet tube was the tube which led through the helix, the length of the hot zone of the inlet tube being at least 10 cms. This length was calculated as being ample for the gas to reach the temperature of the capillary. The calculations were based on an analysis by Goldstein (177), where a characteristic length L for heat transfer is determined for a heater tube through his expression θ .

θ expresses the mean temperature of the gas along the tube, weighted with respect to the fluid velocity for the case of Poiseuillian flow through a pipe with constant wall temperature, as

$$\theta = 0.819 \exp(-x/L) + 0.0976 \exp(-6.1\, x/L)$$

with

$$\theta = (T-Tw)/(To-Tw)$$

where T is the mean temperature at distance x from the entrance of the hot zone, Tw the temperature of the walls and To the inlet temperature of the gas.

Thus $T = Tw + (To-Tw)\theta \approx Tw + (To - Tw)\, 0.819 \exp(-x/L)$

L is given by

$$L = \frac{4u_m r^2}{14.6\, k}$$

where u_m is the mean fluid velocity and k the thermal diffusivity defined by $\frac{\kappa}{c_p \rho}$, with κ being the thermal conductivity, c_p the specific heat at constant pressure per gram of the fluid and ρ the fluid density.

Even for the worst possible conditions in this experiment L was less than 0.3 cm; with the capillary at 1500°K, then, at only 1/4 of the distance along the heat exchanger, $x \approx 7L$ and the mean temperature of the gas calculated from the above equation would be within 1° of the wall temperature. Thus when the gas ultimately enters the capillary it would be essentially in complete thermal equilibrium with the walls.

(a) Platinum capillary (Plate 2)

Length 100 cms; Diameter 0.42 mm.i.d., 1.5 mm.o.d.; Helix diameter 44 mm. The leads were approximately 26 cm x 2.0 mm.i.d., 3.0 mm.o.d. tubing. The diameter of capillary tubes was measured by three methods; direct observation through a microscope, by weighing an accurately measured length of the tube and by inserting drills of known diameter into the capillary. All methods gave the same value. The capillary ends were widened so that the lead tubes could be smoothly welded on to them (Plate 5). The other ends of the lead tubes were silver soldered to 10 cm lengths of Kovar tube which were connected to pyrex tubing through a suitable graded seal. A water cooling jacket was fixed over the Kovar-platinum join. The cooling water was kept at 30°C to prevent mercury vapour from entering the capillary when the capillary was at room temperature. The whole capillary appeared as in Plate 4.

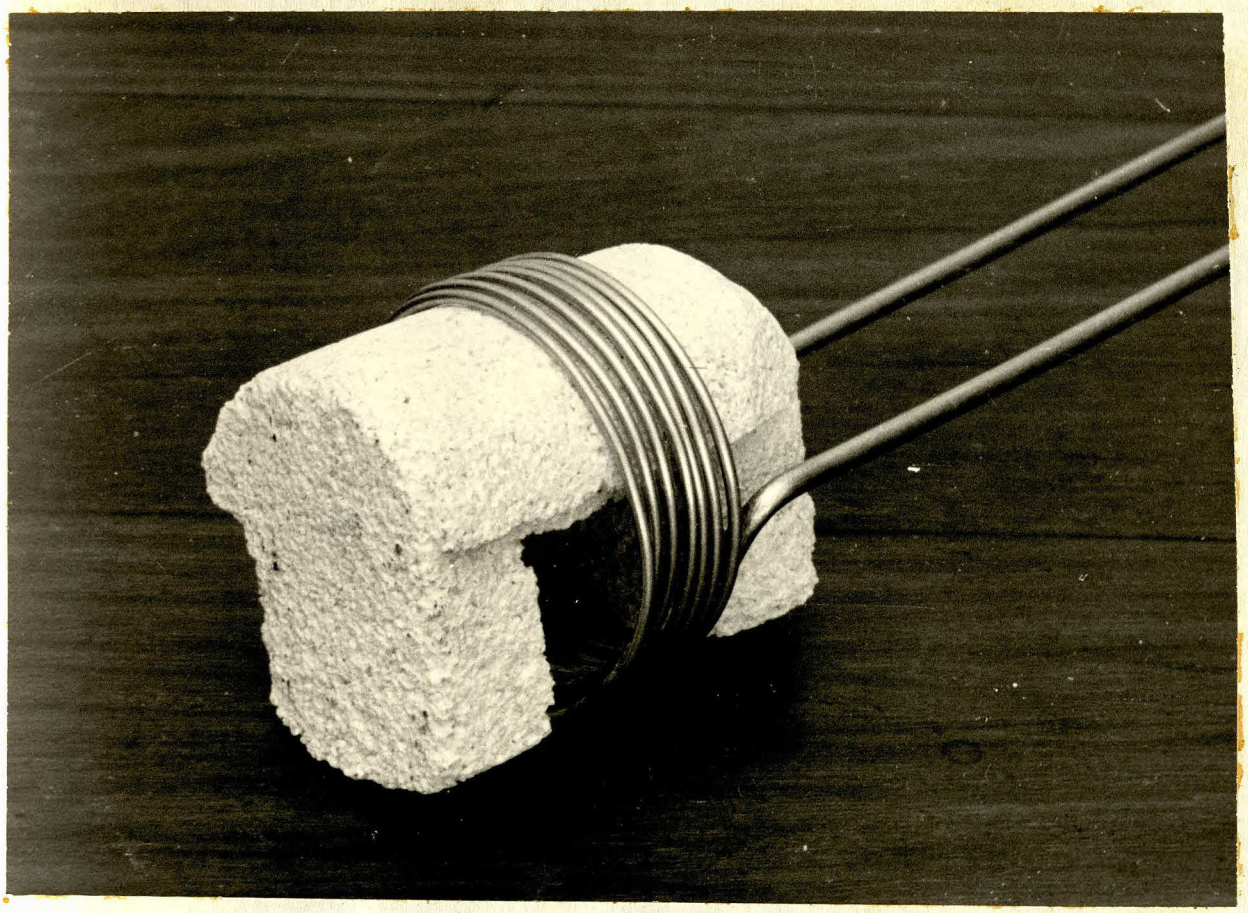


PLATE 2 THE PLATINUM CAPILLARY.

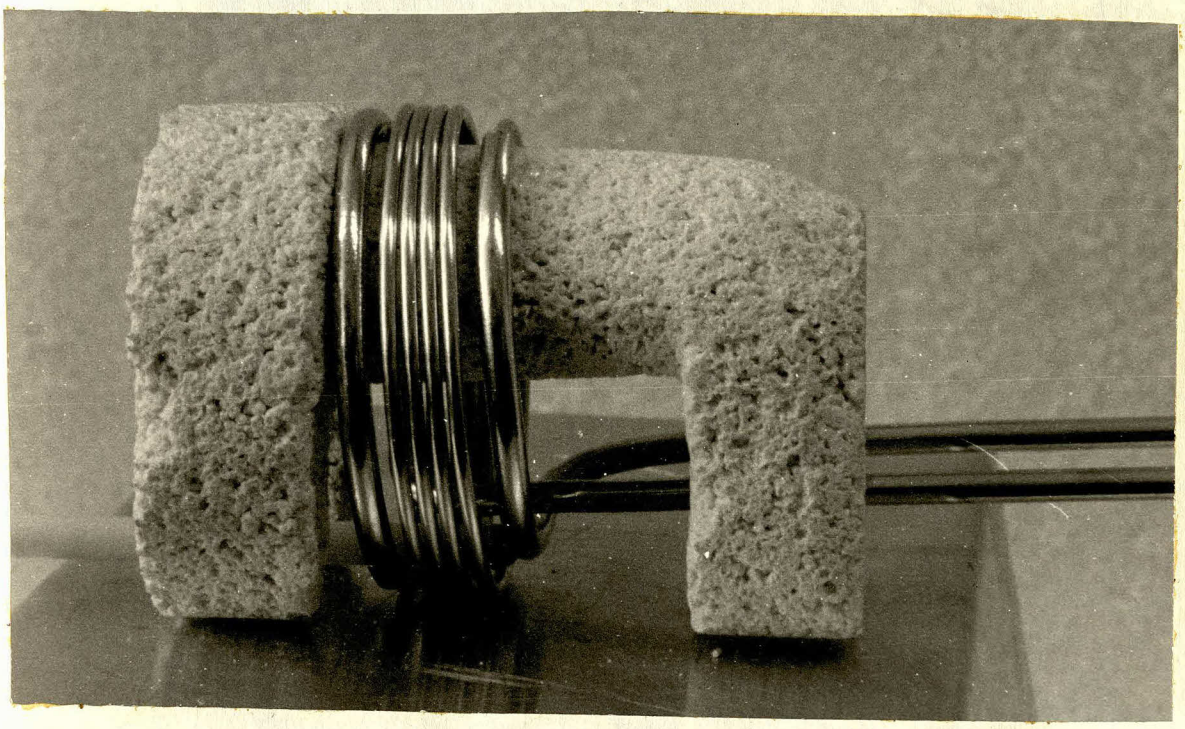


PLATE 3 THE PLATINUM -RHODIUM CAPILLARY.

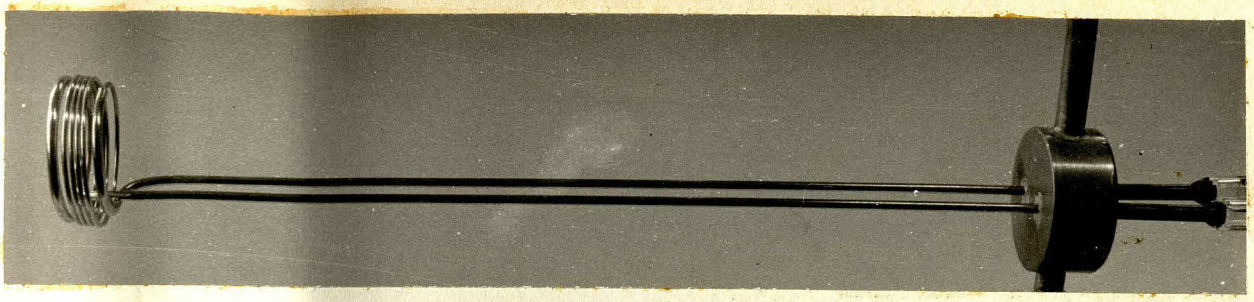


PLATE 4 THE COMPLETE CAPILLARY.

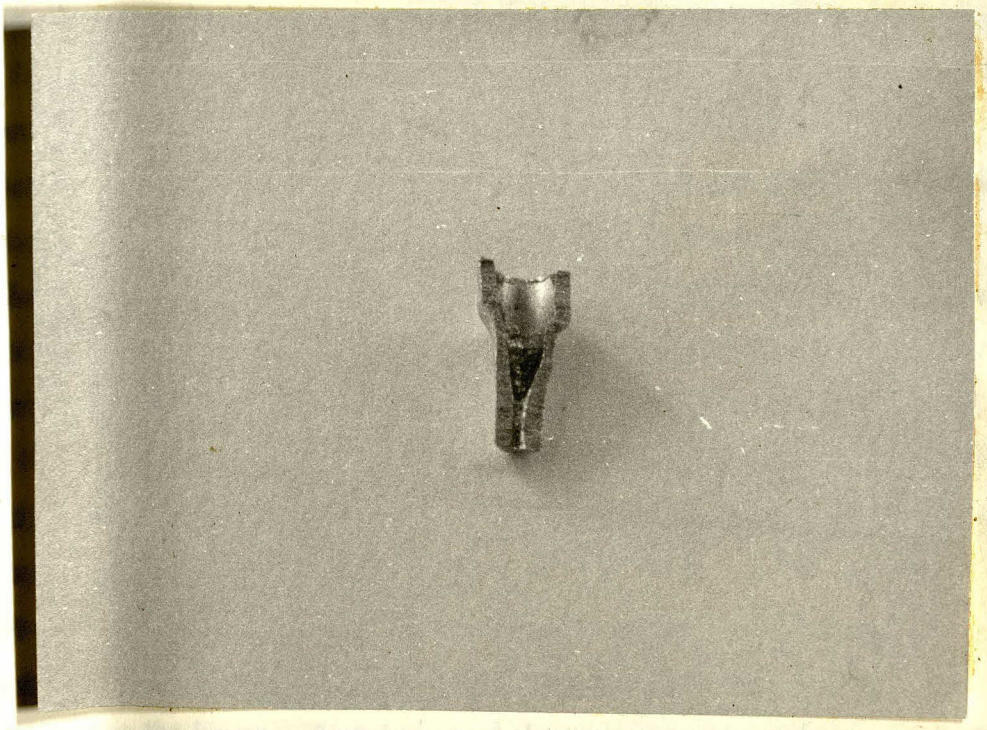


PLATE 5 THE SMOOTH JOIN CAPILLARY AND LEAD TUBE.

The capillary was mounted so that the helix was centrally placed in the furnace. Metallurgical expert opinion considered it unnecessary to support it. Above the annealing temperature pure platinum is very ductile and, contrary to this metallurgical advice, the helix keeled over under its own weight at 1520°K. A supporting bridge made from an A.P. Green G.30 refractory brick was then constructed and fitted to the helix (Plate 2).

b. Platinum 20% Rhodium (Plate 3)

Length 60 cms; Diameter 0.37 mm.i.d., 1.5 mm.o.d.; Helix diameter 44 mm. The leads were approximately 26 and 36 cms x 2.0 mm.i.d., 3.0 mm o.d. in length.

The capillary was essentially the same as (a) except that the inlet tube had a turn of the helix before joining the capillary; this was to ensure that the temperature of the gas had reached the capillary temperature. The cooling coil was of the same design as in (a) and the cooling water again kept at 30°C. A bridge was made from A.P. Green 30 G refractory brick, and the whole capillary together with a thermocouple in position is shown in Plate 3.

Platinum 20% rhodium is much harder than platinum and did not soften even at the highest temperature attempted, 1680°K. However the surface appeared after this heat treatment to be grey, but at the end of experimentation, only the cooler parts of the leads were still grey. Bonilla et al (178) observed a similar colour change with their capillary of platinum-iridium alloy, but say that it did not affect their results. Some variation in times were experienced as the capillary was heated; this was attributed to changes in surface effects of the capillary and will be discussed later.

After some six months in use, water from the cooling coil was observed in the apparatus. This was due to the acid flux, kovar and water reacting in such a way as to corrode the kovar. Stainless steel sleeves were then affixed so that the

cooling coil was over an alloy-stainless steel join and the stainless steel-kovar join was outside the cooling jacket. The accident did not seem to affect the times of flow.

(c) The Silica capillary

Length 164 cms; Diameter 0.44 mm.i.d.; Helix diameter 9.4 cms, depth 9 cms. The leads were approximately 24 and 35 cm x 0.5 mm.i.d. silica tubing.

The capillary was first used by Dr. M. Rigby (175) and was modified to reduce the heat exchanger volume. The original capillary was wound by Wesley Coe (Cambridge) Ltd.

Pyrex-silica graded seals were fitted so that the capillary could be joined to the rest of the apparatus. It was mounted vertically in its furnace unlike (a) and (b).

The Furnace

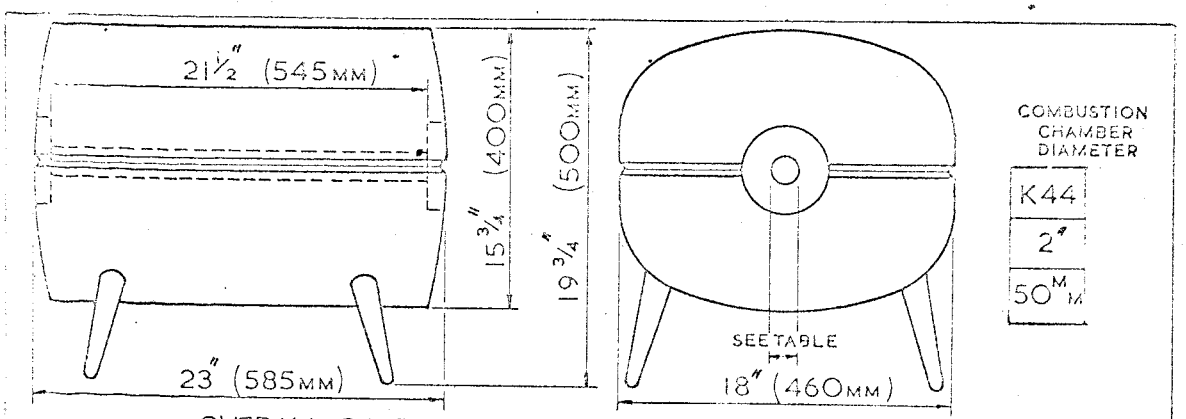
Two furnaces were used:-

(a) for high temperatures, 800-1700°K.

(b) for lower temperatures 300-1000°K.

(a) High Temperatures 800-1700°K

A Johnson Matthey and Co. Ltd. K44 horizontal furnace was used with the dimensions as shown below.



OVERALL DIMENSIONS OF TYPE K44 FURNACE-FIGURE(3.3)

The furnace was wound with platinum 10% rhodium wire, the windings being embedded in high grade alumina refractory, and these elements were fitted inside heat resistant cartridges. Two platinum-platinum 10% rhodium thermocouples were embedded in the refractory close to the heating element, so they did not obstruct the bore of the element and also were protected from mechanical damage. They operated at a potential above earth. One of the thermocouples provided the signal for an automatic temperature regulator and the other was connected to an over-temperature protecting device. The control unit, also bought from Johnson Matthey and Co. Ltd. catalogue number C12, consisted of essentially two Ether Ltd. control boxes, a 991 and a 990. The Ether 991 box controlled the furnace temperature and regulated the power to the furnace through a mercury relay. The 990 unit acted as the over-temperature protector. An energy regulator, controlling the initial heating rate, completed the control circuit.

The Ether control boxes each consisted essentially of a d'Arsonval galvanometer (179). They were scaled 0-1600°C and were suitably insulated to withstand the applied potential on the thermocouples. The temperature was indicated on the calibrated scale by a galvanometer pointer to which was attached a small flag. This flag was free to pass between a photo-transistor and a light source. When the light beam was interrupted the transistor de-energised and operated a relay circuit which altered the current flowing through the furnace. The controller 991 was fitted with an auxiliary circuit to give an anticipatory action (180,181) which reduced the 'overshoot' and 'undershoot' normally experienced with on/off controllers. This system controlled the furnace to within ±1°C. The 'over temperature protection' instrument isolated the furnace by means of a separate switch when the control thermocouple, control galvanometer or mercury relay failed and led to the temperature exceeding the setting on the controller.

Although the scales of the instruments were calibrated, accurate temperature measurements were made with thermocouples. The temperature gradients inside the empty furnace were small, there being 20 cms of hot zone constant to 10° at 1300°K. However when the metal capillaries were placed in the furnace, due to the cooling jacket drawing heat down the lead tubes, a thermocouple placed near the inside of the helix showed a gradient of some 5° over the helix length of 2.4 cm at 1500°K. This was reduced to 2° when the supporting bridge was added, since it acted as a heat sink. The pitch of the platinum 20% rhodium capillary was made closer so that the helix was only 1.4 cm in length with the turns touching, and the gradient of the surroundings was then reduced to less than 1.5°. As the thermal conductivity of platinum is high, the temperature of the capillary was probably uniform to 1° over its whole length. This was taken to be that of the middle turn of the helix and was measured by a thermocouple placed on the capillary as shown in Plate 3.

(b) Lower Temperatures, 300-1000°K

A Gallenkamp vertical box furnace was used to heat the silica capillary. The vitreous silica furnace tube had a diameter 12 cms and length 36 cms. The capillary was sited in the middle of the furnace tube on a vitreous silica tripod, 10 cms in height. A small temperature gradient between the wall and centre of the tube was observed (4° at 800°K), but since all the capillary was uniformly 1 cm from the wall, the capillary was assumed to be at a constant temperature.

The temperature was controlled by an on/off control box made in the Physical Chemistry Laboratory. It worked on a Wheatstone bridge circuit system with the signal to it given by a platinum resistance thermometer. The heating current was controlled by a variac and rheostat in a conventional circuit, shown overleaf.

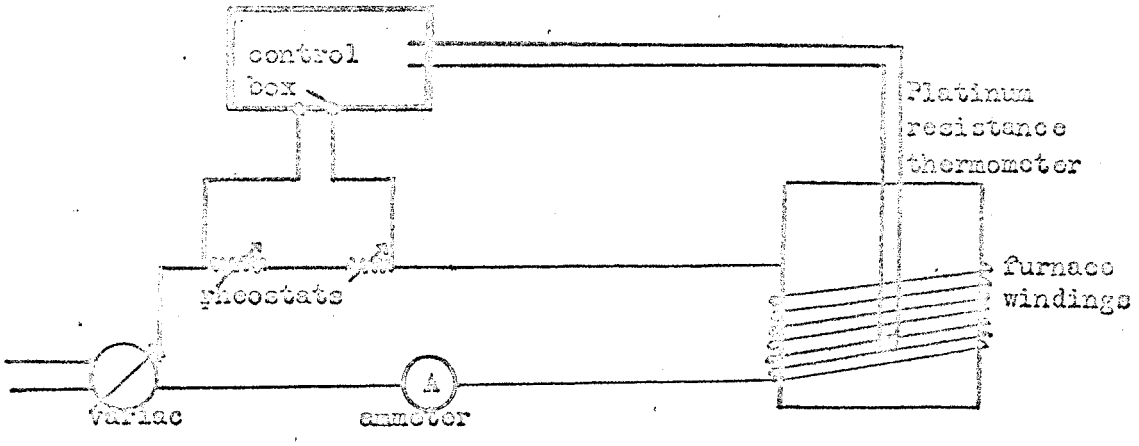


Figure (3.4) - showing control circuit for the Gallenkamp furnace.

The temperature was controlled to $\pm 0.5^{\circ}$ and was measured by certified mercury-in-glass thermometers to 573°K and a platinum/platinum 13% rhodium thermocouple above 573°K. At 573° the two instruments agreed to within 0.3° .

Temperature Measurement

The temperature of furnace (a) was measured by three platinum/platinum 13% rhodium thermocouples made by Johnson Matthey and Co.Ltd. with wire certified to give an E.M.F. which would not deviate from the standard tables by more than the equivalent of 1°C at the gold point (1336°K). Two were made with 28 swg wire whilst the other with 0.5 mm wire; all were 36" in length. The thermocouples were protected from impurities in the atmosphere by recrystallised alumina sheathing. The wires were insulated from each other by enclosing one of the wires in tubing,(0.6 mm.i.d., 1.1 mm.o.d.) and the thermocouple sheathed in a tube (2.0 mm.i.d., 4.0 mm.o.d) closed at one end. The recrystallised alumina tubing was bought from Bush, Beach and Segner Bayley Ltd. (Degussit). The

other ends of the thermocouple wires were separately connected to pure copper wire, either by welding together or lightly soldering, and each separately sheathed in a thin glass tube closed at one end and sealed at the other with picien wax. These tubes were kept in a thermos of ice chips and water. The central parts of the thermocouple wires were encased in plastic sheathing so that the wires were completely insulated from each other over their whole length.

The thermocouples were placed in the furnace around the capillary. The one centrally placed on the capillary can be seen in Plate 3. All three agreed to within 1° at 1300°K when placed close together and agreed to 0.3° with a certified mercury in glass thermometer at 573°K. The E.M.F. from the thermocouples were measured on a Pye Precision Vernier Potentiometer (type number 7568) to ±2 μ-volts in 10 mV (i.e. ±0.2° at 1273°K) and the temperature read from Tables 3 and 4 of the Tables for Thermocouples, British Standard Institute (182). The temperature at 1600°K as given by the thermocouples was compared with the reading of a recently recalibrated disappearing filament pyrometer. The pyrometer was focussed on the tip of the thermocouple sheath, and the agreement was closer than ±20°, which is about the limit of the pyrometer. This gave added confidence in the thermocouples, that they were indicating the correct temperature.

The Vacuum Line (figure 3.1)

Wide bore tubing was used to enable fast pumping speeds, 2.2 cm.o.d. for the main line and 1.4 cm.i.d. for the remainder. A mercury diffusion pump backed by a rotary oil pump evacuated the apparatus. A liquid nitrogen trap was placed between the pumps and the main gallery to prevent mercury vapour entering the vacuum line and condensable vapours reaching the pumps. A 4l. globe was placed between the mercury pump and the oil pump and acted as an oil trap and a static vacuum reservoir. A polythene tube led any vapour from the pump exit to the fume cupboard.

A manometer measured the pressure to 0.3 cm of mercury, and a Vacuum Industrial Appliances thermocouple gauge, which plugged into a B.10 ground glass socket below tap M, measured the pressure to 5×10^{-3} mm of mercury.

The Gas Line (figure 3.1)

Xenon and Krypton were stored in 5l. globes as shown. By suitable manipulation of the taps U and V, and W and X and liquid nitrogen around the cold fingers, gas could be distilled into V_f and V_b or returned into the globes. The high purity nitrogen, argon, helium and neon were taken from cylinders, passed through a P_2O_5 drying column if needed, and admitted to the line via the B.10 ground glass joints below taps N, O and C.

The line could be connected to the pumps via stopcock R, or to V_f and V_b by the needle valves V_1 and V_2 or taps K and L. Tap P connected the blow-off to the line, and could be closed if pressures above 1 atmosphere were required.

Materials Used

Nitrogen:- British Oxygen Company 'white spot' nitrogen was used. No impurities could be detected using the laboratory M.S.10 mass spectrometer (i.e. less than 0.1% impurity).

Argon:- British Oxygen Company 99.995% guaranteed purity argon was used. No impurity could be detected by analysis with the mass spectrometer.

Helium:- British Oxygen Company mineral helium was used. A sample analysis from B.O.C. guaranteed helium not less than 99.995%. No impurities could be detected by analysis with the mass spectrometer.

Neon:- Air Products Ltd. industrial grade neon was used. This was stated to be 99.97% neon. No measurable impurity was found on analysis by mass spectrometer.

Krypton and Xenon:- British Oxygen Company Grade X 1 litre globes were used.

Grade X is stated to be better than 99.9% pure with the balance being the other member of the pair. Mass spectrographic analysis showed less than 0.2% impurities; there being a little air contamination and a very small amount of Xe and Kr respectively in each. The gases were stored in 5l. globes and were frozen and lightly pumped before distilling into the apparatus when needed.

Mercury:- doubly distilled mercury was used.

Tap Grease:- all taps were greased with Apieson L grease.

Stop-watches:- the stop-watches employed had the main dial recording 60 seconds sub-divided into 0.2 second intervals, with a subsidiary dial recording up to 30 minutes. They had two co-axial second hands which could be operated together by pushing the winder button, or one hand could be stopped and then made to rejoin the other, which runs steadily, by pressing a side plunger. Thus a number of concurrent runs could be timed by one watch.

Experimental Procedure

Two procedures were used:-

(a) if the mean pressure was below an atmosphere

(b) if the mean pressure was above an atmosphere.

(a) The mean pressure below an atmosphere

The whole viscometer was evacuated to about 5 μ. Tap A to the side arm and tap H to one side of the manometer were closed. The pressures in V_f and V_b were now the heights of the mercury columns in the two vessels respectively. Taps B, F, C and G were closed. If gas from a cylinder was being used, all delivery tubes were repeatedly flushed out with the gas. Gas was then let into V_b through the needle valve V_2 until the mercury level had nearly reached the required pointer (if from a cylinder, gas was allowed to blow-off at the same time, so preventing gas contamination should a valve or delivery tube have been defective). The gas was allowed to equilibrate with its surroundings, then more gas was gently let through V_2 until the accurate setting was reached - either flickering at the pointer or to the required number of graticule divisions (page 57). V_2 was closed. V_1 was opened and V_f filled to the required pointer. The mercury level was set to the pointer so that the light bulb was alight, but on tapping the side-arm, it flickered. The pressure set in this way was estimated to be reproducible to better than ±0.1 mm of mercury.

Taps to the capillary were then opened: first G then F. For certain longer runs a stop-watch was started as F was opened. There was an initial drop in pressure as the capillary and leads filled with gas, but steady flow was achieved within 10 seconds. The pressure in V_f then dropped whilst the pressure rose in V_b. The pointer circuit was switched to the second pointer and as the mercury surface broke from the pointer the light went out and the stop-watch started. (If the

watch had been started on opening F, one of the co-axial second hands, controlled by the side button, was stopped and the time noted.) The circuit was again switched and the time taken for the pressure to drop to this pointer was recorded by stopping the following hand of the stop-watch. This procedure continued for the run. The apparatus was then re-evacuated by opening taps B and C to the pumps, (unless Kr or Xe were being run, when these were first returned to their respective globes through taps K and L before pumping out any remaining gas).

(b) The mean pressure above an atmosphere

Here the experimental conditions were virtually identical to those of Trautz (125).

Tap I and stopcock J were closed since these parts of the apparatus were not required. The rest of the viscometer was evacuated. All taps experiencing pressures above an atmosphere had elastic bands round them as a precaution against their flying out. Tap E was closed. Gas, whilst blowing-off at P, was admitted through V_1 until the viscometer was filled to atmospheric pressure. Tap F was closed to isolate the capillary from V_f. Tap B was then closed and tap D opened; only V_f was now connected to the gas supply, the rest of the apparatus being at atmospheric pressure. The tap P to the blow-off was closed and the pressure in V_f allowed to rise until the mercury had risen to (usually) above the top pointer. The pressure in V_f was now ($P_{atm} + P_f$) and in V_b, P_{atm} (P_{atm} = atmospheric pressure). The atmospheric pressure was measured before and after a run on an accurate Fortin barometer.

Tap F was then opened and the times recorded for the mercury level to drop from pointer to pointer. These times were corrected to a standard pressure of 760 mm of mercury before any ratios were calculated (Appendix 3).

CHAPTER 4

RESULTS

The primary quantity measured in this work is the time taken for the mercury column in the front vessel to drop between the pointers using various backing pressures. This reflects the pressure drop and mass flow through the capillary and can, in the simplest treatments, be related simply to the viscosity of the gas. In the more accurate work considered here the many corrections described in Chapter 2 have to be applied before the viscosity can be evaluated. The calculations are based on equation (2.50) which is

$$\frac{dn}{dt} = -\frac{\pi r^4}{8\eta RT}\frac{PdP}{dx}\left(1+\frac{C\lambda}{r}\right) \qquad \begin{matrix}(2.50)\\(4.1)\end{matrix}$$

Due to the term in r^4, a very precise knowledge of the dimensions and other characteristics of the apparatus is required, so that the direct calculation of the viscosity is liable to be inaccurate. Hence the viscosities are usually related to some reference. Two methods have been used: the so-called RELATIVE method, where the viscosity of the gas is compared with that of a standard gas at the same temperature, and by the so-called STANDARD method, where a standard value for the gas at temperature T_0 is assumed and the viscosities at other temperatures calculated relative to it.

The relative method requires a knowledge of gas-dependent corrections. In principle it is capable of very high accuracy, however there are no reliable data above room temperature available from the literature, so the value of the reference used may be doubtful. The standard method requires accurate measurements of the temperature and expansion coefficient of the capillary as well as the temperature dependence of the various corrections. In these comparative methods the apparatus constants cancel, and usually the effects of any correction are to some extent

reduced as they are applicable to both conditions.

The equations used, the corrections assumed and the experimentally determined viscosities will now be discussed.

The Equations Used

Using (2.3), (2.4) and (2.6), the slip correction factor of (4.1) becomes,

$$\left(1 + \frac{C\lambda}{r}\right) = \left(1 + \frac{C2\eta}{r\rho\bar{c}}\right) = \left(1 + \frac{C\eta}{rP}\left(\frac{\pi RT}{2M}\right)^{\frac{1}{2}}\right) = \left(1 + \frac{K'}{P}\right)$$

where $$K' = \frac{C\eta}{r}\left(\frac{\pi RT}{2M}\right)^{\frac{1}{2}}$$

so that (4.1) may be written

$$\frac{dn}{dt} = -\frac{\pi r^4}{8\eta RT} P\frac{dP}{dx}\left(1 + \frac{K'}{P}\right) \qquad (4.2)$$

where P is the average pressure of the element of length dx.

Integrating over the length of the capillary,

$$\frac{dn}{dt} = -\frac{\pi r^4}{8\eta lRT}\int_{P_f}^{P_b} PdP - \frac{K'\pi r^4}{8\eta lRT}\int_{P_f}^{P_b} dP$$

$$= \frac{\pi r^4}{16\eta lRT}(P_f^2 - P_b^2)\left(1 + \frac{K'}{\overline{P}_c}\right) \qquad (4.3)$$

where the mean pressure $\overline{P}_c$ in the tube is $(P_f + P_b)/2$.

The rate of flow is measured by the change in pressure of the front vessel. For this purpose the front vessel is the total volume before the capillary including the small volume of the entrance lead tube, which is at the temperature of the

furnace and so will be temperature dependent.

At any instant for the front vessel, assuming ideal gas conditions,

$$P_f \left(\frac{V_f}{T_f} + \frac{V_c}{T_c} \right) = nR$$

where n moles of gas at the pressure P_f are contained in the front vessel of volume V_f at temperature T_f and the lead tubes of volume V_c at the temperature T_c of the capillary.

The rate of pressure drop is related to the mass flow rate by

$$-\frac{dP_f}{dt}\left(\frac{V_f}{T_f} + \frac{V_c}{T_c} \right) = \frac{dn}{dt} R \qquad (4.4)$$

assuming V_f varies so slowly with pressure that it can be regarded as constant for the time interval dt (see below).

$V_c \approx 1$ cc and $V_f \approx 1000$ cc so, since $T_c > T_f$, the effect of V_c/T_c varying with temperature is negligible and (4.4) becomes

$$-\frac{dP_f}{dt}\frac{V_f}{RT_f} = \frac{dn}{dt} \qquad (4.5)$$

so that (4.3) may be written

$$\frac{-dP_f}{dt} = \frac{r^4}{16\,l}\,\frac{T_f}{T_c V_f}\,(P_f^2 - P_b^2)\left(1 + \frac{K'}{\overline{P}_c}\right) \qquad (4.6)$$

The mean pressure $\overline{P}_c$ varies very slowly during a pressure drop ΔP_f (see Appendix 3) so may be assumed constant at the mean pressure $\overline{P}$ for each pressure drop, where, denoting the beginning of a run as i and the end as t,

$$\overline{P} = (\overline{P}_c^{\,i} + \overline{P}_c^{\,t})/2$$

For the pressure drop from P_f^i to P_f^t, integrating with respect to time

$$-\int_{P_f^i}^{P_f^t} \frac{V_f \, dP_f}{(P_f^2 - P_b^2)} = \frac{\pi r^4}{16 \eta l} \frac{T_f t}{T_c} \left(1 + \frac{K'}{\bar{P}} \right) \qquad (4.7)$$

where t is the time. $V_f (= V_o + kh_f)$ depends on the volume of the mercury removed into the side-arm of V_f. V_o is the volume of the front vessel when h_f (the height of the mercury column in the side-arm) is zero. k is the area of the side-arm tube - its value and the determination of V_o are recorded in Appendix 4.

The Relative Method

For two gases, under identical conditions so that V_f, P_f, P_b, r^4/l, T_f, T_c and $\bar{P}$ are the same, the ratio of the times using (4.7) is

$$\frac{tx}{ty} = \frac{\eta x}{\eta y} \frac{(1 + K'y/\bar{P})}{(1 + K'x/\bar{P})} \qquad (4.8)$$

If $K'x/\bar{P}$ is small, then by the binomial expansion

$$\frac{tx}{ty} \simeq \frac{\eta x}{\eta y} \left(1 + \frac{K'y - K'x}{\bar{P}}\right) \qquad (4.9)$$

Thus if the ratio of times of flow tx/ty is plotted against $1/\bar{P}$ (the mean of the average pressure in the capillary) a straight line should be obtained with the intercept being the ratio of the viscosities and the slope providing information about the slip coefficient. The times of flow must be first corrected for kinetic energy and gas imperfection.

Since the ratio of the viscosities varies only slowly with temperature, the temperature of the capillary need not be known with great accuracy; it must, though, be the same for both gases.

The Standard Method

For one gas under identical conditions but at two different temperatures T_c' and T_o, V_f, P_f, P_b, T_f and $\bar{P}$ are the same. The factor r^4/l depends on the expansion coefficient of the material. Dimensionally this factor is (length)^3 and so a term $r_o^4 (1 + \alpha (T_c' - T))^3/l_o$ occurs, where r_o and l_o are the dimensions of the capillary at the reference temperature T, and α the linear coefficient of expansion. The ratio of the times of flow using (4.7) is

$$\frac{t_o}{t'} = \frac{\eta_o T_o (1 + \alpha (T_c' - T))^3 (1 + K_c'/\bar{P})}{\eta' T_c' (1 + \alpha (T_o - T))^3 (1 + K_o'/\bar{P})} \qquad (4.10)$$

where subscript o refers to the lower temperature. If $K_o'/\bar{P}$ is small, then by the binomial expansion

$$\frac{t_o}{t'} \simeq \frac{\eta_o T_o}{\eta' T_c'} \frac{(1 + 3\alpha (T_c' - T))}{(1 + 3\alpha (T_o - T))} \left(1 + \frac{(K_c' - K_o')}{\bar{P}}\right) \qquad (4.11)$$

Thus if the ratio of the times of flow t_o/t' is plotted against $1/\bar{P}$, a straight line should be obtained with the intercept giving the ratio of viscosities, provided the expansion term and the temperatures are known. The slope gives some information about the slip coefficient. Before this analysis, the times of flow must be corrected as described below.

The temperatures T_c' and T_o need to be known with as great an accuracy as is possible.

Corrections Applied

The corrections to be applied to the simple Poiseuille flow formula have

been discussed in Chapter 2. The slip correction has already been applied as described in the earlier sections. A further discussion of the slip coefficient is given in Chapter 5. The calculation of the corrections for the kinetic energy, gas imperfection and curved-pipe flow will now be described.

Kinetic Energy

The viscosity η as calculated from Poiseuille's formula needs to be corrected for kinetic energy effects by the factor given by (2.62) where

$$\eta' = \eta\left(1 - \frac{1.12M}{8\pi\eta' l}\frac{dn}{dt}\right) = \eta / \left(1 + \frac{1.12M}{\eta' l 8\pi}\frac{dn}{dt}\right) \qquad \begin{matrix}(2.62)\\(4.12)\end{matrix}$$

η' is the true corrected value. A mean value of dn/dt, the mass flow in moles/sec may be obtained from the pressure drop in the front vessel, thus

$$\frac{dn}{dt} \simeq \frac{\Delta P_f}{RT_f}\frac{V_f}{t}$$

where t is the time the pressure in the front vessel drops ΔP_f.

So (4.12) becomes $$\eta' = \eta / 1 + \frac{1.12M}{\eta' l 8\pi}\frac{P_f V_f}{RT_f t} = \eta/(1+H) \qquad (4.13)$$

where $$H = \frac{1.12M\,\Delta P_f V_f}{8\pi\eta' l RT_f t}$$

From (4.7), the uncorrected viscosity η (i.e. the viscosity derived if Poiseuille's formula was strictly obeyed) is proportional to t, the time of flow. Thus ignoring other correction terms, from (4.13)

$$\eta' \propto t/(1+H)$$

and comparing two viscosities,

$$\frac{\eta'a}{\eta'b} = \frac{ta(1 + Hb)}{tb(1 + Ha)} \qquad (4.14)$$

This comparative methods used in the analysis of the work here minimises the effects of the Hagenbach correction due to the partial cancellation of terms.

The factor (1 + H) diminishes as the capillary temperature rises due to the increase in both the times of flow and the viscosity, but is proportional to the molecular weight. The values applied to the times of flow at room temperature are given in Appendix 8. The greatest effect occurs for the pressure range $\bar{P}_b$ 0-1 (see Appendix 3) and the factors over the temperature range 300-1500°K for $\bar{P}_b$ 0-1 for the platinum capillary are

Temp °K	He	Ne	Ar	Kr	Xe	N_2
300	1.0003	1.0005	1.0030	1.0046	1.0077	1.0033
500	1.0001	1.0001	1.0008	1.0011	1.0017	1.0008
1000	1.0000	1.0000	1.0002	1.0003	1.0005	1.0001
1500	1.0000	1.0000	1.0000	1.0000	1.0001	1.0000

For each temperature this is the largest effect, as it diminishes rapidly for the lower pointers (see Appendix 8). Most of the Xe and Kr times where (1 + H) is of significance (i.e. greater than 0.1%) have been ignored for the determination of the ratio of viscosities Xe/N_2 and Kr/N_2, because curved-pipe flow effects are also present. Above 500°K for the relative ratios He/N_2, Ne/N_2 and Ar/N_2 the corrections due to the kinetic energy effects will always be much less than 0.1%. For the standard ratios, the effects will be negligible in all cases for He and Ne, and for most points for Ar and N_2 it will be less than 0.1%.

Gas Imperfection

The viscosity as calculated from the simple Poiseuille formula needs to be corrected for gas imperfections. For the gas in the capillary the relation (equation (2.68)),

$$\eta' = \eta \left(1 - \frac{2B(T_c)\,(P_f^3 - P_b^3)}{3RT_c\,(P_f^2 - P_b^2)}\right) \qquad \begin{matrix}(2.68)\\(4.15)\end{matrix}$$

where $B(T_c)$ is the second virial coefficient at the temperature of the capillary, is required.

The rate of flow dn/dt of equation (4.1) is observed by the pressure drop in the front vessel; this is also dependent on gas imperfections and must be corrected.

For the front vessel,

$$P_f V_f = n RT_f(1 + B(T_f)P_f/RT_f) = n RT_f(1 + nB(T_f)/V_f)$$

For a small change in pressure, at constant volume,

$$V_f dP_f = dn\, RT_f(1 + 2n\, B(T_f)/V_f) = dn\, RT_f(1 + 2P_f B(T_f)/RT_f) \qquad (4.16)$$

thus ignoring other correction terms, (2.66) becomes

$$\frac{dn}{dt} = -\frac{dP_f}{dt}\,\frac{V_f}{RT_f(1 + 2P_f B(T_f)/RT_f)} = -\frac{\pi r^4}{8\eta RT_c} P_c(1 - \frac{B(T_c)P_c}{RT_c})\frac{dP_c}{dx} \qquad (4.17)$$

where subscript c and f refers to the capillary and front vessel respectively.

P_f varies slowly with time so if the mean value of the front vessel pressure $\bar{P}_f$ $(= (P_f^i + P_f^t)/2)$ is taken (4.17) becomes

$$-\frac{dP_f}{dt}\,\frac{V_f}{RT_f(1 + 2B(T_f)\bar{P}_f/RT_f)} = -\frac{\pi r^4}{8RT_c\,\eta} P_c \frac{dP_c}{dx} + \frac{\pi r^4}{8RT_c\eta}\,\frac{B(T_c)P_c^2}{RT_c}\,\frac{dP_c}{dx} \qquad (4.18)$$

which becomes on integrating for the length of the capillary,

$$-\int_{P_f^i}^{P_f^t} V_f dP_f = \frac{\pi r^4 T_f t}{16 \eta T_c l}\left(1 + \frac{2\bar{P}_f B(T_f)}{RT_f}\right)(P_f^2 - P_b^2)\left(1 - \frac{2B(T_c)}{3RT_c}\frac{(P_f^3 - P_b^3)}{(P_f^2 - P_b^2)}\right) \quad (4.19)$$

The true viscosity η', neglecting other correction terms, is thus proportional to

$$\eta' \propto t\left(1 + \frac{2\bar{P}_f B(T_f)}{RT_f}\right)\left(1 - \frac{2B(T_c)}{3RT_c}\frac{\bar{P}_f^3 - \bar{P}_b^3}{\bar{P}_f^2 - \bar{P}_b^2}\right) \quad (4.20)$$

The first factor depends only on the front pressure, and so is the same for the pressure ranges 1-6, and is independent of the capillary temperature. The values are given below for $\bar{P}_f$ = 100, 50, 40, 30, 20 and 10 cms of Hg. The virial coefficients are given in cos/mole and are taken from (70).

	He	Ne	Ar	Kr	Xe	N_2
B(298°K)	+11.6	+11.0	-15.6	-52.7	-135.0	-5.6
100	1.0010	1.0010	0.9986	0.9944	0.9856	0.9995
50	1.0005	1.0005	0.9992	0.9972	0.9928	0.9998
40	1.0004	1.0004	0.9994	0.9977	0.9942	0.9998
30	1.0003	1.0003	0.9995	0.9983	0.9957	0.9999
20	1.0002	1.0002	0.9996	0.9988	0.9974	0.9999
10	1.0001	1.0001	0.9998	0.9994	0.9987	1.0000

Thus the relative calculations He/N_2, Ne/N_2 and Ar/N_2 have very small corrections, and with the standard method this factor cancels exactly, because it is the same at both temperatures. The Kr and Xe corrections are significant amounting

to over 0.5% at the higher pressures for Xe. The values used are given in Appendix 8.

The second term depends on the capillary temperature, the pressures at the ends of the capillary and on the second virial coefficient for the gases at the temperature of the capillary. These diminish rapidly for Xe and Kr so that at 773°K, B is zero for Xe, + 12 cos/mole for Kr and the other gases have values in the range +10-20 cos/mole. Thus the second correction factor will be negligible, even for Xe, at 773°K.

At 500°K taking the pressure range P_b30-1 (see Appendix 3) where $\overline{P_f}$ = 49.63 and $\overline{P_b}$ = 30.91 cms of Hg and taking B typically as + 20 cos/mole, the correction factor is 1.0003. The values of B at 500°K are given below,

	He	Ne	Ar	Kr	Xe	N_2
B cos/mole	+11	+13	+6	-6	-37	+17

so that each gas has corrections of less than 0.05% for all the experimental conditions to which it is subjected at this temperature.

The values for the correction at 293°K are given below for the conditions of the pressure range P_b30-1.

	He	Ne	Ar	Kr	Xe	N_2
B(293) cos/mole	+11.4	+11.2	-16.2	-56.1	-139.2	-6.3
factor	0.9998	0.9998	1.0003	1.0012	1.0031	1.0001

Thus it is approximately 1/3 the value of the first correction, and at room temperature tends to reduce the effects of it. A full table for the imperfection terms at 293°K appears in Appendix 8.

Curved Pipe Flow

Dean (165) stated that the effect of curved-pipe flow is some function of the Dean Number $D = \frac{2r\rho v}{\eta}\sqrt{\frac{r}{R'}}$, where v is the fluid velocity and R' the radius of the helix.

v in terms of experimental quantities may be taken as

$$v = \frac{M}{\rho \pi r^2}\frac{dn}{dt}$$

using (2.41)

$$D = \frac{2M}{\pi r \eta}\frac{dn}{dt}\sqrt{\frac{r}{R'}} = \frac{r^3 M (\bar{P}_f^2 - \bar{P}_b^2)}{8\eta^2 R T_c l}\sqrt{\frac{r}{R'}} \qquad (4.21)$$

The velocity has been calculated at the point where the gas pressure in the capillary is $(\bar{P}_f + \bar{P}_b)/2$. D varies with pressure and so the mean values of P_f and P_b are taken. The final correction is a non-linear function of D. As T_c increases D decreases, so the effects of curved-pipe flow decrease. The threshold value of D, the value below which curved-pipe flow is regarded as negligible (i.e. $< 0.1\%$), was taken as 3.0. For the determination of the viscosity ratios the times were not taken into account for any pressure range where $D > 3.0$.

The largest value of D occurred within the pressure range P_b0-1 where $\bar{P}_f = 49.63$ and $\bar{P}_b = 2.05$ cm of Hg and the following values are attained at the temperatures indicated.

°K	He	Ne	Ar	Kr	Xe	N_2
300	2.3	4.8	18.2	31.4	59.2	21.4
400	1.1	2.4	9.2	15.1	30.4	10.8
500	0.5	1.2	4.4	6.8	12.4	5.2
600	0.2	0.6	2.2	3.6	6.4	2.9

By 700°K it would be expected that curved-pipe flow effects are negligible even for Xe. He and Ne should not be affected even at 300°K and Ar and Ne should cease completely to be affected by 600°K.

An experimental investigation of curved-pipe flow occuring in this apparatus will be discussed in Chapter 5.

The Method of Correcting Results

The times of flow must be corrected before using the analysis of (4.9) and (4.11) since the correction factors also vary with pressure. From (4.14) and (4.20), the relative ratio equation (4.3) becomes

$$\frac{t_x}{t_y}\frac{(1+H_y)(1+g_x)}{(1+H_x)(1+g_y)} = \frac{\eta_x}{\eta_y}\left(1+\left(\frac{K'_y - K'_x}{\bar{P}}\right)\right) \qquad (4.22)$$

where $(1+g) = \left(1+\frac{2\bar{P}_f B(T_f)}{RT_f}\right)\left(1-\frac{2B(T_c)}{3RT_c}\left(\frac{\bar{P}_f^3 - \bar{P}_b^3}{\bar{P}_f^2 - \bar{P}_b^2}\right)\right)$

and the standard ratio (4.11) becomes

$$\frac{t_o(1+H_o)(1+G_o)}{t'(1+H')(1+G')} = \frac{\eta_o T_o}{\eta' T'_c}\left(\frac{1+3\alpha(T'_c - T)}{1+3\alpha(T_o - T)}\right)\left(1+\frac{(K'_c - K'_o)}{\bar{P}}\right) \qquad (4.23)$$

where $(1+G) = \left(1-\frac{2B(T_c)(\bar{P}_f^3 - \bar{P}_b^3)}{3RT_c(\bar{P}_f^2 - \bar{P}_b^2)}\right)$

If each time ratio is corrected for these kinetic energy and gas imperfection terms, then the relative calculation is,

$$\left(\frac{t_x}{t_y}\right)_{corr} = \frac{\eta_x}{\eta_y}\left(1+\frac{K'_y - K'_x}{\bar{P}}\right) \qquad (4.24)$$

and the standard calculation becomes,

$$\frac{t^o}{t'_{corr}} = \frac{\eta_o \; T_o}{\eta' \; T'} \left(\frac{1 + 3\alpha (T_c' - T)}{1 + 3\alpha (T_o - T)}\right)\left(1 + \frac{K_c' - K_o'}{\bar{P}}\right) \qquad (4.25)$$

The intercepts should now give the true ratio of viscosities. Where any correction term was less than 0.05% it was neglected, and as seen from (4.22) and (4.23), in most cases the correction terms partially cancelled, so reducing any error.

The Expansion Coefficient

For the standard method of calculation, the expansion of the capillary needs to be taken into account. At temperature T_c the dimensions of the capillary are $r = r_o (1 + \alpha (T_c - T)$ and $l = l_o (1 + \alpha (T_c - T))$, where α is the linear coefficient of thermal expansion of the capillary material at temperature T_c, and r_o and l_o the radius and length of the capillary measured at room temperature T. Thus,

$$\frac{a^4}{l} = \frac{a_o^4 (1 + \alpha(T_c - T))^4}{l_o (1 + \alpha(T_c - T))} \simeq \frac{a_o^4}{l_o} (1 + 3\alpha(T_c - T)) = \frac{a_o^4}{l_o} \; fe \qquad (4.26)$$

where fe is the thermal expansion factor $(1 + 3\alpha (T_c - T))$.

The expansion coefficient for platinum and rhodium are essentially identical: thus at 1273°K, the ratio L/L_o for platinum is 1.01019 and for rhodium 1.01080 (182-186) so for the purposes of (4.25), the linear coefficient for both the platinum and the platinum 20% rhodium capillaries is taken as

$$L = L_o(1 + 8.868 \times 10^{-6}(T_c - 273) + 1.324 \times 10^{-9} (T_c - 273)^2)$$

where T_c is measured in °K, and L is the length at T_c and L_o the length at 273°K, so that

$$fe = 1 + 2.6604 \times 10^{-5}(T_c - 273) + 3.972 \times 10^{-9}(T_c - 273)^2 \qquad (4.27)$$

A plot of fe against T_c is given in figure (4.1).

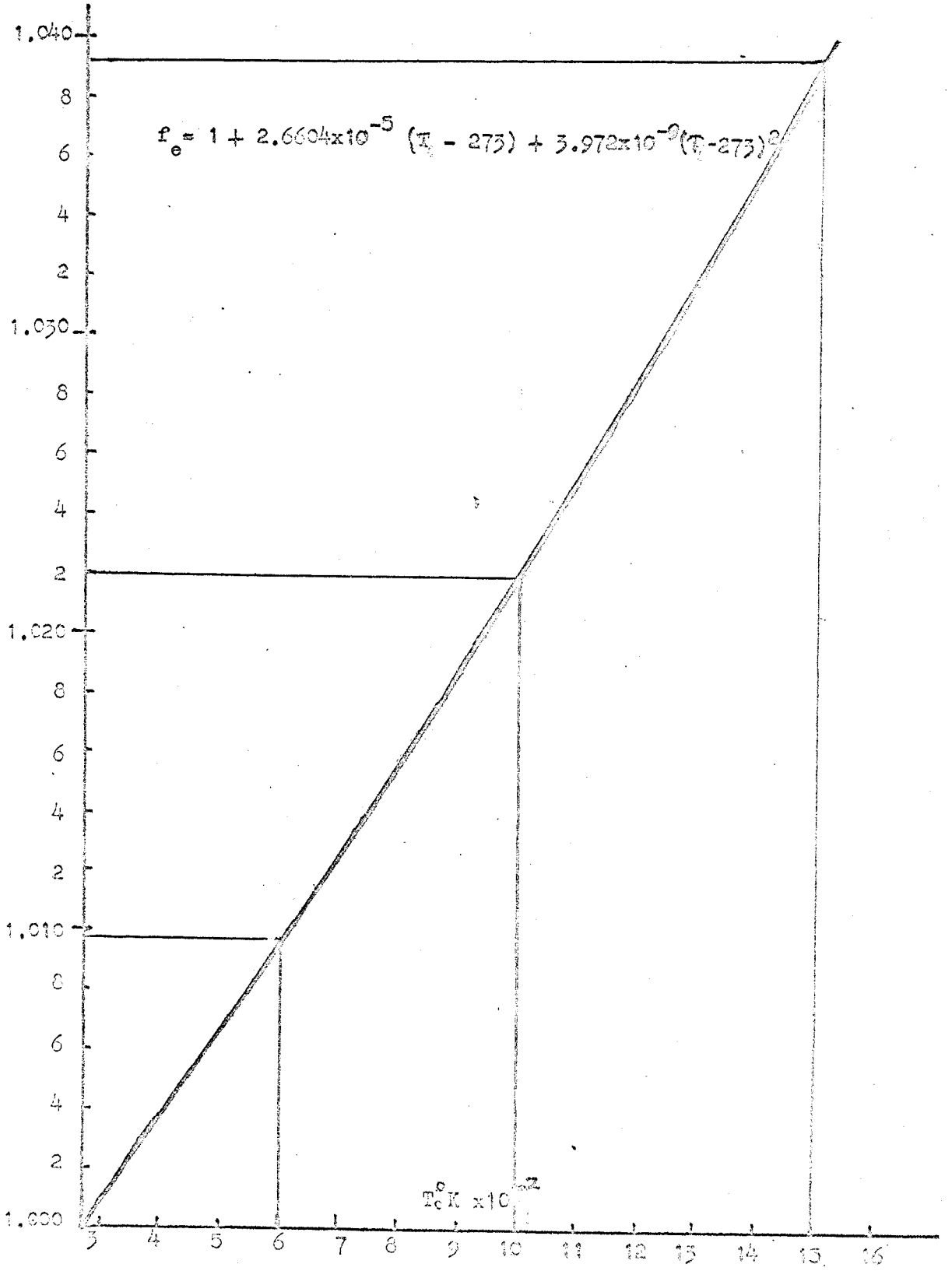


Figure (4.1) f_e against $T_c^\circ K$

The expansion coefficient for the silica capillary is given (184) as $\alpha = 0.54 \times 10^{-6}$, thus

$$f_e = (1 + 1.62 \times 10^{-6} (T_c - 273)) \quad (4.28)$$

and so for the temperatures at which measurements were made in this work, f_e takes the values

T_c °K	f_e
373	1.00016
474	1.00032
566	1.00048
673	1.00064
803	1.00086
948	1.00108

Analysis of Times of Flow

Some 10,000 times of flow were recorded and the averages at each temperature are given in tables in Appendix 5. The readings at each temperature are recorded in separate tables in the order in which they were obtained. Experimental difficulties affecting the capillary are noted at the head of certain tables. The reproducibility of the times was usually better than ± 1 second or 0.2%. The pressure ranges are given in code for convenience (Appendix 3).

Specimen calculations will be given here for both the relative and standard methods of determining the viscosities. The values of the slopes and intercepts of equations (4.24) and (4.25), together with their standard deviations as determined by the analysis of Appendix 6, will be presented in the following tables. Then summary tables of the smoothed data obtained by fitting the experimental data to polynomial functions are given, and these values compared with the literature values. Finally in this Chapter, an evaluation of the errors and accuracy of this work will be made.

Specimen Calculation by the Relative Method

The determination of the ratio of the viscosities of Xe/N_2 at 926°K will be given in full as a typical example of the determination of viscosities by the relative method.

The evaluation is made through equation (4.24) where the corrected time ratios should give a straight line when plotted against $1/\bar{P}$; $\bar{P}$ being the average pressure in the capillary. Due to experimental uncertainties the points may not lie exactly on the line, so a least means square analysis is used. The derivation of this analysis and the computer programme used are given in Appendix 6.

The maximum Dean Number (4.21), which occurs at $P_b U=1$, is for Xe 2.3 and for N_2 1.2; so no curved-pipe flow effects would be expected.

The maximum Hagenbach correction (4.13) which occurs at P_b 0-1 is 1.0005 for Xe and 1.0001 for N_2; so kinetic energy effects are always negligible.

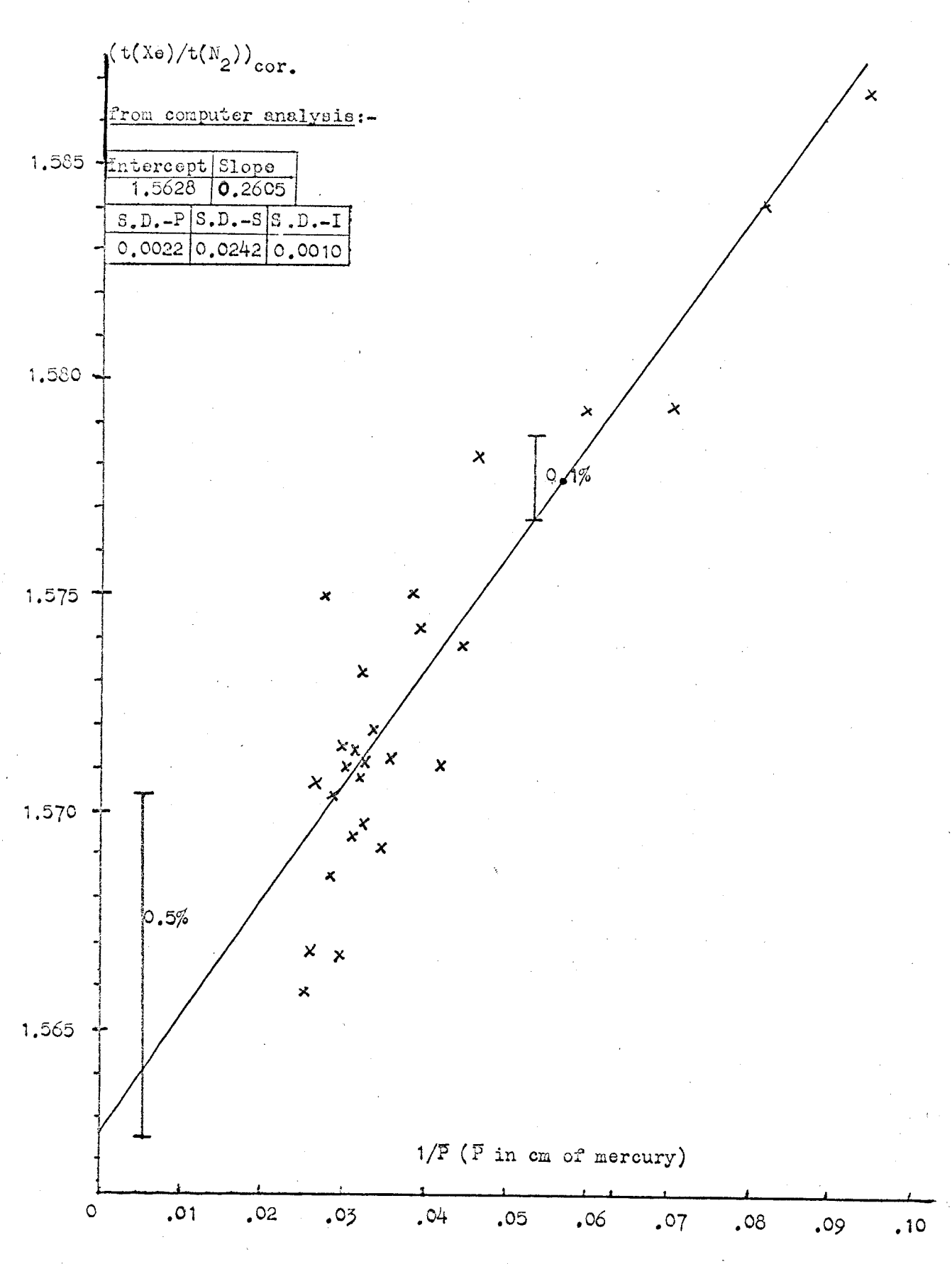
The imperfection term is applied in two parts (4.20). The first term, the front vessel correction is significant for Xe, amounting in some cases to 0.7%; the values are given in Appendix 8. For N_2, the correction factor is negligible, its maximum value being 0.9998 i.e. 0.02%. The second term is negligible as $B(926^\circ K)$ is approximately + 10ccs/mole for Xe and + 30 ccs/mole for N_2: thus the factor is always less than 1.0001 for Xe and 1.0002 for N_2.

The following table gives the raw data, the corrected times and the corrected ratios. The graph of $(t(Xe)/t(N_2))_{corr.}$ vs. $1/\bar{P}$ is shown in figure (4.2) together with the computer analysis. The intercept when $1/\bar{P} = 0$ is 1.5628 with a standard deviation of 0.00103.

Thus the ratio $\eta(Xe)/\eta(N_2)$ at 926°K is 1.5628 ±0.001.

The data for the relative calculation Xe/N_2 at 926°K

$\bar{p}$		Xe		N_2		
Code	Values	t_{raw}	t_{corr}	t_{raw}	t_{corr}	$(t(Xe)/t(N_2))_{corr}$
P_b30-1	40.27	1015.0	1007.7	643.6	643.6	1.5657
-2	38.76	1817.4	1804.7	1151.8	1151.8	1.5668
-3	37.47	2192.2	2179.4	1383.7	1383.7	1.5750
P_b25-1	38.38	883.3	876.9	558.2	558.2	1.5709
-2	36.87	1418.1	1408.2	897.9	897.9	1.5683
-3	35.34	1356.0	1348.1	858.1	858.1	1.5710
-4	34.75	1367.9	1360.4	866.0	866.0	1.5709
P_b20-1	35.75	770.8	765.3	487.3	487.3	1.5705
-2	34.27	1138.6	1130.6	721.6	721.6	1.5665
-3	33.02	955.5	950.0	604.5	604.5	1.5716
-4	32.24	810.4	805.9	512.9	512.9	1.5713
P_b15-1	33.62	709.0	703.9	447.9	447.9	1.5715
-2	32.15	1004.2	997.2	635.5	635.5	1.5692
-3	30.88	791.6	787.0	500.3	500.3	1.5731
-4	30.06	629.6	626.1	398.4	398.4	1.5715
P_b10-1	30.56	653.2	648.5	413.1	413.1	1.5698
-2	29.08	887.2	881.0	561.5	561.5	1.5690
-3	27.81	663.0	659.1	419.4	419.4	1.5715
-4	17.02	502.4	499.6	317.1	317.1	1.5755
P_b0-1	25.84	619.4	614.9	390.5	390.5	1.5746
-2	24.36	811.8	806.1	513.1	513.1	1.5711
-3	23.09	580.7	577.3	366.8	366.8	1.5738
-4	22.30	424.3	422.0	267.4	267.4	1.5782
P_f36-1	16.57	2956.0	2943.2	1863.6	1863.6	1.5793
-2	14.25	2521.4	2510.5	1589.4	1589.4	1.5795
P_f26-1	12.19	2201.0	2195.3	1385.8	1385.8	1.5841
-2	10.68	3929.8	3919.6	2470.0	2470.0	1.5868



Figure(4.2) The Plot of $(t(Xe)/t(N_2))_{cor.}$ vs. $1/\bar{P}$ at 926°K .

The Relative Ratios

The following tables give the computer analysis for the relative calculation of the times of flow given in Appendix 5, corrected as described in the last sections. The intercepts i.e. viscosity ratios were fitted to the polynomial function ($\log N = \log_{10} N$),

$$\text{Log (Ratio)} = A \log T + B/T + C/T^2 + D$$

by the method of least squares using the University computer KDF9 programme STAT 15. The coefficients are given at the top of each page. The standard deviations of the ratios from the smooth curve are given at the end of each table.

The columns show:- 1) the capillary used, 2) the temperature, 3) the intercept of the straight line, when $1/T = 0$, 3a) the reciprocal of 3) if the slip effects for gas x, equation (4.24), are larger than gas y, 4) the slope of the line - this will be discussed in Chapter 5, 5) the standard deviation of the points from the line multiplied by 10^3, 6) the standard deviation of the slope multiplied by 10^2, 7) the standard deviation of the intercept multiplied by 10^3 and 8) the % difference between the experimental values of the ratios and the calculated value.

Helium/Nitrogen Ratios

The intercepts were fitted to the following equation:

$\log \eta(He)/\eta(N_2) = 0.12177 \log T + 31.990/T - 1139.20/T^2 - 0.351033.$

Helium has the larger slip coefficient, so the straight line intercept ratio $\eta(N_2)/\eta(He)$ was plotted. The column labelled 1/Intercept gives the ratio $\eta(He)/\eta N_2$.

Cap	T°K	Int	1/Int	Slope	SD-P	SD-S	SD-I	%
Pt-Rh	292	0.90201	1.1086	0.128	1.5	0.9	0.7	-0.14
Pt	293	0.90134	1.1095	0.160	1.0	0.6	0.5	-0.03
Pt-Rh	293	0.90374	1.1065	0.164	1.9	1.2	1.0	-0.36
Pt-Rh	293	0.89837	1.1131	0.215	1.3	1.0	1.0	0.30
Pt-Rh	293	0.90094	1.1100	0.210	1.6	1.2	1.2	0.00
Silica	293	0.89846	1.1130	0.179	1.4	0.9	0.7	0.12
Silica	373	0.91231	1.0961	0.253	1.4	1.2	0.8	0.02
Silica	474	0.91883	1.0883	0.401	1.7	1.5	0.8	-0.13
Silica	566	0.91703	1.0905	0.442	2.0	1.6	0.9	0.24
Silica	673	0.91491	1.0930	0.630	1.9	1.7	0.9	0.52
Pt	794	0.91076	1.0980	0.874	2.2	1.6	0.9	0.01
Pt-Rh	798	0.90961	1.0993	1.072	0.8	1.8	0.9	0.08
Pt-Rh	799	0.90960	1.0992	0.513	1.5	1.2	0.6	0.08
Pt-Rh	800	0.90980	1.0990	0.739	1.7	0.9	0.5	0.07
Pt-Rh	801	0.91490	1.0930	1.131	2.2	3.4	1.4	-0.39
Silica	803	0.90800	1.1011	0.760	2.1	1.8	0.0	0.24
Pt-Rh	804	0.91400	1.0940	1.000	1.6	1.5	0.8	-0.48
Pt	926	0.90350	1.1068	1.430	2.2	2.2	0.9	0.15
Silica	948	0.89940	1.1118	0.980	1.9	1.5	0.7	0.52
Pt	1044	0.90097	1.1100	1.453	3.7	2.1	1.4	-0.19
Pt	1047	0.89603	1.1160	1.769	1.8	2.0	1.0	0.33
Pt-Rh	1144	0.8954	1.1167	1.300	1.0	1.9	0.8	-0.10
Pt-Rh	1146	0.89720	1.1140	1.330	1.6	1.6	0.6	-0.37
Pt	1153	0.89300	1.1200	1.920	1.7	1.6	0.7	0.12
Pt-Rh	1273	0.8920	1.1210	1.900	2.3	3.3	1.3	-0.07
Pt-Rh	1275	0.88710	1.1272	1.510	2.5	2.8	1.2	0.09
Pt-Rh	1275	0.89050	1.1220	1.575	2.0	2.1	1.0	-0.26
Pt-Rh	1275	0.8910	1.1223	1.971	1.9	2.8	0.9	-0.35
Pt-Rh	1275	0.8910	1.1223	1.905	1.5	1.7	0.7	0.19
Pt	1287	0.88597	1.1287	1.905	1.5	1.7	0.7	0.19
Pt	1304	0.88705	1.1273	2.242	1.4	2.0	1.1	-0.03
Pt-Rh	1457	0.8789	1.1377	2.220	3.0	4.2	1.8	0.10
Pt-Rh	1457	0.8798	1.1365	2.495	2.1	6.0	1.3	0.02
Pt	1530	0.8751	1.4270	2.788	2.4	4.6	1.2	0.17

Standard deviation of the ratios from the smooth curve = 0.24%

Argon/Nitrogen Ratios

The intercepts were fitted to the following equation:

$$\text{Log } \eta \text{ (Ar)}/\eta \text{ (N}_2\text{)} = 0.001733 \log T - 9.41093/T + 95.8263/T^2 + 0.1310053$$

Cap	T°K	Int	Slope	SD-Pt	SD-SI	SD-I	%
Silica	293	1.2738	-0.044	1.5	1.0	0.8	0.19
Pt-Rh	293	1.2700	-0.018	2.1	1.2	1.0	-0.13
Pt-Rh	293	1.2708	-0.019	2.2	1.3	1.1	-0.05
Pt	293	1.2702	-0.045	1.9	1.1	0.9	-0.10
Silica	373	1.2896	-0.024	1.4	1.2	0.7	-0.10
Silica	474	1.3076	-0.053	2.7	2.4	1.2	0.06
Silica	566	1.3170	-0.036	2.8	2.3	1.2	0.03
Silica	673	1.3255	-0.070	2.5	2.0	1.2	0.06
Pt	794	1.3303	-0.156	2.5	6.5	2.2	-0.09
Pt-Rh	799	1.3317	-0.066	1.8	1.4	0.7	0.00
Pt-Rh	800	1.3320	-0.084	1.6	0.8	0.4	0.02
Silica	803	1.3322	-0.055	2.3	1.9	0.9	0.02
Pt	926	1.3365	-0.060	1.8	1.7	0.6	-0.03
Silica	948	1.3380	-0.080	2.3	2.2	1.3	0.02
Pt	1044	1.3402	-0.116	2.1	1.7	0.9	-0.03
Pt	1047	1.3409	-0.141	1.7	1.9	0.9	0.01
Pt-Rh	1146	1.3440	-0.150	2.5	2.3	1.0	0.05
Pt	1153	1.3430	-0.140	2.1	2.1	0.8	-0.03
Pt-Rh	1275	1.3472	-0.145	1.8	2.0	1.9	0.07
Pt-Rh	1275	1.3470	-0.155	2.8	3.3	1.4	0.07
Pt	1285	1.3449	-0.110	1.9	2.2	0.9	-0.11
Pt	1304	1.3447	-0.178	2.4	3.9	2.2	-0.15
Pt-Rh	1457	1.3495	-0.200	2.3	3.8	1.5	0.02
Pt	1530	1.3512	-0.288	1.5	3.3	0.9	0.07

Standard deviation of the ratios from the smoothed curve = 0.08 %

Neon/Nitrogen Ratios

The following equation was fitted to the values of 1/Intercept.

$\log \eta\ (Ne)/\eta\ (N_2) = 0.024072 \log T + 10.50365/T + 591.453/T^2 + 0.148377$

Neon has the larger slip coefficient so the ratios $t(N_2)/t(Ne)$ were plotted.

Cap	T°K	1/Int	Int	Slope	SD-P	SD-S	SD-I	%
Pt	293	1.7795	0.56190	0.070	0.6	1.0	0.8	0.05
Pt.Rh	293	1.7750	0.56339	0.073	0.7	1.0	0.7	0.30
Pt-Rh	293	1.7797	0.56190	0.079	0.9	0.7	0.7	0.05
Silica	293	1.7892	0.55888	0.077	0.7	0.4	0.4	0.49
Silica	373	1.7494	0.57161	0.097	0.8	0.7	0.4	0.04
Silica	474	1.7278	0.57876	0.144	1.3	1.2	0.6	-0.02
Silica	566	1.7166	0.58254	0.149	1.2	1.5	0.7	-0.08
Silica	673	1.7150	0.58300	0.255	0.9	0.7	0.4	0.21
Pt-Rh	801	1.7030	0.58715	0.330	1.5	1.9	0.9	-0.25
Silica	803	1.7100	0.58485	0.270	1.0	0.8	0.4	0.16
Pt-Rh	804	1.7020	0.58760	0.326	1.5	1.4	0.7	-0.30
Silica	948	1.7140	0.5834	0.366	0.8	0.7	0.4	0.52
Pt-Rh	1059	1.7010	0.158800	0.550	1.8	3.1	1.2	-0.21
Pt-Rh	1273	1.7040	0.58740	0.660	1.7	2.8	1.1	-0.06
Pt-Rh	1503	1.7070	0.58558	0.928	2.4	4.5	1.9	0.03

Standard deviation of the ratios from the smoothed curve = 0.23%

Neon/Helium Ratios

The intercepts were fitted to the following equation

$\log \eta (Ne)/\eta (He) = -0.036710 \log T - 4.46558/T - 142.513/T^2 + 0.362260$

where T lies between 293-1300°K

Cap	T°K	Int	Slope	SD-P	SD-S	SD-I	%
Pt	293	1.6050	0.080	3.0	1.7	1.1	0.00
Pt-Rh	293	1.6047	0.133	2.9	1.6	1.0	0.00
Silica	293	1.6081	0.093	2.9	1.5	1.0	0.19
Silica	373	1.5964	0.164	2.7	2.2	1.2	-0.06
Silica	474	1.5879	0.286	3.6	3.2	1.6	0.08
Silica	566	1.5762	0.352	4.0	3.6	2.4	0.03
Silica	673	1.5675	0.420	1.3	1.3	0.7	0.06
Pt-Rh	801	1.5573	0.844	4.8	5.7	2.5	0.13
Silica	803	1.5550	0.570	3.2	2.6	1.2	-0.15
Pt-Rh	804	1.5548	0.795	4.8	4.2	1.9	-0.01
Silica	948	1.5490	0.650	3.0	2.6	1.4	-0.05
Pt-Rh	1278	1.5230	1.044	4.1	7.0	2.7	0.02

Standard deviation from the smoothed curve = 0.09%

Krypton/Nitrogen Ratios

The intercepts were fitted to the following equation:

$$\log \eta (Kr)/\eta (N_2) = -0.032623 \log T - 39.7811/T + 2694.75/T^2 + 0.339326$$

Cap	T°K	Int	Slope	SD-P	SD-S	SD-I	%
Silica	293	1.4259	0.010	1.4	0.9	0.9	-0.08
Silica	373	1.4744	-0.026	2.1	1.8	1.1	0.11
Silica	474	1.5115	0.052	0.9	1.2	1.0	-0.17
Silica	566	1.5407	0.051	1.6	1.5	1.0	0.01
Pt	791	1.5838	0.019	1.9	2.7	1.4	-0.20
Silica	803	1.5809	0.085	2.1	2.2	1.6	-0.07
Pt	926	1.5980	0.061	2.8	3.2	1.3	0.19
Silica	948	1.5940	0.096	2.4	2.7	2.2	-0.17
Pt	1044	1.6026	0.153	2.2	3.1	1.6	-0.09
Pt	1153	1.6122	0.112	3.3	3.6	1.5	0.10
Pt-Rh	1275	1.6128	0.206	2.2	5.1	2.5	-0.20
Pt	1288	1.6163	0.132	1.8	2.7	1.5	-0.02
Pt-Rh	1457	1.6242	0.161	0.9	2.1	1.2	0.13
Pt	1530	1.6244	0.134	2.7	16.9	5.7	0.02

Standard deviation from the smooth curve = 0.12%

Xenon/Nitrogen Ratios

The intercepts were fitted to the following equation:

$$\text{Log } \eta(Xe)/\eta(N_2) = -0.022589 \log T - 57.1777/T + 4082.66/T^2 + 0.31673$$

Cap	T°K	Int	Slope	SD-P	SD-S	SD-I	%
Silica	293	1.3008	0.024	1.9	2.6	3.2	0.17
Silica	373	1.3652	-0.009	0.8	1.4	1.3	0.11
Silica	474	1.4216	0.123	2.4	2.2	1.2	-0.12
Silica	566	1.4661	0.127	2.7	2.6	1.6	-0.02
Pt	791	1.5374	0.184	1.4	2.0	1.0	0.29
Silica	803	1.5371	0.128	1.4	1.5	1.0	0.10
Pt	926	1.5628	0.260	2.2	2.4	1.0	0.27
Silica	948	1.5575	0.313	1.1	2.7	1.4	-0.29
Pt	1044	1.5739	0.421	2.0	2.9	1.5	-0.13
Pt	1153	1.5908	0.391	2.9	3.3	1.4	0.13
Pt-Rh	1275	1.5995	0.473	1.4	3.2	1.6	-0.11
Pt	1288	1.5986	0.482	1.8	2.6	1.3	-0.18
Pt	1304	1.5988	0.539	1.6	2.9	1.8	-0.26
Pt-Rh	1457	1.6149	0.557	2.4	5.6	3.0	0.04
Pt	1530	1.6235	0.527	3.0	18.5	6.3	0.29

Standard deviation of the ratios from the smoothed curve = 0.20%

Specimen Calculation for the Standard Method

The determination of the ratio He(1153°K)/He(293°K) using the platinum capillary will be given in full as a typical example.

Equation (4.25) is used. The corrections for gas imperfection and kinetic energy effects are all less than 0.05%, so are neglected. The times of flow are given in Appendix 5. The ratio t(293)/t(1153) vs. $1/\bar{P}$ is shown in figure (4.3) together with the computer analysis. The ratio is plotted this way round so that the smaller slip correction (i.e. that at 293°K) is the one expanded by the binomial expansion. The intercept is 0.10049 with a standard deviation of 0.00016.

From (4.25), the intercept is $$\frac{\eta_0 T_0 (1 + 3\alpha(T_c' - T))}{\eta' T' (1 + 3\alpha(T_c' - T))}$$

Thus $$0.10049 = \frac{\eta_{293}}{\eta_{1183}} \times \frac{293}{1153} \times 1.0260$$

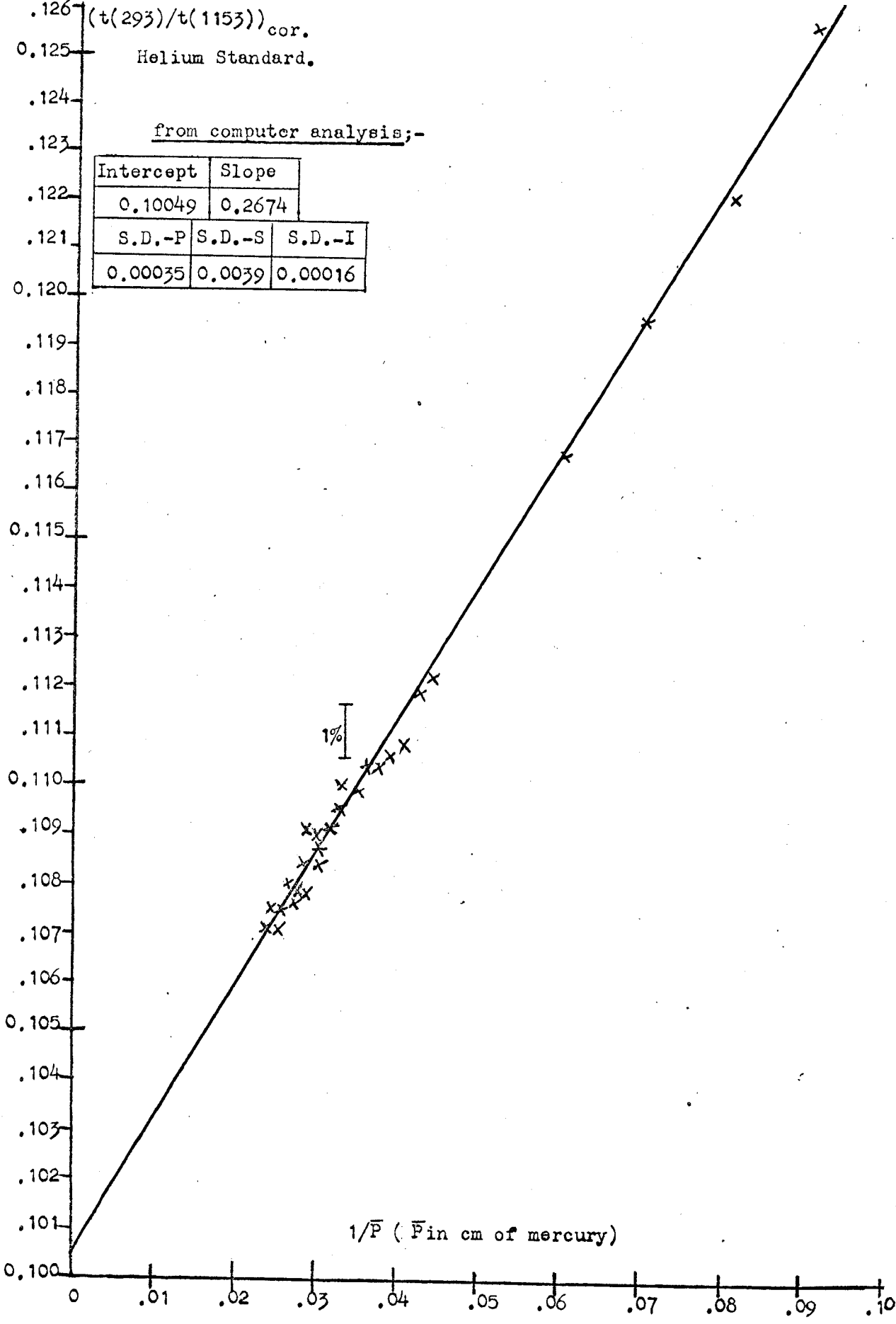
using the value of the expansion coefficient given in (4.27).

Hence

$$\frac{\eta_{1183}}{\eta_{293}} = 2.59_7 = 2.60 \pm .005.$$

It must be noted that the accuracy of the determination depends on the accuracy with which the temperature is known.

The following tables give the computer analysis for the standard calculation for the times of flow given in Appendix 5, corrected as described in the last section. The calculations were performed with each temperature in turn as the standard temperature. The agreement between the direct calculation of $\eta(T_1)/\eta(T_2)$ and the indirect calculation through, for example,



Figure(4.3) The Plot of (t(293)/t(1153))Helium vs $1/\bar{P}$

$\frac{\eta(T_1)}{\eta(T_3)} \times \frac{\eta(T_3)}{\eta(T_4)} \times \frac{\eta(T_4)}{\eta(T_2)}$ was better than 0.5% in all cases and in most within 0.2%. This indirect method was used to estimate the ratio $\eta(T)/\eta(293)$ when there were not sufficient data for the direct calculation. These calculations are shown in the 7th column by the two figures: the top figure is the ratio indicated in column 1 and the bottom figure is the ratio $\frac{\eta(T)}{\eta 293} = \frac{\eta(T)}{\eta(T_1)} \times \frac{\eta(T_1)}{\eta 293}$.

The ratios $\eta(T)/\eta(293)$ were fitted to the polynomial function ($\log N \equiv \log_{10} N$)

$$\text{Log (Ratio)} = A \log T + B/T + C/T^2 + D$$

by the method of least squares using the University computer KDF9 programme STAT 15. The coefficients are given at the top of each page. As seen in the last column of the tables, there are a few ratios deviating by over 0.5% from this curve, due probably to slight temperature errors (discussed in a later section). These ratios make the standard deviation given at the bottom of each table fairly large.

The tables give information similar to that given in the relative tables. The intercepts are for $\eta(T_1)/\eta(T_2)$ where $T_{(1)}$ is the lower temperature and the ratio column is for $\eta(T_2)/\eta(T_1)$. The final column gives the % difference between the calculated value using the polynomial at the head of the table and the experimental value.

Nitrogen Standard Ratios

The standard ratios η (T)/ η (293) were fitted to the equation

$$\log (\text{Ratio}) = 0.661586 \log T + 17.7886/T - 5639.68/T^2 - 1.627077$$

Temp. Ratio	Int	Slope	SD-P	SD-S	SD-I	Ratio	%
Pt Capillary							
793/293	0.1877	0.036	0.7	0.8	0.6	1.997	-0.79
926/293	0.1439	0.071	0.3	0.4	0.3	2.240	0.02
1044/293	0.1193	0.063	0.2	0.2	0.2	2.404	-0.39
1047/293	0.1172	0.077	0.3	0.5	0.4	2.420	0.26
1131/293	0.1009	0.067	0.2	0.3	0.2	2.563	0.43
1285/293	0.0833	0.060	0.4	0.6	0.4	2.756	0.00
1304/793	0.4456	0.280	2.1	3.7	1.8	1.387	
						2.771	-0.41
1330/926	0.4476	0.193	1.5	2.9	0.8	1.375	
						3.080	-0.12
Pt.Rh Capillary							
799/292	0.1837	0.041	0.4	0.3	0.2	2.018	
						2.010	-0.79
800/293	0.1834	0.060	0.4	0.2	0.2	2.027	-0.13
1146/293	0.1023	0.075	0.2	0.3	0.2	2.562	0.15
1275/293	0.0861	0.071	0.2	0.3	0.2	2.745	0.31
1144/800	0.5624	0.149	1.2	2.1	0.9	1.260	
						2.554	-0.03
1457/800	0.3828	0.258	0.7	1.3	0.6	1.466	
						2.980	-0.26
804/293	0.1811	0.093	0.1	0.2	0.2	2.042	0.28
1059/804	0.6437	0.129	1.5	2.6	1.1	1.189	
						2.428	-0.07
1273/804	0.4777	0.225	1.0	1.6	0.7	1.343	
						2.744	0.05
1505/804	0.3641	0.260	1.6	3.6	1.7	1.501	
						3.065	0.29

Silica Capillary							
373/293	0.6515	0.032	1.3	1.3	1.0	1.205	-0.11
474/293	0.4315	0.061	1.3	1.3	1.0	1.433	-0.05
566/293	0.3197	0.061	1.2	1.2	0.9	1.620	0.36
673/293	0.2397	0.058	1.2	1.5	1.3	1.817	0.23
803/293	0.1785	0.065	0.8	0.8	0.6	2.046	0.48
948/366	0.4258	0.113	1.4	1.4	0.9	$\frac{1.403}{2.275}$	0.50

Standard deviation of points from smooth curve = 0.35 %

Helium Standard Ratios

The standard ratios $\eta(T)/\eta(293)$ were fitted to the equation

$$\log(\text{Ratio}) = 0.759644 \log T + 32.3787/T - 3965.49/T^2 - 1.93824$$

Temp. Ratio	Int	Slope	SD-P	SD-S	SD-I	Ratio	%
Pt Capillary							
793/293	0.1888	0.181	0.9	0.8	0.4	1.986	0.04
926/293	0.1449	0.272	0.5	0.7	0.3	2.226	0.18
1044/293	0.1191	0.242	0.6	0.3	0.2	2.407	-0.07
1047/293	0.1178	0.277	0.4	0.5	0.2	2.429	0.17
1153/293	0.1005	0.267	0.3	0.3	0.2	2.594	0.14
1285/293	0.0838	0.236	0.3	0.3	0.2	2.804	0.23
1304/293	0.0817	0.268	0.2	0.3	0.2	2.837	0.54
1530/926	0.4326	0.902	0.9	1.8	0.5	$\frac{1.423}{3.165}$	-0.10
Pt-Rh Capillary							
799/292	0.1849	0.126	0.5	0.3	0.2	$\frac{2.018}{2.013}$	0.40
800/293	0.1849	0.175	0.6	0.3	0.2	2.010	0.43
1146/293	0.1021	0.208	0.6	0.7	0.3	2.569	-0.41
1144/293	0.1026	0.184	0.2	0.4	0.2	2.560	-0.48
1275/293	0.0848	0.202	0.4	0.5	0.2	2.790	0.20
1457/293	0.0684	0.236	0.3	0.5	0.2	3.050	-0.08
801/293	0.1851	0.248	0.4	0.4	0.3	1.999	-0.20
1273/293	0.0862	0.254	0.2	0.5	0.2	2.762	-0.37
801/293	0.1869	0.255	0.6	0.5	0.3	1.987	-0.65

Silica Capillary							
373/293	0.6629	0.071	1.0	0.8	0.4	1.185	0.02
474/293	0.4433	0.150	1.3	1.2	0.6	1.395	-0.11
566/293	0.3277	0.141	0.9	0.7	0.4	1.580	0.21
673/293	0.2452	0.177	1.0	0.9	0.5	1.776	-0.04
803/293	0.1815	0.174	0.7	0.6	0.3	2.012	0.17
948/293	0.1368	0.181	1.1	1.1	0.7	2.260	0.30

Standard deviation of the ratios from the smooth curve = 0.29 %

Argon Standard Ratios

The standard ratios η (T)/ η (293) were fitted to the equation

log (Ratio) = 0.638420 log T - 6.93683/T - 3374.72/T^2 - 1.51196

Temp.Ratio	Int	Slope	SD-P	SD-S	SD-I	Ratio	%
Pt Capillary							
793/293	0.1789	0.048	1.6	6.9	2.7	2.096	-0.60
926/293	0.1372	0.065	0.3	0.4	0.3	2.350	0.12
1044/293	0.1133	0.068	0.3	0.4	0.3	2.532	-0.15
1047/293	0.1115	0.074	0.2	0.4	0.3	2.565	0.45
1153/293	0.9568	0.070	0.3	0.6	0.4	2.725	0.08
1288/923	0.8134	0.087	0.2	0.5	0.4	2.889	-0.68
1804/793	0.4357	0.428	2.3	14.7	5.7	1.418 2.960	0.50
1530/926	0.4422	0.297	0.8	1.9	0.5	1.392 3.270	0.15
Pt-Rh Capillary							
799/293	0.1736	0.048	0.3	0.3	0.3	2.120	-0.15
800/293	0.1749	0.063	0.4	0.3	0.2	2.124	-0.26
1146/293	0.0969	0.070	0.3	0.4	0.2	2.707	-0.25
1273/293	0.0812	0.074	0.4	0.6	0.3	2.910	0.18
1457/800	0.3786	0.270	1.6	2.0	0.9	1.482 3.150	0.39

Silica Capillary							
373/293	0.6412	0.028	1.7	1.5	1.1	1.221	-0.15
474/293	0.4208	0.058	1.4	1.4	0.9	1.469	0.02
566/293	0.3087	0.062	1.3	1.2	0.8	1.677	0.30
673/293	0.2296	0.067	1.8	2.2	1.9	1.987	0.17
803/293	0.1707	0.063	1.3	1.4	1.1	2.139	0.18
948/566	0.4192	0.127	1.6	1.8	1.4	$\frac{1.424}{2.396}$	0.22

Standard deviation of the points from the smooth curve = 0.32%

Neon Standard Ratios

The standard ratios η (T)/ η (293) were fitted to the equation

log (Ratio) = 0.62959 log T - 5.01472/T - 186.203/T^2 - 1.53381

Temp.Ratio	Int	Slope	SD-P	SD-S	SD-I	Ratio	%
Pt-Rh Capillary							
804/293	0.1897	0.182	0.8	1.0	0.5	1.950	0.29
1059/293	0.1228	0.180	0.5	1.1	0.5	2.305	-0.48
1273/293	0.0909	0.180	0.3	0.7	0.3	2.162	-0.06
1505/293	0.0694	0.182	0.4	0.9	0.4	2.923	0.13
801/293	0.1916	0.172	1.0	1.0	0.5	1.938	-0.08
Silica Capillary							
373/293	0.6676	0.048	1.5	1.2	0.6	1.177	0.06
474/293	0.4489	0.096	1.8	1.6	0.8	1.377	-0.11
566/293	0.3342	0.094	1.0	1.4	0.9	1.550	-0.02
673/293	0.2515	0.125	1.2	1.1	0.7	1.732	-0.06
803/293	0.1877	0.123	1.0	0.9	0.5	1.945	0.11
948/293	0.1427	0.130	1.0	1.0	0.6	2.167	0.23

Standard deviation of points from smooth curve = 0.21%

Summary Table - (4-1)

The Coefficients for the Smoothed Curves

The equation used was

$\log_{10}(\text{Ratio}) = A \log_{10} T + B/T + C/T^2 + D$

and was fitted by least squares analysis to the data given in the previous tables.

Ratio	A	B	C	D
Relative Ratios				
He/N_2	0.1217705	31.9901	-1139.198	-0.3510326
Ne/N_2	0.0240717	10.5036	591.4527	0.1483773
Ne/He	-0.0367095	-4.465581	-142.515	0.3622598
Ar/N_2	0.0017333	-9.410934	95.82634	0.1310053
Kr/N_2	-0.0326233	-39.78117	2694.757	0.3393269
Xe/N_2	-0.0225894	-57.17776	4082.663	0.316731
Standard Ratios				
$N_2(T)/N_{293}$	0.6615863	17.78868	-5639.681	-1.627077
$He(T)/He_{293}$	0.7596445	32.37878	-3965.492	-1.938237
$Ne(T)Ne_{293}$	0.6295918	-5.01472	-186.2027	-1.53381
$Ar(T)/Ar_{293}$	0.6384201	-6.936534	-3374.716	-1.511957
$Kr(T)Kr_{293}$*	0.628963	-21.99249	-2944.924	-1.44248
$Xe(T)Xe_{293}$*	0.638997	-39.48908	-1557.018	-1.424289

* calculated using the relation $\frac{Kr(T)}{Kr(293)} = \frac{N_2(T)}{N_2(293)} \frac{N_2(293)}{Kr(293)} \frac{Kr(T)}{N_2(T)}$, and similarly for Xe.

so $\log(\text{Ratio}) = \log(N_2(T)/N_2(293)) - \log Kr(293)/N_2(293) + \log Kr(T)/N_2(T)$

where $\log Kr(293)/N_2(293) = \log 1.428 = 0.154728$, and $\log Xe(293)/N_2(293) = \log 1.300 = 0.113943$.

Summary Table - (4-2)

Ratios Relative to Nitrogen calculated by the Smoothed Curves

°K	He/N_2	Ne/N_2	Ne/He	A/N_2	Kr/N_2	Xe/N_2
293	1.1098	1.7800	1.6050	1.2700	1.4271	1.3000
300	1.1081	1.7766	1.6044	1.2735	1.4317	1.3048
400	1.0931	1.7417	1.5946	1.2960	1.4854	1.3821
500	1.0890	1.7247	1.5838	1.3099	1.5223	1.4379
600	1.0900	1.7155	1.5735	1.3195	1.5484	1.4792
700	1.0934	1.7103	1.5640	1.3264	1.5674	1.5105
800	1.0982	1.7073	1.5553	1.3318	1.5816	1.5348
900	1.1037	1.7057	1.5474	1.3359	1.5925	1.5542
1000	1.1095	1.7049	1.5400	1.3393	1.6009	1.5699
1100	1.1155	1.7046	1.5332	1.3421	1.6076	1.5828
1200	1.1215	1.7048	1.5270	1.3445	1.6129	1.5935
1300	1.1274	1.7052	1.5211	1.3466	1.6171	1.6026
1400	1.1333	1.7058		1.3483	1.6205	1.6103
1500	1.1390	1.7065		1.3498	1.6233	1.6169
1600	1.1447	1.7073		1.3512	1.6255	1.6226

Summary Table - (4-3)

The Standard Ratios calculated by the Smoothed Curves

	N_2	He	Ne	Ar	Kr*	Xe*
293	1.0000	1.0000	1.0000	1.0000	1.0000	1.0000
300	1.0195	1.0171	1.0162	1.0206	1.0221	1.0232
400	1.2695	1.2432	1.2323	1.2906	1.3204	1.3496
500	1.4843	1.4484	1.4277	1.5266	1.5823	1.6418
600	1.6783	1.6410	1.6084	1.7407	1.8198	1.9096
700	1.8582	1.8246	1.7778	1.9390	2.0396	2.1590
800	2.0276	2.0014	1.9381	2.1256	2.2457	2.3938
900	2.1887	2.1727	2.0909	2.3025	2.4409	2.6167
1000	2.3432	2.3393	2.2374	2.4716	2.6270	2.8297
1100	2.4921	2.5019	2.3785	2.6340	2.8054	3.0342
1200	2.6361	2.6611	2.5147	2.7907	2.9773	3.2313
1300	2.7758	2.8170	2.6468	2.9424	3.1434	3.4220
1400	2.9119	2.9702	2.7751	3.0896	3.3044	3.6069
1500	3.0445	3.1208	2.8999	3.2328	3.4608	3.7867
1600	3.1741	3.2691	3.0217	3.3725	3.6131	3.9618

*See Summary Table (4-1)

Summary Table - (4-4)

The Viscosities calculated by the Standard Method (x 10^{-6} g cm^{-1} sec^{-1})

The viscosities were calculated from Summary Table 4-3 using literature values for η (293) (see Appendix 7).

	N_2	He	Ne	Ar	Kr*	Xe*
293	175.7	196.0	313.8	222.8	250.8	228.4
300	179.1	199.3	318.9	227.4	256.3	233.7
400	223.0	243.7	386.7	287.6	331.2	308.2
500	260.8	283.9	448.0	340.1	396.8	375.0
600	294.9	321.6	504.7	387.8	456.4	436.2
700	326.5	357.6	557.9	432.0	511.5	493.1
800	356.2	392.3	608.2	473.6	563.2	546.8
900	384.6	425.9	656.1	513.0	612.2	597.7
1000	411.7	458.5	702.1	550.7	658.9	646.3
1100	437.9	490.4	746.4	586.9	703.6	693.0
1200	463.2	521.6	789.1	621.8	746.7	738.0
1300	487.7	552.1	830.6	655.6	788.4	781.6
1400	511.6	582.2	870.8	688.4	828.7	823.8
1500	534.9	611.7	910.0	720.3	868.0	864.9
1600	557.7	640.7	948.2	751.4	906.2	904.9

*See Summary Table (4-1)

Summary Table - (4-5)

Viscosities Relative to Nitrogen (x 10^{-6} g cm^{-1} sec^{-1})

The viscosities were calculated from Summary Table(4-2), using the standard N_2 values given in Summary Table (4-4).

	N_2 (Standard)	He	Ne	Ar	Kr	Xe
290	175.7	195.0	312.7	223.1	230.7	228.4
300	179.1	198.4	318.2	228.1	236.5	233.7
400	223.0	243.8	388.5	289.1	331.3	308.3
500	260.8	284.0	449.8	341.6	397.0	375.0
600	294.9	321.4	505.9	389.1	456.6	436.2
700	326.5	357.0	558.4	433.1	511.7	493.1
800	356.2	391.2	608.2	474.4	563.4	546.8
900	384.6	424.4	653.9	513.8	612.4	597.7
1000	411.7	456.8	701.9	551.4	659.1	646.3
1100	437.9	488.4	746.4	587.7	703.9	693.0
1200	463.2	519.4	789.6	622.7	747.0	738.1
1300	487.7	549.9	831.6	656.7	788.7	781.6
1400	511.6	579.8	872.7	689.8	829.1	823.9
1500	534.9	609.3	912.8	722.1	868.3	864.9
1600	557.7	638.4	952.1	753.5	906.5	904.9

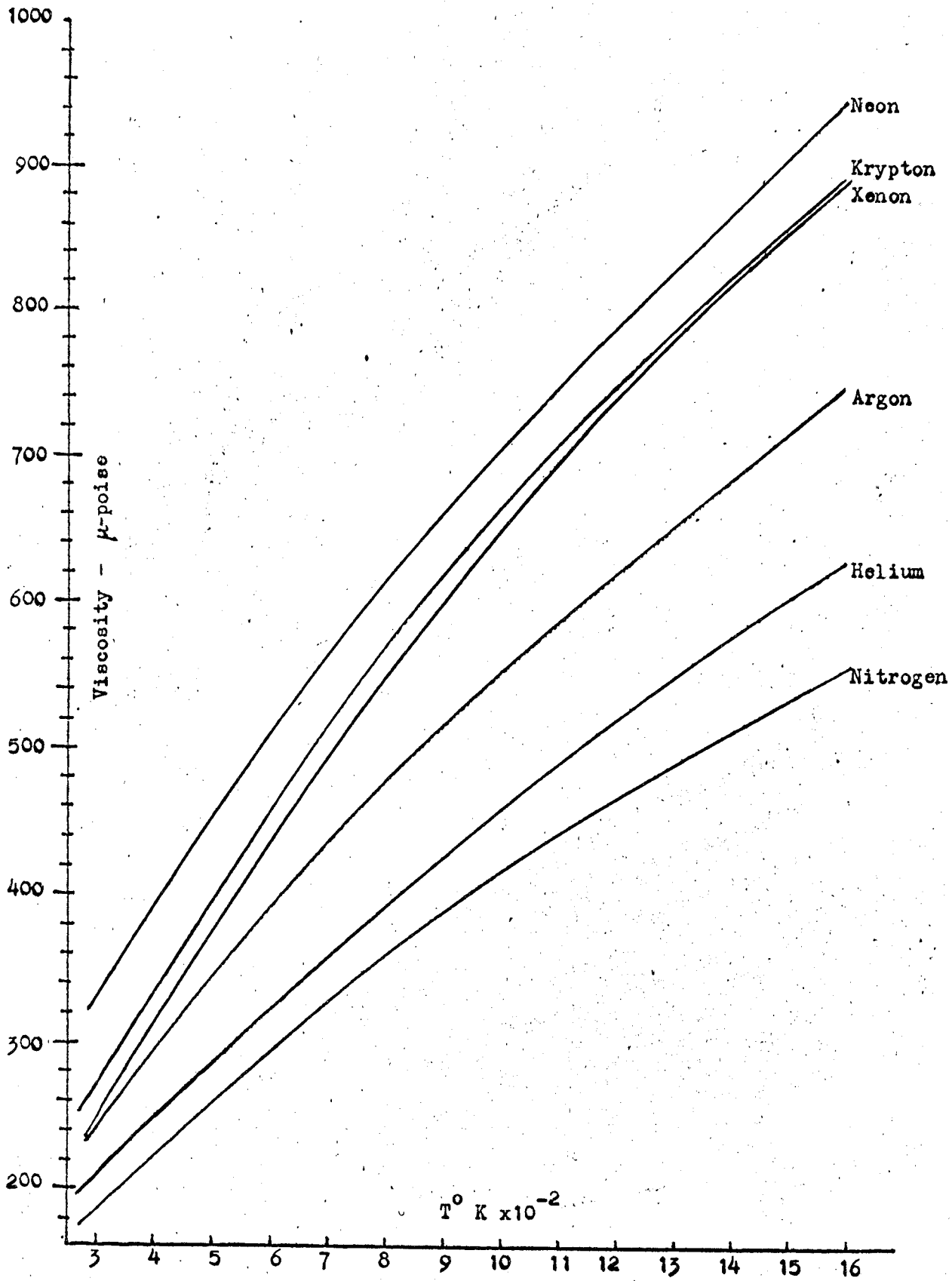
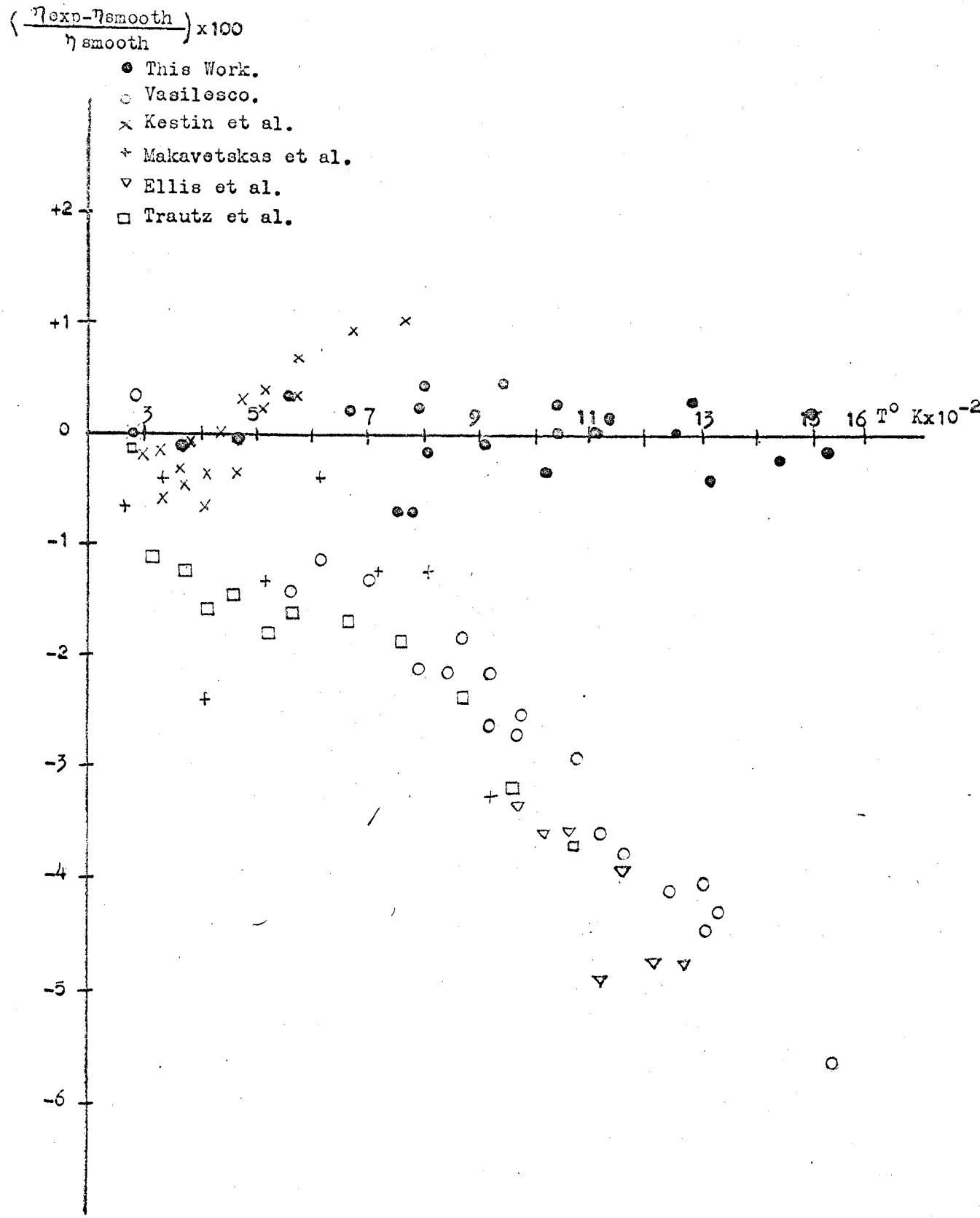
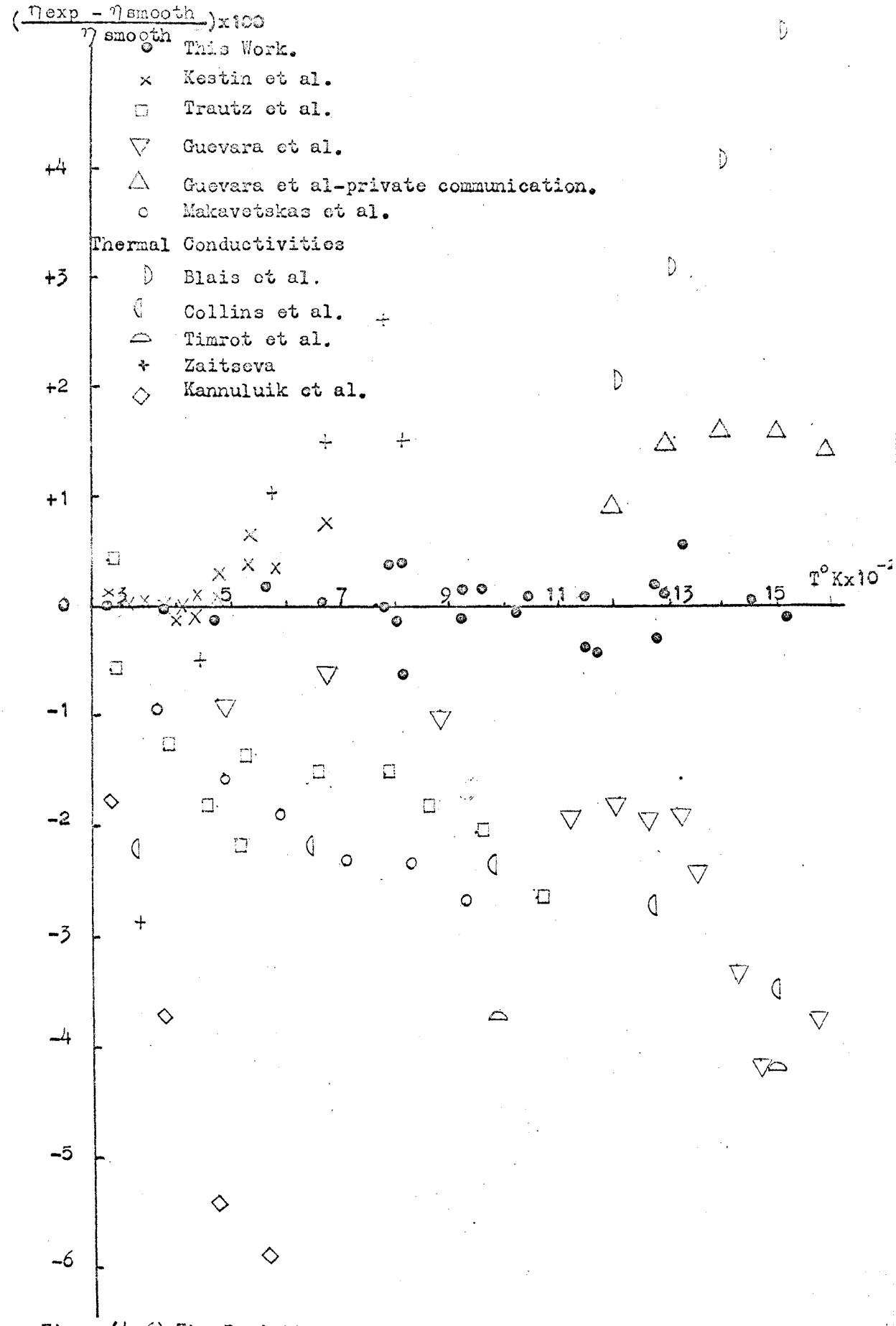


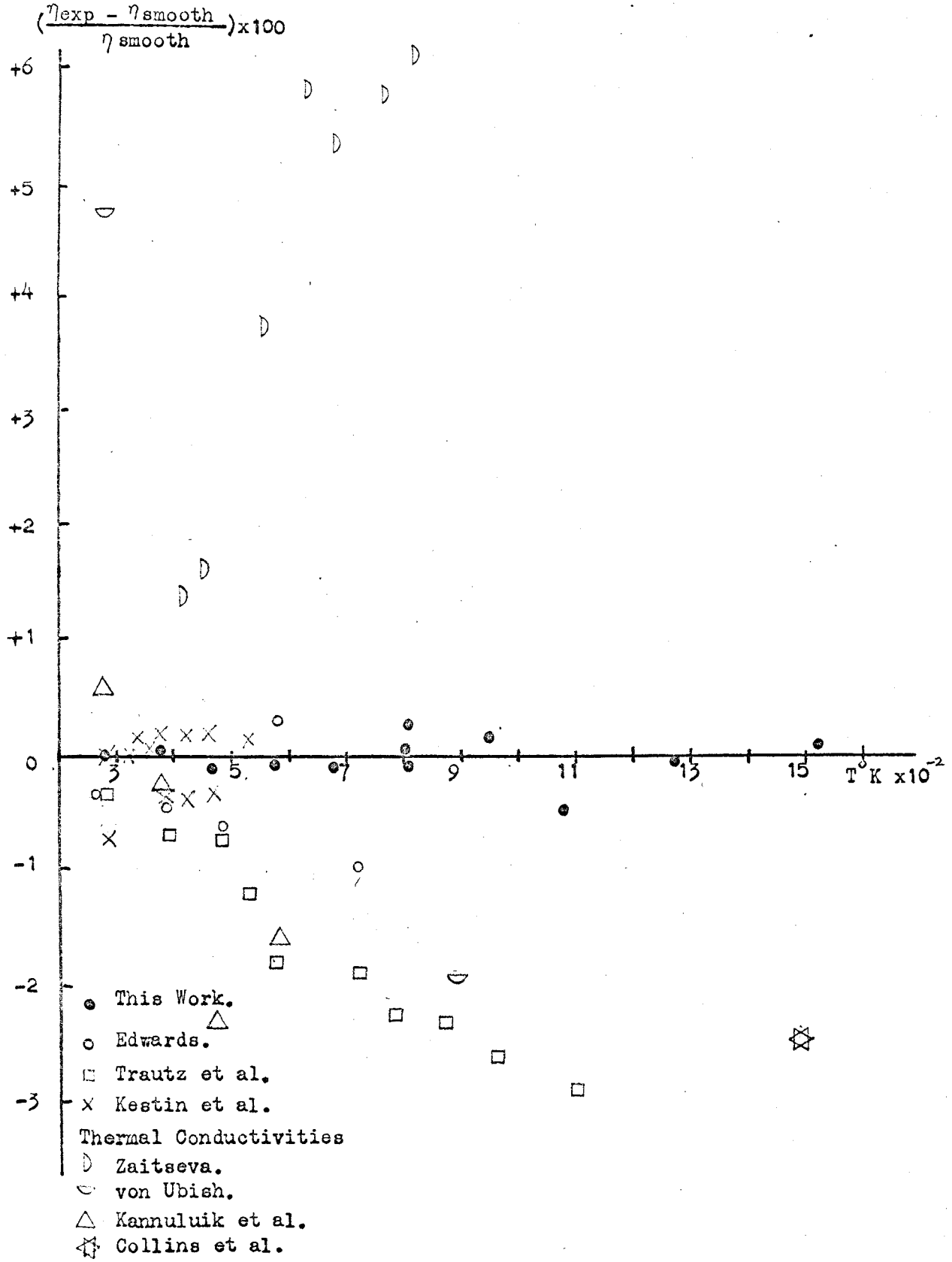
Figure (4.4) The Viscosities of the Gases studied.
(taken from the smooth curves)



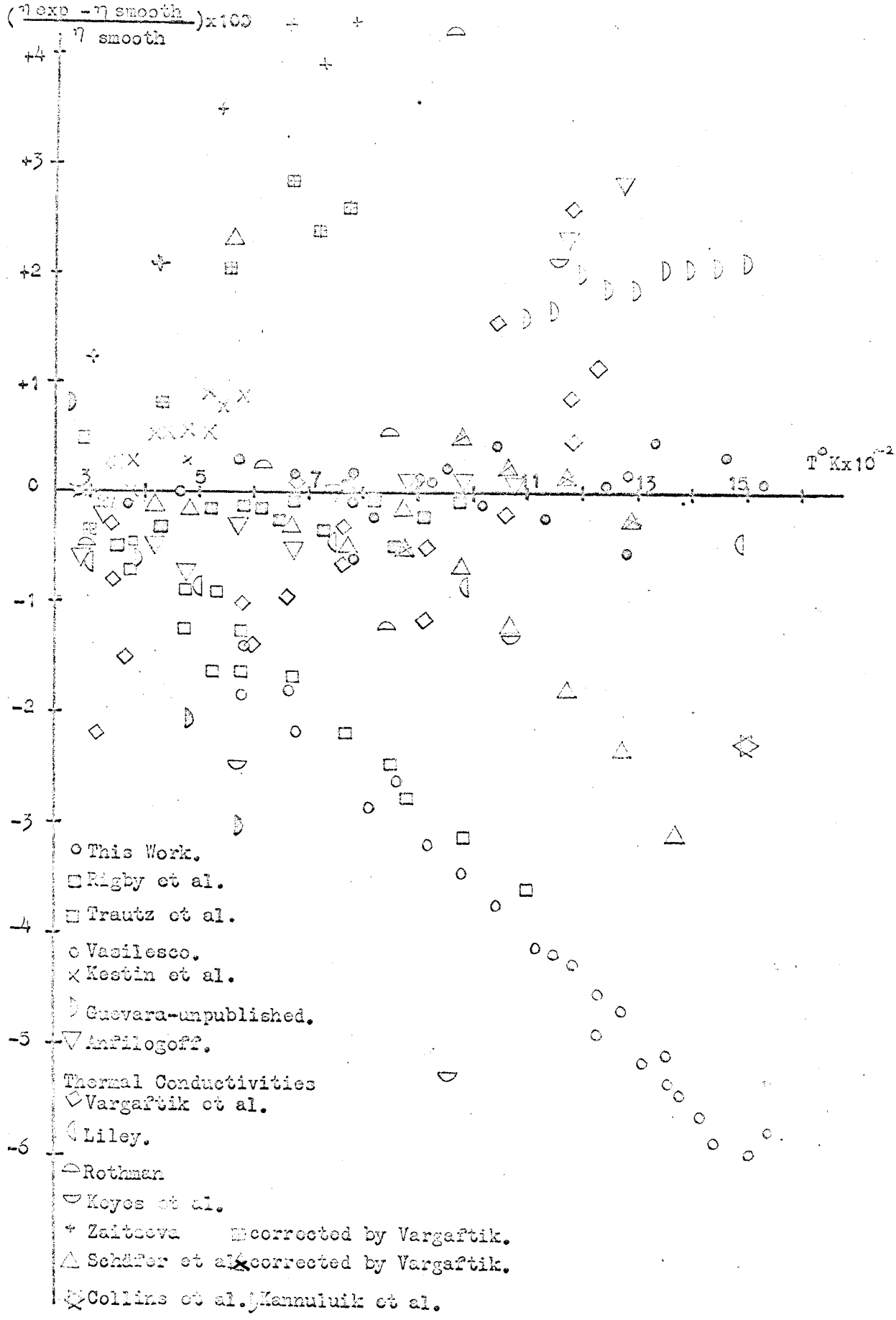
Figure(4.5) The Deviation of Nitrogen Data from the Smooth Curve of This Work.



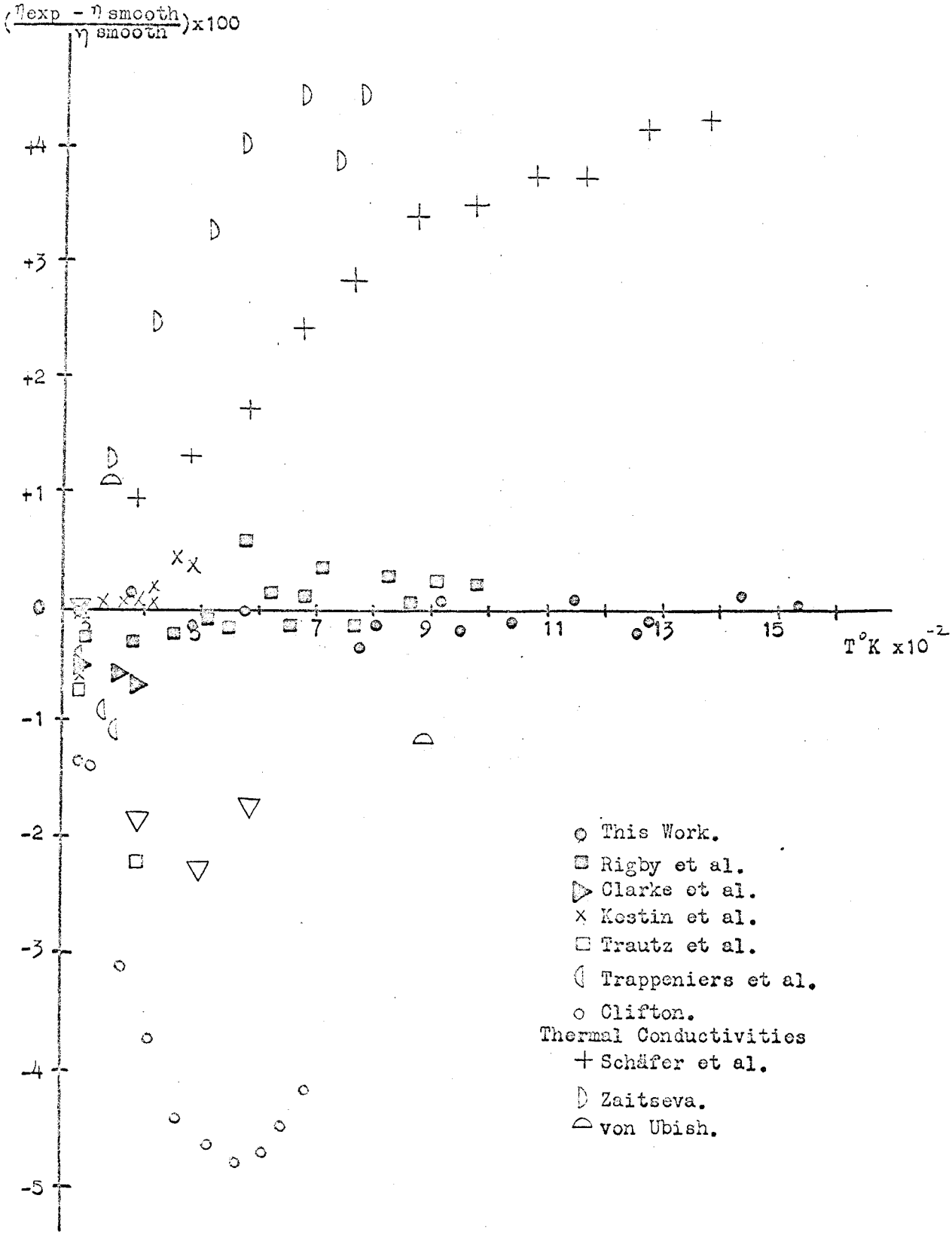
Figure(4.6) The Deviation of Helium Data from the Smooth Curve of This Work



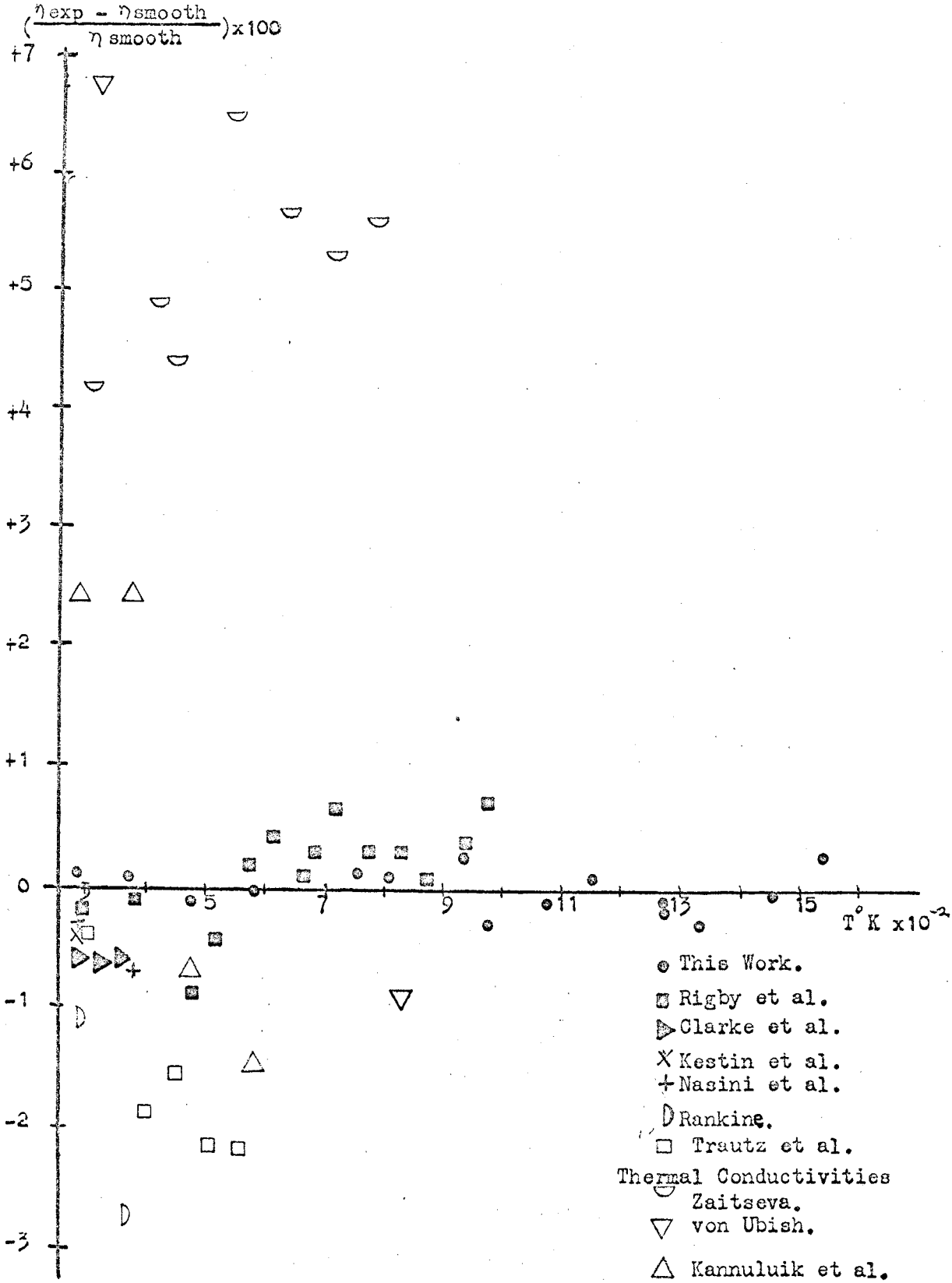
Figure(4.7) The Deviation of Neon Data from the Smooth Curve of This Work.



Figure(4.8) The Deviation of Argon from the Smooth Curve of This Work



Figure(4.9) The Deviation of Krypton from the Smooth Curve of This Work.



Figure(4.10) The Deviation of Xenon Data from the Smooth Curve of This Work.

A Comparison with other Data

The values of the viscosities of nitrogen, helium, neon, argon, krypton and xenon in the temperature range 293–1600°K as given by the smoothed curves are presented in Summary Tables (4–4) and (4–5). If the accepted standard values at 293°K for table (4–4) or the accepted standard nitrogen viscosities (based on η (293) for nitrogen being 175.7 μ-poise) should subsequently be redetermined, the values in these tables may easily be recalculated by multiplying the ratios of Tables (4–2) and (4–3) by the new standard. A discussion of the errors and accuracy expected in this work appears in the next section.

Values of the viscosity coefficient for the rare gases and nitrogen reported in the literature are given in Appendix 7. Where necessary the data have been adjusted if the standard used by the author differed from that used here. The published and corrected data and the percentage difference between them and the values established in this work are given. High temperature thermal conductivity data have also been surveyed, since the rare gas values can easily be converted using equation (2.32) into the corresponding viscosity values. As can readily be seen the data are not very reliable. Figures (4–4) - (4–10) show the smoothed curves and the differences between the smoothed values and the data of some other workers. Many determinations have been made in the temperature range between room temperature and 373°K. Such data, if obtained prior to 1930, are not included in the figures or further discussion, although they are tabulated in Appendix 7 together with percentage deviations from the smooth curves.

There are few data which extend over a wide temperature range. The work of Vasilesco (see Appendix 7 for source in the literature) and of Trautz and his co-workers for argon and nitrogen have, until recently, been regarded as authoritative but in the last few years doubt has been cast on their accuracy, although no experimental evidence has been produced to support this view. The new data reported in this work show unequivocally that the results of Trautz and Vasilesco are

too low at high temperatures. The relative viscosities of Rigby and Smith up to 972°K are the only values reported for krypton and xenon at these temperatures. Guevara et al. are in the process of reporting their high temperature work up to 2000°K using a very short molybdenum capillary. Their preliminary results for helium and argon seem to be in good agreement with this work. All the above workers have used capillary-flow methods. DiPippo and Kestin are developing an oscillating disc technique and at present they have reported data up to 773°K in close agreement with this work. However the difficulties of the torsion fibre have not yet been fully overcome so higher temperatures have not been attempted.

The values obtained from the literature given in Appendix 7 will now be critically compared with the results presented in Table (4-5), although no reasons for any discrepancy can be put forward with confidence. The viscosities for each gas will be considered separately and finally a brief critique of the thermal conductivity data will be given.

Nitrogen

Following a suggestion by Kestin (133), nitrogen is used here as the standard gas, so its value needs to be known with very great accuracy. There are, however, very few data above 470°K with which to compare the values obtained in this work.

Kestin and Whitelaw* using a high pressure oscillating disc viscometer give data up to 538°K. At this temperature they have a value higher than that given by our smooth curve by 0.7%. DiPippo and Kestin using a low pressure oscillating disc differ by only 0.3% from the curve at this temperature, although at their maximum temperature of 773°K they differ from it by 1.0%. The results at high temperatures most often quoted were obtained by Trautz and Zink (to 1098°K) and Vasilesco (to 1695°K), both using low pressure capillary-flow techniques. Their results deviate

---

* See Appendix 7 for values and references.

systematically from this work so that at 1098°K Trautz et al. differ by -3.7%, and at 1564°K Vasilesco differs by -5.5%. They differ from each other at 1098°K by about 1%. No definite reasons for these discrepancies can be given but incomplete correction for curved pipe flow effects may contribute to Vasilesco's difference. The data of Ellis and Raw between 973°K and 1273°K vary between 3.2% and 4.8% lower than the work reported here. The results of Clarke and Smith to 373°K agree to within 0.35% of our curve i.e. within their experimental error. The high temperature work of Makovetskas using a high pressure capillary is within 3.5% of our smooth curve, which is within their estimated accuracy.

The value of N_2 taken from the literature as the standard value at 293°K is 175.7 μ-poise. This is in agreement with the high precision work of Kestin and Leidenfrost.

Helium

Helium has large slip effects which can cause some inaccuracy in determining the viscosity. Guevara et al. have recently published some very high temperature data up to 2340°K using a very short (0.25 cm) molybdenum capillary, but their results may have some error due to viscous end effects. At 1462°K they are lower than our curve by some 4%. However in a recent private communication they have modified their data considerably as a result of further experimental work, so that at 1500°K they are now 1.6% higher than the data of this work.

The data obtained from the various oscillating disc apparatuses lie within about 0.2% of the values of Table (4-5) except at the highest temperature attained by each instrument, when Kestin and Whitelaw suddenly jump to 0.8% at 520°K and DiPippo and Kestin rise to 1.0% at 673°K. Possibly the experimental difficulties with the torsion wire and the thermal expansion of the structural parts of the apparatus become too great to enable accurate readings to be obtained.

Trautz and Zink deviate systematically from our data and at 1090°K they are

lower by some 2.5%. The Russian workers Makavetskas et al. also differ from our smoothed values by -2.5% at 918°K, but this is within their stated error.

At room temperature (293°K) the standard value of helium has been taken as 196.0 μ-poise in keeping with the supposedly accurate absolute determination of Kestin and Leidenfrost, although this value of helium is higher than the majority of other workers as seen in Appendix 7, and the value at 293°K calculated by the ratio with N_2 is 195.0 μ-poise. The absolute value probably lies between these two.

Argon

The gas most studied is argon and there are many reported data between 293°K and 373°K which will not be discussed here, but the values and sources can be found in Appendix 7.

Trautz et al. and Vasilesco are the major sources of data at high temperatures. They again deviate systematically from our work and at the highest temperatures reached, Trautz (1100°K) differs by -3.5% and Vasilesco (1511°K) by -5.8%. At 1100°K they differ from each other by about 0.7%.

The values obtained by the oscillating disc technique again jump suddenly away from our data at the highest temperatures attained so that at 537°K both the Kestin and Whitelaw, and the DiPippo apparatuses give results which are 0.9% higher than the viscosities in Table (4-5).

Up to 374°K Clarke and Smith agree to within 0.1% of the results in this work whereas De Rocco's results are some 1% lower over most of their temperature range (300°K - 471°K). The work of Anfilogoff up to 1288°K, although not published in full detail except in his Ph.D. thesis, agrees very closely (always within 0.6%) with the results here. This work has received very little attention but seems to be of a high calibre.

Hanley and Childs (11) have quoted the unpublished work of Guevara et al. who used a very short molybdenum capillary. These data seem to be higher than the

work here by some 2%, although the results may be subject to modifications, since the comparatively large corrections for viscous end effects due to the shortness of the capillary may still be incomplete (195,11).

The ratio results of Rigby and Smith up to 972°K are in very close agreement with the present work, lying usually within 0.2%.

The standard value at 293°K is taken as 222.8 μ-poise, which is the value quoted by most workers (Page 34). The value calculated through the N_2 ratio is 223.1 μ-poise in very close agreement.

Neon

There are few data above 500°K for neon. Kestin and Whitelaw and DiPippo, both using oscillating discs, have viscosity values in close agreement with the values reported here at about 500°K. Edwards, using a capillary viscometer, gives values up to 717°K all of which lie within 1% of our curve but Trautz et al., who give values up to 1100°K differ by up to -2.9% from the data of this work.

At the lower temperatures many workers report data, which lie usually within their quoted error of the smooth curve, although Trappeniers deviates at 348°K by some -1.8%.

The standard value taken at 293°K is the value obtained by Kestin and Leidenfrost of 313.8 μ-poise, and the value calculated by the N_2 ratio is 312.7 μ-poise, in good agreement.

Krypton

There are few data above 373°K reported for krypton. Rigby and Smith have given relative viscosities up to 972°K which are, in general, within 0.2% of the smooth curve, and Clarke and Smith give standard viscosities at lower temperatures up to 360°K which agree to within 0.4% of the values in this work. The data of Clifton using an oscillating disc viscometer appear to be in error when compared with our smooth curve by over -4% at his highest temperature 670°K, so confirming the

conclusions of Rigby and Smith. The new data of DiPippo up to 473°K using his high temperature oscillating disc are in close agreement (0.2%) with this work. At the lower temperatures the data of Trappeniers, Trautz and Thornton lie within 1% of the smooth curve.

The standard taken at 293°K is 250.8 μ-poise which is 0.4% higher than the measurements of Kestin and Leidenfrost.

Xenon

There are few reported data for Xe. Trautz and Heberling give data up to 550°K which are lower than the values in Table (4-5) by up to 2.2%, while the high temperature ratios of Rigby and Smith to 972°K are usually better than 0.4% when compared with Table (4-2) although at 453°K the disagreement is -0.8%. At the lower temperatures the ratio viscosities of Clarke and Smith to 360°K lie lower than our curve by some 0.7%.

The value taken as standard at 293°K is 228.4, which is estimated by the N_2 ratio.

Thermal Conductivity Data

Viscosity coefficients have been calculated from thermal conductivity data through (2.32). This simple conversion is satisfactory until more accurate data are available when the factors (2.27) and (2.28) will have to be included.

The data are often inaccurate probably due to incorrect application of the necessary corrections. Vargaftik has modified a number of data for argon by what he considers to be suitable correction factors for temperature jump. These have been marked * in Appendix 7 with a comment to that effect in the last column. The original data are also given and it can be seen that there is better agreement with the smooth curve for argon. Vargaftik's own work is in good agreement with this work, although the variation from the smooth curve is over ±1.5%.

Kannuluik and Carman have measured the thermal conductivities of all the rare gases up to 579°K. The viscosities calculated from their data at 579°K are within 2.5% of the smooth curve except for He where the difference is 5%. Zaitseva, who has reported values for all the rare gases up to 780°K, has been criticised by Vargaftik for inadequate corrections for temperature jump, and has corrected his data for argon by some 2%. The agreement between the uncorrected data and the smooth curves is about 5%, but the corrected data for argon are much better lying less than 3% away from the curve.

The data for helium obtained by Blais and Mann differ by up to 5% from the smooth curve at 1500°K but their data have been criticised by Timrot as being too high, on the grounds that they did not allow for the loss of heat from the ends of the wire. Timrot's own work differs by some -4% compared with our data.

For the rare gases Xe, Kr and Ne there are few thermal conductivity data, although Kr has been studied by Senftleben up to 673°K and Schäfer et al. up to 738°K whose results have been criticised by Vargaftik, Kannuluik and Carman up to 579°K, von Ubish at 895°K and Zaitseva up to 800°K have measured the thermal conductivities of all the gases. The data of Kannuluik and Carman, as stated above, are usually within 2.5% of the smooth curves, and both von Ubish's and Zaitseva's data are often more than 5% away from the Curve. For Zaitseva's data, Vargaftik has suggested that the error is due to an inadequate temperature jump correction.

Collins has described a novel method of determining thermal conductivities by a shock-tube technique. It is designed for temperatures above 1500°K, but it is not very accurate at 1500°K, since the viscosity data calculated differ by as much as 10% from our curves.

Errors and Accuracy

The apparatus was designed with the intention of measuring viscosities to an accuracy of better than 1%. The analysis of errors which follows indicates that the random errors associated with the method are within the required tolerance. Under certain circumstances the effects of both systematic and random errors are considerably reduced by the comparative techniques employed, though this is not always the case. Each of the factors leading to error will be examined.

The experimental quantities measured are times of flow, heights of mercury columns and temperatures. All the gases used had less than 0.1% impurity, so no significant errors due to impurity would be expected.

Measurement of times of flow: Reproduceability of the times of flow at one temperature were usually to ±1 sec or ±0.2% (whichever is the greater). Thus typically at 1153°K using nitrogen, eight determinations of the times of flow were made with the platinum capillary for the pressure range P_b 0-1. These were recorded as 553.0, 552.8, 553.7, 553.4, 553.7, 553.4, 554.0 and 553.0 secs giving a mean deviation from the average, 553.4, of 0.4 secs i.e. less than 0.1%. Though it was not possible to adjust the furnace exactly to a chosen temperature, a number of check runs were performed to ensure that the capillary constant had not changed during each series of runs. The times of flow within a series at two very similar temperatures, when adjusted for the temperature difference and different slip corrections, always agreed to better than 0.7% e.g. for the platinum capillary at 1044°K and 1047°K the corrected times differ by 0.1%.

The fluctuation of the times of flow could be due to errors in the stop-watch, sticking of the mercury surface at the pointer tips, errors in setting the pressures or temperature fluctuations in the front vessel, the non-thermostatted parts of the connecting tube or the furnace. In all probability temperature fluctuations of the furnace accounted for most of the variations.

The stop-watches used could measure to 0.2 secs and it was estimated that the human reaction time was less than 0.5 sec; however since the watch was both started and stopped by hand the error introduced was probably much less than this. Thus the measured time interval for the mercury column to drop from one pointer to the next could be recorded to within 0.5 secs. The errors so introduced would be usually less than 0.2%. Comparison with B.B.C. radio time-signals showed that the watch lost about 1 sec in an hour. The error in the absolute times is thus about 0.04%. However as the method of calculating the results depends on ratios of times, unless the stop-watch is erratic, the ratios will not be affected.

Sticking at the pointer tips may have occured and was an unknown quantity but probably was less than 1 sec. Unless the behaviour was erratic the ratios should not be much affected. Clean, doubly distilled mercury was used in the apparatus and was kept either under vacuum or argon, so preventing oxygen reacting with the mercury and contaminating the surface.

The method of setting pressure as described in Chapter 3 was very precise. The backing pressure was either zero or set by means of the telescope to within ± 0.01 cm and the front vessel pressure was set to within 0.01 cm. The error caused by any inaccuracy is thus very small (estimated to be less than 0.1%) since the time of flow depends on $1/\tilde{P}\,\Delta P$.

The front vessel temperature variation was less than 0.01° at any one point in the bath since a thermometer reading to 0.01° was not observed to move over a period of weeks, so no error can be attributed to this. Any errors caused by variation of room temperature affecting unthermostatted parts (about 30 cc in volume) were minimised by thermostatting the laboratory to $294 \pm 2^{\circ}$K. The full variation from 292 to 296°K was never observed during a single day. Even if the whole temperature change had occured during the course of one run, little error would be introduced (estimated to be less than 0.01%).

Pressure Measurements In the analysis of (4.24) and (4.25) the mean pressure appears only as $1/\bar{P}$. This, as seen from Appendix 3, varies slowly for a pressure range and since most pressures are of the order of 30 cm, an error as great as 0.2 cm would make only a small difference to the position of the ratio of times in the graphs of the ratio analysis. The pressures were measured to ± 0.02 cm but $\bar{P}$ determined by simple averaging may introduce some small error. This would, though, be the same for all gases. Thus poor setting of the initial pressure described above should only affect the times of flow and not the subsequent data analysis, and any inaccuracies incurred in the measurement of the pressures given in Appendix 3 should affect this analysis only minimally.

Temperature fluctuation and measurement in the furnace The temperature fluctuations in the furnace and the gradients along the capillary are small. For the standard method of calculating the results (4.25) the temperature needs to be known with as great an accuracy as possible, but for the relative method it need not be known so accurately. The temperature of the platinum furnace was controlled to $\pm 1^{\circ}$ and the Gallenkamp furnace to $\pm 0.5^{\circ}$. This fluctuation was probably the major cause of the variation of times of flow.

In the standard method of calculation both the time of flow and the viscosity depend on temperature, so an error of 1% in the absolute measurement of the temperature would cause an error of approximately 2% in the viscosity value. Thus temperature is one of the major factors in determining the accuracy of the viscosities in this work, although the relative ratios of Table (4-2) are not greatly affected by small errors in temperature, the final values of the viscosities in Table (4-5) depend on the standard values obtained for N_2.

The temperature near the capillary when the supporting bridge was present (which was for all runs except the first three for the platinum capillary), varied by about 1° along the inside of the capillary as far as could be measured, since the

support prevented complete probing by the thermocouples. As platinum and rhodium are both good thermal conductors it was assumed that the temperature of the capillary was more uniform than this. The temperature was determined by measuring the E.M.F. from platinum/platinum 13% rhodium thermocouples by an accurate potentiometer. The three thermocouples, made by Johnson Matthey Metals Ltd. had certificates guaranteeing that they would read to within 1° of the gold point ($1336^{\circ}K$). As already discussed in Chapter 3, gross errors in the measurement of temperature by the thermocouples were eliminated by the check at $1660^{\circ}K$ with a disappearing filament pyrometer and by the fact that all three thermocouples gave E.M.F. values which indicated that they agreed to within 1° of each other at all temperatures. At $573^{\circ}K$ the thermocouples were all within 0.3° of an N.P.L. calibrated mercury-in-glass thermometer. Thus, taking $\pm 3^{\circ}$ as the maximum uncertainty in the temperature, the error arising from this source would be less than 0.5%.

Systematic Errors caused by the analysis (4.24) and (4.25) All the correction terms are somewhat uncertain due to the need to assume mean pressure values, so that most correction terms are probably no more accurate than ±10%. However except for the slip factor which will be considered separately, most of the terms are less than 0.5%, and usually only 0.05%. Due to the comparative method of analysis the terms partially cancel and so any error introduced would be expected to be negligible.

The slip term, though, can be large. The factors $(1 + K'_x / \bar{P})^{-1}$ of equation (4.8) and $(1 + K'_o / \bar{P})^{-1}$ of equation (4.10) are expanded by the binomial theorem and terms higher than K'_x and any cross terms are neglected to enable the simple straight-line analysis to be made. Some inaccuracy can be introduced if there is a difference of more than 5% between the slip terms. However this will not affect the ratios Ar/N_2, Kr/N_2, Xe/N_2, $N_2(T)/N_2(293)$, $Ar(T)/Ar(293)$ because

the differences are never as large as this. As $\bar{P}$ increases the slip term decreases and the errors in the assumptions are reduced. In the analysis of (4.24) and (4.25) the errors are greatest at the smaller values of $\bar{P}$ which are furthest from the intercept. Thus it would be expected that any errors should affect the slope of the curve but have little effect on the intercept. Should these higher terms need to be included, then (4.24) and (4.25) need to be replaced by equations of the form,

$$\frac{t_1}{t_2}\left(1 + \frac{t_2}{t_1}\frac{\eta_1}{\eta_2}\left[\frac{(K_1K_2}{\bar{P}2} - \frac{K_1^2)}{\bar{P}2}\right]\right) = \frac{\eta_1}{\eta_2}\left(1 + \frac{(K_2 - K_1))}{\bar{P}}\right)$$

obtained by including the second term of the binomial expansion. From an analysis using the above equation, the same intercept within 0.1% was obtained as by the simple equation, but the slope had changed considerably (10%). In the determination of the slip coefficients in Chapter 5 these higher terms were considered.

The standard deviation of the intercept was usually smaller than 0.2% so defining the ratio with great precision. Thus the relative ratios were expected to be very accurate since only the random errors need to be taken into account, but because the standard ratios also depend on the accuracy with which the temperature is known, their error will be larger.

The accuracy of the determination of the viscosities depends on the accurate measurement of the temperature of the capillary and knowledge of the viscosity standards used in the comparison. As seen in the last section and Appendix 7 there is considerable variation, even at room temperature, of the reported viscosities, so making the choice of the standards difficult. Here the ratio results of Tables (4.2) and (4.3) are unlikely to be in error by more than 0.5% but the absolute values of the viscosities in Tables (4.4) and (4.5) may have errors of up to 1% due to these uncertainties in the standards. The standard deviation of the ratios from the smooth curves are all less than 0.3% with only four points out of a total of 180 deviating by more than 0.5%.

CHAPTER 5

DISCUSSION

Although the primary purpose of this work was to develop a high temperature capillary viscometer, and to measure accurately the viscosities of the inert gases, it is of interest to see what new light the data can shed on the forces which act between simple molecules. This will be considered here taking argon and helium as examples, since these gases have been most extensively studied. Furthermore, as a result of the method of capillary viscometry used, some interesting observations can be made about the slip coefficient and curved pipe flow which, if not recognised and corrected for, can lead to serious errors in viscosity measurements. The conclusions drawn may explain some of the discrepancies between the experimental data and theoretical calculations.

Viscosity and the Potential Function

It is of interest to see how the data reported in this work obey the Principle of Corresponding States (P.C.S.). To do so it is necessary to define suitable characteristic parameters. Traditionally the critical properties have been used (96, 97) but these have been criticised (188) on the grounds that in dense states of matter the uncertainty of non-pairwise additivity of intermolecular energies may lead to irregularities in behaviour at the critical point. The Boyle temperature, T_B, (defined by $B_{(T_B)} = 0$) and the Boyle volume V_B (defined by $V_B = T(dB/dT)$ at $T = T_B$) have a number of advantages (189). However as the determination of the Boyle volume is subject to rather large uncertainties since the slope of the curve of B against T is difficult to measure precisely around T_B, another characteristic volume $B_\circ$ has been suggested (176) and is defined by

$$B_\circ = -B \text{ at } T = 0.7\ T_B$$

This parameter is more easily determined from the experimental data than the Boyle volume while retaining the theoretical advantages of the latter. The values of T_B and $B_\circ$ for the rare gases are given below. For argon, krypton and xenon, they have been taken from (176), where Rigby and Smith (176) estimate the uncertainty in these values to be 2-3%. The values for helium and neon have been estimated from the plot of B against T using the data from (70).

	He	Ne	Ar	Kr	Xe
T_B °K	25	125	410	570	775
$B_\circ$ (ccs/mole)	7.4	10.0	18.3	22.7	29.7

The reduced viscosity η^* may be defined (97)

$$\eta^* = \eta \frac{B_\circ^{2/3} N^{1/3}}{(R.M.T)^{1/2}} \qquad (5.1)$$

and T^* is T/T_B and the reduced second virial coefficient is defined as $B^* = B/B_o$. Data from this work and that of Clarke and Smith (192) have been reduced and the smooth curve is shown in figure (5.1). The deviations of all the points from the curve are within experimental error. The same parameters also yield a reduced second virial coefficient curve with all points lying within experimental error (48). As seen, the data of Trautz et al. (193) and Vasilesco (170) for argon deviate from our curve, as do the data of Clifton (116) for krypton. Due to its low value of T_B there are no points on the curve for helium.

The degree to which the P.C.S. is obeyed suggests that it should be possible to define the potential energy of interaction of these gases in terms of a single function having just two adjustable parameters.

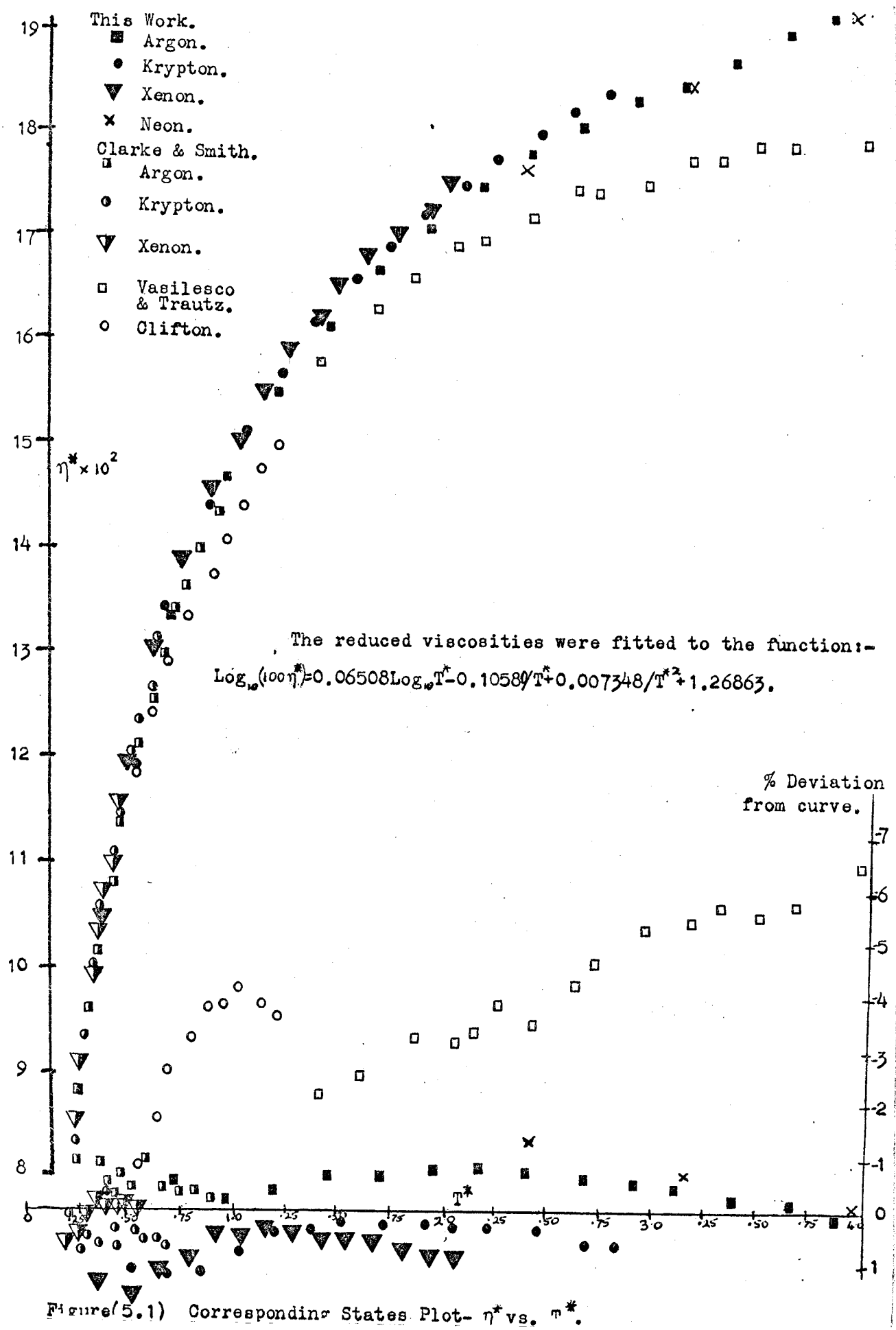
The viscosities are calculated theoretically from the potential function through equation (2.24)

$$\eta = \frac{2.6693\ \sqrt{MT}}{\sigma^2\ \Omega^{(2,2)^*}(T^*)}\ f_\eta \quad \times 10^{-5}\ \text{g cm}^{-1}\text{sec}^{-1} \qquad (5.2)$$

f_η accounts for the higher order approximations of η and is a slowly varying function of T^*, which seldom differs from unity by more than 0.7%, and can be omitted from (5.2) without causing serious error. The true potential should give a reduced viscosity curve coincidental with the experimental curve of figure (5.1). The potential function ϕ (r) may be reduced by the characteristic parameters ε and σ as defined in figure (1.1). The various reduced quantities may be defined in terms of these theoretical parameters. Thus the reduced theoretical second virial coefficient is

$$B^*_T = B/b_o \text{ where } b_o = \frac{2}{3}\pi N \sigma^3 \; ; \; T^*_T = kT/\varepsilon$$

(Subscript T refers to a theoretically reduced quantity.) The value of T^* when



Figure(5.1) Corresponding States Plot- η^* vs. T^*.

$B^*_T = 0$ is the reduced Boyle temperature T^*_B ($= kT_B/\varepsilon$) and at $0.7\ T^*_T$ the value of B^*_T is the reduced theoretical characteristic volume $B_\bigcirc{}^*$. Thus it can be shown that

$$\eta^* = \frac{0.2886\ (B_\bigcirc{}^*)^{2/3}}{\Omega^{(2,2)^*}(T^*)}$$

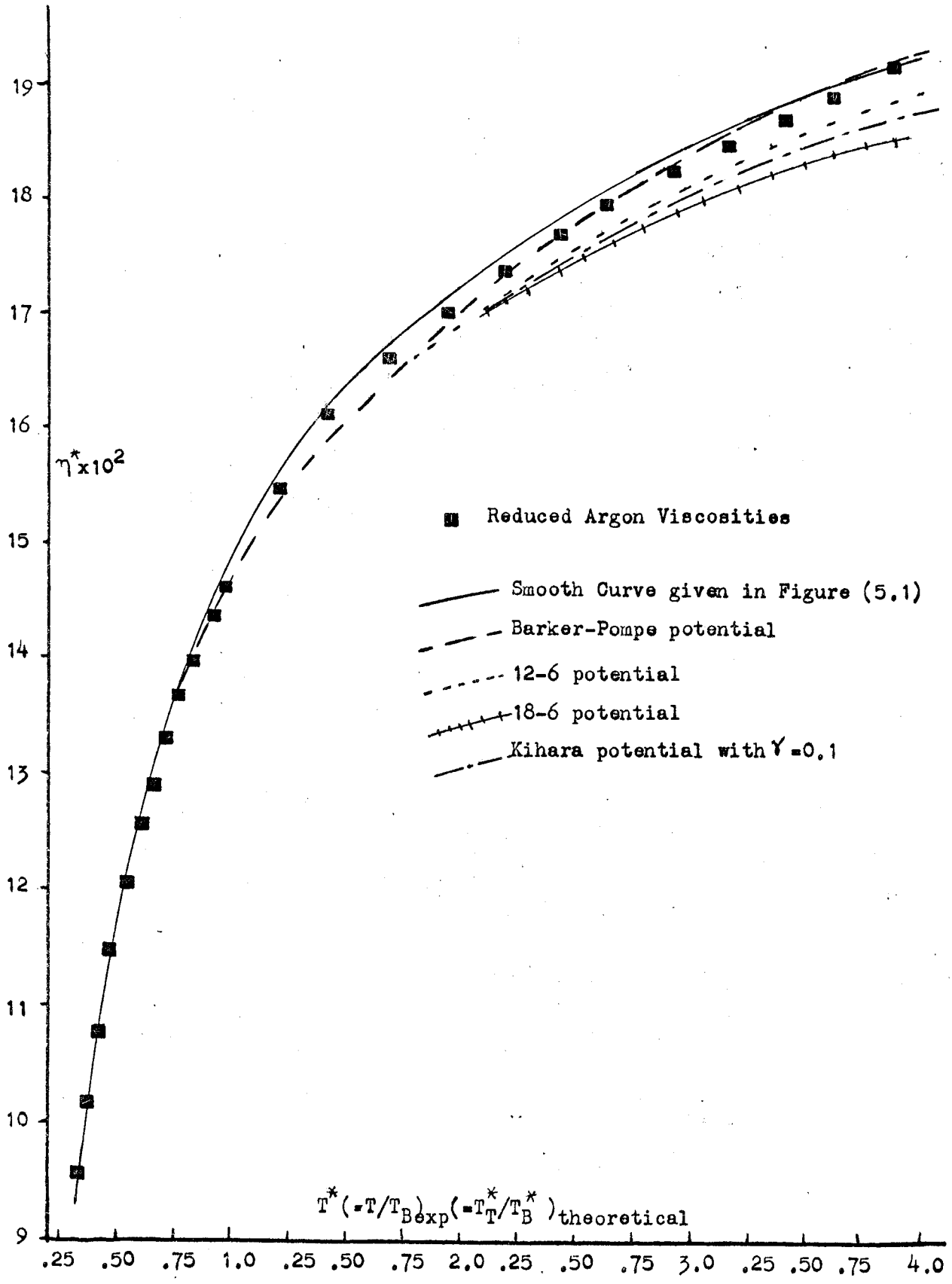
Since $B^*_\bigcirc$ and $\Omega^{(2,2)^*}(T^*)$ have been calculated for a potential function, η^* may be calculated as a function of T^*. The experimental curve is of η^* against T/T_B, so the theoretical values of η^* must be plotted against T^*/T^*_B. Since a suitable function has been found the individual parameters for each gas may then be determined. The theoretical curves for various potentials are shown in figure (5.2), none of which is fully compatible with the data.

Hanley and Childs (11) have shown that potential functions may be classified in terms of families, for example the Lennard-Jones m-n family and, in a number of cases, that if one member of a given family can be fitted to the experimental data via a theoretical expression, a similar fit can be obtained by a member of another family. Alternatively members of different families can be interchanged without materially altering the fit. They have also shown that to test substantially any function, data are needed outside the reduced range,

$$2 < T^*\ (12\text{-}6) < 5$$

where $T^* = (kT/\varepsilon)_{12\text{-}6}$, and $(\varepsilon/k)_{12\text{-}6}$ is the well-depth parameter for the gas obtained from the 12-6 function. They find that data inside this region may be fitted by a large number of potential functions.

Up to now there has been a discrepancy between the theoretically derived viscosity data using parameters obtained from molecular beam scattering experiments, second virial coefficients and quantum mechanically calculated long



Figure(5.2) A Comparison of Theoretical Reduced Viscosities given by Various Potentials and Experimental Reduced Viscosities.

range interaction coefficients, and the experimental viscosity data. There have been many attempts to reconcile this difference with little success. However, as suggested by a number of workers (7-11), the original viscosity data on which these analyses are based are in error, and the new data reported here considerably reduce this discrepancy. Typical of those who have attempted this analysis are Barker and Pompe (10). They give a potential function which they find gives theoretical values in excellent agreement with all properties except transport data. It has the form:-

$$\phi(R) = \varepsilon \left[e^{\alpha(1-r)} \left(\sum_{i=0}^{3} A_i (r-1)^i \right) - \sum_{i=0}^{2} C_{2i+6} / (\delta + r^{2i+6}) \right]$$

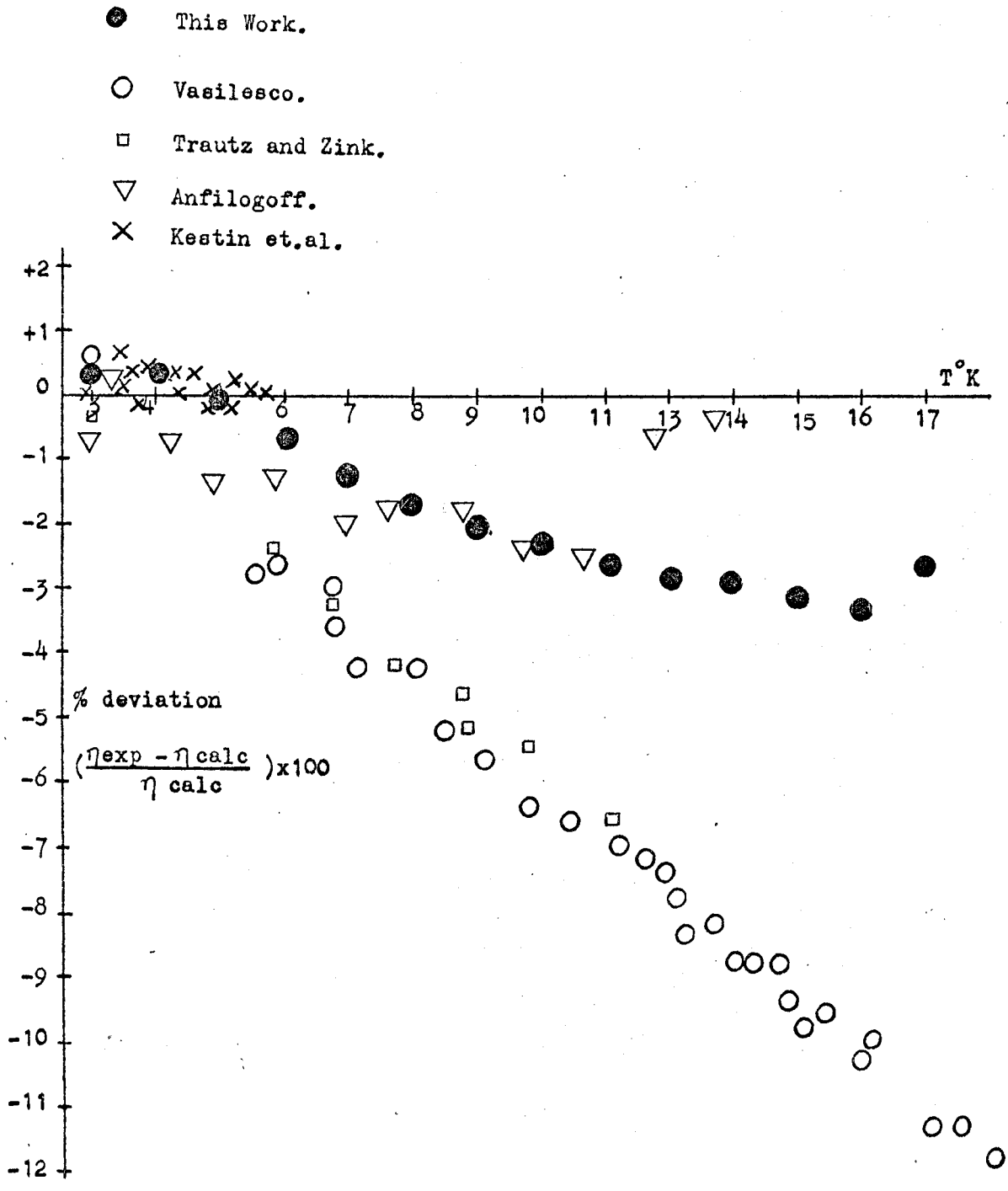
where $r = R/R_m$, and R is the actual separation, R_m the separation at the minimum of the potential function and ε the depth of the potential well. δ is a constant which prevents the occurence of a spurious maximum at small separations.

For argon, the parameters are found to take the following values:-

$\varepsilon/k = 147.0°K$, $b_o = (\frac{2}{3} \pi N R_m^3) = 66.86$ cc/mole,

i.e. $R_m = 3.757 \times 10^{-8}$ cm, $\alpha = 12.5$. $A_0 = 0.2349$, $A_1 = -4.7735$, $A_2 = -10.2194$, $A_3 = -5.2905$, $C_6 = 1.0698$, $C_8 = 0.1642$, $C_{10} = 0.0132$, $\delta = 0.01$.

The collision integrals have been calculated using the programme of Barker, Fock and Smith (72) modified by Dr. M. Rigby for use with the University KDF9 computer. Using the parameters for argon as given by Barker and Pompe, the deviation of the new data from their predicted values is shown in figure (5.3). Also included on the diagram are the data of Trautz et al. (193) and Vasilesco (170) and it can be seen that the agreement between the new data and the potential assumed is very much improved.



Figure(5.3) The Deviation of Argon Data from the predicted values given by the Potential of Barker and Pompe.

The potential of the form,

$$\phi(r) = A \exp(-Br)$$

has been suggested (190) to be the true qualitative form of the repulsive intermolecular potential at moderately small internuclear distances (or equivalently, high temperatures).

Helium has such a small Boyle temperature that it would be expected that at high temperatures only the repulsive part of the potential need be considered.

The collision integrals of the reduced potential

$$\phi^*(r) = 10{,}000 \exp(-Sr^*)$$

where $\phi^* = \phi/E$ and $E = \frac{A}{10{,}000}$, and $r^* = \frac{r}{S}$ and $S = \frac{8}{B}$ have been calculated and are given in Appendix 9. The integrals are identical to those calculated by Monchick (190), who calculated the collision integral $I^{(l,s)}$ as a function of α, where

$$\alpha = \ln(A/kT)$$

and $$\sigma^2 \Omega^{(l,s)^*}(T^*) = \frac{8\alpha^2 B^{-2} I^{(l,s)}}{(s+1)!\left[1 - \frac{1}{2}\left(\frac{1+(-1)^l}{1+l}\right)\right]}$$

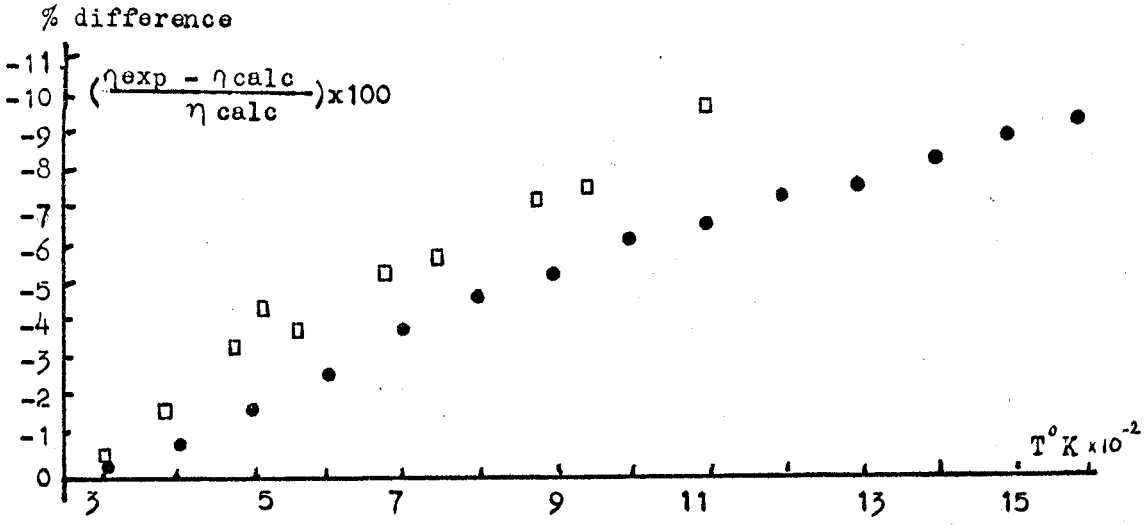
The table of integrals given by Monchick can cover a much wider range of values of A and B than the table in Appendix 9. If $\Omega^{(l,s)^*}$ does not lie in our table for the required value of $T^*(=kT/E)$ a potential with different values of E and S must be used.

For helium, Amdur and Jordan (86) have suggested A = 196 e.v. and B = 4.21 as giving good agreement with high energy molecular beam results and theoretical calculations. The agreement with our experimental data is poor, and at 1500°K the difference between the calculated and experimental values is

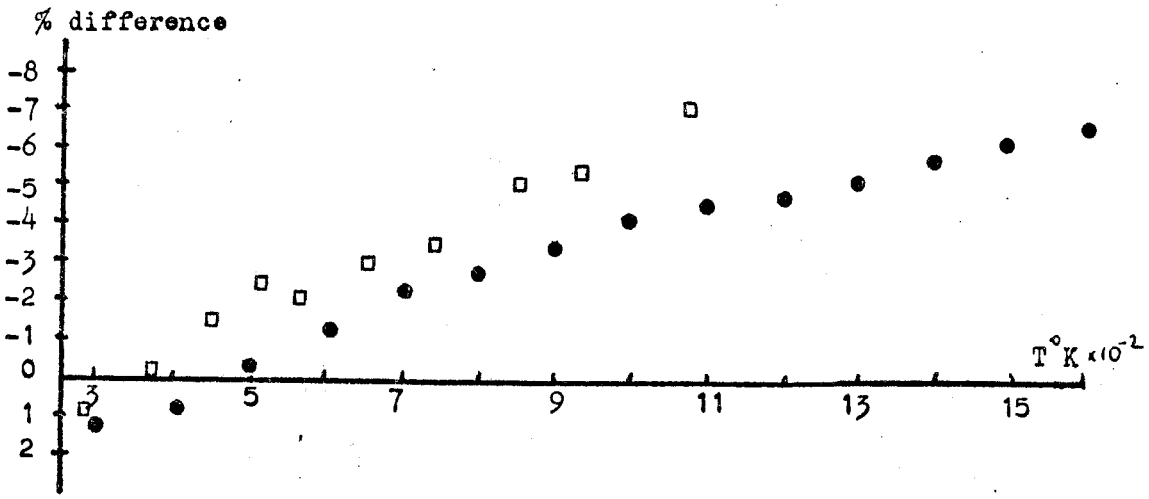
some 9% as seen in figure (5.4). The data of Trautz and Zink (193) are in even worse agreement.

Blais and Mann (194) have suggested that A = 228 e.v. and B = 4.25. The difference between the calculated and experimental values is shown in figure (5. 4). A similar potential having A = 240 e.v. and B = 4.21 gives a fit of our data above 500°K to better than 3%. The difference between the experimental data and theoretical values is also shown in figure (5.4). The values of the repulsive potential energy calculated using this function are in excellent agreement with both theoretical and molecular beam studies as seen in figure (5. 5).

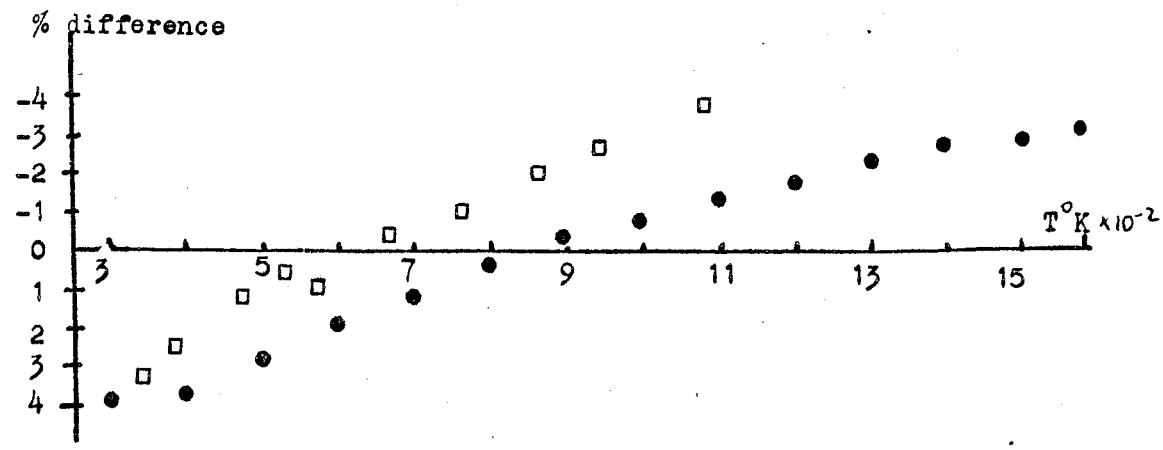
The new data reported in this work do appear to reconcile, at least in part, some of the discrepancy between the parameters derived from transport properties and from other sources.



A= 196 e.v. B= 4.21 - E/k= 227.2°K, S= 1.900A



A= 228 e.v. B= 4.25 - E/k= 264.2°K, S= 1.882A

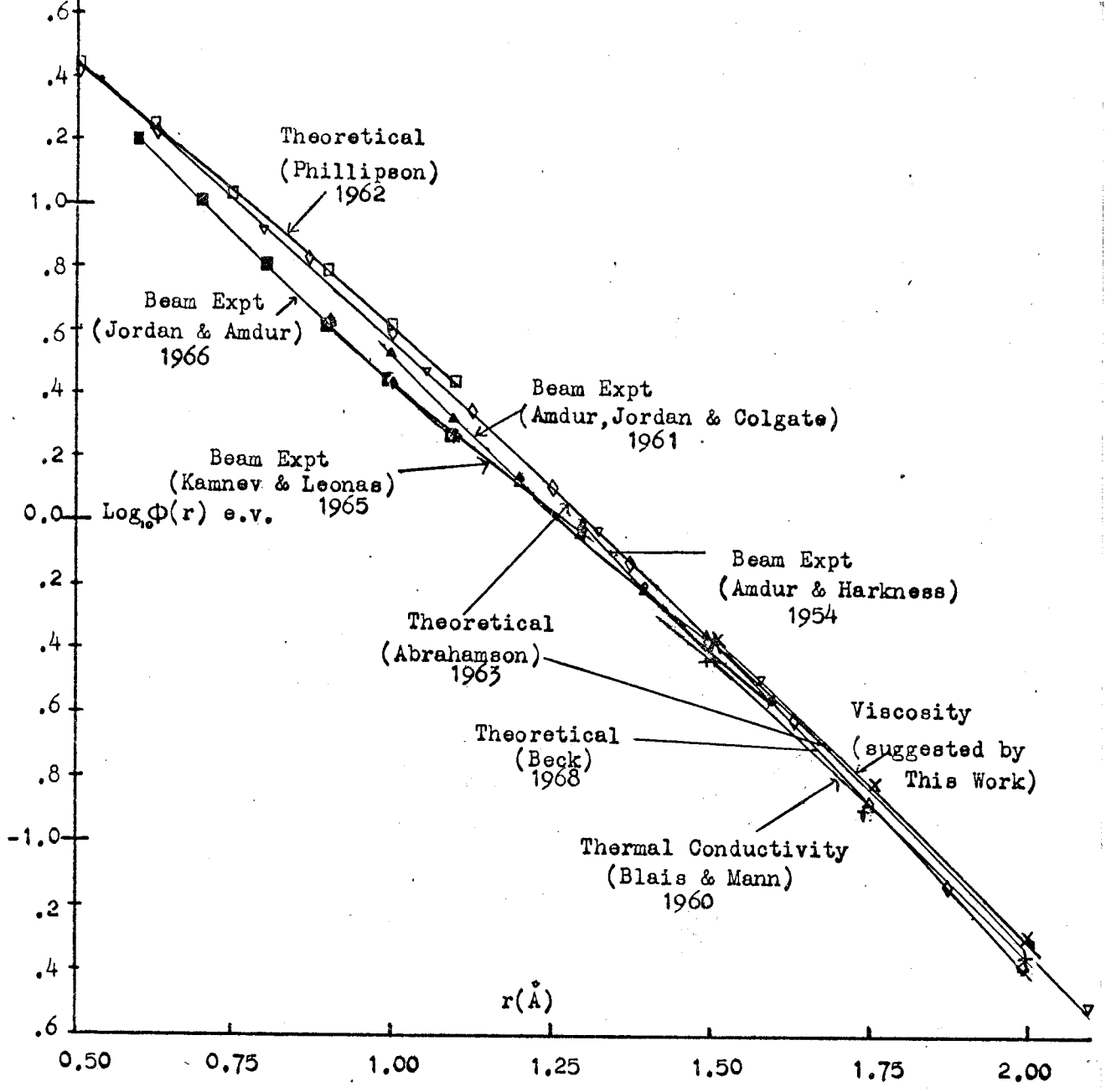


A= 240 e.v. B= 4.21 - E/k= 278.2°K, S= 1.900A

● This Work □ Trautz et al.

Helium Data.

Figure(5.4) The Difference between the Experimental Data and the Theoretical Viscsities calculated by the Exponential Potential



Theoretical Curves:- □ P.E.Phillipson, Phys.Rev., 125 1981 (1962)
◊ A.A.Abrahamson, Phys.Rev., 130 693 (1963)
▽ D.E.Beck, Mol.Phys., 14 311 (1968)

Molecular Beams:- ■ J.E.Jordan and I.Amdur, J.Chem.Phys., 46 165 (1967)
▲ I.Amdur, J.E.Jordan and S.O.Colgate, J.Chem.Phys., 34 1525 (1961)
• I.Amdur and A.L.Harkness, J.Chem.Phys., 22 664 (1954)
♦ A.B.Kamnev and V.B.Leonas, Soviet Physics Doklady, 10 525 (1965)

Experimental Data:- + N.C.Blais and J.B.Mann, J.Chem.Phys., 32 1459 (1960)
× This Work - suggested curve $\Phi(r) = 240 \exp(-4.21r)$ e.v.

Figure(5.5) Repulsive Potential Energy of Helium Atoms. A comparison of beam-derived results with theoretical calculations and with empirical potentials.

The Slip Coefficient

In this work the normal assumption that the slip coefficient is a function of the mean free path is made. This being so, the actual value of the slip coefficient need not be known in order to obtain the correct viscosities of gases. However important information about the coefficient can be derived from the dependence of the results on the mean pressure at which they were obtained.

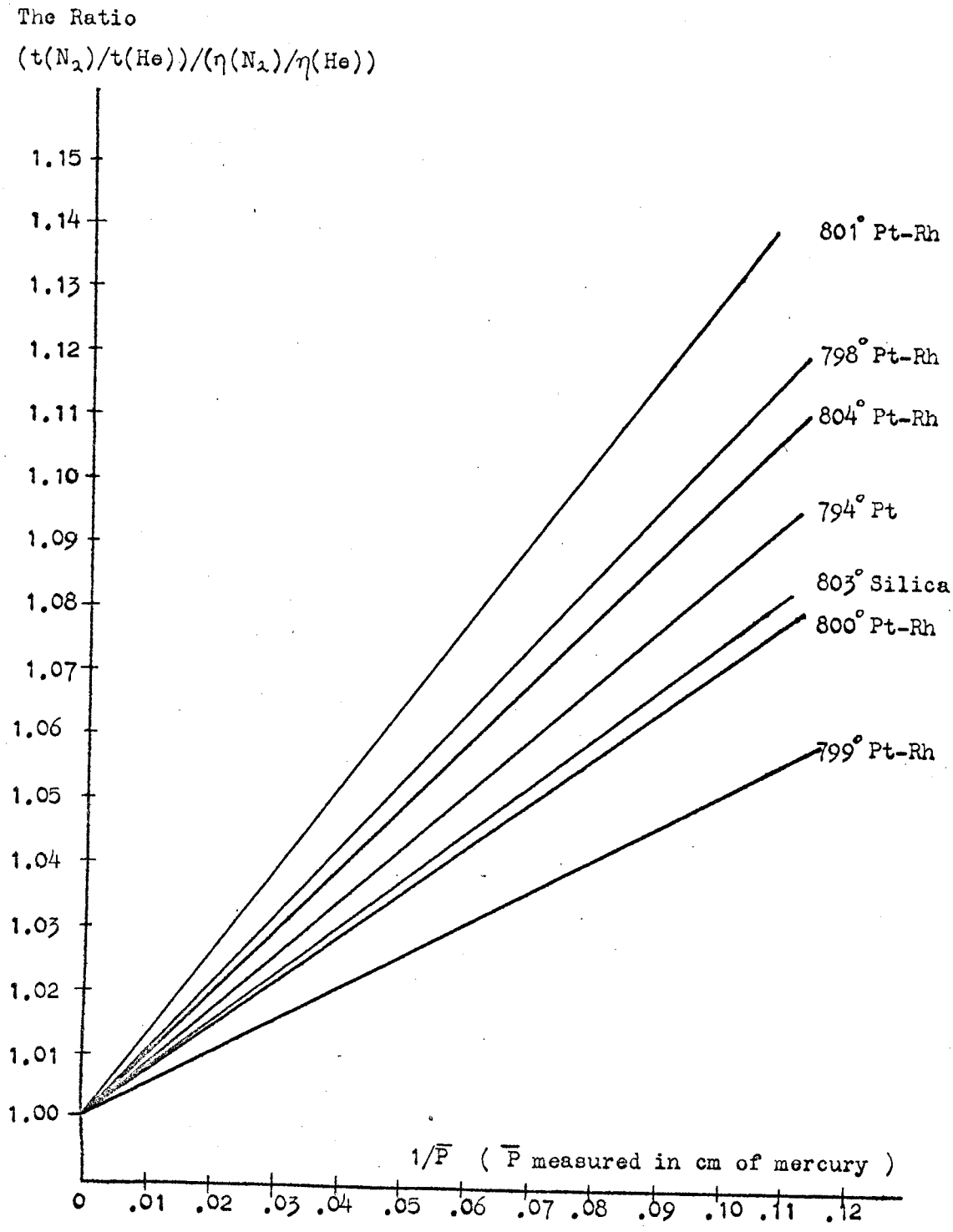
In Chapter 2, equation (2.30) was derived having a slip factor of $(1 + C\frac{\lambda}{r})$ where $C = \left(\frac{2-f}{f}\right) 4k$. $k\lambda$ is the distance the molecules have travelled since their last collision before entering the surface layer of gas, and f is the fraction of molecules diffusely reflected. Thus C has two variables, f and k. Most workers using capillary viscometers have corrected their times of flow for slip effects using Knudsen's slip formula (141) where C has the value 16/3. They have assumed C to be constant at all temperatures, for any capillary regardless of its composition or thermal history.

From equation (4.2)

$$\frac{C\lambda}{r} = \frac{K'}{\bar{P}} = \frac{C\eta}{r\bar{P}} \left(\frac{\pi RT}{2M}\right)^{\frac{1}{2}} ,$$

so that, at constant temperature, for the two gases, x and y, the comparative method of analysis produces equation (4.9). When the ratio of the corrected times of flow is plotted against $1/\bar{P}$, the mean pressure in the capillary, the curve has the slope $(K'y - K'x)\frac{\eta x}{\eta y}$. A similar slope is obtained for the standard equation (4.11) and the discussion is identical, so will not be given here.

If Knudsen's formula is valid, a number of determinations of the relative viscosity ratio at similar temperatures with the same capillary should be identical. As the slope is not very sensitive to temperature, the capillary need not be at exactly the same temperature for all its determinations. However as seen in figure (5.6) for our platinum-rhodium capillary at temperatures around 800°K, the

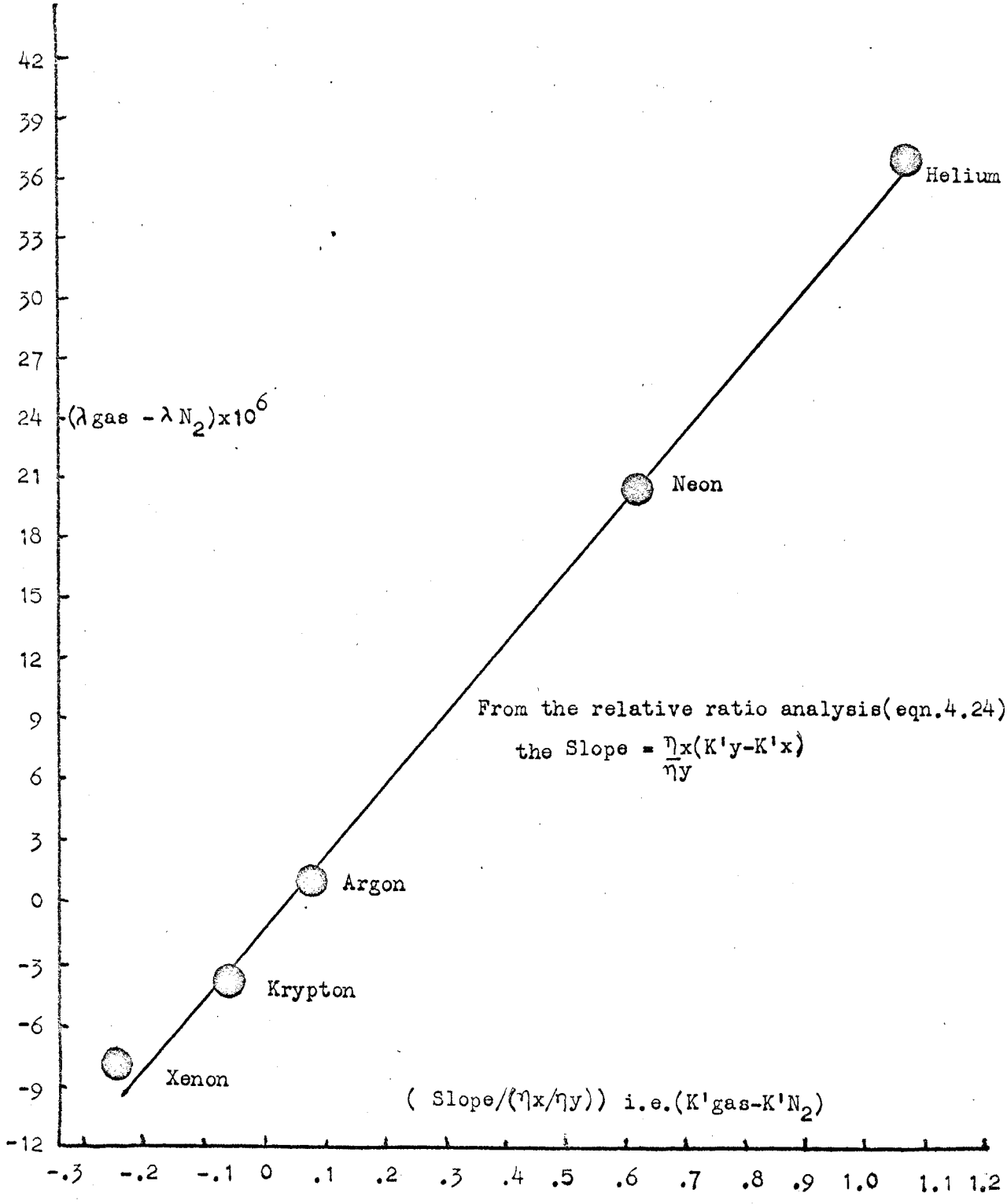


Figure(5. 6) The Plot $(t(N_2)/t(He))/(\eta(N_2)/\eta(He))$ vs. $1/\overline{P}$; showing the slopes for the $(N_2)/(He)$ relative ratios, determined at temperatures around 800°K for the three capillaries.

slope of the nitrogen/helium relative ratio graph varies by a factor of two. C is not constant in this case and depends on the thermal history of the capillary. If instead of our analysis, a straightforward calculation using equation (4.8) or (4.10) of the viscosity ratios is made and a wrong value of C used in determining the slip correction factor, some error will be introduced into the calculation of the viscosity coefficient. This may explain some of the discrepancies in the viscosity data reported in the literature.

The slopes of the equations (4.24) and (4.25) are given in Chapter 4 together with the intercepts. It can be seen that, relative to nitrogen, the magnitude of the slip effect of the gases (i.e. the value of the slope) is approximately proportional to the difference in the mean free paths (see Appendix 2 for typical values of the mean free path). Thus at 948°K using the silica capillary the values of the ratio of slope to intercept for the gas/N_2 ratios are He = 1.1, Ne = 0.6, Ar = 0.06, Kr = -0.06 and Xe = -0.2. These factors should be proportional to the mean free path of the gas less that of nitrogen if the degree of specular reflection is the same for all gases under the same conditions, and indeed an excellent correlation is observed, as shown in figure (5. 7).

Values of C have been calculated from the slopes given by the analyses of (4.24) and (4.25). When the two slip factors are similar, for example argon has a slip factor only 5% larger than nitrogen, the gradient is very small since it depends on the difference between the two slip terms, and so the calculated values of C are liable to gross inaccuracies. Attention was therefore paid mainly to the standard helium and neon and the relative N_2/He and N_2/Ne ratios. For these calculations one of the slip terms dominates the correction factor. The standard deviation of the slope in these cases is less than 10% so the error in C should be no more than ± 10%.



Figure(5.7) - showing the correlation between the slope of the relative ratio analysis and the difference in the mean-free paths of the gas and nitrogen.

Calculation of C using N_2/He slopes

Platinum Capillary		Platinum/rhodium Capillary		Silica Capillary	
T°K	C	T°K	C	T°K	C
796	4.9	292	3.7	293	5.5
794	8.0	293	4.3	373	5.7
798	10.2	293	5.8	474	6.6
1144	9.3	293	5.7	568	5.8
1146	11.8	798	8.7	673	7.8
1153	9.5	799	4.0	803	7.0
1157	9.5	806	5.9	948	7.0
1164	10.0	801	8.9		
1158	11.6	804	8.0		
		1144	6.5		
		1146	6.6		
		1273	8.2		
		1273	6.5		
		1273	6.7		
		1273	8.4		
		1273	8.2		
		1457	10.4		
		1457	12.3		

Calculation of C using helium standard slopes

Platinum Capillary		Platinum-Rhodium Capillary		Silica Capillary	
Temp. ratio	C	Temp. ratio	C	Temp. ratio	C
793/293	7.4	799/292	8.6	373/293	5.8
926/293	10.4	800/293	5.1	474/293	7.8
1044/293	10.0	1146/293	7.8	566/293	6.3
1047/293	11.8	1144/293	7.3	673/293	7.6
1153/293	10.2	1275/293	9.0	803/293	7.2
1289/293	10.4	1457/293	10.2	948/293	6.8
1504/293	12.4	801/293	7.2		
1330/926	11.6	1273/293	11.0		
		801/293	7.4		

Calculation of C using neon standard slopes

Platinum-Rhodium Capillary		Silica Capillary	
Temp. Ratio	C	Temp. Ratio	C
804/293	8.6	370/293	5.8
1039/293	7.8	474/293	6.8
1273/293	7.0	566/293	5.8
1504/293	7.0	673/293	7.4
801/293	8.8	803/293	7.8
		948/293	7.8

As can be seen, C for the platinum and silica capillaries tends to increase slightly with temperature, but for the platinum rhodium capillary it varies considerably. A major change in C was observed when the platinum-rhodium capillary was first heated at 1100°K. This was probably due to annealing effects in the alloy which the pure metal or silica capillaries do not experience. The reasons for any change in the value of C must be due to differing reactions of the surface gas molecules with the capillary wall.

Knudsen's value of C was 5.4, so if the slip correction had been calculated using this value rather than the experimentally observed one, significant errors would have been introduced. Thus Guevara et al. (193) using a molybdenum tube obtained, by a calculation similar to ours, a slip coefficient considerably different from the Knudsen value, which gave viscosities some five percent higher than the values obtained by other workers at 1100°K.

The value of C has been the subject of much discussion since the work of Knudsen (141), and recently Barrer and Nicholson (191) have made a detailed study of specular reflection. If the value of C is determined and a value of k assumed, then f may be deduced or vice versa. Most theoretical discussions e.g. (199) which solve the Boltzmann equation using suitable boundary conditions, assume diffuse reflection i.e. f = 1. The following table lists a number of values of C, k and f obtained from various treatments.

C	k when f = 1	f when k = 1	Authors
4.00	1.00	1.00	Maxwell (137)
3.33	1.30	0.85	Knudsen (141), Fryer (139)
3.30	1.33	0.86	Hanks and Weissberg (200)
3.10	1.28	0.87	Lund and Berman (201)
4.58	1.15	-	* Cercignani et al (199)
4.56	1.14	-	* Willis (202)
6.00	1.50	0.80	Mason et al. (150)

*indicates theoretical calculations, assuming f = 1.

1) Hurlbut (140) and Partington (102) have listed a number of values of f obtained using Maxwell's values for C and k. These have been obtained by measurements of the flow of gases through tubes and of drag in a rotating cylinder device. It is seen that in these experiments the nature of the surface and the gas used affect f.

2) Barrer and Nicholson (191) found that for their glass capillary C varies with gas at low temperatures.

3) If k is assumed to be 1.0, the value of f as indicated by the values of C from this work, may be deduced from the following table. If k takes another value, then $f = 8k/(C + 4k)$

C	f
4.0	1.0
4.9	0.9
6.0	0.8
7.5	0.7
9.3	0.6
12.0	0.5

f is the fraction of diffusely reflected molecules and can be regarded as a measure of the extent to which momentum is exchanged with the surface. (1 - f) is the fraction of specularly reflected molecules and gives an indication of the preponderance of forward direction in the scattering process. In their analysis of specular reflection, Barrer and Nicholson (191) have assumed values of k of 1.0 and 1.125 and have given a quantitative basis to their arguments using values obtained from their experimental measurements. Their conclusions are that specular reflection is influenced by a number of factors, such as the effect of surface roughness in scattering the molecules, and the effects of adsorption of gas molecules on the surface. The elastic scattering where no energy is exchanged with the surface is apparently important only for light gases at low temperatures. Specular reflection for the heavier gases indicates imperfect momentum exchange with the surface rather than non-interaction.

Whether this analysis by Barrer and Nicholson has any real value is open to question until there have been more studies of the reactions of gases with surfaces, and the true value of k experimentally determined. There have been many molecular beam studies of scattering at surfaces (e.g. 140, 196, 197, 204) but in most of the work described, monoenergetic beams react with the cold surfaces of specially cleaved planes of crystals. This does not really represent a capillary tube, the surface of which is hot and uneven on a submicroscopic level, and is approached by gas molecules from all directions with a near Maxwellian distribution. Thus no conclusions concerning f or k can, as yet, be drawn.

In view of the uncertain value of C in the slip coefficient, two procedures are suggested for accurate viscometry work. Either the value C should be determined at every temperature under experimental conditions, or, as in our case, the apparatus designed to eliminate the necessity for an actual slip correction to be evaluated.

Curved Pipe Flow

In a coiled tube extra resistance to flow due to centrifugal forces, which occur at high flow rates, can be considerable. In determining the viscosity ratios, any times of flow which have an associated Dean number, equation (4.21), greater than 3.0 have been neglected. At high temperatures as shown in Chapter 4 (page 79) D is always less than 3.0, but as the temperature drops, the Dean numbers increase in magnitude so that at 293°K there are significant curved pipe flow effects for 60% of the runs. This has allowed an examination of the effects of curved pipe flow with varying Dean numbers due to the different pressure ranges, helix/capillary radius ratios, gases and temperatures. The Dean number of helium never exceeded 2.0 under our experimental conditions because of its low molecular weight, so no curved pipe flow effects were expected. The ratio t(gas)/t (He) calculated from the corrected times of flow, including slip effects, should be constant. However if curved pipe flow effects are present the time $t(gas)_{corr}$, still has not been corrected completely, so will not give the true viscosity ratio. Since all other effects have been corrected, the difference between the ratio of corrected times and the true viscosity ratio gives a measure of the amount of curved pipe flow present. Such an analysis is given in Appendix 8. The graph of F_d/F_s (the quotient of the ratio of corrected times of flow and actual viscosities) against Dean number is given in figures(5.8,9). It can be seen that within experimental error a smooth curve is given. This curve, obtained from data from the platinum and silica capillaries, confirms that the resistance to flow in a coiled tube is some function of the Dean number. The following table gives the value of the increased resistance to flow due to curved pipe flow effects expected with the Dean numbers calculated under our experimental conditions. The values have been read from the best line drawn through the experimental points of a large scale diagram of figure (5. 8).

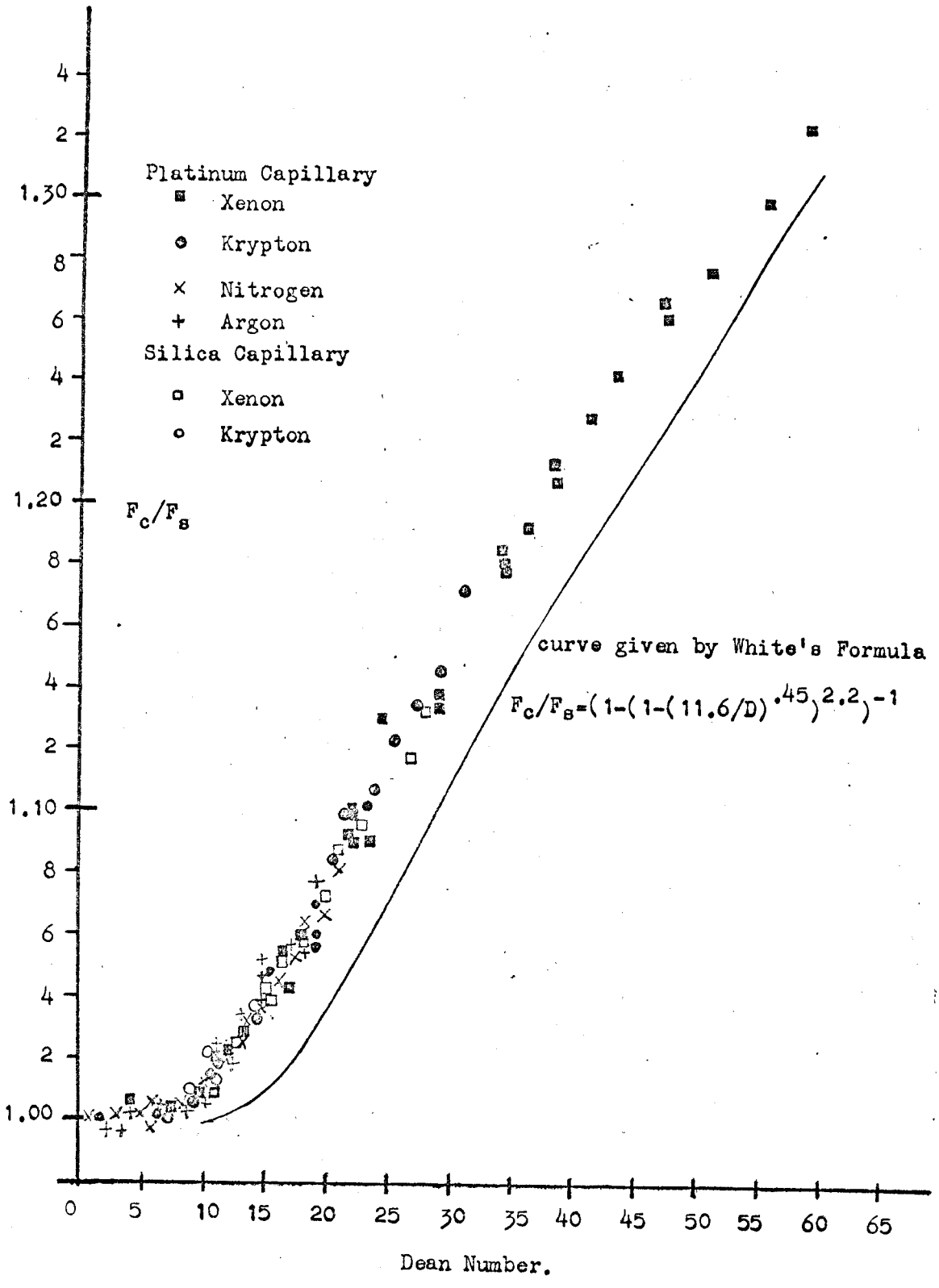
Dean No.	C.P.F.	Dean No.	C.P.F.	Dean No.	C.P.F.
1.0	1.000	8.0	1.009	20	1.08
2.0	1.000	9.0	1.012	25	1.11
3.0	1.000	10	1.017	30	1.15
4.0	1.000	11	1.020	35	1.18
5.0	1.000	12	1.025	40	1.21
6.0	1.001	15	1.05	50	1.27
7.0	1.002	18	1.07	60	1.33

The effects of curved pipe flow increase very rapidly with Dean number but are negligible below a Dean number of 6.0. The times of flow where the Dean number is above 3.0 have been neglected in the determination of the viscosity ratios. As this is well below the threshold value of 6.0, there will be no curved pipe flow effects present.

At 373°K the maximum Dean number for xenon with the silica capillary is 13.1 and the experimental curved pipe flow effect as shown by F_c/F_s is 1.033, which is in excellent agreement with the value of 1.031 given by figure (5. 9). This confirms the temperature dependence of curved pipe flow (see Chapter 4).

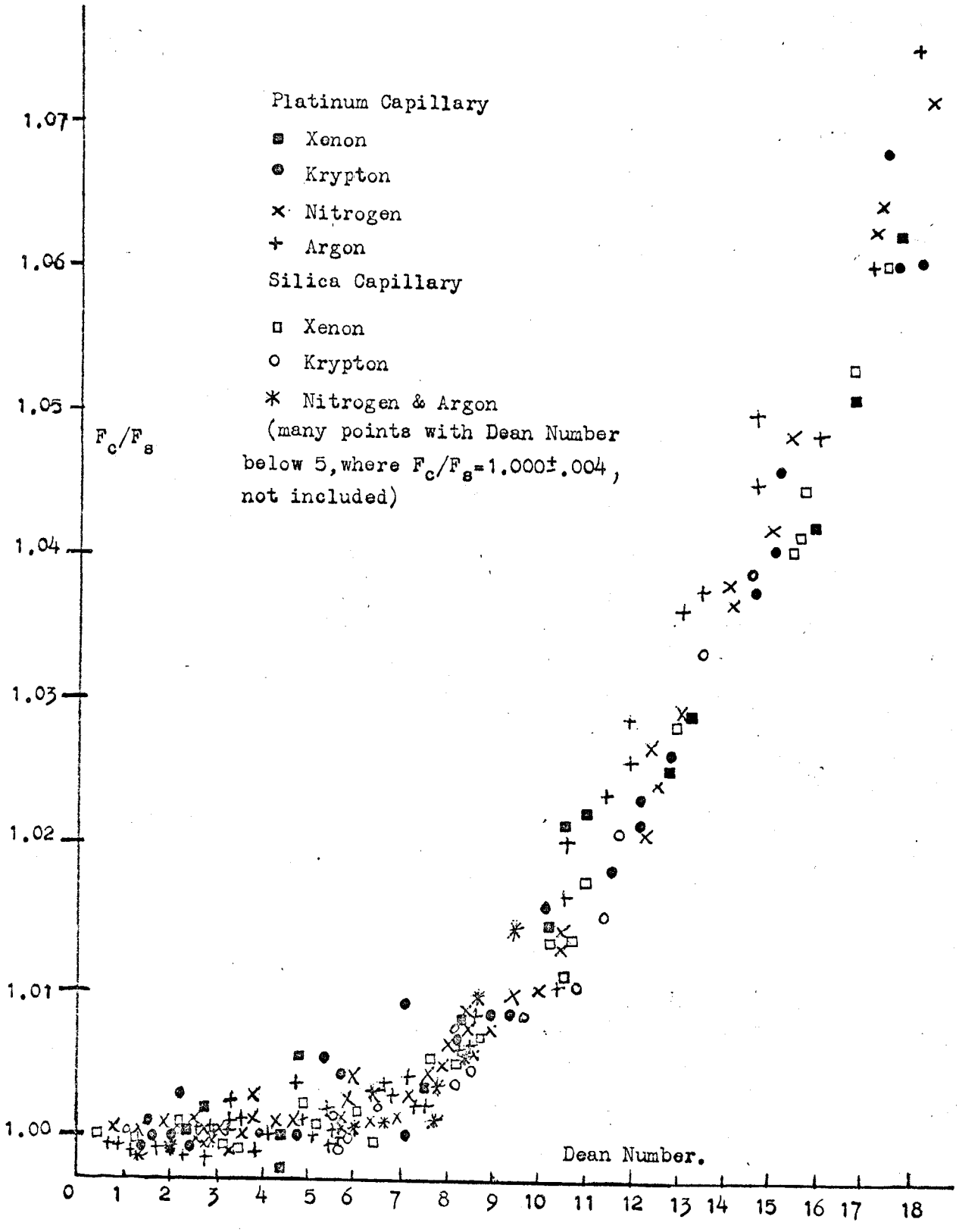
Due to the empirical method of determining the velocity of flow, v , in the Dean number (equation (4.21)), data of different workers may differ. Thus Vasilesco (170) using a similar coiled capillary but with constant pressures acting on his capillary, observed that curved pipe flow effects occured only with Dean numbers greater than 11.6. This is considerably higher than the threshold value observed in this work. However in our work the average of the Dean numbers at the start and end of a run for a gas flowing in a capillary is used, while the values of Dean number for Vasilesco's apparatus were constant for each pressure range, so complete accord is not to be expected. Vasilesco's results fit the curve given by

White (167) (see Chapter 2), whose experimental results were also obtained from measurements with constant driving pressures. This curve is also shown in Figure (5. 8). The similarity of general shape between the curves is striking although, as expected, there is not complete agreement.



(See Appendix 8 for the Actual Values -in this figure not all the points with Dean Number below 10 are shown)

Figure(5.8) The Experimentally Determined Curved-Pipe Flow as a Function of Dean Number.



Figure(5.9) Curved-Pipe Flow as a function of Dean Number, showing the Threshold Value.

APPENDIX 1

GLOSSARY OF SYMBOLS

B	second virial coefficient (p.12)
b	impact parameter (p.23)
C	third virial coefficient (p.12)
	coefficient in slip factor (equation 2.50) where $C = \left(\frac{2-f}{f}\right) 4k$ (p.42)
$C_{6,8,10}$	attractive coefficients in the potential function (p.5)
$C_{p,V}$	molar specific heat at constant pressure, volume.
D	coefficient of diffusion (p.29)
	Dean Number (p.51)
F	force (pp 3, 18)
f	fraction of molecules diffusely reflected (p.40)
(1-f)	fraction of molecules specularly reflected (p.40)
$f_{\eta,K,D}$	correction factors to first order calculation of viscosity (p.30) etc.
G	imperfect gas correction term (p.80)
g	relative velocity (p.23)
H	Hagenbach correction term (p.74)
K	Knudsen Number (p.36)
K'	slip correction term (p.70)
k	Boltzmann constant - 1.3804×10^{-16} erg.deg^{-1}
	constant in slip factor (p.42)
M	gramme molecular weight
m	the mass of one molecule
N	Avogadro's Number - 6.0247×10^{23} mole^{-1}
n	number of moles
P	pressure

Q	collision cross-section (p.27)
	flow rate ($Q = dn/dt\ RT$) (p.45)
R	gas constant - 8.3166×10^7 erg.mole^{-1} $^{\circ}K^{-1}$
Re	Reynold's Number (p.35)
r	intermolecular distance
	radius of tube
S	total cross section (p.26 - $d\sigma$ the differential cross-section p.25)
T	temperature $^{\circ}K$
t	time
V	volume
v	velocity
α	polarisability (p.5)
	linear coefficient of expansion (p.73)
γ	Kihara third parameter (p.9)
ε	coefficient of external friction (p.39)
$-\varepsilon$	maximum attractive energy (p.6)
η	coefficient of shear viscosity (p.18)
θ	angle of orientation (pp.7,23)
κ	coefficient of thermal conductivity (p.29)
λ	mean free path (p.20)
μ	dipole moment (p.5)
	Joule Thomson coefficient (p.13)
	reduced mass (p.23)
ν	coefficient of kinematic viscosity (p.18)
ρ	density
σ	collision diameter (p.6)
$\phi(r)$	intermolecular potential function
χ	angle of deflection (p.23)

$\Omega^{(l,s)}$ collision integrals, where l and s are small positive integers (p.27)

Superscripts

*	indicates a reduction to a dimensionless quantity. e.g. $T^* = T/T_B$, where T_B is the Boyle temperature (pp.16, 120). e.g. $T^*_T = kT/\varepsilon$, the theoretically reduced quantities in terms of σ and ε (pp.28, 124)
i,f	refer to initial and final values.

Subscripts

B	e.g. T_B, refers to Boyle properties (p.120)
b,c,f	refer to quantities belonging to the back vessel, the capillary and the front vessel respectively.
m	e.g. r_m, refers to the value at a maximum or minimum (e.g. p.6)
a,b,x,y	refer to quantities belonging to species a,b,x and y respectively.

Mean values are indicated $\bar{P}$, $\bar{c}$ etc.

Molar quantities are indicated $\tilde{V}$ etc.

A bracket after a quantity indicates it is either a function of the quantity in the bracket e.g. $\phi(r)$ - the potential energy is a function of the intermolecular distance r; or is the value of the quantity at the value indicated. e.g. $B(293^\circ K)$ indicates the second virial coefficient at temperature $293^\circ K$ and $\eta(T)$ indicates the viscosity at temperature T.

APPENDIX 2

USEFUL DATA FOR THE GASES USED

	He	Ne	Ar	Kr	Xe	N_2
Molecular Weight	4.003	20.183	39.944	83.8	131.3	28.01
Atomic Number	2	10	18	36	54	7
B(293°K) cc/mole	11.4	11.2	-16.2	-36.1	-139.2	-6.3
T_B °K (Boyle Temp)	23	125	410	575	775	325
$-B_{0.7}\ T_B$ cc/mole	7.4	10.3	18.3	22.7	29.7	25.5
η (293°K) x 10^{-6} g cm^{-1} sec^{-1}	196.0	310.8	222.6	250.6	228.4	175.7
$\bar{c}$ x 10^{4} cm/sec (eqn. 2.3)	12.3	5.5	3.9	2.7	2.1	4.6
λ (1 atm 293°K) x 10^{-6} cm (eqn 2.4)	18.6	13.2	6.6	5.1	3.7	6.3
σ x 10^{-8} cm (eqn 2.6)	2.2	2.6	3.6	4.2	4.8	3.8

Data taken from (16), (70) and this work.

APPENDIX 3

PRESSURE MEASUREMENTS

The pressures were measured by a cathetometer and are reported here in cms of mercury. The cathetometer can read to ±0.001 cm but the readings are probably no better than ±0.02 cm. The pressures at the various pointer tips are given first, then the pressures during a run are tabulated for each of the ranges used.

Front Vessel

	Colour of sheathing of connecting wire		Pressure
1	Grey	(Gy)	50.14 ±0.02
2	Brown	(Br)	52.02
3	Red	(R)	47.26
4	Mauve	(Ma)	42.05
5	Yellow	(Y)	38.93
6	Green	(Gn)	36.91
7	White	(W)	26.33
8	Black	(Bk)	21.38
9	Orange	(O)	16.25
10	Blue	(Bl)	11.14
11	Pink	(P)	8.15

Back Vessel

1	Green	29.12
2	Yellow	25.13
3	Red	20.05
4	Black	13.70
5	Blue	9.54

The Pressure Range

V_f and V_b were filled to various pressures. There were 10 ranges in all with the mean pressure in the capillary (defined below) varying from over 100 cms to 5 cms of mercury.

In reporting the times of flow the various pressure drops of the ranges are coded for convenience, e.g. P_b 10-3, P_f 26-2 and A-6. The front portion of the code indicates the approximate setting of the front and back pressures, and the figure after the dash shows which pressure drop is being considered. A P_b code means that P_f is initially 55.14 cms and the initial value of P_b is approximately the number shown. A P_f code means that P_b is zero with the pressure in V_f set approximately at the number following P_f. The runs with the code beginning A are atmospheric runs (Range 10).

Thus P_b 10-3 means the third pressure drop (i.e. between the 'mauve' and 'yellow' pointers) of Range 5, and that V_f and V_b are initially filled so that P_f = 55.14 and P_b = 9.54 (i.e. approximately 10).

The various headings in the following table indicate:-

P_f - the pressure in V_f at the pointer (the letter indicates the colour of the plastic sheathing connecting the pointer to the selection switch).

ΔP_f - the difference in pressure between two consecutive pointers in V_f.

$\bar{P}_f$ - the average pressure in V_f between these pointers i.e. $(P_f^i + P_f^f)/2$.

P_b - the pressure in V_b at the instant when the front vessel is at P_f.

ΔP_b - the pressure rise in V_b for the drop of ΔP_f in V_f.

$\bar{P}_b$ - the average pressure in V_b during the pressure drop i.e. $(P_b^i + P_b^f)/2$

$\bar{P}_c$ - the average pressure in the capillary when the pressure in V_f is P_f i.e. $(P_f - P_b)/2$

$\bar{P}$ - the mean pressure in the capillary during the pressure drop from one pointer to the next i.e. $(P_f^i + P_f^f + P_b^i + P_b^f)/4$.

ΔP_c - the pressure difference between the ends of the capillary when the front vessel is at P_f i.e. $(P_f - P_b)$.

$\Delta\bar{P}$ - the mean pressure difference in the capillary during the pressure drop from one pointer to the next i.e. $(\bar{P}_f - \bar{P}_b)$ where subscript i = initial and subscript f = final values of the pressure in a pressure drop.

Pressure Range 1 - Code, P_b30

Initially filled to $P_f = 55.14$, $P_b = 29.12$

	P_f	ΔP_f	$\overline{P_f}$	P_b	ΔP_b	$\overline{P_b}$	$\overline{P_c}$	ΔP_c	$\overline{P}$	ΔP
Br	52.02			29.95			40.98	22.07		
1		4.76	49.64		1.90	30.92			40.28	18.72
Rd	47.26			31.88			39.36	15.37		
2		5.21	44.65		2.10	32.88			38.77	11.77
Mc	42.05			33.89			37.97	8.16		
3		3.12	40.49		1.20	34.46			37.48	6.03
Y	38.93			35.03			36.98	3.90		
4		2.02	37.92		0.76	35.43			36.68	2.49
Gr	36.91			35.82			36.36	1.09		

Pressure Range 2 - Code, [illegible]25

Initially filled to P_f = 53.14, P_b = 26.13

	P_f	ΔP_f	$\bar{P}_f$	P_b	ΔP_b	$\bar{P}_b$	$\bar{P}_c$	ΔP_c	$\bar{P}$	ΔP
Br	52.02			26.07			39.05	25.95		
1		4.78	49.64		2.13	27.14			38.38	22.50
Rd	47.26			28.20			37.73	19.04		
2		5.21	44.65		1.78	29.09			36.87	15.51
Mo	42.05			29.98			36.02	12.07		
3		3.12	40.49		1.24	30.60			35.55	9.89
Y	38.93			31.22			35.08	7.71		
4		2.02	37.92		0.73	31.59			34.75	6.34
Gn	36.91			31.95			34.43	4.96		

Pressure Range 3 - P_b 20

Initially filled to P_f = 55.14, P_b = 20.05

	P_f	ΔP_f	$\bar{P}_f$	P_b	ΔP_b	$\bar{P}_b$	$\bar{P}_c$	ΔP_c	$\bar{P}$	ΔP
Br	52.02			20.94			36.48	31.08		
1		4.78	49.64		1.87	21.87			35.75	27.76
Rd	47.24			22.81			35.08	24.44		
2		5.21	44.63		2.17	23.88			34.27	20.77
Ave	42.03			24.98			33.51	17.07		
3		3.12	40.44		1.15	25.55			33.02	14.94
Y	38.93			26.13			32.53	12.80		
4		2.02	37.92		0.75	26.55			32.24	11.37
Gn	36.91			26.88			31.89	10.03		

Pressure Range 4 - Code, P_b La

Initially filled to P_f = 32.14, P_b = 1[illegible]

	P_f	ΔP_f	$\overline{P}_f$	P_b	ΔP_b	$\overline{P}_b$	$\overline{P}_c$	ΔP_c	$\overline{P}$	ΔP
Br	32.02			16.65			34.34	35.37		
1		4.78	49.64		1.92	17.61			33.62	32.03
Rd	47.26			18.57			32.94	28.69		
2		5.21	44.65		2.16	19.65			32.15	25.00
Wh	42.05			20.73			31.39	21.32		
3		3.12	40.49		1.09	21.28			30.86	19.22
Y	38.93			21.82			30.38	17.11		
4		2.02	37.92		0.78	22.21			30.07	15.71
Gn	36.91			22.60			29.76	14.31		

Pressure Range, S = [illegible], [illegible]

Initially filled to P_f = 55.14, P_b = [illegible]

	P_f	ΔP_f	$\overline{P_f}$	P_b	ΔP_b	$\overline{P_b}$	$\overline{T_c}$	ΔT_c	$\overline{T}$	ΔT
Br	52.62			10.48			31.25	41.84		
1		4.78	49.64		1.98	11.49			30.36	38.15
[illegible]	47.26			12.34			29.88	34.76		
2		5.21	44.63		2.00	13.32			29.09	31.13
[illegible]	42.05			14.55			28.36	27.36		
3		3.12	40.49		1.15	15.12			27.81	25.37
Y	38.93			16.78			27.32	23.23		
4		3.02	37.92		0.87	16.12			27.02	21.81
Cn	36.91			16.53			26.72	20.38		
S		10.58	31.62		3.84	13.45			25.14	13.17
[illegible]	26.33			24.37			23.35	5.96		

Pressure Range 5 - Scale, P_b =

Initially filled to P_f = 33.14, P_g = [illegible]

	P_f	ΔP_f	$\bar{P}_f$	P_b	ΔP_b	$\bar{P}_b$	P_c	ΔP_c	$\bar{P}$	Δ
Br	32.02			1.04			26.53	30.98		
1		4.78	49.64		2.01	2.05			25.84	47.59
Rd	47.26			3.05			25.15	44.21		
2		5.21	44.65		2.05	4.08			24.36	40.58
No	42.05			5.13			23.58	36.95		
3		3.12	40.49		1.20	5.70			23.09	34.79
Y	38.93			6.90			22.62	32.63		
4		2.02	37.92		0.77	6.68			22.38	31.24
Gn	36.91			7.05			21.98	29.85		
5		10.58	31.62		3.94	9.02			20.32	22.60
W	26.33			10.99			18.66	15.34		
6		4.96	23.85		1.80	11.90			17.87	11.91
Bk	21.37			12.80			17.09	8.57		
7		5.06	18.83		1.82	13.71			16.26	5.12
[illegible]	16.31			14.62			15.46	1.69		

Pass range 7 [illegible]

Initially filled to $p_f = 36.91$, $p_b = [illegible]$

	p_f	Δp_f	$\bar{p}_f$	p_b	Δp_b	$\bar{p}_b$	$\bar{p}_c$	Δp_c	$\bar{p}$	Δp
Cn	36.26			[illegible]			16.13	36.26		
1		9.93	31.29		3.70	1.85			16.57	29.44
[illegible]	26.33			3.70			15.02	22.63		
2		4.96	28.35		1.90	4.62			14.25	19.21
B[illegible]	21.37			5.60			13.48	15.77		
3		5.06	18.34		1.75	6.40			12.65	13.36
C	16.31			7.35			11.33	8.96		
4		5.14	13.74		1.72	8.21			10.78	5.53
B1	11.17			9.07			10.12	2.10		

Initially filled to [illegible]

	T_f	ΔT_f	$\bar{T}_f$	T_b	ΔT_b	$\bar{T}_b$	$\bar{T}_c$	ΔT_c	$\bar{T}$	ΔT
W	25.7			[illegible]			15.65	10.72		
1		4.36	23.54		1.67	[illegible].84			12.19	22.70
Bk	21.37			1.67			11.52	19.70		
2		5.12	18.81		1.78	[illegible].56			10.68	16.65
	16.25			2.45			9.85	17.88		
3		5.11	13.67		1.76	4.29			9.41	9.36
Bl	11.14			5.21			8.17	5.93		
4		2.99	9.66		1.81	5.71			7.68	3.93
P	8.15			6.22			7.16	1.93		

Pressure Range 9 - Code, [illegible]16

Initially filled to P_f = 16.25, P_c = 0.00

	P_f	ΔP_f	$\overline{P}_f$	P_b	ΔP_b	$\overline{P}_b$	$\overline{P}_c$	ΔP_c	$\overline{P}$	ΔP
	16.25			0.00			8.12	16.25		
1		5.11	13.76		1.70	0.85			7.31	12.93
B1	11.14			1.70			8.42	9.44		
2		3.06	9.66		1.09	2.24			5.95	7.96
F	8.15			2.79			5.48	5.39		

Pressure Range 10 - Code, A

Atmospheric pressure range

$P_f = P'_f + A$; $P_b = A$ where $A = 76.00$ cm of Hg.

The superscript ' indicates the actual height of mercury; the non superscripted the actual pressure.

	P'_f	ΔP_f	$\bar{P}'_f$	$\bar{P}'_c$	ΔP_c	$\bar{P}'$	$\bar{P}$	ΔP
Cy	33.14			17.57	33.14			
1		3.12	33.58			26.79	102.79	53.57
Br	32.02			26.31	32.02			
		4.77	49.64			24.82	100.82	49.63
	47.26			23.63	47.26			
		3.20	44.65			23.33	98.32	44.65
	42.05			21.03	42.05			
4		3.12	40.49			20.24	96.25	40.49
Y	38.93			19.96	38.93			
		2.02	37.92			18.96	94.96	37.92
Cn	36.91			18.45	36.91			
6		10.58	31.62			15.81	91.81	31.62
	26.33			13.16	26.33			
7		4.95	23.85			11.93	87.92	23.85
Bk	21.38			10.69	21.38			
8		5.13	18.82			9.41	86.41	18.82
	16.25			8.12	16.25			
9		5.11	13.69			6.85	82.85	13.70
Bl	11.14			5.67	11.14			
10		2.99	9.64			4.82	80.82	9.65
0	18.15			4.07	8.15			

APPENDIX 4

VOLUME MEASUREMENTS

The volumes of the front vessel V_f, its side-arm and the backing vessel V_b were determined by pressure measurements. The pressures were measured as heights of mercury and are presented here as such. Dry nitrogen was used and ideal gas conditions assumed. No greater degree of accuracy was necessary since these volumes do not come directly into the equations used in our analyses (4.24), (4.25).

The Front Vessel V_f (see figure (A4.1))

The volume of V_f depends on the volume of mercury which has flowed from it into the side-arm. Let h be the height of the mercury column measured from the mercury level in V_f, and let y be the height of the mercury column measured from the mercury level in V_f when h is zero. Let V_o be the volume of V_f enclosed by taps B, F, K and V_1 (figure (3.1)) when h is zero and P_o the external pressure acting on V_f when h is zero.

If V is the volume of V_f when the height of the mercury column is h and P the total pressure acting on V_f,

$$V = V_o + \pi r^2 y \quad \text{and} \quad P = h + P_{ext}$$

where r is the radius of the side-arm (assumed constant over its length) and P_{ext} the external pressure acting on the side-arm. This was measured by the manometer of V_b, by having taps A and I open.

By Boyle's law,

$$P_o V_o = P(V_o + \pi r^2 y)$$

which on rearranging gives,

$$y = \frac{P_o V_o}{\pi r^2} \left(\frac{1}{P} - \frac{V_o}{\pi r^2} \right)$$

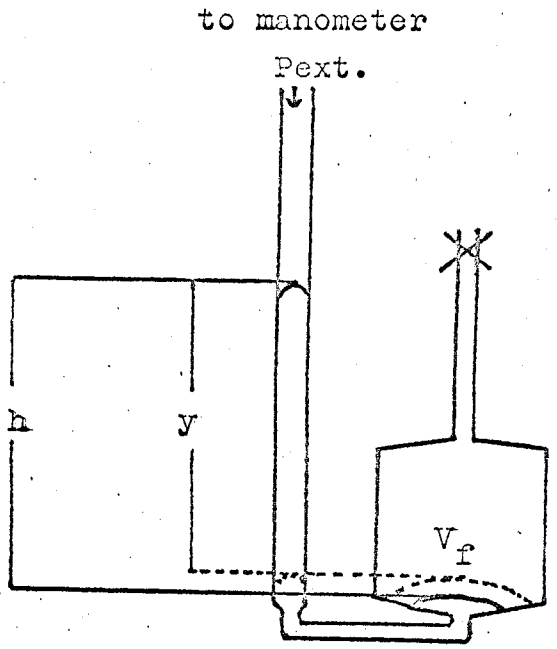


Figure A4.1

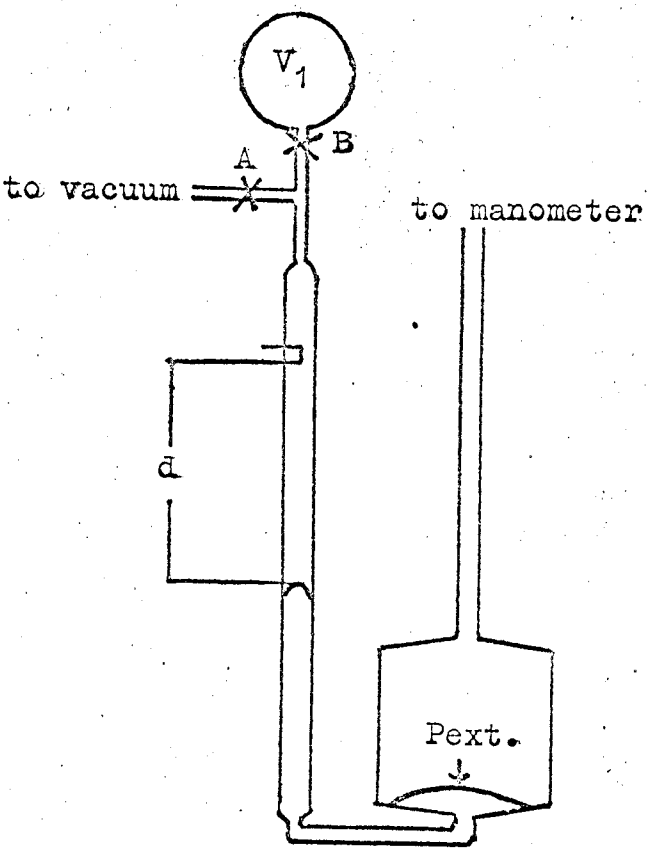


Figure A4.2

Thus if the pressure P acting on a mass of gas enclosed in V_f is varied, a plot of y against 1/P should give a straight line with a slope of $\frac{P_o V_o}{\pi r^2}$.

At $y = 0$, $P = P_o$, so $\frac{V_o}{\pi r^2}$ may be deduced.

The pressures, (i.e. heights of mercury) were measured by a cathetometer to ± 0.005 cm.

Five determinations were made using different initial pressures P_o, and the mean value of $\frac{V_o}{\pi r^2}$ was found to be 366 cm.

The determination of πr^2 (figure A4.2)

A bulb of known volume V_1 was fitted on to the side-arm as shown in figure (A4.2), and was filled with dry nitrogen to a pressure P_1, measured on the manometer of V_b. Tap B was closed and the side-arm was evacuated. Tap A was then closed and Tap B opened, so that the gas in V_1 now filled the space in the side-arm above the mercury surface. The pressure in V_f (now the external pressure) was varied so that the mercury column in the side-arm varied, and hence so did the volume of the gas in the side-arm.

At the distance d (the distance of the mercury surface from the top pointer tip), the volume of the gas will be V, where

$$V = \pi r^2 d + V_1 + V_2$$

and V_2 is the volume between the top pointer tip and taps A and B.

If P is the pressure acting on the enclosed gas (where $P = P_{ext} - h$ and P_{ext} is the pressure of V_f measured by the manometer of V_b), then

$$P_1 V_1 = P(\pi r^2 d + V_1 + V_2)$$

which on rearranging gives,

$$d = \frac{P_1 V_1}{\pi r^2} \frac{1}{P} + \frac{(V_1 + V_2)}{\pi r^2}$$

Thus if the pressure acting on a mass of gas enclosed in the space above the mercury surface in the side-arm and Tap A is varied, a plot of d against $1/P$ should give a straight line with a slope of $\frac{P_1 V_1}{\pi r^2}$. Since P_1 and V_1 are known, $\frac{1}{\pi r^2}$ may be determined, and hence the volume of the front vessel V_o.

From two determinations it was found that $\pi r^2 = 2.91\ cm^2$, and hence V_o is 1070 cc. The errors involved in this method of determination were estimated to be ± 50 cc.

The Backing Vessel V_b

The volume of V_b may be deduced from the pressure rise in V_b with pressure drop in V_f, when the two vessels are connected. If V_b is initially at zero pressure, then

$$P_f^i V_f^i - P_f^t V_f^t = P_b^t V_b$$

where the superscripts i and t refer to the initial and final conditions. After making minor corrections for the small volume of the connecting tubes V_b was estimated to be 2900 ± 100 ccs.

APPENDIX 5

THE TIMES OF FLOW

The times of flow in seconds for the pressure ranges are presented here in the order in which they were obtained: the code for the pressures is explained in Appendix 3. When more than one time was actually recorded, the average is given. The various comments at the head of some tables indicate any noteworthy factors influencing the experimental conditions. The data must be corrected as explained in Chapter 4 for gaseous imperfections and kinetic energy effects before analysis for slip. The times affected by curved-pipe flow are marked * and were neglected in the analysis for the viscosity coefficients.

The atmospheric runs have been corrected to 76.00 cm pressure since they cannot be compared otherwise. From equation 2.41, it can be seen that the time of flow is inversely proportional to $\overline{P}.\Delta P$. ΔP is a constant under these conditions so the time depends on $1/\overline{P}$. $\overline{P}$ itself depends on the atmospheric pressure as $\overline{P} = P_{atm} + (P_f^i + P_f^t)/4$. A correction $(1 + (P_{atm} - 76.0)/100)$ to the times suffices.

The room temperature runs were corrected to 293°K since there were fluctuations of $\pm 1°$. A correction $(1 + (293.1 - T)/200)$ was used: this accounts for the temperature variation and the associated variation of the viscosity (approximately 0.5 μ-poise per °).

Platinum capillary

t 794°K

Code	N_2	He	Ar
P_b30-1	503.0	538.9	665.8
-2	897.2	961.9	1188.3
-3	1066.6	1142.0	1411.4
P_b29-1	435.0		577.7
-2	698.6		928.3
-3	662.4		880.5
-4	673.0		897.9
P_b20-1	380.8	407.0	504.3
-2	563.8	602.0	747.2
-3	469.0	501.0	621.2
-4	402.7	428.9	534.0
P_b19-1	349.9		463.9
-2	495.9		657.1
-3	387.8		515.3
-4	313.1		414.8
P_b10-1	323.0	343.8	427.0
-2	439.7	467.5	581.2
-3	326.8	346.9	432.1
-4	250.3	265.4	331.3
-5	2565.2	2701.9	3394.7
P_b 9-1	306.0	323.9	405.0
-2	401.6	425.0	531.7
-3	285.8	302.0	378.9
-4	211.8	223.4	279.9
-5	1697.8	1780.0	2244.0
-6	1628.3	1704.2	2155.5
P_f36-1	-	-	
-2	1252.2	1282.0	
-3	2206.8	2239.2	
-4	6440.0		
P_f26-1	-	-	
-2	1960.4	1978.0	
-3	4098.8	4069.0	
-4	7019.2	6861.0	

At 1285°K

	N_2	He	A
p_b30-1	1080.9	1158.3	1452.4
-2	1932.9	2069.5	2589.2
-3	2310.7	2466.0	3096.4
p_b25-1	939.1	1003.8	1258.4
-2	1583.8	1609.4	2022.8
-3	1434.9	1524.2	1925.2
-4	1455.0	1548.2	-
p_b20-1	818.5	870.4	1096.4
-2	1212.4	1286.0	1624.6
-3	1010.3	1068.0	1352.4
-4	864.4	914.7	1160.0
p_b15-1	751.7	798.9	1009.4
-2	1064.5	1127.7	1428.3
-3	838.2	882.6	1120.3
-4	669.3	706.2	897.8
p_b10-1	692.4	728.3	928.6
-2	941.3	987.4	1261.8
-3	698.4	732.9	939.8
-4	534.1	557.7	717.8
p_b 8-1	654.3	681.7	877.1
-2	857.8	889.5	1149.1
-3	611.1	631.4	819.6
-4	449.1	462.9	602.3
p_b6-1	3100.4	3090.2	4147.4
-2	2633.6	2579.8	3521.4
p_b4-1	2295.6	2203.6	3060.6
-2	4058.4	3818.2	5421.4

At 1044°K

	N_2	He	Ar	Kr	Xe	Ne
P_b30 -1	778.8	832.6	1040.2	1257.2	1247.8	
-2	1392.6	1486.0	1861.8	2247.8	2227.5	
-3	1666.2	1772.6	2231.8	2690.8	2657.8	
P_b20 -1	589.3	626.6	787.8			
-2	872.0	925.6	1164.6			
-3	726.7	770.7	971.7			
-4	623.0	658.1	833.2			
P_b10 -1	498.0	525.0	666.3			
-2	677.6	712.2	905.5			
-3	504.2	528.7	673.5			
-4	384.8	403.0	515.3			
P_b0 -1	472.2	494.7	630.9	762.5	756.4	
-2	620.8	647.5	827.4	1000.2	994.7	
-3	441.9	458.9	590.0	712.8	708.5	
-4	325.8	338.0	433.8	525.8	521.7	
P_f36 -1	2240.4	2268.0	2990.0			
-2	1913.2	1901.0	2546.0			
-3	3357.8	3306.1	4485.0			
P_f26 -1	1668.0	1626.0	2217.8	2703.6	2698.0	2668.6
-2	2974.0	2839.0	3943.0	4817.4	4810.0	4694.4
-3	6178.0					
P_f16 -1	5146.6	4670.4	6821.0			
-2	6502.0	5674.6				

At 791°K

		N_2	Kr	Xe	Ne
P_b^{36}	-1	499.0	792.5	775.5	
	-2	892.3	1415.3	1384.2	
	-3	1065.7	1694.3	1653.8	
P_b^{0}	-1	303.8	482.1	472.1	
	-2	398.1	632.6	619.2	
	-3	283.9	451.8	441.4	
	-4	208.9	331.7	325.2	
P_F^{26}	-1	1083.4	1718.6	1686.4	1759.0
	-2	1934.4	3071.7	3014.7	3100.0
	-3	4035.6			6368.0

At 1288°K

		N_2	Kr	Xe	Ne
P_b^{30}	-1	1088.3	1767.3	1765.5	
	-2	1944.7	3158.7	3154.8	
	-3	2324.1	3775.6	3772.3	
P_b^{0}	-1	658.9	1068.2	1070.8	
	-2	861.5	1401.1	1404.5	
	-3	613.1	997.5	999.7	
	-4	451.9	735.3	736.0	
P_F^{26}	-1	2312.4	3767.0	3799.4	3628.3
	-2	4101.4	6686.6	6758.8	6358.1

At 1304°K

Before these runs an attempt was made to take readings at 1500°K. However contrary to metallurgical advice, the helix keeled over under its own weight due to it being so ductile at these temperatures. A supporting bridge was made from A.P. Green G.30 refractory brick. This made the temperature gradients of the surroundings about the capillary uniform to ±0.7° at 1273°K. The effects of this accident were not serious - the intercept of the straight line analysis plot (equation 4.7) were within experimental error but the gradients had changed. This was ascribed to surface effects and is discussed in Chapter 5.

	N_2	He	Ar	Xe	Kr
P_b30 -1	1109.8	1178.4	1490.4		
-2	1990.0	2100.8			
P_b0 -1	670.6	689.2	895.4	1093.6	1091.0
-2	879.5	897.6	1177.6	1436.8	1430.8
-3	626.4	637.6	837.8	1023.6	
-4	458.4	464.2	611.2	748.0	
P_f26 -1	2349.4	2194.0	3125.6	3867.6	
-2	4160.4	3789.6	5526.4	6887.0	

At 1047°K

	N_2	He	Ar
P_b30 -1	786.1	835.0	1050.2
-2	1408.5	1493.5	1883.7
-3	1691.8	1793.0	2262.2
P_b20 -1	593.6	626.9	792.0
-2	878.8	927.4	1174.8
-3	732.7	772.5	979.4
-4	624.3	656.1	834.2
P_b10 -1	502.4	527.3	672.2
-2	684.4	716.5	915.1
-3	508.6	530.5	679.0
-4	386.4	403.6	518.1
P_b0 -1	474.6	491.6	633.7
-2	624.0	644.2	832.6
-3	444.5	456.8	593.9
-4	325.2	333.8	433.4
P_f36 -1	2266.0	2254.2	3016.0
-2	1932.6	1888.0	2572.8
-3	3398.0	3273.6	4514.4
P_f26 -1	1678.0	1617.0	2233.4
-2	2984.0	2822.7	3974.5

At 293°K

The effects of curved-pipe flow were observed at this temperature

		N_2	He	Ar	Kr	Xe	Ne
P_b30	-1	97.1*	104.1	122.6*	144.8*	147.9*	
	-2	170.0*	186.7	215.2*	246.4*	241.3*	
	-3	201.8*	222.4	256.5*	289.3*	268.8*	
	-4	346.0	382.1	439.3	496.4*	455.6*	
P_b25	-1	85.2*	90.2	107.5*	128.8*	131.9*	
	-2	133.0*	145.2	168.0*	195.3*	195.5*	
	-3	125.1*	137.8	158.4*	180.4*	172.6*	
	-4	126.3*	139.2	160.4*	181.4*	168.6*	
P_b20	-1	75.9*	78.6	94.7*	115.0*	118.3*	
	-2	108.6*	117.0	136.9*	161.2*	164.2*	
	-3	88.9*	97.4	112.3*	129.6*	128.2*	
	-4	75.6*	83.2	95.9*	108.9*	104.9*	
P_b15	-1	70.6*	72.8	88.1*	107.6*	110.8*	
	-2	96.8	102.8	121.4*	145.0*	148.0*	
	-3	74.1*	80.6	93.6*	109.4*	109.8*	
	-4	58.9*	64.4	74.6*	85.5*	84.4*	
P_b10	-1	66.0*	67.3	82.3*	100.7*	104.2*	
	-2	86.6*	90.9	108.8*	131.0*	134.4*	
	-3	63.1*	68.0	79.2*	93.5*	95.5*	
	-4	47.5*	51.5	60.0*	69.9*	70.1*	
	-5	484.6*	532.7	614.2*	696.9*	659.7*	
P_b0	-1	63.5*	68.4	78.7*	96.9*	100.4*	
	-2	80.3*	83.0	100.8*	122.0*	125.9*	
	-3	56.1*	59.4	70.5*	84.3*	86.0*	
	-4	40.5*	43.5	51.1*	60.5*	61.6*	
	-5	322.2*	352.1	407.9*	467.4*	457.4*	
	-6	308.0	388.4	391.7	441.3	409.1*	
	-7	913.8	1003.1	1159.8	1316.6	1212.0*	
P_f36	-1	279.0*	303.8	352.7*	405.8*	399.2*	
	-2	237.3	259.7	301.0	340.2	319.1*	
	-3	417.6	457.5	529.3	598.4	548.7*	
	-4	1232.2	1347.9	1563.8	1766.2	1617.4	
P_f26	-1	207.5	226.8	262.3	297.0	278.6*	365.7
	-2	371.5	405.2	470.4	531.4	489.6*	653.5
	-3	781.0	850.0	988.3	1117.3	1019.9	1372.5
P_f16	-1	659.1	712.6	832.1	942.7	862.3	1154.9
	-2	848.2	912.0	1071.6	1210.2	1106.0	1479.8

At 1153°K

At this temperature 'atmospheric' runs were introduced

	N_2	He	Ar	Kr	Xe	Ne
P_b30 -1	914.5	972.7	1226.6	1479.2	1473.1	
-2	1636.1	1736.2	2195.0	2649.0	2632.4	
-3	1964.0	2076.3	2634.2	3173.0	3172.0	
P_b25 -1	792.0	839.0	1058.7	1281.3	1278.8	
-2	1272.4	1345.0	1701.3	2055.4	2046.8	
-3	1212.8	1279.8	1624.6	1966.5	1957.4	
-4	1226.8	1290.2	1640.4	1992.2	1980.0	
P_b20 -1	692.1	730.3	925.0	1120.2	1114.4	
-2	1025.0	1078.9	1369.6	1656.8	1650.2	
-3	855.7	898.4	1143.6	1385.0	1380.4	
-4	728.2	764.1	976.0	1181.6	1173.8	
P_b15 -1	635.4	667.0	852.0	1031.0	1026.8	
-2	899.6	943.2	1205.8	1460.2	1453.4	
-3	705.8	738.8	948.2	1150.4	1144.0	
-4	564.0	588.2	755.2	913.0	909.2	
P_b10 -1	585.9	611.4	783.4	949.2	946.2	
-2	796.7	828.0	1066.3	1290.4	1285.8	
-3	593.9	615.2	792.3	962.8	959.2	
-4	450.4	466.3	602.5	727.5	726.6	
P_b0 -1	553.4	572.9	740.9	896.8	896.1	
-2	726.5	749.6	971.1	1175.5	1173.1	
-3	518.6	530.8	689.3	839.5	838.7	
-4	379.0	387.9	506.7	613.6	612.0	
P_f36 -1	2628.0	2603.0	3503.2	4257.4	4253.0	
-2	2237.0	2173.0	2978.2	3630.0	3633.0	
P_f26 -1	1948.0	1857.4	2594.0	3166.0	3169.0	3064.0
-2	3458.0	3223.0	4601.0	5621.0	5650.0	5371.0

	N_2	H_e	Ar
1	96.0	165.4	129.1
2	160.6	176.5	215.3
3	193.5	213.0	259.6
4	126.9	139.1	170.2
5	87.6	95.9	117.3
6	563.0	610.2	754.6
7	354.1	387.9	474.2
8	461.5	516.0	619.3
9	651.8	714.0	871.6
10	552.3	604.7	739.2

At 926°K

	N_2	He	Ar	Kr	Xe	Ne
P_b30-1	643.6	684.9	860.5	1033.4	1015.0	
-2	1151.8	1223.4	1540.6	1846.4	1817.4	
-3	1383.7	1468.0	1846.0	2223.3	2192.2	
P_b25-1	558.2	595.8	745.2	896.0	883.3	
-2	897.9	954.0	1198.2	1442.0	1418.1	
-3	858.1	908.5	1146.4	1380.2	1356.0	
-4	866.0	916.8	1154.8	1392.4	1367.9	
P_b20-1	487.3	517.6	650.4	780.4	770.8	
-2	721.6	764.4	962.4	1155.1	1138.6	
-3	604.5	638.8	806.4	967.5	955.5	
-4	512.9	541.0	683.5	823.0	810.4	
P_b15-1	447.9	472.3	597.4	720.0	709.0	
-2	635.5	668.0	847.4	1019.8	1004.2	
-3	500.3	524.9	667.6	802.4	791.6	
-4	398.4	416.6	531.0	638.8	629.6	
P_b10-1	413.1	434.8	552.0	662.6	653.2	
-2	561.5	589.1	750.1	898.8	887.2	
-3	419.4	439.2	560.9	671.2	663.0	
-4	317.1	331.9	424.0	509.4	502.4	
P_b 0 -1	390.5	408.9	522.3	626.1	619.4	
-2	513.1	538.9	684.9	821.3	811.8	
-3	366.8	380.8	489.5	586.8	580.7	
-4	267.4	277.2	357.2	428.0	424.3	
P_f36-1	1863.6	1884.1	2486.2	2994.0	2956.0	3038.8
-2	1589.4	1581.7	2117.6	2552.6	2521.4	2564.4
P_f26-1	1385.8	1360.9	1842.3	2227.6	2201.0	2243.4
-2	2470.0	2373.0	3286.1	3986.4	3929.8	3926.2
A 1	68.1*	73.8	90.5*			
2	113.4	123.2	151.5			
3	136.2	148.5	182.0			
4	89.6	97.3	119.7			
5	61.5	67.0	82.1			
6	396.8	432.2	530.3			
7	249.2	271.5	333.1			
8	325.6	354.2	434.8			
9	459.3	499.3	612.3			
10	388.9	422.9	519.1			

At 1530°K

		N_2	He	Ar	Kr	Xe
P_b30	-1	1426.0	1507.4	1916.9	2328.0	2342.2
	-2	2555.0	2688.2			
P_b0	-1	859.0	873.3	1151.4	1400.8	1414.6
	-2	1124.6	1136.2	1540.8	1838.0	1857.8
	-3	802.9	807.0	1076.2		
	-4	585.9	586.3			
A	1	150.2	166.4	202.8		
	2	252.6	278.7	339.8		
	3	303.0	336.5	408.8		
	4	199.8	220.5	269.6		
	5	136.8	152.0	184.4		
	6	883.0	976.3			
	7	554.6	612.4			

Platinum - 20% Rhodium capillary

	At 292°K		At 293°K	
	N_2	He	N_2	Ar
P_b30 -1	139.6*	150.9	140.0*	176.4*
-2	245.0*	269.7	246.0*	312.4*
-3	292.1	322.4	291.8	370.2
-4	491.6	543.4		
P_b25 -1	121.9*	130.8	122.6*	154.2*
-2	192.0*	209.8	192.8*	244.4*
-3	181.5	200.3	182.2	231.0
-4	182.3	201.4	183.2	233.2
P_b20 -1	108.2*	114.4	108.2*	135.8*
-2	156.0*	169.0	156.6*	197.8*
-3	128.9*	141.1	128.6*	163.8**
-4	109.1*	120.0	109.2*	138.6
P_b15 -1	100.0*	105.2	100.4*	126.2*
-2	138.2*	148.8	139.0*	175.4*
-3	107.5*	117.3	108.0*	136.2*
-4	85.0*	93.1	85.2*	108.4*
P_b10 -1	93.0*	97.1	93.8*	117.2*
-2	123.7	132.1	123.8*	156.2*
-3	91.0*	98.4	91.2*	115.0*
-4	68.0*	74.6	68.4*	86.8*
-5	700.6*	774.4	703.8*	892.8*
P_b0 -1	89.9*	92.1	90.2*	112.4*
-2	114.6	120.7	115.0*	144.6*
-3	80.8*	86.3	80.6*	102.0*
-4	58.3*	63.4	59.0*	73.8*
-5	467.6*	511.2	468.0*	594.0*
-6	447.7	492.4	448.8	568.6
P_f36 -1	404.7*	440.5	405.0*	512.4*
-2	344.0	377.0	344.6	437.4
-3	604.6	664.0	605.6	768.6
P_f26 -1	300.2	328.6	302.0	381.8
-2	537.2	587.2	539.2	683.6
-3	1129.2	1236.0	1132.0	1435.8
P_f16 -1	953.0	1036.0	957.2	1212.6
-2	1222.0	1321.0	1224.8	1553.4

At 799°K

	N_2	He	Ar
P_b30 -1	739.7	801.4	948.4
-2	1320.5	1433.6	1756.6
-3	1578.7	1712.7	2098.2
P_b25 -1	640.2	694.0	853.9
-2	1029.6	1115.0	1370.0
-3	980.4	1060.6	1305.0
-4	989.8	1069.8	
P_b20 -1	560.2	606.8	745.4
-2	828.5	898.0	1101.9
-3	692.0	749.3	919.9
-4	587.6	635.5	780.7
P_b15 -1	516.0	557.2	685.0
-2	730.4	789.0	972.2
-3	574.4	620.3	762.6
-4	458.2	493.7	607.6
P_b10 -1	477.1	513.9	633.8
-2	648.4	699.0	863.4
-3	483.1	520.7	643.2
-4	365.7	394.2	
P_b0 -1	450.4	482.9	597.4
-2	591.3	633.6	784.8
-3	421.9	451.9	560.0
-4	308.6	330.6	410.8
P_f36 -1	2154.0	2288.4	2860.0
-2	1839.0	1945.2	2443.6
P_f26 -1	1606.6	1691.4	2128.6
-2	2860.6	2992.2	3786.4
P_f16 -1	5025.6	5100.4	6652.4
-2	6389.0	6389.0	

At 1146°K

At this temperature the times of flow decreased continuously at first. This was due to the Pt/Rh reannealing, although it had been annealed in the workshop. Accordingly the capillary was heated to 1500°K for some hours to speed up the process. The times of flow were then reproducible, although some 10% lower than the original times. The effects due to slip had doubled: this is discussed further in Chapter 5.

The capillary surface had turned a dull grey colour but still had great tensile strength (unlike the platinum capillary).

	N_2	He	A
P_b30 -1	1171.8	1261.2	1568.6
-2	2095.2	2249.8	2805.6
-3	2510.0	2688.6	3356.0
P_b25 -1	1014.6	1090.0	1357.8
-2	1634.2	1751.0	2185.8
-3	1551.6	1659.0	2079.8
-4	1572.4	1679.2	2100.8
P_b20 -1	885.4	946.0	1186.2
-2	1310.0	1399.8	1756.6
-3	1094.4	1165.8	2713.2
-4	929.8	990.6	
P_b15 -1	814.6	870.9	1094.4
-2	1156.8	1234.8	1550.6
-3	907.4	966.2	1217.6
-4	724.2	769.0	969.0
P_b10 -1	748.8	794.2	1003.2
-2	1018.6	1077.0	1362.4
-3	758.4	800.2	1015.4
-4	576.2	606.8	768.8
P_b0 -1	704.6	740.8	944.2
-2	925.0	969.6	1236.0
-3	659.6	689.2	885.0
-4	480.8	502.0	644.8
P_f36 -1	2853.2	2883.0	3810.2
P_f26 -1	4415.0	4319.1	5860.0

		N_2	He	Ar
A	1	122.5	135.4	165.3
	2	205.6	226.2	275.9
	3	248.0	272.3	333.8
	4	163.0	179.0	218.8
	5	112.0	122.6	150.8
	6	722.0	792.8	968.5
	7	454.4	498.7	610.5
	8	590.0	645.6	791.8
	9	836.4	919.6	1127.4
	10	709.6	776.0	954.7

At 293°K

	N_2	He	Ar
P_b30 -1	125.0*	135.0	158.0*
-2	220.2*	241.0	280.0
-3	261.6	288.0	332.4
P_b25 -1	109.4*	117.0	137.6*
-2	172.0*	187.8	218.0*
-3	162.4	178.4	205.6
-4	163.8	179.6	207.8
P_b20 -1	97.0*	102.2	122.2*
-2	139.8*	151.8	177.2*
-3	115.4*	126.2	146.0*
-4	97.4	107.6	124.0
P_b15 -1	90.2*	94.0	113.0*
-2	124.4*	133.6	156.6*
-3	96.4*	104.4	121.6*
-4	76.0	83.8	96.8
P_b10 -1	84.6*	87.1	105.8*
-2	111.6*	118.5	140.4*
-3	81.6*	88.2	103.0*
-4	62.0*	67.0	78.0*
-5	629.4	691.6	800.2
P_b0 -1	81.0*	82.2	101.4*
-2	103.4*	108.0	130.2*
-3	72.2*	77.2	91.0*
-4	52.6*	56.4	66.2*
-5	418.6*	457.2	531.6*
-6	400.6	439.4	508.8
P_f36 -1	362.2*	392.2	457.6*
-2	307.8	335.8	390.4
-3	541.0	589.8	686.2
P_f26 -1	269.4	293.2	342.0
-2	482.6	525.2	611.0
-3	1013.6	1102.2	1288.0
P_f16 -1	855.0	922.6	1083.6
-2	1095.4	1174.4	1389.4

At 800°K

		N_2	He	Ar
P_b30	-1	661.4	713.6	878.2
	-2	1183.8	1274.8	1573.2
	-3	1415.2	1524.2	1884.2
P_b25	-1	573.0	615.8	763.0
	-2	921.0	992.6	1224.8
	-3	877.6	943.2	1168.0
	-4	886.0	951.8	1176.0
P_b20	-1	500.4	538.8	665.0
	-2	741.8	798.2	987.2
	-3	619.2	665.4	822.6
	-4	527.2	564.6	699.6
P_b15	-1	460.6	494.2	612.4
	-2	653.6	700.8	869.0
	-3	512.8	548.8	682.2
	-4	409.4	438.8	544.6
P_b10	-1	424.4	453.8	565.8
	-2	577.6	619.2	770.0
	-3	431.0	460.6	573.4
	-4	326.2	348.8	434.0
P_b0	-1	403.2	429.0	535.8
	-2	529.4	561.6	703.8
	-3	377.6	401.0	501.2
	-4	275.6	292.0	367.0
P_f36	-1	1920.0	2008.0	2551.0
	-2	1640.0	1705.0	2176.8
P_f26	-1	2544.0	2596.8	3365.0
P_f16	-1	5661.6	5471.6	7460.4
A	1	69,7*	75.3	92.7*
	2	116.8*	125.8	155.3*
	3	140.1	152.5	186.5
	4	91.8	99.5	122.5
	5	63.1	68.8	84.0
	6	407.2	442.0	542.3
	7	256.0	278.5	341.0
	8	333.5	362.0	443.4
	9	471.1	512.6	627.7
	10	399.0	431.7	528.1

At 1143°K

	N_2	He	Ar
P_b30 -1	1169.6	1259.6	
-2	2095.6	2233.1	
P_b20 -1	884.8	948.6	
-2	1310.6	1404.0	
P_b10 -1	749.4	799.6	
-2	1019.8	1087.0	
-3	759.0	807.4	
P_b0 -1	707.6	744.0	
-2	928.6	979.0	
-3	662.8	696.8	
-4	484.0	507.2	
P_f36 -1	3355.6	3446.4	
P_f26 -1	2498.0	2494.2	
A 1	123.1	135.6	165.2
2	206.1	226.9	276.0
3	248.6	273.6	333.6
4	162.7	179.6	218.1
5	111.8	123.4	150.1
6	723.3	796.0	971.0
7	454.1	499.9	1402.9
8	590.6	651.6	
9	838.9	922.2	
10	710.6	777.1	

At 1275°K

	N_2	He	Ar
P_b30-1	1388.2	1501.0	1866.0
-2	2486.4	2681.3	3337.6
-3	2980.2	3204.0	4001.0
P_b25-1	1202.6	1301.2	1615.0
-2	1935.0	2089.4	2598.0
-3	1843.6	1987.4	2480.8
-4	1858.6	1998.6	2497.4
P_b20-1	1050.2	1126.4	
-2	1557.4	1668.8	
-3	1298.0	1387.4	
-4	1102.0	1181.4	
P_b15-1	965.0	1039.0	1296.2
-2	1369.8	1471.6	1840.0
-3	1073.6	1153.0	1443.4
-4	856.4	917.4	1147.0
P_b10-1	889.4	946.8	1192.4
-2	1209.4	1286.2	1620.2
-3	899.4	953.6	2125.4
-4	680.6	723.4	
P_b 0 -1	837.2	883.8	1124.0
-2	1098.8	1155.0	1474.0
-3	784.4	821.8	1050.2
-4	572.2	598.6	768.6
-1	3970.0	4047.0	5313.4
P_p36 -2	3376.0	3388.0	4503.2
-1	2941.2	2914.0	3929.8
P_p26 -2	5194.4	5058.4	6932.2
A 1		161.7	
2	244.2	270.8	
3	296.0	326.7	
4	194.2	214.9	
5	132.9	147.2	
6	858.7	948.9	
7	540.6	597.4	
8	705.9	777.7	
9	992.6	1096.2	

At 1275°K

Having nearly completed all the desired runs, water was observed in the lead tubes to the capillary. This was due to flux, water and kovar reacting in such a way as to corrode the kovar. Stainless steel sleeves were inserted as indicated in Chapter 3. The slip factor was slightly affected by this mishap.

	N_2	He	Ar	Kr	Xe
P_b30 -1	1383.3	1490.3	1838.2	2246.2	2245.2
-2	2476.0	2656.6	3324.4		
P_b20 -1	1044.4	1118.4	1405.8		
-2	1554.2	1657.7			
P_b10 -1	885.9	937.1	1189.8		
-2	1207.0	1272.3			
-3	896.6	948.8			
P_b0 -1	835.5	877.5	1116.8	1355.2	1362.8
-2	1094.8	1145.2	1468.8	1779.0	1784.8
-3	781.6	812.5	1044.6	1271.4	1272.2
-4	571.4	594.6			
P_f36 -1	3942.0	3997.0			
-2	3360.0	3348.2			
P_f26 -1	2908.0	2853.0	3882.6	4746.0	4777.4
-2	5150.6	4968.6	6864.4		
A 1	146.9	161.7	196.8		
2	245.0	270.6	329.2		
3	295.3	325.6	397.2		
4	193.8	214.0	259.6		
5	133.2	147.0	178.0		
6	859.0	949.0	1153.5		
7	539.5	597.0	725.6		
8	704.0	776.2			

At 1457°K

	N_2	He	Ar	Kr	Xe
P_b30-1	1697.4	1815.4	2286.0	2771.8	2787.2
P_b20-1	1285.6	1364.6			
P_b10-1	1086.0	1139.0	1456.2		
-2	1480.8	1550.0			
P_b0 -1	1023.0	1064.0	1373.0	1671.6	1684.4
-2	1346.0	1388.4	1807.0		
-3	958.6	985.4	1283.6		
-4	698.4	715.2			
P_f36 -1	4813.0	4722.0			
P_f26 -1	3545.8	3347.2	4730.2	5813.6	5910.0
A 1		199.8	240.8		
2	301.0	333.7	406.8		
3	362.4	401.6	489.6		
4	237.7	265.0	320.0		
5	164.0	181.9	220.0		
6	1056.0	1168.6	1423.1		
7	666.0	730.9	897.6		
8	863.4	956.8			

At 1457° K

	N_2	He
P_b30 -1	1693.0	1798.4
P_b0 -1	1017.2	1040.7
-2	1332.4	1358.0
A 1	179.2	198.1
2	299.7	330.8
3	360.9	399.8
4	237.6	263.0
5	163.9	180.0

At 1275° K

	N_2	He
P_b30 -1	1361.4	1446.0
P_b0 -1	818.3	844.1
P_f26 -1	2839.4	2700.0
A 1	143.9	158.4
2	241.0	264.0
3	290.2	318.6
4	190.8	209.5
5	131.1	144.1

At 798°K

	N_2	He
P_b30 -1	648.2	692.0
P_b0 -1	392.8	413.4
P_f26 -1	1388.0	1391.2
A -1	69.0	73.7
-2	114.6	122.9
-3	138.0	149.2
-4	90.3	97.6
-5	62.2	66.9

At 293°K

Neon from a cylinder was used; before B.D.H. C. spectrally pure Ne obtained from 1 litre flasks was used.

	N_2	He	Ne
P_b30-1	123.7*	134.0	214.1
-2	217.3*	239.0	382.3
-3	258.1	286.2	455.7
P_b20-1	96.4*	101.2	163.0
-2	138.8*	150.0	240.8
-3	114.4*	125.4	201.0
-4	96.8*	106.2	170.6
P_b10-1	83.6*	86.0	138.4
-2	110.4*	117.6	188.4
-3	80.6*	87.4	139.8
-4	60.8*	66.0	106.4
-5	623.2	686.2	1101.0
P_b0 -1	80.4*	81.8	131.4
-2	102.4*	107.2	172.6
-3	71.6*	76.4	122.8
-4	52.0*	55.7	89.8
-5	415.4*	453.7	727.4
-6	396.6	435.8	700.0
P_f36 -1	359.0*	389.1	626.2
-2	305.4*	333.0	536.0
-3	536.8	586.3	944.0
P_f26 -1	266.8	291.1	
-2	477.0	518.7	836.0
-3	1004.2	1089.2	1755.0
P_f16 -1	846.0	910.6	
-2	1082.6	1159.0	

At 804°K

	N_2	He	Ne
P_b30-1	638.1	700.3	1100.0
-2	1175.4		1975.5
-3	1406.2		2367.6
P_b20-1	497.9	527.8	832.0
-2	736.4		1235.5
-3	615.0		1031.0
-4	520.8		873.0
P_b10-1	422.0	445.2	706.0
-2	574.0	607.2	958.0
-3	427.6		712.8
-4	324.2		540.0
P_b0 -1	399.6	418.4	666.0
-2	525.2	550.0	871.0
-3	374.0		621.8
-4	272.8		453.0
P_f36 -1	1898.8	1950.0	3111.0
P_f26 -1	1413.0	1418.0	2294.0
-2	2510.2		4055.0
P_f16 -1	4365.0	4155.4	6933.4
A 1		75.0	117.2
2		125.4	196.0
3		151.5	236.1
4	91.7	98.6	154.8
5	62.9	68.1	106.6
6	405.5	439.5	686.4
7	254.5	275.5	431.4
8	333.0	360.2	561.1

At 1059°K

	N_2	Ne
P_b30 -1	1015.4	1694.8
P_b20 -1	769.4	1276.6
P_b10 -1	652.0	1070.6
-2	885.8	1457.6
P_b0 -1	615.6	1009.0
-2	809.0	1324.2
-3	575.4	943.0
-4	421.6	685.2
P_f26 -1	2158.2	3413.2
A -1	107.1	181.6
-2	179.8	303.3
-3	216.4	365.0
-4	142.1	238.8
-5	97.1	163.8
-6	629.2	1061.8
-7	397.0	666.4
-8	514.7	869.6

At 1505°K

	N_2	Ne
P_b30 -1	1775.0	2915.0
P_b10 -1	1139.4	1833.8
P_b0 -1	1065.8	1711.0
-2	1396.2	2237.2
P_f26 -1	3669.4	5566.4
A -1	188.5	316.6
-2	314.9	529.5
-3	379.1	639.4
-4	248.3	418.2
-5	170.8	288.4

At 1273°K

	N_2	He	Ne
P_b30 -1	1365.0	1450.1	2258.0
P_b20 -1	1029.6	1087.0	1699.4
P_b10 -1	872.4	910.6	1428.8
	1182.8	1232.6	
P_b0 -1	821.1	848.6	1337.8
-2	1076.4	1108.0	1750.0
-3	766.0	787.6	1244.6
-4	558.3	571.3	909.6
P_f36 -1	3862.6	3828.8	
P_f26 -1	2849.3	2720.7	4442.8
A -1	144.2	159.4	243.4
-2	241.2	266.4	405.7
-3	291.5	319.0	489.3
-4	190.3	209.2	322.4
-5	130.4	143.7	220.9
-6	845.0	928.1	1420.6
-7	530.6	584.1	891.5
-8	689.1	761.6	

At 801°K

	N_2	He	Ne
P_b30-1	650.6	691.4	1094.0
P_b20-1	492.0	519.7	825.0
-2	730.6	771.3	1229.8
P_b10-1	417.3	437.4	698.6
-2	569.0	595.0	949.2
-3	424.0	443.1	708.6
-4	320.4	334.7	533.0
P_b0 -1	396.0	411.6	658.4
-2	518.6	539.4	861.8
-3	370.4	384.6	614.8
-4	270.7	280.0	450.4
P_f36 -1	1882.0	1918.6	3097.0
P_f26 -1	1399.0	1392.6	2288.2
P_f16 -1	4325.0	4068.6	6797.0
A 1		73.8	115.4
2		123.4	192.8
3		148.6	233.0
4	90.4	97.4	153.4
5	62.1	67.0	106.4
6	401.7	434.7	678.8
7	252.0	272.9	

At 293°K

	N_2	He	Ne
P_b30-1	123.4*	133.4	214.2
-2	216.9*	238.0	382.0
-3	257.5	284.3	457.7
P_b20-1	95.6*	101.0	162.4
-2	138.4*	149.4	240.0
-3	113.6*	124.6	200.4
-4	96.4*	105.8	169.8
P_b10-1	83.6*	85.6	138.4
-2	109.8*	116.7	188.0
-3	80.9*	86.7	139.6
-4	60.3*	65.7	106.0
-5	621.6	682.6	1098.0
P_b0-1	80.4*	81.4	131.6
-2	101.9*	106.8	171.8
-3	71.5*	75.9	122.8
-4	51.6	55.3	89.2
-5	414.0*	450.6	725.2
-6	395.2	433.8	698.0
P_f36-1	357.5*	387.4	624.6
-2	304.1	331.0	533.8
-3	535.2	583.0	941.0
P_f26-1	265.8	288.6	466.1
-2	475.8	516.8	835.0
-3	999.6	1081.6	1754.0
P_f16-1	842.3	903.6	1469.0
-2	1078.6	1152.6	1875.6

Silica Capillary

At 293°K

	N_2	He	Ar	Kr	Xe	Ne
P_b30-1	147.5*	163.0	187.4*	211.8*	202.6*	261.4
-2	259.6	287.4	330.8	371.3	343.9*	462.5
-3	299.4	332.0	381.8	428.6	391.8	533.8
P_b20-1	113.4*	124.7	143.7*	164.0*	160.7*	200.8
-2	166.7*	183.8	211.7*	239.0*	226.4*	295.7
-3	137.9	152.4	174.9	197.2	182.9*	245.7
-4	116.1	128.8	147.3	166.0	152.7	207.2
P_b10-1	97.3*	106.5	123.8*	141.8*	141.2*	171.6
-2	131.6*	144.7	167.0*	189.5*	183.9*	233.0
-3	97.5	107.4	124.1	140.1*	132.6*	173.4
-4	73.8	81.4	93.4	105.3	98.9*	131.0
-5	736.6	835.7	962.9	1082.3	993.3*	1345.4
P_b0 -1	93.0*	101.0	117.8*	136.3*	136.2*	163.3
-2	121.7*	132.5	153.8*	175.9*	171.7*	213.7
-3	86.2*	94.6	109.6*	124.2*	118.9*	152.6
-4	63.0*	68.9	80.2*	90.2*	85.0*	111.5
-5	509.1	561.3	647.6	727.8	673.9*	904.0
-6	487.5	535.3	620.0	695.8	637.4*	864.9
P_f36-1	422.2	463.3	536.2	602.6	558.7*	747.2
-2	376.9	413.2	479.0	539.1	492.8	669.0
-3	662.7	725.4	841.0	947.2	864.5	1173.6
P_f26-1	303.6	333.0	385.0	434.7	396.4	538.2
-2	590.9	645.3	750.0	844.0	772.8	1044.2
-3	1243.2	1353.6	1576.0	1776.1	1621.0	2192.4
P_f16-1	1010.2	1095.2	1282.8	1443.1	1317.7	1773.0
-2	1347.5	1451.0	1707.5	1925.3	1761.6	2363.2

At 373°K

	N_2	He	Ar	Kr	Xe	Ne
P_b30-1	225.9	245.0	290.6	332.1	310.4*	392.8
-2	397.7	433.2	513.5	587.0	545.6	691.7
-3	459.2	499.8	591.1	677.9	631.6	800.3
P_b20-1	173.0	187.3	222.4	254.7*	239.0*	300.8
-2	254.2	276.4	327.9	374.9	350.0*	441.6
-3	211.0	229.3	271.8	311.4	289.5	367.5
-4	178.0	193.8	229.5	263.2	243.5	310.3
P_b10-1	147.6	159.8	190.0	218.0*	206.7*	255.6
-2	200.6	217.4	257.9	295.7	277.7*	348.0
-3	148.6	161.0	191.7	219.7	204.4*	258.8
-4	112.5		145.0	166.2	154.6	195.9
P_b0 -1	140.6*	151.6	181.4*	208.0*	198.5*	243.0
-2	183.8	199.0	236.8	272.0*	256.8*	319.4
-3	131.0	142.1	168.6	193.4	181.1*	227.3
-4	95.9	103.6	123.6	141.6	132.0*	166.4
P_f36 -1	644.4	694.4	830.4	950.4	882.6	1116.4
-2	575.2	619.2	741.6	848.0	787.4	995.0
P_f26 -1	465.6	498.6	600.0	684.8	636.8	804.4
-2	901.4	965.8	1160.4	1330.1	1233.2	1553.2
P_f16 -1	1540.1	1624.3	1979.8	2266.4	2102.4	2630.0

At 566°K

	N_2	He	Ar	Kr	Xe	Ne
P_b30-1	456.0	490.7	601.1	705.0	673.0	777.1
-2	806.7	869.0	1061.8	1248.0	1193.0	1379.2
-3	935.4	1007.7	1234.0	1443.8	1385.8	1591.3
P_b20-1	349.1	375.3	457.9			
-2	515.6	553.2	678.3			
-3	427.0	459.3	1562.1			
-4	360.9	389.5	476.6			
P_b10-1	297.8	319.5	390.8			
-2	404.8	434.8	532.9			
-3	301.5	322.3	395.4			
-4	227.4	244.8	300.5			
P_b0 -1	283.2	302.2	371.8	457.3	419.2	480.4
-2	371.7	396.2	488.5	574.8	551.3	632.0
-3	265.0	283.3	348.2	410.1	393.3	450.8
-4	193.2	206.3	254.5	299.1	285.8	327.2
P_f36-1	1303.4	1381.0	1712.0			
-2	1158.6	1223.6	1524.0			
P_f26-1	940.6	985.8	1237.2	1456.2	1390.4	1585.6
-2	1810.6	1891.0	2377.8			3039.2
P_f16-1	3082.1	3151.4	4044.0	4770.4	4580.4	5102.4

At 803°K

	N_2	He	Ar	Kr	Xe	Ne
P_b30-1	811.8	875.1	1079.1	1290.0	1263.0	1376.1
-2	1438.2	1547.5	1911.5			2431.5
-3	1664.4	1789.8	2214.2			
P_b20-1	620.4	668.0		983.8	963.4	1046.4
-2	919.4	984.6				1547.4
-3	761.8	816.6				1285.0
-4	642.2	689.9				1081.6
P_b10-1	528.2	567.6				
-2	718.6	769.8				
-3	536.5	572.0				
-4	403.9	432.8				
P_b 0 -1	502.1	535.0	667.4	796.8	781.2	843.8
-2	658.4	702.1	875.7	1045.6	1023.4	1105.3
-3	470.2	498.9	625.5			788.2
-4	342.1	364.9	453.8			574.3
P_f36 -1	2309.3	2422.6	3068.5			3845.4
P_f26 -1	1663.9	1719.4	2212.0	2650.0	2594.9	2749.6
P_f16 -1	5378.6	5306.8	7116.8	8564.0	8438.8	8633.4
A 1	86.2	94.2	116.0			146.5
2	144.0	157.9	192.5			245.7
3	174.1	190.0	231.9			296.0
4	114.1	124.5	152.4			193.6
5	78.6	86.1	104.1			133.4
6	507.1	553.5	675.7			860.3
7	318.8	347.2	422.9			541.8
8	414.3	452.7	552.4			704.6

At 948°K

	N_2	He	Ar	Kr	Xe	Ne
P_b30 -1	1066.8	1153.5	1422.0		1681.0	1799.1
P_b20 -1	814.2	877.4				1371.6
P_b10 -1	691.8	742.6		1109.2		1164.4
P_b0 -1	656.6	700.4	875.1		1039.0	1098.4
-2	862.2	918.4	1150.3		1363.4	1439.0
P_f26 -1	2173.2	2226.3	2896.2	3487.4	3448.8	3547.6
P_f16 -1	6972.0	6732.8	9238.0	11207.6		10996.2
A 1	112.9	124.4	151.4			192.4
2	189.1	208.0	252.5			321.0
3	227.9	250.5	305.5			387.3
4	149.4	164.0	199.9			254.5
5	103.1	113.1	137.6			175.8
6	665.1	732.1	891.0			1131.8
7	419.2	458.9	559.4			713.9
8	544.9	599.6	731.8			928.2

At 673°K

	N_2	He	Ar	Ne
P_b30 -1	607.0	652.4	803.2	1029.5
-2	1074.8	1154.0	1426.8	
P_b20 -1	463.2	497.4	613.3	785.5
-2	686.2	734.6	907.5	1161.7
P_b10 -1	396.0	422.8		
-2	537.6	575.8		
-3	401.1	426.8		
-4	303.5	322.2		
P_b0 -1	375.8	399.8	496.9	634.0
-2	492.6	524.1	652.9	831.0
-3	352.1	373.8	465.0	593.0
-4	257.7	272.9	339.5	432.1
P_f36 -1	1732.4	1818.4	2287.4	2897.5
P_f26 -1	1249.6	1294.6	1653.2	2072.2
P_f16 -1	4070.8	4044.4	5333.6	6574.8
A 1	64.5	700.0	85.2	
2	107.7	116.5	142.5	183.1
3	129.7	140.8	172.0	220.9
4	85.0	92.2	112.6	145.1
5	58.6	63.5	77.6	99.9
6	378.2	410.1	501.2	644.6
7	237.9	258.2	315.1	405.7
8	309.4	335.8	410.9	528.0
9	437.8	475.4	580.2	747.4

At 474°K

	N_2	He	Ar	Kr	Xe	Ne
P_b30-1	338.4	364.2	441.9		486.5*	581.4
-2	599.1	643.6	780.5		856.9	1025.8
-3	692.4	744.6	906.0		995.1	1194.8
P_b20-1	258.4	278.1	337.4		371.4*	444.4
-2	381.8	410.7	500.3		547.8*	655.6
-3	317.2	340.1	413.3		454.8	544.7
-4	267.6	288.0	349.8		384.2	458.7
P_b10-1	221.0	236.7	288.7		318.4*	377.4
-2	300.2	322.1	392.5		431.7*	514.0
-3	223.1	239.4	291.8		319.6	382.3
-4	169.0	181.2	220.7		242.3	289.0
P_b0 -1	210.2	224.4	274.3	320.4	304.5*	359.0
-2	275.4	294.8	360.5	419.2	396.9*	471.4
-3	196.7	210.1	256.5	298.4	282.4*	336.2
-4	144.0	153.4	187.0	218.4	206.8	245.0
P_f36-1	967.1	1026.0	1261.0	1468.6	1386.4	1649.4
P_f26-1	698.6	737.0	910.0	1059.8	1002.0	1184.4
P_f16-1	2294.3	2352.0	2986.6	3486.0	3308.8	3833.1

APPENDIX 6

THE STATISTICS OF THE STRAIGHT LINE (187)

A straight line is given by the equation

$$y = a + bx \qquad (A6.1)$$

where a is a constant and b the gradient.

If the measured values of y do not lie exactly on the line then provided the errors in x are small compared with the errors in y, a least squares analysis may be performed. Assuming equal weighting for all points, the error of a measurement y at x is

$$(y - y') = y - (a + bx) \qquad (A6.2)$$

where y' is the true value given by (A6.1) at x.

The best straight line through all the points is the one in which a and b give a minimum to the sum of the squares of the errors, i.e. $\sum (y - y')^2$ is a minimum.

Thus

$$\frac{d}{da} \sum (y - a - bx)^2 = \frac{d}{da} \sum (y^2 - 2ay + a^2 + 2abx - 2bxy + b^2x^2) = 0$$

and $$\frac{d}{db} \sum (y - a - bx)^2 = 0$$

Hence $$\frac{d \sum}{da}(y - a - bx)^2 = \sum (-2y + 2a + 2bx) = 0$$

and $$\frac{d \sum}{db}(y - a - bx)^2 = \sum (2ax - 2xy + 2bx^2) = 0$$

so

$$a = \frac{\sum y - b \sum x}{n} \qquad A(10)$$

where n is the number of values of y.

and $$b = \frac{n\Sigma xy - \Sigma x \Sigma y}{n\Sigma x^2 - (\Sigma x)^2} \qquad A(9)$$

The standard deviation of the points from the line is given by

$$SD - P = \left[\frac{1}{n-2} \left(\Sigma y^2 - \frac{(\Sigma y)^2}{n} - \frac{(\Sigma xy - \frac{\Sigma x \Sigma y}{n})^2}{\Sigma x^2 - \frac{(\Sigma x)^2}{n}} \right) \right]^{\frac{1}{2}} \qquad A(12)$$

n-2 is used since the data have been used to estimate b. The standard deviation for the slope A(14) is given by

$$SD - S = \frac{A(12)}{(\Sigma x^2 - \frac{\Sigma x^2}{n})^{\frac{1}{2}}} \qquad A(14)$$

The standard deviation for the intercept A(19) is given by

$$SD - I = A(12) \left(\frac{\Sigma x^2}{n\Sigma x^2 - (\Sigma x)^2} \right)^{\frac{1}{2}} \qquad A(19)$$

A programme written in Fortran suitable for the laboratory Elliott 903 computer is given overleaf. The numbers A(n) indicate the formula calculated in the programme.

```
      GLOBAL,VISDAT,SQRT]
      DIMENSION  A(50),V(30),Z(20)
      WRITE(2,91)
      READ(1)L                    NO.OF DATA SETS
      J=0
      K=0
    2 J=J+1
      P=0
      LT=0
      READ(1)  ZZ,LA               CODE,  NO.OF P̄
      DO6K=1,30
    6 A(K)=0
    3 READ(1) W,M,I                P̄,  NO.OF TIMES FOR GAS(1),GAS(2)
      X=1/W                        X=1/P̄
      DO 7LR=1,M
    7 READ(1) V(LR)                TIMES FOR GAS(1)
      DO8LS=1,I
    8 READ(1) Z(LS)                TIMES FOR GAS(2)
      DO 9LR=1,M
      DO 10LS=1,I
      Y=V(LR)/Z(LS)                Y=TIME(1)/TIME(2)
      P=P+1                        P=NO.OF RATIOS
      A(1)=A(1)+X                  ΣX
      A(2)=A(2)+Y                  ΣY
      A(3)=A(3)+X**2               ΣX²
      A(4)=A(4)+Y**2               ΣY²
   10 A(5)=A(5)+X*Y                ΣXY
    9 CONTINUE
      LT=LT+1
      IF(LA-LT)12,12,3
   12 A(6)=A(1)**2                 (ΣX)²
      A(7)=A(2)**2                 (ΣY)²
      A(8)=1/P
      A(21)=P*A(5)-A(1)*A(2)                  A(9)=NΣXY-ΣXΣY = b
      A(22)=P*A(3)-A(6)                        NΣX² - (ΣX)²
      A(9)=A(21)/A(22)
      A(10)=A(8)*A(2)-A(9)*A(1)*A(8)          A(10)=1/N Σ Y- b/N Σ X = a
      A(15)=A(5)*A(9)-A(1)*A(2)*A(9)*A(8)
      LM=P-2
      A(11)=(A(4)-A(8)*A(7)-A(15))/LM
      A(12)=SQRT(A(11))
      A(13)=SQRT(A(3)-A(8)*A(6))
      A(14)=A(12)/A(13)
      A(23)=P*A(3)-A(6)
      A(17)=A(3)/A(23)
      A(18)=SQRT(A(17))
      A(19)=A(12)*A(18)
      A(20)=1/A(10)
      WRITE(2,93)
      WRITE(2,92) ZZ,P,A(9),A(10),A(20)
      WRITE(2,94)
      WRITE(2,95) A(12),A(14),A(19)
      IF (L-J)4,4,2
   91 FORMAT(37HDAWE VISDATA-LEAST SQRS.FIT FOR TIMES)
   93 FORMAT(/44H   CODE  PTS    SLOPE    INTERCEPT 1/INTERCEPT)
   92 FORMAT(F7.2,I4,F10.6,F10.6,1X,F10.6)
   94 FORMAT(35H  S.D.PTS     S.D.SLP .  S.D.INT     )
   95 FORMAT(F9.6,2X,F9.6,2X,F9.6)
    4 END
```

APPENDIX 7

REVIEW OF PREVIOUS DATA

The data published by other workers in the range 290-1600°K is summarised here. The survey of viscosities and thermal conductivities of each gas is given in a separate table and each table is divided into three parts, 1) viscosity data, 2) ratio data, either by a relative or a standard method, 3) thermal conductivities. The viscosity data are given in μ- poise ($g\ cm^{-1} sec^{-1}$) and the thermal conductivity data are given in 10^{-5} cal $cm^{-1} sec^{-1} {}^{o}K^{-1}$.

Most workers have not used an absolute method, so have had to use some standard. If this standard differed from the one accepted here i.e. η air (296°K) = 1833 x 10^{-6} poise, N_2(293°K) =175.7 x 10^{-6} poise the data have been corrected. In part 1 of the tables the raw data which needed correcting are given in the second column and the corrected data in the third column. Where no correction was needed, the data only appear in column 3. The fourth column gives the % difference of the data from the smooth curves given in summary Table (4-1). The source of the data is given in the fifth column, with the literature reference given at the end of the Appendix.

In part 2 of the tables the ratio data are compared with the suitable smooth curve.

In part 3 of the tables the thermal conductivities of the rare gases are given in the second column and have been converted in the third column to viscosities using equation (2.32) where

$$\kappa = \frac{5}{2} \frac{Cv}{M} \eta$$

Cv being the specific heat per mole at constant volume and M the molecular weight. Thus the factor for converting thermal conductivities into viscosities is,

He	Ne	Ar	Kr	Xe
0.53682	2.7110	5.3548	11.246	17.621

Occasionally a worker has used some other system of units. Thus Makovetskas et al uses kg sec/m^2 for viscosities (1 unit = 98.1 μpoise) and Brain uses watts/cm ^{o}K for thermal conductivities (1 unit = 2.388×10^{-7} cal cm^{-1} sec^{-1} $^{o}K^{-1}$).

A fuller survey of literature values may be found in the "Retrieval guide to thermophysical properties research literature" Purdue Univ. (Y.S. Touloukian Ed.) 1960 & subsequent editions.

NITROGEN

η (293) taken as 175.7 μ-poise.

T	η_{lit}	η_{corr}	%	Reference
344		198.4	-0.59	24
371		210.2	-0.49	
419.3		229.4	-0.65	
472		249.9	-0.36	
524		270.5	0.41	
566		276.2	0.71	
293		175.7	-0.05	22
273		166.5	0.52	20
283		171.9	0.06	
300		178.6	-0.35	
273		165.6	-0.02	28
296		177.5	-0.42	
323		189.6	-0.26	
348		200.2	-0.67	
373		209.8	-1.07	15
298		177.1	-0.64	
303		180.2	-0.26	11
278.1		166.3	0.37	52
556.6		274.4	-1.49	
613		295.7	-1.20	
703.6		323.5	-1.30	
804.5		350.2	-2.09	
855.1		364.2	-2.15	
875.1		370.2	-1.88	
912.1		380.0	-2.09	
917.4		379.3	-2.64	
977.4		393.0	-2.68	
997		400.5	-2.59	
1083		421.6	-2.91	
1122		428.0	-3.55	
1161		436.5	-3.78	
1259		458.5	-4.08	
1307		470	-4.02	
1314		469.5	-4.45	
1321		472.0	-4.27	
1564		519.5	-5.52	
973		391.6	-3.24	14
1021		401.7	-3.79	
1059		411.9	-3.65	

1120		421.6	-4.88	
1166		437.4	-3.85	
1220		446.1	-4.76	
1273		458.2	-4.82	
298		177.9	-0.19	12
303		180.2	-0.26	
323		190	-0.06	
348		200.8	-0.27	
373		211.6	-0.22	
395		220.2	-0.06	
423		231.5	-0.34	
453		243.6	-0.06	
483		255.7	0.34	
523		269.8	0.28	
573		287.1	0.34	
673		321.4	0.96	
773		352.1	1.02	
273		166.1	0.28	5
299.1		178.6	-0.10	
322.7		189.6	-0.19	
344.8		199.2	-0.37	
374.6		212.1	-0.30	
300	178.1	179.0	-0.12	47
400	219.1	220.2	-1.33	
500	255.9	257.2	-1.43	
550	272.8	274.2	-1.50	
293	174.6	175.5	-0.16	45
373	208.6	209.6	-1.17	
473	246.3	247.3	-1.46	
523	262.9	264.2	-1.80	
290	173.1	174.0	-0.17	43
325.0	188.0	188.9	-1.11	
373	208.4	209.4	-1.26	
425	228.1	229.2	-1.66	
473	246.1	247.2	-1.58	
523	262.3	264.0	-1.88	
293	174.6	175.5	-0.16	49
572	279.7	281.1	-1.64	
681	314.1	315.6	-1.63	
763	337.4	339.1	-1.88	
873	366.4	368.2	-2.40	
986	393.0	394.9	-3.26	
1098	419.2	421.3	-3.72	

[illegible]		216.2	1.95	30
[illegible]		[illegible]	2.16	
[illegible]		[illegible]	1.16	
[illegible]		175.9	0.06	35
[illegible]		184.9	-0.29	
[illegible]		196.7	-0.50	
[illegible]		[illegible]	-0.63	
[illegible]		[illegible]	-0.82	
[illegible]	172.3*	176.2	-0.65	27
[illegible]	200.6	196.8	-0.61	
[illegible]	230.0	[illegible]	-2.42	
[illegible]	270.0	264.9	-1.38	
[illegible]	306.4	[illegible]	-0.46	
[illegible]	332.5	328.2	-1.25	
[illegible]	362.5	355.6	-1.25	
[illegible]	395.[illegible]	[illegible]	-2.20	
[illegible]		176.6	3.00	31
[illegible]		216.3	1.99	
[illegible]		236.1	1.96	
[illegible]		291.6	1.92	
[illegible]		323.9	1.75	
[illegible]		353.6	1.43	
[illegible]		[illegible]	0.99	
[illegible]		397.3	-1.83	
[illegible]		431.9	0.16	
1173		[illegible]	[illegible]	
[illegible]		477.3	-0.82	
[illegible]		519.4	-1.81	

* given in 10^6 kg sec m^{-2}

HELIUM

η (293) standard, from the literature 196.0 μ-poise.
calculated from N_2 ratio 195.0 μ-poise.

T°K	η lit.	η corr.	%	Reference
298.2		197.3	0.00	24
37[illegible].1		231.2	-0.22	
37[illegible].3		232.7	-0.22	
42[illegible].0		252.5	-0.22	
47[illegible].[illegible]		273	-0.14	
52[illegible].[illegible]		293.3	0.60	
293		196.1	0.04	22
27[illegible]		185.4	-0.38	29
29[illegible]		195.2	-0.35	
296		196.9	-0.22	
29[illegible]		197.7	-0.29	
286	194.2	193.6	0.35	32
37[illegible]	232.2	232.4	0.34	
37[illegible]		231.2	-0.38	15
29[illegible]		198.5	0.06	
293		196.0	0.00	11
303		200.8	0.03	
298		198.5	0.06	10
3[illegible]		200.9	0.02	
32[illegible]		209.7	-0.23	
348		220.7	-0.22	
37[illegible]		231.4	-0.30	
423		252.6	-0.22	
453		264.6	-0.23	
483		277.3	0.00	
523		293.1	0.17	
573		312.3	0.27	
673		350.6	0.75	
27[illegible]	187.4	186.5	0.21	30
287	194.3	193.3	0.16	
373	233.2	233.2	0.38	
293	194.1	195.0	-0.36	44
373	228.1	229.2	-1.25	
473	267.2	268.3	-1.81	
523	285.3	286.7	-2.12	

291	194.6	195.6	0.34	49
333	299.2	300.7	-1.32	
680	343.6	345.3	-1.34	
739	370.6	372.4	-1.58	
879	408.7	410.7	-1.90	
949	430.3	432.4	-2.11	
1090	471.3	473.6	-2.85	
375		230.0	-1.00	33
423		251.4	-0.76	
473		271.2	-0.80	
283.6	193.2*	191.5	0.00	27
369	232.2	228.0	-1.00	
488	280.0	274.7	-1.67	
594	318.6	312.5	-1.90	
705	357.3	350.7	-2.40	
811	393.5	386.0	-2.45	
918	428.5	420.3	-2.85	
293	195.6	196.6	0.26	53
313	204.6	205.6	0.13	
333	213.4	214.6	0.00	
353	222.0	223.3	-0.10	
371.0	229.5	230.66	-0.30	
291	194	194.0	-0.50	40
	192			

*given in 10^6 kg-sec cm^{-2}

T°K	η (T)/ η (293)	%	Reference
476	1.386	-1.04	16
675	1.766	-0.75	
875	2.108	-1.05	
1163	2.508	-1.95	
1214	2.635	-1.79	
1262	2.704	-1.96	
1311	2.782	-1.84	
1363	2.840	-2.53	
1412	2.889	-3.35	
1462	2.938	-4.11	
1596	3.143	-3.68	

T°K	K	η	%	Reference
273	34.06	182.8	-1.84	21
373	41.65	223.6	-3.76	
491	49.47	275.5	-5.37	
579	55.05	295.5	-5.81	
302	36.7	197.0	-1.59	50
693	73.6	395.1	-6.77	
347	40.3*	216.0	-2.15	54
445	48.6	260.9	-0.52	*units originally given in k cal m^{-1} hr^{-1} deg^{-1}
563	57.9	310.8	1.00	
677	66.1	354.8	1.54	
745	70.4	376.0	2.70	
866	74.5	400.6	1.55	
1300	110.0	590.5	-3.45	7
1200	98.9	531.0	-2.81	
960	81.1	435.0	-2.32	
640	61.3	329.0	-2.05	
320	38.0	204.0	-2.20	
1000	82.2*	441.2	-3.83	39
1300	109.4	587.2	-4.06	*units originally given in k cal m^{-1} hr^{-1} deg^{-1}
1200	99.1	532.0	2.13	2
1300	105.9	568.5	3.18	
1400	112.6	604.4	4.10	
1500	119.4	641.0	5.10	

NEON

η (293) standard from the literature 313.8 μ poise
calculated from N_2 ratio 312.7 μ poise

T°K	η_{lit}	η_{corr}	%	Reference
296.0		313.7	-0.72	24
371.0		366.2	-0.44	
424.0		400.2	-0.43	
468.3		428.0	-0.30	
519.0		459.2	0.19	
293		313.8	-0.00	22
273		296.7	-0.79	19
290		312.1	-0.54	
296		314.3	-0.53	
298		315.8	-0.51	
286	307.6	309.1	-0.34	13
373	365.6	367.4	-0.47	
457	417.7	419.7	-0.62	
573	490.1	492.6	0.34	
717.3	558.4	561.2	-1.00	
287	308.0	307.2	-0.72	32
373	365.2	365.5	-0.98	
373		368.5	-0.17	15
298		317.8	0.02	
293		314.5	0.22	23
303		322.1	0.33	
293		314.0	0.06	11
303		321.3	0.08	
298		317.3	-0.04	10
303		320.8	-0.07	
323		335.8	0.18	
348		352.9	0.14	
373		370.1	0.26	
423		402.8	0.38	
433		421.5	0.39	
296		314.3	-0.95	4
292.6		313.2	-0.10	18

293	311.1	312.6	-0.38	44
373	364.6	366.4	-0.74	
470	424.8	426.9	-0.76	
526	453.2	455.5	-1.28	
292	310.4	312	-0.34	49
536	470.8	473.1	-1.72	
703	545.4	548.1	-1.93	
775	580.2	583.1	-2.14	
867	623.0	626.1	-2.23	
939	662.6	665.9	-2.37	
1100	721.0	724.5	-2.93	
371		369	-0.63	33
423		299.3	-0.49	
473		426.5	-1.50	
290	311.8	313.4	-0.13	53
313	325.8	327.4	-0.23	
333	339.5	342.2	-0.27	
353	352.9	354.7	-0.30	
371.8	364.5	366.7	-0.30	
298		317.3	-0.04	42
323		329.4	-1.73	
343		345.9	-1.84	
291	307	311	-0.39	40
	308			
	310			
	313			

T°K	K		%	Reference
273	11.1	300.9	0.62	21
373	13.57	367.9	-0.33	
491	15.95	432.4	-2.33	
579	17.89	485.0	-1.65	
302	12.37	338.4	4.71	36
893	23.6	640.0	-1.97	
413	14.78*	400.8	1.47	34
444	15.53	421.0	1.61	
555	16.36	497.7	3.75	
620	20.08	544.4	5.38	
697	21.61	585.8	5.30	
762	23.21	623.5	5.79	
811	23.81	645.5	6.14	
1300	32.75	887.8	-2.44	6

* units originally given in k cal m^{-1} hr^{-1} deg^{-1}

ARGON

η (293) standard, from the literature 222.8 μ-poise
calculated from N_2 ratio 223.0 μ-poise

T°K	η_{lit}	η_{corr}	%	Reference
296		225.0	0.11	24
336.7		250.6	-0.01	
349		258.1	-0.04	
371		271.1	-0.11	
420.0		301.7	0.14	
469.6		325.6	0.26	
516.8		350.4	0.56	
567.2		361.4	0.85	
293.0		222.8	0.01	22
273		210.0	0.39	19
293		222.7	-0.03	
296		224.6	-0.07	
298		225.7	-0.17	
289	220.4	219.8	-0.14	32
373	270.2	270.5	-0.63	
373		271.3	-0.34	15
293		225.6	-0.21	
293		223.0	0.10	23
303		229.8	0.20	
293		222.8	0.01	11
363		229.4	0.02	
298		226.2	0.06	10
308		229.2	-0.06	
323		243.2	0.44	
348		258.3	0.32	
373		273.2	0.36	
423		301.5	0.44	
453		317.8	0.52	
473		328.4	0.58	
523		354.8	0.93	
573		379.0	0.98	
291	221 220	221.0	-0.25	40
272.3		209.7	0.41	5
299.1		226.9	0.05	
322.7		242.0	0.02	
344.8		255.3	-0.10	
374.6		273.1	-0.02	

273		210.5	0.62	
569.2		366.8	-1.81	
572.1		369.6	-1.42	
574.3		369.5	-1.71	
674		414.0	-1.62	
678		413.3	-2.28	
682.1		417.5	-1.61	
685.3		416.5	-2.16	
692.2		419.0	-2.26	
8[illegible]3.1		463.0	-2.49	
819.1		467.5	-2.86	
827.3		470.2	-2.96	
845.1		476.8	-3.01	
858.2		481.5	-2.69	
873.2		487.5	-3.01	
909.4		500.5	-3.12	
913.3		501.6	-3.19	
975.9		523.0	-3.46	
997.1		529.5	-3.66	
1033.3		549.0	-3.71	
1111.4		567.0	-4.04	
1124.3		570.8	-4.14	
1158.1		582.5	-4.08	
1193.1		593.0	-4.26	
1220.		600.0	-4.55	
1230		601.5	-4.83	
1265.4		614.0	-4.66	
1307.1		624.5	-5.08	
1311.1		626.2	-5.01	
1313.3		626.5	-5.07	
1325		630.0	-5.10	
1353		639.0	-5.06	
1358		638.3	-5.39	
1371		643.5	-5.27	
1383		645.5	-5.47	
1407		651.5	-5.66	
1423		656.0	-5.72	
1458		669.0	-5.37	
1503		678.5	-5.92	
1511		682.0	-5.77	

288	219.6	220.7	0.38	46
373	368.8	270.1	-0.78	
473	320.7	322.3	-1.29	
523	344.4	346.1	-1.53	
293	221.7	222.8	0.01	44
373	269.5	270.8	-0.52	
473	322.3	323.9	-0.80	
523	346.4	348.1	-0.95	
273		210.2	0.48	9
293		222.0	-0.35	
300		226.7	-0.30	
311		234.0	-0.22	
320		238.9	-0.56	
328		244.6	-0.27	
338		249.9	-0.60	
345		252.3	-0.85	
353.4		259.2	-0.58	
368.6		267.4	-0.84	
381.3		273.5	-1.26	
396.4		281.9	-1.27	
409.1		289.6	-1.02	
423.7		297.1	-1.15	
438.9		305.0	-1.20	
448.2		309.9	-1.09	
461.9		317.0	-1.18	
471.4		322.1	-1.10	
293	221.2	222.3	-0.21	49
575	368.5	370.6	-1.51	
674	411.5	413.6	-1.72	
770	448.4	450.6	-2.33	
807	481.5	484.1	-2.45	
983	525.7	529.4	-2.75	
1100	563.2	566.0	-3.55	
567	366.1	367.9	-1.24	
701	423.1	425.2	-1.68	
796	459.4	461.7	-2.17	
894	494.1	496.6	-2.76	
978	523.1	525.7	-3.10	

1298		670.4	2.89	1
1190		633.7	2.49	
1068		575.6	0.01	
995		549.4	0.12	
891		510.5	0.19	
762		457.7	-0.08	
695		427.4	-0.58	
589		382.0	-0.20	
493		334.2	-0.72	
431		304.7	-0.59	
325		243.8	0.09	
296		223.4	-0.60	
293	222.8	223.9	0.51	53
313	235.7	236.9	0.47	
333	247.6	246.8	0.18	
336	259.2	260.3	-0.07	
371	269.7	271.0	-0.02	

T°K	η (T)/ η (293)	%	Reference
1100	2.676	1.59	17
1150	2.759	1.69	
1200	2.847	2.02	
1250	2.922	1.91	
1300	2.997	1.86	
1350	3.080	2.11	
1400	3.155	2.12	
1450	3.226	2.03	
1500	3.000	2.07	

T°K	η (A)/ η (N_2)	%	Reference
293	1.2610	-0.82	34
363	1.2840	-0.39	
453	1.2984	-0.44	
503	1.3096	-0.07	
553	1.3130	-0.18	
575	1.3151	-0.17	
610	1.3174	-0.22	
654	1.3215	-0.15	
678	1.3250	-0.01	
723	1.3231	-0.36	
773	1.3306	0.00	
821	1.3310	-0.13	

855	1.3277	-0.49	
921	1.3335	-0.24	
972	1.3388	0.03	
280	1.2650	-0.18	5
300	1.2708	-0.21	
320	1.2760	-0.24	
340	1.2808	-0.24	
360	1.2850	-0.26	

T°K	K	η	%	Reference
373	5.10	273.1	0.32	37
423	5.51	295.0	-1.73	
473	6.07	325.0	-0.46	
523	6.51	348.6	-0.82	
573	7.00	374.8	-0.14	
623	7.42	397.3	-0.24	
673	7.79	417.1	-0.78	
723	8.12	434.8	-1.58	
773	8.41	450.3	-2.66	
773	8.81*	471.7	1.97	*corrected by 51
316	4.42**	236.7	-0.42	54
444	5.86	313.8	0.77	
550	6.95	372.1	2.09	**corrected by 51
654	7.92	424.1	2.92	
728	8.50	455.2	2.55	
788	8.98	480.9	2.60	
316	4.50***	241.0	1.38	54
444	5.99	318	2.11	
550	7.05	377.5	3.57	*** units originally given in k cal m^{-1} hr^{-1} deg^{-1}
654	8.02	429.4	4.21	
728	8.61	461.0	3.85	
788	9.11	487.8	4.07	
273	3.96	212.0	1.34	36
373	5.08	272.0	-0.08	
473	6.09	326.0	-0.15	
573	6.99	374.3	2.29	
673	7.83	419.3	-0.26	
773	8.59	460.0	-0.56	
873	9.40	503.3	0.15	

973	10.15	543.5	0.53*	*corrected by 51
1073	10.80	578.3	0.19*	
1173	11.45	613.1	0.10*	
1273	12.03	644.2	-0.36*	
873	9.33	499.6	-0.58*	
973	10.02	536.6	-0.75	
1073	10.65	570.3	-1.20	
1173	11.24	601.9	-1.72	
1273	11.79	631.3	-2.36	
1373	12.30	658.6	-3.09	
273	3.94	211.0	0.86	21
373	5.06	271.0	-0.45	
491	6.14	328.8	-2.03	
579	6.85	366.8	-3.00	
273	3.90	208.8	-0.19	29
298	4.20	224.9	-0.52	
313	4.38	234.5	-0.55	
325	4.50	241.0	-0.47	
348	4.81	257.5	0.01	
426	5.61*	300.4	-0.47	3
449	5.85	313.2	-0.27	* units originally given watts/cm °K
485	6.04	323.4	-2.77	
522	6.52	349.1	-0.54	
553	6.68	358.2	-2.11	
302	4.34	232.4	1.62	50
893	9.14	489.4	-4.10	
327	4.55	243.6	-0.42	35
633	7.54	403.8	0.26	
831	8.98	480.9	-1.05	
849	9.26	495.9	0.56	
961	10.44	559.0	4.26	
962	10.52	563.3	4.99	
533	6.82	365.2	2.49	25
923	9.22	493.7	-5.39	
1033	10.40	556.9	-1.04	
1173	11.70	626.5	2.29	
273	3.91	209.4	0.10	38
298	4.21	225.4	-0.30	
323	4.50	241.0	-0.47	
373	5.09	272.6	0.14	
423	5.69	304.7	1.50	

473	6.28	336.3	3.00	
573	7.46	399.5	6.44	
673	8.65	463.2	10.19	
413	5.51	295.0	0.09	25
523	6.48	347.2	-1.21	
573	6.87	368.1	-1.93	
620	7.12	381.5	-3.88	
311	4.28	229.1	-2.31	51
316	4.43	237.2	-0.21	
327	4.54	243.1	-0.62	
336	4.60	246.3	-1.56	
577	6.97	373.2	-1.06	
586	7.03	376.4	-1.31	
661	7.68	411.2	-0.95	
669	7.83	419.3	0.16	
777	8.64	462.6	-0.35	
787	8.70	465.9	-0.51	
916	9.58	513.0	-1.18	
926	9.72	520.5	-0.47	
1036	10.70	573.0	1.62	
1048	10.60	567.0	-0.21	
1182	11.80	631.8	2.64	
1189	11.65	623.8	0.94	
1198	11.66	624.4	0.53	
1202	11.75	629.2	1.14	
300	4.22	226.0	-0.61	26
500	6.30	337.4	-0.80	
750	8.43	451.4	-0.37	
1000	10.2	546.2	-0.81	
1500	13.4	717.5	-0.38	
1500	13.14	703.6	-2.31	8

KRYPTON

η (293) taken as standard 250.8 μ-poise

obtained from N_2 ratio 250.7 μ-poise

T°K	η lit	ηcorr	%	Reference
291	247 248 249	249.0	0.12	40
293		249.6	-0.41	22
289	245.8	245.2	-0.86	32
373	306.3	306.6	-1.74	
303		257.3	-0.57	10
323		274.9	0.11	
348		293.8	0.04	
373		312.3	0.08	
423		347.6	0.19	
453		368.4	0.41	
473		381.2	0.37	
272		233.6	0.00	5
299		254.5	-0.44	
322		273.0	-0.50	
344		289.4	-0.65	
374		311.9	-0.41	
298		251.3	-1.34	6
300		252.6	-1.46	
350		286.1	-3.08	
400		318.6	-3.79	
450		349.2	-4.31	
500		378.4	-4.65	
550		406.9	-4.77	
600		435.1	-4.67	
650		463.0	-4.43	
690		485.1	-4.16	
273	231.8	230.6	-1.41	30
288	243.6	242.4	-1.67	
373	306.2	306.2	-1.87	
273	231.4	232.5	-0.60	48
373	303.6	305.1	-2.23	
298		253.2	-0.60	41, 42
323		272.0	-0.95	
348		290.6	-1.05	

T°K	$\eta(Kr)/\eta(N_2)$	%	Reference
293	1.4233	-0.27	34
363	1.4641	-0.25	
453	1.5043	-0.15	
505	1.5225	-0.09	
553	1.5329	-0.13	
575	1.5533	0.69	
610	1.5522	0.11	
654	1.5570	-0.15	
678	1.5660	0.15	
725	1.5772	0.37	
775	1.5756	-0.18	
821	1.5888	0.29	
853	1.5902	0.14	
921	1.5977	0.20	
972	1.6020	0.20	
280	1.4122	-0.44	5
300	1.4257	-0.42	
320	1.4384	-0.40	
340	1.4505	-0.35	
360	1.4722	-0.28	

T°K	K	η	%	Reference
273	2.08	233.9	0.00	21
373	2.72	305.9	-1.97	
491	3.40	382.4	-2.25	
579	3.88	436.3	-1.80	
302	2.32	260.9	1.14	50
893	5.34	600.5	-1.37	
273	1.95	219.3	-6.24	38
298	2.07	232.8	-8.61	
323	2.20	247.4	-9.91	
373	2.44	274.4	-12.06	
423	2.68	301.4	-13.13	
473	2.90	326.1	-14.14	
573	3.36	377.9	-14.27	
673	3.83	430.7	-13.34	
273	2.14	240.7	2.91	36
373	2.80	314.9	0.92	
473	3.42	384.6	1.26	
573	3.99	448.7	1.79	
673	4.53	509.4	2.49	

773	5.03	565.7	2.94	
873	5.51	619.7	3.42	
973	5.95	669.1	3.50	
1073	6.38	717.5	3.73	
1173	6.78	762.5	3.71	
1273	7.19	808.5	4.02	
1372	7.58	852.5	4.26	
314	2.41*	271.0	1.29	54
415	3.11	349.7	2.40	
508	3.69	415.0	3.28	
579	4.11	462.2	4.03	
666	4.58	515.0	4.42	
727	4.86	546.6	3.96	
798	5.22	587.0	4.41	
1500	6.91	777.1	-10.47	8

* units originally given in K cal m^{-1} hr^{-1} deg^{-1}

XENON

η (293) taken as standard 228.4 μ-poise

obtained from N_2 ratio 228.0 μ-poise

T	η lit	η Corr	%	Reference
298		231.0	-0.48	22
289	223.5	224.6	-0.38	45
293	226.0	227.1	-0.44	
400	300.9	302.4	-1.90	
450	335.1	336.8	-1.64	
500	365.2	367.0	-2.13	
550	395.4	397.4	-2.16	
288	222.2	221.6	-1.11	32
373	282.7	283.0	-2.80	
272		211.4	0.01	5
299		231.4	-0.68	
322		249.4	-0.82	
344		265.5	-1.03	
374		287.6	-0.88	
273	212.2	211.1	-0.33	30
289	225.0	223.9	-0.44	
373	287.1	287.1	-0.66	
291	225	225.0	-0.67	40
	224			

T°K	η (Xe)/ η (N_2)	%	Reference
293	1.2946	-0.29	34
363	1.3552	-0.09	
453	1.4026	-0.80	
505	1.4354	-0.34	
575	1.4723	0.16	
610	1.4886	0.40	
654	1.4983	0.08	
678	1.5080	0.25	
725	1.5267	0.63	
775	1.5347	0.35	
821	1.5448	0.36	
855	1.5476	0.10	
921	1.5633	0.36	
972	1.5765	0.68	

280	1.2794	-0.53	5
300	1.2964	-0.64	
320	1.3132	-0.69	
340	1.3294	-0.70	
360	1.3450	-0.67	

T°K	K	η	%	Reference
273	1.23	216.7	2.32	21
373	1.68	296.0	2.42	
491	2.08	366.5	-0.74	
579	2.37	417.6	-1.44	
302	1.43	251.4	6.85	50
893	3.34	588.5	-0.96	
306	1.41	248.4*	4.17	54
425	1.94	341.8	4.99	
443	2.00	352.4	4.34	
560	2.49	438.8	6.44	
650	2.79	491.6	5.70	
720	3.01	530.4	5.22	
793	3.25	572.7	5.45	

* units originally given in k cal m^{-1} hr^{-1} deg^{-1}

VISCOSITY REFERENCES

1. N. Anfilogoff, Ph.D. Thesis, London (1932)
2. N.C. Blais and J.B. Mann, J.Chem.Phys. 32 1459 (1960)
3. T.J.S. Brain, Internat.J.Heat and Mass Transfer 10 737 (1967)
4. J.W. Buddenberg and C.R. Wilke, J.Phys.Chem 53 1491 (1951)
5. A.G. Clarke and E.B. Smith, J.Chem.Phys. 48 3988 (1968)
6. E.G. Clifton, J.Chem.Phys. 40 1123 (1963)
7. D.J. Collins, R. Grief and A.E. Bryson, Internat.J.Heat and Mass Transfer 8 1209 (1965)
8. D.J. Collins and W.A. Menard, J.Heat Transfer 88C 52 (1964)
9. A.G. De Rocco and J.O. Halford, J.Chem.Phys. 28 1152 (1958)
10. R. DiPippo, Ph.D. Thesis, Brown University (1966)
11. R. DiPippo, J. Kestin and K. Oguchi J.Chem.Phys. 46 4758 (1967)
12. R. DiPippo, J. Kestin and J.H. Whitelaw, Physica 32 2064 (1966)
13. R.S. Edwards, Proc.Roy.Soc. A119 578 (1928)
14. C.P. Ellis and C.J.G. Raw, J.Chem.Phys. 30 574 (1959)
15. C.P. Flynn, R.V. Hanks, N.A. Le Maire and J. Ross J.Chem.Phys. 38 154 (1963)
16. F.A. Guevara and W.E. Wageman, U.S. At Energy Commission L.A. 3319 (1965)
17. F.A. Guevara, B.B. McInteer, W.E. Wageman, Private communication see H.J.M. Hanley and G.E. Childs, Science 159 1114 (1968)
18. A. van Itterbeek and O. van Paemel, Physica 7 265 (1940)
19. H.L. Johnson and E.R. Grilly, J.Phys.Chem. 46 948 (1942)
20. H.L. Johnson and K.E. McLaskey, J.Phys.Chem. 44 1038 (1940)
21. W.G. Kannuluik and E.H. Carmen, Proc.Phys.Soc. 65B 701 (1952)
22. J. Kestin and W. Leidenfrost, Physica 25 1) 537 (1959)
    2) 1033 (1959)
23. J. Kestin and A. Nagashima, J.Chem.Phys. 40 3648 (1964)
24. J. Kestin and J.H. Whitelaw, Physica 29 335 (1963)
25. K.G. Keyes and R.G. Vines, J. Heat Transfer 87C 177 (1965)
26. P.E. Liley (comment), J. Heat Transfer 88C 55 (1966)

27. R.A. Makavetskas, V.N. Popov and N.V. Tsederberg, High Temp. 1 169 (1963)

28. A. Michels and R.O. Gibson, Proc.Roy.Soc. A134 288 (1931)

29. A. Michels, J.V. Sengers, J.L.M. van de Klundert, Physica 29 149 (1963)

30. A.G. Nasini and C. Rossi, Gazz, Chim.Ital. 58 433 (1928)

31. E. Rammler and K. Breitling, Die Wärme, Z. für Dampfkessel und Maschienenbetrieb 60 620 (1937)

32. A.O. Rankine, Proc.Roy.Soc. A83 516 (1910)
A84 181 (1911)

33. E.G. Reynes and G. Thodos, J.Chem.Eng.Data 11 137 (1966)

34. M. Rigby and E.B. Smith, Trans.Faraday Soc. 62 54 (1966)

35. A.J. Rothman and L.A. Bromley, Ind.Eng.Chem. 47 899 (1955) and U.S. Atomic Energy Comm. U.C.R.L. 2339 (1954)

36. K. Schäfer and F.W. Reiter, Z.Elektrochem. 61 1230 (1957)

37. W.F. Schottky, Z. Elektrochem. 56 889 (1952)

38. H. Senftleben, Z. Angew,Phys. 17 86 (1964)

39. D.L. Timrot and A.S. Umanskii, High Temp. 3 345 (1965)

40. E. Thornton, Proc.Phys.Soc. 76 104 (1960)
77 1166 (1961)
80 1172 (1962)

41. N.J. Trappeniers, A. Botzen, C.A. Ten Seldam, H.R. van den Berg and J. van Oosten, Physica 31 1681 (1965)

42. N.J. Trappeniers, A. Botzen, H.R. van den Berg and J. van Oosten, Physica 30 985 (1964)
31 945 (1965)

43. M. Trautz and P.B. Baumann, Ann.Physik (Lpz) 2 733 (1929)

44. M. Trautz and H.E. Binkele, Ann.Physik 5 561 (1930)

45. M. Trautz and R. Heberling, Ann.Physik 10 155 (1931)
20 118 (1934)

46. M. Trautz and W. Ludewigs, Ann.Physik 3 409 (1929)

47. M. Trautz and A. Melster, Ann.Physik 7 409 (1930)

48. M. Trautz and H. Zimmermann, Ann.Physik 22 189 (1935)

49. M. Trautz and R. Zink, Ann. Physik 7 427 (1930)

50. H. von Ubish, Arkiv Fysik 16 93 (1959)

51. N.B. Vargaftik and N. Kh. Zimina, High Temp. 2 645 (1964)

52. V. Vasilesco, Ann. Physique 20 137 (1945)
292

53. R. Wobser and F. Müller, Kolloid-Beihefte 52 165 (1941)

54. L.S. Zaitseva, Soviet. Phys. Tech. Phys. 4 444 (1959)

APPENDIX 6

CURVED PIPE FLOW EVALUATION

If curved pipe flow effects are present, then the ratio t(gas)/t(He) corrected for slip, gas imperfections and kinetic energy effects will not be the true ratio of viscosities but will be larger. (Due to its low molecular weight He may be assumed not to have curved-pipe flow effects under the experimental conditions here.) The ratio of the experimental value of the time ratio and the ratio of viscosities gives a measure of the curved-pipe flow effects present. By plotting this ratio against Dean Number (Page 79) a smooth curve is obtained (see Chapter 5).

The tables given here are:-

1) Dean Numbers for the Platinum and Silica capillaries at 293°K, using (4.21). The values for the Platinum-Rhodium capillary may be obtained by multiplying the values for the Platinum capillary by 0.9. At 373°K, the D.N's are approximately half that at 293°K and at 473°K approximately 1/3.

2) Gas Imperfection corrections (Page 76). The two terms of (4.20) are considered separately. (a) The first term depends on $B(T_f)$, T_f and P_f, so is independent of the capillary temperature or which capillary is being used. (b) The second term is given here for $T_c = 293°K$. It diminishes rapidly with increasing temperature due to $B(T_c)$ decreasing.

3) Kinetic Energy corrections (Page 74). The corrections for the Platinum capillary at 293°K are given (equation (4.13)). For the Platinum-Rhodium capillary H increases by about 20% and for the Silica capillary it decreases by 1/3.

4) Slip correction factors for the Platinum capillary at 293°K, using C' (4.2) as $C\left(\frac{\pi A}{2}\right)^{1/2}$ = 32,600. C was evaluated from the slope of the graph $(t(N_2)/t(He))_{corr}$ vs. $1/\bar{P}$, for the times of flow unaffected by curved-pipe flow. Each temperature, T_c, may

have a different value of C since it varies with capillary and temperature (see Chapter 5). For the Silica capillary at 293°K, $C' = 52{,}000$.

5) The tables of run times for the Platinum capillary at 293°K given in Appendix 5 are corrected for imperfection, kinetic energy and slip effects.

6) The ratios t(Gas)/t(He) are given for the Platinum capillary at 293°K. If no curved-pipe flow effects are present each ratio should be η (Gas)/ η (He).

7) The ratio (t(Gas)/t(He)) ÷ η (Gas)/ η (He)) where the value is not 1.000 ± 0.002, curved-pipe flow effects are probably present. This table gives the ratio Fc/Fs (Page 52).

(I) - DEAN NUMBERS (PLATINUM CAPILLARY AT 293°K)

	He	Ne	Ar	Kr	Xe	N_2
P_b30-1	1.4	3.0	11.2	19.3	36.3	13.1
-2	0.9	1.8	6.8	11.7	22.0	7.9
-3	0.4	0.9	3.3	5.8	10.9	3.9
-4	0.2	0.4	1.4	2.3	4.4	1.6
P_b25-1	1.6	3.4	12.8	22.1	41.7	15.1
-2	1.1	2.2	8.3	14.7	24.6	10.0
-3	0.7	1.4	5.2	9.0	16.9	6.1
-4	1.4	0.9	3.3	5.6	10.6	3.8
P_b20-1	1.9	3.9	14.7	25.4	47.8	17.3
-2	1.4	2.8	10.6	18.3	34.6	12.5
-3	0.9	1.9	7.3	12.6	23.8	8.6
-4	0.7	1.3	5.4	9.4	17.6	5.9
P_b15-1	2.0	4.2	16.0	27.5	51.3	18.7
-2	1.3	3.1	11.9	20.5	38.7	14.0
-3	1.1	2.3	8.8	15.2	28.6	10.3
-4	0.9	1.9	7.0	12.1	22.8	8.2
P_b10-1	2.2	4.5	17.3	29.8	56.1	20.3
-2	1.7	3.5	13.4	23.1	43.6	15.8
-3	1.3	2.7	10.3	18.0	34.0	12.3
-4	1.1	2.3	8.7	15.1	28.4	10.3
-5	0.6	1.4	4.9	8.4	15.9	5.7
P_b 5 -1	2.3	4.8	18.2	31.4	59.2	21.4
-2	1.9	3.8	14.6	25.3	47.6	17.2
-3	1.5	3.1	11.9	20.5	38.7	14.0
-4	1.3	2.7	10.3	17.8	33.5	12.1
-5	0.9	1.8	6.8	11.7	22.1	8.0
-6	0.4	0.8	3.2	5.4	10.2	3.7
-7	0.1	0.2	0.8	1.4	2.6	0.9
P_f36-1	0.9	1.8	7.2	12.5	23.5	8.5
-2	0.5	1.0	4.1	7.0	13.2	4.8
-3	0.3	0.6	2.3	4.0	7.5	2.7
-4	0.1	0.3	0.9	1.6	2.9	1.1
P_f26-1	0.5	1.0	4.1	7.1	13.3	4.8
-2	0.3	0.7	2.6	4.4	8.4	3.0
-3	0.1	0.3	1.3	2.2	4.1	1.5
P_f16-1	0.1	0.3	1.4	2.4	4.6	1.6
-2	0.1	0.2	0.7	1.2	2.2	0.8

DEAN NUMBERS - SILICA CAPILLARY AT 293°K

	He	Ne	Ar	Kr	Xe	N_2
P_b30-1	0.7	1.4	5.3	8.8	16.7	6.0
-2	0.4	0.9	3.1	5.3	10.1	3.6
-3	0.2	0.4	1.6	2.7	5.0	1.9
P_b20-1	0.9	1.8	6.7	11.7	21.9	7.9
-2	0.6	1.3	4.9	8.4	15.8	5.7
-3	0.4	0.9	3.4	5.8	10.9	4.2
-4	0.3	0.7	2.5	4.3	8.1	2.8
P_b10-1	1.1	2.2	7.9	13.7	25.7	9.3
-2	1.0	1.7	6.1	10.6	20.0	7.2
-3	0.6	1.2	4.8	8.2	15.6	5.6
-4	0.5	1.1	4.0	6.9	13.0	4.7
-5	0.3	0.6	2.3	3.9	7.3	2.8
P_b0 -1	1.2	2.4	8.3	14.3	27.0	9.2
-2	0.9	1.8	6.7	11.6	21.8	7.8
-3	0.7	1.5	5.4	9.3	17.7	6.4
-4	0.6	1.3	4.7	8.2	15.3	5.6
-5	0.4	0.9	3.1	5.4	10.3	3.8
-6	0.2	0.4	1.4	2.3	4.7	1.7
-7	0.0	0.1	0.4	0.6	1.2	0.4
P_p30-1	0.4	0.9	3.2	5.7	10.8	4.1
-2	0.2	0.4	1.9	3.2	6.0	2.2
-3	0.1	0.3	1.1	1.8	3.5	1.3
-4	0.1	0.1	0.4		1.4	0.5
P_p26 -1	0.2	0.4	1.9	3.3	6.1	2.3
-2	0.2	0.3	1.2	2.0	3.8	1.4
-3	0.1	0.1	0.6	1.0	1.9	0.6
P_p16 -1	0.1	0.1	0.7	1.1	2.1	0.7
-2	0.0	0.1	0.3	0.5	1.0	0.3

(2) GAS IMPERFECTION CORRECTION AT 293°K

a) $1 + \frac{2\bar{P}_f B(T_f)}{RT_f}$ term.

$\bar{P}_f$	He, Ne	N_2	Ar	Kr	Xe
B(296)	+11.6, 11.0	-5.6	-15.6	-52.7	-135 ccs/mole
49.6	1.0005	0.9997	0.9992	0.9972	0.9928
44.6	1.0004	0.9997	0.9993	0.9975	0.9936
40.3	1.0004	0.9997	0.9993	0.9977	0.9942
37.9	1.0004	0.9997	0.9994	0.9979	0.9945
31.6	1.0003	0.9997	0.9994	0.9983	0.9955
23.8	1.0002	0.9998	0.9996	0.9987	0.9966
18.8	1.0002	0.9998	0.9996	0.9990	0.9973
13.7	1.0001	0.9999	0.9997	0.9993	0.9979
9.7	1.0001	0.9999	0.9998	0.9995	0.9985

b) $1 - \frac{2}{3}\frac{B(T_c)}{RT_c}\frac{(\bar{P}_f^3 - \bar{P}_b^3)}{(\bar{P}_f^2 - \bar{P}_b^2)}$ term. The pressure factor $P = \frac{(\bar{P}_f^3 - \bar{P}_b^3)}{(\bar{P}_f^2 - \bar{P}_b^2)}$ is first evaluated. At 293°K with the following values of P, the factor becomes

$\bar{P}$ (cms. Hg)	He, Ne	N_2	Ar	Kr	Xe
60	0.9998	1.0001	1.0002	1.0014	1.0031
50	0.9998	1.0001	1.0002	1.0013	1.0025
40	0.9999	1.0000	1.0001	1.0013	1.0020
30	0.9999	1.0000	1.0002	1.0009	1.0015
20	1.0000	1.0000	1.0000	1.0005	1.0010
10	1.0000	1.0000	1.0000	1.0002	1.0005

(3) KINETIC ENERGY CORRECTION (PLATINUM CAPILLARY 293°K)

		He	Ar	Kr	Xe	N_2
P_b30	-1	1.0002	1.0019	1.0031	1.0052	1.0022
	-2	1.0001	1.0012	1.0019	1.0035	1.0014
	-3	1.0001	1.0006	1.0011	1.0018	1.0007
	-4	1.0000	1.0002	1.0003	1.0007	1.0002
P_b25	-1	1.0003	1.0022	1.0035	1.0058	1.0025
	-2	1.0002	1.0016	1.0024	1.0043	1.0017
	-3	1.0001	1.0010	1.0016	1.0028	1.0011
	-4	1.0001	1.0006	1.0010	1.0019	1.0007
P_b20	-1	1.0003	1.0025	1.0040	1.0064	1.0027
	-2	1.0002	1.0020	1.0029	1.0051	1.0022
	-3	1.0002	1.0014	1.0022	1.0038	1.0016
	-4	1.0001	1.0011	1.0017	1.0031	1.0012
P_b15	-1	1.0004	1.0027	1.0042	1.0069	1.0030
	-2	1.0003	1.0022	1.0032	1.0057	1.0025
	-3	1.0002	1.0016	1.0026	1.0044	1.0020
	-4	1.0002	1.0013	1.0022	1.0038	1.0016
P_b10	-1	1.0004	1.0029	1.0045	1.0072	1.0032
	-2	1.0003	1.0025	1.0035	1.0063	1.0027
	-3	1.0002	1.0020	1.0031	1.0050	1.0023
	-4	1.0002	1.0017	1.0027	1.0046	1.0019
	-5	1.0001	1.0008	1.0014	1.0026	1.0069
P_b0	-1	1.0004	1.0030	1.0046	1.0077	1.0033
	-2	1.0003	1.0027	1.0038	1.0068	1.0029
	-3	1.0003	1.0022	1.0034	1.0055	1.0026
	-4	1.0002	1.0020	1.0031	1.0053	1.0022
	-5	1.0002	1.0013	1.0025	1.0039	1.0014
	-6	1.0001	1.0006	1.0010	1.0020	1.0007
	-7	1.0000	1.0002	1.0004	1.0007	1.0002
P_f36	-1	1.0002	1.0015	1.0025	1.0044	1.0017
	-2	1.0001	1.0008	1.0014	1.0025	1.0009
	-3	1.0000	1.0005	1.0008	1.0014	1.0006
	-4	1.0000	1.0001	1.0003	1.0005	1.0001
P_f26	-1	1.0001	1.0009	1.0016	1.0029	1.0001
	-2	1.0000	1.0005	1.0009	1.0016	1.0006
	-3	1.0020	1.0002	1.0004	1.0007	1.0003
P_f16	-1	1.0000	1.0003	1.0005	1.0009	1.0004
	-2	1.0000	1.0000	1.0002	1.0004	1.0002

(4) SLIP CORRECTION (PLATINUM CAPILLARY 293°K)

		He	Ne	Ar	Kr	Xe	N_2
P_b30	-1	1.0070	1.0050	1.0026	1.0021	1.0014	1.0024
	-2	1.0073	1.0052	1.0028	1.0021	1.0014	1.0024
	-3	1.0075	1.0054	1.0029	1.0022	1.0015	1.0026
	-4	1.0077	1.0055	1.0030	1.0022	1.0015	1.0026
P_b25	-1	1.0073	1.0052	1.0028	1.0022	1.0015	1.0026
	-2	1.0077	1.0055	1.0029	1.0022	1.0016	1.0026
	-3	1.0080	1.0057	1.0030	1.0024	1.0016	1.0028
	-4	1.0082	1.0058	1.0030	1.0025	1.0016	1.0029
P_b20	-1	1.0079	1.0057	1.0028	1.0022	1.0015	1.0028
	-2	1.0083	1.0059	1.0030	1.0024	1.0016	1.0029
	-3	1.0084	1.0061	1.0031	1.0025	1.0016	1.0030
	-4	1.0087	1.0063	1.0033	1.0025	1.0017	1.0031
P_b15	-1	1.0084	1.0059	1.0030	1.0024	1.0016	1.0028
	-2	1.0088	1.0063	1.0033	1.0025	1.0017	1.0029
	-3	1.0092	1.0065	1.0033	1.0026	1.0018	1.0030
	-4	1.0094	1.0067	1.0034	1.0028	1.0018	1.0032
P_b10	-1	1.0093	1.0064	1.0033	1.0025	1.0020	1.0030
	-2	1.0098	1.0069	1.0035	1.0026	1.0020	1.0033
	-3	1.0102	1.0073	1.0037	1.0028	1.0021	1.0034
	-4	1.0104	1.0075	1.0039	1.0030	1.0022	1.0035
	-5	1.0113	1.0080	1.0041	1.0032	1.0024	1.0039
P_b6	-1	1.0111	1.0078	1.0040	1.0029	1.0022	1.0038
	-2	1.0116	1.0083	1.0042	1.0033	1.0024	1.0041
	-3	1.0123	1.0087	1.0046	1.0034	1.0026	1.0042
	-4	1.0128	1.0090	1.0048	1.0035	1.0026	1.0043
	-5	1.0140	1.0100	1.0051	1.0038	1.0028	1.0046
	-6	1.0158	1.0111	1.0057	1.0044	1.0030	1.0054
	-7	1.0174	1.0123	1.0064	1.0048	1.0035	1.0058
P_b36	-1	1.0171	1.0120	1.0062	1.0047	1.0033	1.0057
	-2	1.0200	1.0142	1.0073	1.0053	1.0039	1.0067
	-3	1.0231	1.0162	1.0085	1.0064	1.0047	1.0077
	-4	1.0260	1.0180	1.0095	1.0072	1.0053	1.0087
P_b35	-1	1.0231	1.0161	1.0085	1.0064	1.0047	1.0077
	-2	1.0266	1.0188	1.0098	1.0073	1.0053	1.0090
	-3	1.0317	1.0224	1.0116	1.0088	1.0064	1.0106
P_b16	-1	1.0391	1.0280	1.0144	1.0109	1.0079	1.0131
	-2	1.0479	1.0340	1.0176	1.0134	1.0096	1.0163

(5) TIMES OF FLOW CORRECTED (PLATINUM CAPILLARY 293°K)

		He	Ar	Kr	Xe	N_2
P_b30	-1	104.8	122.5	144.1	146.2	97.0
	-2	188.0	215.3	245.7	239.2	170.0
	-3	224.0	256.6	288.8	267.2	202.0
	-4	385.0	440.0	496.1	453.4	346.6
P_b23	-1	90.8	107.5	128.2	130.4	85.2
	-2	146.3	168.0	194.8	193.7	133.0
	-3	138.9	158.5	180.0	171.4	125.2
	-4	140.3	160.6	181.2	167.6	126.3
P_b20	-1	79.2	94.6	114.4	116.9	73.9
	-2	118.0	136.8	160.6	162.5	108.6
	-3	98.2	112.4	129.3	127.2	88.9
	-4	83.9	96.0	108.7	104.2	75.7
P_b15	-1	73.4	88.0	107.0	109.4	70.6
	-2	103.7	121.4	144.5	146.4	96.8
	-3	81.3	93.7	109.1	108.9	74.1
	-4	65.0	74.6	85.3	83.7	59.0
P_b10	-1	67.9	82.2	100.2	102.8	66.0
	-2	91.8	108.8	130.5	133.7	86.6
	-3	68.7	79.3	93.3	94.7	63.1
	-4	52.2	60.1	69.8	69.5	47.6
	-5	538.7	615.8	696.7	656.3	485.9
P_b0	-1	64.1	78.7	96.4	99.1	60.5
	-2	84.0	100.9	121.6	124.4	80.3
	-3	60.1	70.6	84.0	85.2	56.1
	-4	44.0	51.2	60.4	61.0	40.6
	-5	357.0	409.2	467.2	454.8	322.9
	-6	343.7	393.4	442.4	408.1	309.4
	-7	1020.5	1166.2			918.6
P_t36	-1	309.0	354.2	406.0	397.0	279.8
	-2	264.9	302.7	341.1	318.4	238.6
	-3	468.0	533.2	601.1	549.0	420.6
	-4	1383.0	1577.8	1776.6	1620.7	1242.7
P_t26	-1	232.0	264.2	297.9	278.1	208.9
	-2	416.0	474.6	534.3	490.0	374.7
	-3	876.9	999.3	1125.8	1022.9	769.3
P_t16	-1	740.5	843.6	951.9	866.5	667.7
	-2	955.5	1090.2	1225.5	1115.1	862.0

(6) RATIO $(t(Gas)/t(He))_{corr}$ (PLATINUM CAPILLARY 293°K)

	Ar	Kr	Xe	N_2
P_b30 -1	1.1688	1.3750	1.3950	1.0804
-2	1.1452	1.3069	1.2723	1.1059
-3	1.1455	1.2890	1.1928	1.1089
-4	1.4428	1.2884	1.1777	1.1107
P_b25 -1	1.1639	1.4118	1.4361	1.0657
-2	1.1483	1.3315	1.3240	1.1007
-3	1.1411	1.2958	1.2340	1.1094
-4	1.1446	1.2915	1.1946	1.1091
P_b20 -1	1.1945	1.4444	1.4760	1.0434
-2	1.1593	1.3610	1.3771	1.0865
-3	1.1446	1.3167	1.2953	1.1047
-4	1.1442	1.2956	1.2420	1.1083
P_b15 -1	1.1989	1.4577	1.4904	1.0400
-2	1.1706	1.3934	1.4118	1.0713
-3	1.1525	1.3420	1.3395	1.0972
-4	1.1477	1.3120	1.2877	1.1017
P_b10 -1	1.2106	1.4757	1.5140	1.0288
-2	1.1852	1.4216	1.4564	1.0600
-3	1.1543	1.3581	1.3784	1.0887
-4	1.1513	1.3371	1.3314	1.0966
-5	1.1470	1.2963	1.2183	1.1086
P_b 0 -1	1.2278	1.5039	1.5460	1.0094
-2	1.2012	1.4476	1.4809	1.0461
-3	1.1747	1.3976	1.4176	1.0713
-4	1.1636	1.3227	1.3864	1.0837
-5	1.1462	1.3086	1.2739	1.1056
-6	1.1446	1.2860	1.1874	1.1108
P_t36 -1	1.1463	1.3139	1.2847	1.1044
-2	1.1427	1.2876	1.2020	1.1102
-3	1.1393	1.2844	1.1731	1.1127
-4	1.1409	1.2845	1.1720	1.1129
P_t26 -1	1.1388	1.2841	1.1990	1.1106
-2	1.1409	1.2843	1.1780	1.1102
-3	1.1395	1.2838	1.1660	1.1109
P_t16 -1	1.1392	1.2854	1.1700	1.1090
-2	1.1409	1.2825	1.1670	1.1109

(7) RATIO $F_c/F_s = (t(gas)/t(He))_{corr} \div (\eta(gas)/\eta(He))$ - PLATINUM CAPILLARY 293°K

	Ar	Kr	Xe	N_2
η (Gas)/ η (He)	1.1421	1.2840	1.1690	1.1120
	Ar	Kr	Xe	N_2
P_b30 -1	1.023	1.071	1.193	1.029
-2	1.003	1.018	1.090	1.005
-3	1.003	1.004	1.022	1.003
-4	1.000	1.003	1.007	1.001
P_b25 -1	1.036	1.100	1.228	1.043
-2	1.005	1.037	1.132	1.010
-3	0.999	1.009	1.055	1.003
-4	1.002	1.005	1.021	1.002
P_b20 -1	1.045	1.125	1.262	1.065
-2	1.015	1.060	1.178	1.024
-3	1.002	1.026	1.109	1.007
-4	1.002	1.009	1.062	1.004
P_b15 -1	1.050	1.135	1.275	1.069
-2	1.025	1.085	1.207	1.038
-3	1.007	1.045	1.147	1.013
-4	1.004	1.021	1.102	1.009
P_b10 -1	1.060	1.146	1.295	1.081
-2	1.037	1.107	1.241	1.049
-3	1.010	1.060	1.181	1.021
-4	1.008	1.040	1.138	1.014
-5	1.004	1.009	1.042	1.003
P_b5 -1	1.075	1.171	1.322	1.102
-2	1.051	1.124	1.267	1.062
-3	1.029	1.085	1.212	1.038
-4	1.020	1.070	1.185	1.026
-5	1.003	1.015	1.091	1.006
-6	1.002	1.001	1.015	1.001
P_f36 -1	1.003	1.023	1.099	1.007
-2	1.000	1.005	1.029	1.001
-3	0.998	1.000	1.003	0.999
-4	0.999	1.000	1.003	0.999
P_f26 -1	0.997	1.000	1.025	1.001
-2	0.999	1.000	1.008	1.001
-3	0.998	1.000	0.997	1.000
P_f16 -1	0.998	1.000	1.000	1.003
-2	0.999	0.999	1.000	1.001

Fc/Fs FOR SILICA CAPILLARY 293°K

		Ar	Kr	Xe	N_2
$\bar{P}_b$36	-1	1.001	1.004	1.052	1.001
	-2	1.001	0.997	1.013	0.999
	-3	1.001	0.997	1.001	0.998
$\bar{P}_b$26	-1	1.002	1.015	1.088	1.006
	-2	1.001	1.003	1.042	1.002
	-3	0.999	1.000	1.017	1.000
	-4	0.997	0.995	1.005	0.997
$\bar{P}_b$16	-1	1.010	1.033	1.118	1.009
	-2	1.004	1.010	1.074	1.004
	-3	1.004	1.005	1.044	1.002
	-4	0.998	0.998	1.029	1.001
	-5	1.000	1.000	1.005	0.999
$\bar{P}_b$6	-1	1.012	1.039	1.136	1.016
	-2	1.008	1.021	1.093	1.013
	-3	1.005	1.009	1.060	1.004
	-4	1.000	1.007	1.040	1.006
	-5	1.001	0.998	1.011	0.998
	-6	1.003	1.000	1.003	1.002
$\bar{P}_t$36	-1	1.000	0.998	1.013	1.001
	-2	1.001	1.000	1.002	0.999
	-3	1.000	1.000	0.999	0.999
$\bar{P}_t$26	-1	0.997	1.000	0.996	1.000
	-2	1.000	1.000	1.000	1.001
	-3	1.000	1.000	0.998	0.998
$\bar{P}_t$16	-1	1.000	0.998	0.997	1.000
	-2	1.000	1.000	1.000	1.001

APPENDIX 9

THE REDUCED COLLISION INTEGRALS FOR THE POTENTIAL

$$\Omega^*(r^*) = 10{,}000 \exp(-8r^*)$$

T^*	$\Omega^*(1,1)$	$\Omega^*(1,2)$	$\Omega^*(2,2)$	$\Omega^*(2,3)$
0.30	1.5054	1.4040	1.7849	1.6709
0.40	1.4192	1.3209	1.6896	1.5780
0.50	1.3542	1.2582	1.5875	1.5077
0.60	1.3022	1.2080	1.5298	1.4514
0.70	1.2590	1.1664	1.4818	1.4046
0.80	1.2222	1.1310	1.4409	1.3647
0.90	1.1902	1.1002	1.4052	1.3300
1.00	1.1619	1.0730	1.3737	1.2993
1.10	1.1366	1.0487	1.3455	1.2719
1.20	1.1138	1.0268	1.3200	1.2471
1.30	1.0930	1.0068	1.2967	1.2245
1.40	1.0739	0.9885	1.2754	1.2037
1.50	1.0563	0.9716	1.2557	1.1846
1.75	1.0175	0.9344	1.2122	1.1424
2.00	0.9845	0.9027	1.1752	1.1064
2.25	0.9558	0.8753	1.1436	1.0751
2.50	0.9305	0.8511	1.1146	1.0475
2.75	0.9080	0.8295	1.0891	1.0228
3.00	0.8876	0.8100	1.0662	1.0005
3.50	0.8521	0.7761	1.0261	0.9617
4.00	0.8219	0.7473	0.9920	0.9286
4.50	0.7958	0.7224	0.9623	0.8998
5.00	0.7728	0.7005	0.9362	0.8745
6.00	0.7338	0.6634	0.8917	0.8315
7.00	0.6874	0.6194	0.8388	0.7804
10.00	0.6300	0.5649	0.7729	0.7166
15.00	0.5535	0.4929	0.6836	0.6294
20.00	0.5028	0.4461	0.6222	0.5656
25.00	0.4660	0.4129	0.5771	0.5095

REFERENCES

1. J.O. Hirschfelder, C.F. Curtiss and R.B. Bird "Molecular Theory of Gases and Liquids", Wiley, N.Y. (1954)
2. R.D. Present, "Kinetic Theory of Gases", McGraw-Hill (1958)
3. S. Chapman and T.G. Cowling, "Mathematical Theory of Non-Uniform Gases", Cambridge University Press, London (1952)
4. K.S. Pitzer, Adv.Chemical Physics, 2 59 (1959)
5. C.A. Coulson, "Valence", Oxford University Press, (1961)
6. D.A. Jonah and J.S. Rowlinson, Trans.Faraday Soc., 62 1067 (1966)
7. E.A. Mason and W.E. Rice, J.Chem.Phys. 22 843 (1954)
8. R.J. Munn, Disc. Faraday Soc. 40130 (1965)
9. R.J. Munn and F.J. Smith, J.Chem.Phys., 43 3998 (1965)
10. J.A. Barker and A. Pompe - private communication (to be published) see Ref.(17)
11. H.J.M. Hanley and G.E. Childs, Science, 159 1114 (1968)
12. R. DiPippo, J. Kestin and J.H. Whitelaw, Physica, 32 2064 (1966)
13. F.M. Devienne, Advances in Heat Transfer, 2 272 (1965)

    "The Solid-Gas Interface" E.A. Flood, Ed., Vol 2, Ch.27, Arnold, London (1967)
14. N.B. Vargaftik and N. Kh.Zimina, High Temp. 2 645 (1964)
15. D.L. Timrot and A.S. Umanski, High Temp. 3 345 (1965)
16. E.H. Kennard, "Kinetic Theory of Gases", McGraw-Hill Book Co., New York (1938)
17. E.B. Smith, Ann.Reports Chem.Soc. 63 13 (1966)
18. D.D. Fitts, Ann.Rev. Phys.Chem. 17 59 (1966)
19. J.A. Pryde, "The Liquid State", Hutchinson University Library, London (1966)
20. Discuss. Faraday Soc., 40 (1965) (Intermolecular Forces)
21. H. Pauly and J.P. Toennies, Adv.Atomic and Molecular Physics, 1 302 (1965)
22. J.O. Hirschfelder Ed., Advances in Chem.Phys. 12 (1968) (Intermolecular Forces) - especially Chapter 7 by E.A. Mason and L. Monchick.

23. R.A. Buckingham, Trans.Faraday Soc. 54 547 (1954)
24. A.A. Abrahamson, Phys.Rev. 130 693 (1963)
25. ref. 1. page 28.
26. F. London, Z. Phys.Chem. B11 222 (1930)
27. F. London, Trans. Faraday. Soc. 33 8 (1937)
28. J.C. Slater and J.G. Kirkwood, Phys.Rev. 37 682 (1931)
29. H. Margenau, Rev.Mod.Phys. 11 1 (1939)
30. A. Dalgarno, Adv.Atomic and Molecular Physics, 2 2 (1966)
31. R.J. Bell, Proc.Phys.Soc. 86 17 (1965)
32. P.R. Fontana, Phys.Rev. 123 1865 (1961)
33. B.M. Axilrod and E. Teller, J.Chem.Phys. 11 299 (1943)
34. T. Kihara, Adv.Chem.Phys. 1 267 (1958)
35. L. Jansen, Phys.Rev. 125 1798 (1962)
36. A.E. Sherwood and J.M. Prausnitz, J.Chem.Phys. 41 413 (1964)
37. B.M. Axilrod, J.Chem.Phys. 19 719 (1951)
38. J.E. Walkley, J.Chem.Phys. 44 2417 (1966)
39. A.E. Sherwood, A.G. De Rocco and E.A. Mason, J.Chem.Phys. 44 2984 (1966)
40. J.A. Barker and A. Pompe, See Refs. 10 and 17.
41. Ref. 2 page 31.
42. J.E. Lennard-Jones, Proc.Roy.Soc. A106 463 (1924)
43. J.H. Dymond, M. Rigby and E.B. Smith, Phys.Fluids, 9 1222 (1965)
44. S.D. Hamann and J.A. Lambert, Australian J.Chem. 7 1 (1954)
45. T. Kihara, Rev.Mod.Phys. 25 831 (1953)
46a. R.A. Buckingham and J. Corner, Proc.Roy.Soc. A189 118 (1947)
b. J. Corner, Trans.Faraday Soc. 44 914 (1948)
47. E.A. Guggenheim and M.L. McGlashan, Proc.Roy.Soc. A255 456 (1960)
48. J.H. Dymond, M. Rigby and E.B. Smith, J.Chem.Phys. 42 2801 (1965)

49. R.J. Munn, J.Chem.Phys. 40 1439 (1964)

50. S.F. Boys and L. Shavitt, Nature, 178 1340 (1956)

51. J.H. Dymond, M. Rigby and E.B. Smith, Nature, 204 678 (1964)

52. Ref. 1. page 1035.

53. M. Rigby, D.Phil.Thesis, Oxford (1965)

54. Ref. 1. Chapters 4 and 9.

55. J.A. Barker, "Lattice Theories of the Liquid State", Pergamon, London, (1963)

56. Discuss. Faraday Soc. 43 (1967) (The Structure and Properties of Liquids)

57. H. Eyring and J.O. Hirschfelder, J.Phys.Chem. 41 249 (1937)

58. Ref. 1, Chapter 4.

59. N. Metropolis, A.W. Rosenbluth, M.N. Rosenbluth, A.H. Teller and E. Teller, J.Chem.Phys. 21 1087 (1953)

60. M.A.D. Fluendy and E.B. Smith, Quart.Rev.Chem.Soc., 16 241 (1962)

61. B.J. Alder and J.W. Wainwright, J.Chem.Phys. 27 1208 (1957)
31 459 (1959)

62. P.G. Mikolaj and C.J. Pings, J.Chem.Phys. 46 1401, 1412 (1967)

63. Ref. 1 Chapter 3.

64. M. Klein, J. of Research of Nat.Bur.Standards 70A 259 (1966)

65. J.B. Keller and B. Zumino, J.Chem.Phys. 30 1351 (1959)

66. H.L. Frisch and E. Helfand, J.Chem.Phys. 32 269 (1960)

67. P.E. Phillipson, Phys.Rev. 125 1981 (1962)

68. J.S. Rowlinson, Disc.Faraday Soc. 40 19 (1965)

69. E.S. Burnett, J.Appl.Mech. 3A 137 (1936)

70. J.H. Dymond and E.B. Smith, "The Virial Coefficients of Gases", The Clarendon Press, Oxford (1968)

71. D.G. Francis and G.R. Luckhurst, Trans.Faraday Soc. 59 667 (1963)

72. J.A. Barker, W. Fock and F. Smith, Phys.Fluids, 7 897 (1964)

73. Ref. 2, Chapter 7.

74. Ref. 1, Chapter 7.

75. S.C. Saxena and B.P. Mathur, Rev.Mod.Phys. 37 316 (1965)

76. S.C. Saxena and B.P. Mathur, Rev.Mod.Phys. 38 380 (1966)

77. E.A. Mason, R.J. Munn and F.J. Smith, Adv.At.Mol.Phys. 2 33 (1966)

78. B.E.F. Fender, J.Chem.Phys. 35 2243 (1961)

79. T.I. Morgan and W.W. Watson, Phys.Rev. 109 1184 (1958)

80. R.B. Bernstein, Science, 144 141 (1964)

81. R.B. Bernstein, Chapter 8 Ref. 22.

82. J. Ross, Ed. Advances in Chem.Phys. 10 (1966) (Molecular Beams)

83. E.A. Mason and J.T. Vanderslice, "Atomic and Molecular Processes", D.R. Bates ed. Academic Press, New York (1962) Chapter 17.

84. J.B. Hasted, "Physics of Atomic Collisions", Butterworth, Washington D.C., (1964)

85. A.R. Blythe, M.A.D. Fluendy and K.P. Lawley, Quart.Revs.Chem.Soc. 20 465 (1966)

86. I. Amdur and J.E. Jordan, Adv. in Chem.Phys. Vol.10 (1966) (Ref.82) Chapter 2.

87. J.E. Jordan and I. Amdur, J.Chem.Phys. 46 165 (1967)

88. R.B. Bernstein, Adv. in Chem.Phys. Vol.12 (1968) Ref. 81, page 393.

89. E.A. Mason and L. Monchick, Adv. in Chem.Phys. 10 (1968) Ref. 22, Chapter 7.

90. R.G. Breene Jr. "The Shift and Shape of Spectral Lines" Pergamon Press, New York (1961)

91. G.P. Reck, H. Takebe and C.A. Mead, Phys.Rev. 137 A683 (1965)

92. G. Birnbaum, Adv. in Chem.Phys. 12 (1968) Ref. 22, Chapter 9.

93. M. Bloom, Adv. in Chem.Phys. 12 (1968) Ref. 22, Chapter 10.

94. T.L. Cottrell and J.C. McCoubrey, "Molecular Energy Transfer in Gases", Butterworth, London (1961)

95. K. Pitzer, J.Chem.Phys. 7 583 (1939)

96. E.A. Gugenheim, Rev.Pure Appl.Chem. 3 1 (1953)
J.Chem.Phys. 7 253 (1945)

97. J.S. Rowlinson and J.R. Townley, Trans.Faraday Soc. 49 20 (1953)

98. J.D. van der Waals, Verh K.Akad.Wetens Amsterdam 21 No.5 (1881)

99. N.G. Parsonage, "The Gaseous State", The Commonwealth and International Library, Pergamon Press (1966)

100. L.B. Loeb, "The Kinetic Theory of Gases", McGraw-Hill Book Co. (1934)

101. H.S. Taylor and S. Glasstone, "A Treatise on Physical Chemistry", Vol.2, "States of Matter", D. van Nostrand Co. New York (1951)

102. J.R. Partington, "An Advanced Treatise on Physical Chemistry", Vol.1, "Fundamental Principles and Properties of Gases", Section VIIF, Longmans, Green and Co.Ltd., London (1949)

103. J.H. Jeans, "An Introduction to the Kinetic Theory of Gases", Cambridge University Press, London (1946)

104. L. Monchick, Y.S. Yun and E.A. Mason, J.Chem.Phys. 39 654 (1963)

105. S. Chapman, Phil.Trans.Roy.Soc. A211 433 (1912)

106. D. Enskog, Phys.Zeit. 12 56, 533 (1911)

107. H. Goldstein, "Classical Mechanics", Addison Wesley, Reading U.S.A. (1950)

108. K.W. Ford and J.A. Wheeler, Ann.Phys. (N.Y.) 7 259, 287 (1959)

109. N.F. Mott and H.S.W. Massey, "The Theory of Atomic Collisions", Oxford University Press, London (3rd Ed. 1965)

110. T. Kihara, "Imperfect Gases", Tokyo; Asakusa Bookstore, 1949, Translated by U.S. Office of Air Research, Wright Patterson Air Force Base, Dayton, Ohio.

111. J.O. Hirschfelder, J.Chem.Phys. 26 282 (1957)

112. E.A. Mason and L. Monchick, J.Chem.Phys. 36 1622 (1962)

113. S.C. Saxena, M.P. Saksena and R.S. Gambhir, Brit.J.Appl.Phys. 15 843 (1964)

114. H.L. Johnson and K.E. McCloskey, J.Phys.Chem. 44 1038 (1940)

115. A. van Itterbeek and C. van Paemel, Physica 5 1009 (1938)

116. E.G. Clifton, J.Chem.Phys. 38 1123 (1963)

117. J. Kestin and W. Leidenfrost, Physica 25 1033 (1959)

118. M.N. States, Phys.Rev. 21 662 (1923)

119. J. Kestin and J.H. Whitelow, Physica, 29 335 (1963)

120. R. DiPippo, Ph.D. Thesis, Brown University (1966)

121. J.A. Bearden, Phys.Rev. 56 1023 (1939)

122. R.A. Millikan, Phil.Mag. 34 1 (1917)

123. Y. Ishida, Phys.Rev. 21 350 (1923)

124. G.P. Flynn, R.V. Hanks, N.A. LeMaire and J. Ross, J.Chem.Phys. 38 154 (1963)

125. M. Trautz and W. Weizel, Ann.Phys. 78 305 (1925)

126. V. Vasilesco, Ann de Phys. 20 137, 292 (1945)

127. V.D. Hopper and T.G. Laby, Proc.Roy.Soc. A178 243 (1941)

128. R.T. Birge, Nuovo Cimento Supp. 6 39 (1957)

129. R.T. Birge, Am.J. of Physics, 13 63 (1945)

130. R.T. Birge, Rev.Mod.Phys. 1 1 (1929)

131. J.W.M. DuMond and E.R. Cohen, Rev.Mod.Phys. 25 691 (1953)

132. E.L. Harrington, Phys.Rev. 8 738 (1916)

133. J. Kestin, (Comment) Trans. A.S.M.E. 78 1288 (1956)

134. R.J. Taylor, "Chemical Engineering", A Unilever Education Booklet, Advanced Series (1967)

135. J.O. Hinze, "Turbulence", McGraw-Hill Book Co., New York (1959)

136. O.E. Meyer, Pogg.Ann. 127 253 (1866)

137. J.C. Maxwell, Phil.Trans. 170 231 (1879)

138. Ref. 2, page 62

139. G.M. Fryer, Proc.Roy.Soc. A293 329 (1966)

140. F.C. Hurlbut, in "Methods of Experimental Physics", Vol.1, "Classical Methods", page 184, I. Estermann Ed. Academic Press, (N.Y.) (1959)

141. M. Knudsen, Ann.Phys. 28 75 (1909)

142. P. Clausing, Ann.Phys. 7 569 (1930)

143. H. Adzumi, Bull.Chem.Soc.Japan 12 199, 285 (1937)

144. S. Visner, Phys.Rev. 82 297 (1951)

145. P.C. Carman, Proc.Roy.Soc. A203 35 (1950)
"Flow of Gases through Porous Media" Butterworth, London (1956)

146. W.G. Pollard and R.D. Present, Phys.Rev. 73 762 (1948)

147. D.S. Scott and F.A.L. Dullien, A.I.Ch.E.J. 8 293 (1962)

148. S. Weber, Mat-Fys Medd. 28 No.2 (1954)

149. R.M. Barrer, App. Materials Research 2 129 (1963)

150. E.A. Mason, A.P. Malinauskas and R.B.Evans III, J.Chem.Phys. 46 3199 (1967)

151. E. Creutz and L.R. Zumwalt, J.Appl.Phys. 33 2883 (1962)

152. R.M. Barrer and D. Nicholson, British J.Appl.Phys. 17 1091 (1966)

153. M. Knudsen, "The Kinetic Theory of Gases" Methuen and Co.Ltd. London (3rd Ed. 1950)

154. R.B. Evans III, G.M. Watson and E.A. Mason, J.Chem.Phys. 35 2076 (1961)

155. E.A. Mason, R.B. Evans III and G.M. Watson, J.Chem.Phys. 38 1808 (1963)

156. S. Simons, Proc.Roy.Soc. A301 387 (1967)

157. C. Cercignani and A. Daneri, J.Appl.Phys. 34 3509 (1963)

158. C. Cercignani and F. Semagiotto, Phys. Fluids, 9 40 (1966)

159. E. Hagenbach, Pogg.Ann. 109 385 (1860)

160. G. Barr, "A Monograph of Viscometry", Oxford University Press (N.Y.) (1931)

161. M. Couette, Ann.de Chimie et de Physique, 21 433 (1890)

162. R.L. Hanks and H.L. Weissberg, J.Appl.Phys. 35 142 (1964)

163a. See Ref. (124)

b. R.E. Wellman, R. Dewitt and R.B. Ellis, J.Chem.Phys. 44 3070 (1966)

164. S. Goldstein Ed. "Modern Developments in Fluid Dynamics", Oxford University Press, London (1938) page 299 (Now published by Dover Publications Ltd.)

165. W.R. Dean, Phil.Mag. 4 208 (1927)

166. W.R. Dean, Phil.Mag. 5 673 (1928)

167. C.M. White, Proc.Roy.Soc. A123 645 (1929)

168. S. Goldstein, Ref. 164, page 312

169. G.I. Taylor, Proc.Roy.Soc. A124 243 (1929)

170. V. Vasilesco, Ann. Physique, 20 137, 292 (1945)

171. N.L. Anfilogoff, Ph.D. Thesis, London (1932)

172. C.Y. Liu, Phys. Fluids 11 481 (1968)

173. O. Reynolds, Phil. Trans. 174 935 (1883)

174. F.C. Hurlbut, J. Appl. Phys. 28 844 (1957)

175. M. Rigby, D. Phil. Thesis, Oxford (1963) Chapter 1

176. M. Rigby and E.B. Smith, Trans. Faraday Soc. 62 54 (1966)

177. S. Goldstein Ed. Ref. (164) Vol. II page 616.

178. C.F. Bonilla, S.J. Wang and H. Weiner, Trans. A.S.M.E. 78 1285 (1956)

179. Ether Ltd. Handbook for Transitrol Temperature Controllers, Types 990 and 991

180. C.H.L. Goodman, J. Sci. Instrum. 43 393 (1966)

181. A.J. Jewell, J. Sci. Instrum. 44 81 (1967)

182. Tables for Thermocouples, British Standards Institution, London (1952)

183. B. Barter and A.S. Darling, Platinum Metals Rev. 4 138 (1960)

184. "A Handbook of Chemistry and Physics", Chemical Rubber Publishing Co. (1966)

185. L. Holborn and A.L. Day, Ann. Physik, 4 347 (1914)

186. H. Holzmann, Festschrift 50 jahrigen, Siebert G.M.B.H., Hanau, Germany, 147 (1931)

187. W.J. Youden, "Statistical Methods for Chemists", Chapter 3, John Wiley and Sons, Inc. (1951)

188. K.J. Munn, J. Chem. Phys. 40 1439 (1964)

189. T. Kihara, Rev. Mod. Physics, 25 831 (1953)

190. L. Monchick, Phys. Fluids, 2 695 (1959)

191. R.M. Barrer and D. Nicholson, Canadian J. Chem. 43 896 (1965)

192. A.G. Clarke and E.B. Smith, J. Chem. Phys. 48 3988 (1968)

193. M. Trautz and R. Zink, Ann. Physik, 7 427 (1930)

194. N.C. Blais and J.B. Mann, J. Chem. Phys. 32 1459 (1960)

195. F.A. Guevara and W.E. Wageman, Los Alamos Scientific Laboratory Report, L.A. - 3319 (1965)

196. A number of articles in "Advances in Applied Mathematics - Rarefied Gas Dynamics" Academic Press (1961 and onwards.).

197. K.E. Stickney, Ad.At. and Mol.Phys. 3 143 (1967)

198. F.C. Hurlbut and F.S. Sherman, Phys. Fluids, 11 486 (1968)

199. S. Albertoni, C. Cercignani and L. Gotusso, Phys.Fluids 6 993 (1963)

200. R.W. Hanks and H.L. Weissberg, J.Appl.Phys. 35 142 (1964)

201. L.M. Lund and A.S. Berman, J.Appl.Phys. 37 2489, 2496 (1966)

202. D.R. Willis, Phys. Fluids, 5 127 (1962)

203. Ref. (140) page 161

204. R.M. Logan and R.E. Stickney, J.Chem.Phys. 44 195 (1966) and references therein.